

**THE CELL KINETICS OF
HUMAN BREAST CANCER**

PETER DAVID STANTON

B Med Sci (Hons), MB, BS (Hons), FRCS, FRACS

**A Thesis Submitted to the University of Glasgow
for the Degree of Doctor of Philosophy**

**Dept. of Surgery (Royal Infirmary)
University of Glasgow**

© April, 1995

ProQuest Number: 11007735

All rights reserved

INFORMATION TO ALL USERS

The quality of this reproduction is dependent upon the quality of the copy submitted.

In the unlikely event that the author did not send a complete manuscript and there are missing pages, these will be noted. Also, if material had to be removed, a note will indicate the deletion.



ProQuest 11007735

Published by ProQuest LLC (2018). Copyright of the Dissertation is held by the Author.

All rights reserved.

This work is protected against unauthorized copying under Title 17, United States Code
Microform Edition © ProQuest LLC.

ProQuest LLC.
789 East Eisenhower Parkway
P.O. Box 1346
Ann Arbor, MI 48106 – 1346

Theirs
10122
Copy 1

GLASGOW
UNIVERSITY
LIBRARY

ABSTRACT

Tumour growth has been studied for many years in the hopes of gaining prognostic information, guiding cancer therapy, and better understanding the control of cellular proliferation within tumours. Recent methods have applied the technology of flow cytometry, using its ability to characterise many cells in a short space of time. This thesis examines the potential for two of these techniques to contribute to the study of tumour cell kinetics in the context of breast cancer, one of the commonest tumours, one of the most studied, and yet one where patient outcome has improved little in recent years.

The first method involves staining of tumour nuclei with fluorescent stoichiometric DNA dyes in order to obtain a frequency distribution of DNA contents within the tumour cell population. From this, the amount of nuclear DNA of the tumour cells relative to the norm (tumour ploidy), and the proportion of cells in the S phase of the cell cycle (the S phase fraction, SPF) can be estimated. These parameters have been described as being of prognostic significance in breast cancer. In 293 cases studied here, there was a non-statistically significant worse prognosis for aneuploid tumours relative to diploid (relative hazard in multivariate analysis 1.20, 95%CI 0.81-1.76), whilst SPF shows an also non-significant trend toward poor survival associated with high SPF (relative hazards 1.31, 95%CI 0.87-1.98). In view of theoretical and logistical shortcomings of the methodology, studies of the reproducibility of the SPF were carried out, indicating very large variations in repeated estimates (95% CI for estimates of $\pm 40\%$ or more). This may contribute to the limited prognostic power of this parameter.

The second technique, which also provides information about the rate of cell cycle transit, involves the administration of the DNA precursor bromodeoxyuridine prior to tumour biopsy. Staining of nuclear suspensions for both DNA content as above, and for bromodeoxyuridine content, analysed by multiparameter flow cytometry, allows estimation of the proportion of cells in S phase (the bromodeoxyuridine labelling index, BLI), the length of that phase (T_s), and the potential doubling time (T_{pot}) of the tumour. This information has been gained in 84 women, out of 89 labelled. This has demonstrated that the technique can be successfully applied to most breast cancers. Median values for the three parameters were: LI- 3.2%, T_s - 12.7hrs, T_{pot} - 14.6days. Prognostic information is not yet available, but the relationship to other prognostic factors. Kinetics were closely related to histological grade, but not tumour size or nodal status. Although oestrogen receptor status was known for only a minority of tumours, within this group ER negative tumours showed significantly higher BLI. In terms of reproducibility, this method emerges as superior to the estimation of SPF

(95%CI for estimations of BLI $\pm 30\%$). Its own limitations are considered, principally the inability to allow for cell loss within tumours, or to deal with variation in kinetic parameters in different areas of tumour.

The potential to use this technique as a means of exploring tumour biology was addressed in a further study of type I growth factor expression in the same group of breast tumours. Two members of this family of cell surface proteins were studied, the epidermal growth factor receptor (EGFR) and the *c-erbB-2* oncoprotein. Both are known to be expressed in a significant minority of breast cancers, and in each case expression has been shown to be associated with poorer prognosis. This has led to the hypothesis that they act to give growth advantage to tumours in which they are overexpressed, which was tested here by looking at the relationship between expression and cell kinetics. In the case of *erbB-2*, there was a trend toward higher BLI in positive tumours, but this was not statistically significant ($p=0.28$). For the study of EGFR, a quantitative immunohistochemical method not previously used in breast cancers was used. This involves application of radio-iodinated antibody to tissue sections, the binding of which is demonstrated by covering the slide with autoradiographic emulsion. Quantification is possible by counting the number of grains developed in the emulsion, using an image analysis system. In all, 105 tumours were studied this way, as well as 9 normal breast controls. This demonstrated that 97% of tumours had levels of EGFR expression lower than that in normal breast. Tumours with preserved expression of any degree did have significantly higher BLI (rank correlation, $p=0.019$), and lower T_{pot} ($p=0.039$).

ACKNOWLEDGEMENTS

I was introduced to this fascinating area of research, and then supported and encouraged through it, by Tim Cooke. Working for him has been easy and agreeable, which is reflected in the fact that I remain actively involved in this area well beyond the completion of the experiments described here. I think that I have been very fortunate to have benefitted from this level of commitment from someone who appreciates the primacy of basic research in determining the future of surgery.

At a technical level, the second and third parts of this thesis were supported greatly by the efforts of Sarah Oakes and Gill Forster, both in developing these techniques within the labs at the Glasgow Royal Infirmary and then in studying the many specimens. I also benefitted from the parallel work of Brendan Bolger and Lyn Cooke in the fields of cervical and head and neck cancer respectively. Some data kindly provided by Gill and Brendan is included in Chapter 9, and is credited there. James Going in the Department of Pathology of the hospital spent many hours in vetting H&E sections to grade the tumours, and to count labelling indices on immunocytochemical preparations for us, and I am very grateful for the enormous amount of work that this involved.

I would also like to express my debt to Mr David Smith at the Victoria Infirmary, Glasgow, for allowing me to include his patients in the bromodeoxyuridine labelling studies, and to Greg Keogh who contributed considerably to the refinement of this manuscript.

STATEMENT

This thesis contains no material which has been accepted for the award of any other degree or diploma in any tertiary institution. To the best of my knowledge and belief it contains no material previously published or written by another person, except where due reference is made in the text.

TABLE OF CONTENTS

	Page
Part I - Background Information and Historical Review	1
Chapter 1: Basic Theory of Growth of Cell Populations	2
Chapter 2: Overview of Methods in Tumour Cell Kinetics	9
Chapter 3: Review of Static Methods in Breast Cancer	17
Chapter 4: Review of Dynamic Methods in Breast Cancer	45
Statement of Aims	55
Part II - S Phase Fraction as a Prognostic Factor	57
Introduction to Experimental Parts of the Thesis	58
Overview of Ploidy Studies	58
Chapter 5: Patients and Methods	59
Chapter 6: Results	76
Chapter 7: Discussion and Conclusions	88
Part III - <i>in vivo</i> Bromodeoxyuridine in Breast Cancer	100
Overview of Bromodeoxyuridine Studies	101
Chapter 8: Patients and Methods	102
Chapter 9: Results	117
Chapter 10: Epidermal Growth Factor Receptor Expression	141
Chapter 11: Discussion and Conclusions	157
General Discussion	165
References	170
Appendices	190

CONTENTS IN DETAIL

	Page
Part I - Background Information and Historical Review	1
Chapter 1: Basic Theory of the Growth of Tumour Cell Populations	2
Section i: Development of Models of the Cell Cycle	2
Section ii: Kinetic Description of the Cell Cycle	3
Section iii: Mechanisms of Cell Loss	5
Section iv: Control of the Cell Cycle	6
Section v: Cell Cycle Response to External Stimuli	8
Chapter 2: Overview of Methods in Tumour Cell Kinetics	9
Section i: Why Study Tumour Cell Kinetics?	9
Section ii: Why Use Breast Cancer as the Model?	10
Section iii: Summary of Methods Available	11
Chapter 3: Review of Static Methods applied to Breast Cancer	17
Section i: Direct Measurement of Tumour Growth	17
Section ii: Use of the Mitotic Index	23
Section iii: Staining for Cell Cycle Specific Antigens	24
Section iv: Thymidine Labelling Index	27
Section v: Flow Cytometric S Phase Fraction	35
Chapter 4: Review of Dynamic Methods applied to Breast Cancer	45
Section i: Theoretical Basis for the Use of Bromodeoxyuridine	45
Section ii: Application of the Bromodeoxyuridine Method	51
Statement of Aims	55
Part II - S Phase Fraction as a Prognostic Factor in Breast Cancer	57
Introduction to Experimental Parts of the Thesis	58
Overview of Ploidy Studies	58
Chapter 5: Patients and Methods	59
Section i: Patients Studied	59
Section ii: Tissue Available	60
Section iii: Preparation and Staining of Nuclear Suspensions	60
Section iv: Flow Cytometry	62
Section v: Data Storage	66
Section vi: Allocation of Tumour Ploidy	66
Section vii: Estimation of S Phase Fraction	68
Section viii: Statistical Methods	71
Section ix: Reproducibility Studies	75

	Page
Chapter 6: Results	76
Section i: Patient Characteristics	76
Section ii: Basic Ploidy Data	76
Section iii: Prognostic Power of Tumour Ploidy	78
Section iv: Basic Data on S Phase Fractions	79
Section v: Prognostic Power of S Phase Fraction	81
Section vi: Multivariate Analysis	81
Section vii: Reproducibility Studies	84
a) Comparison of different models of S phase	
b) Inter-observer variation	
c) Intra-observer variation	
Chapter 7: Discussion and Conclusions	88
Part III - <i>in vivo</i> Administration of Bromodeoxyuridine in Breast Cancer	100
Overview of Bromodeoxyuridine Studies	101
Chapter 8: Patients and Methods	102
Section i: Patients Studied	102
Section ii: Bromodeoxyuridine Labelling	102
Section iii: Specimen Collection	103
Section iv: Patient and Tumour Data Noted	103
Section v: Specimen Preparation	104
Section vi: Flow Cytometry	106
Section vii: Data Storage	108
Section viii: Determination of Cell Kinetic Parameters	108
Section ix: Other Data Accumulated	115
a) Immunohistochemical Counts of Labelling	
b) Expression of c-erbB-2	
Section x: Statistical Methods	116
Chapter 9: Results	117
Section i: Patient Characteristics	117
Section ii: Basic Cell Kinetic Data	118
Section iii: Relationship of Length of S Phase to Labelling Index	121
Section iv: Relationship of Length of S Phase to Labelling Time	122
Section v: Flow versus Immunohistochemical Labelling Indices	123
Section vi: Comparison of Kinetics in Tumour and Normal Breast	125
Section vii: Comparison of Labelling Index and S Phase Fraction	126
Section viii: Relationship of Kinetics to Prognostic Factors	129
Section ix: Relationship of Kinetics to Ploidy	130

	Page
Section x: Relationship of Kinetics to c-erbB-2 Expression	132
Section xi: Reproducibility Studies	135
a) Results from serial sections	
b) Results from tumour segments	
c) Inter- and intra-observer variation	
Section xii: Comparison with Kinetics of Squamous Tumours	139
Chapter 10: Epidermal Growth Factor Receptor Expression	141
Section i: Introduction	141
Section ii: Methods	144
a) Patients studied and material available	
b) Antibody iodination	
c) Incubation	
d) Film autoradiography	
e) Emulsion autoradiography	
f) Counterstaining	
g) Grain counting	
h) Calculation of EGFR expression	
i) Controls	
Section iii: Results	151
a) Counts in cell pellets	
b) Counts in normal breast	
c) Counts in breast cancers	
d) Lower limit of detection	
e) Relationship to cell proliferation	
f) Relationship to pathological variables	
Chapter 11: Discussion and Conclusions	157
General Discussion	165
References	171
Appendices	190
Appendix I: Ploidy and S Phase Fraction in 281 patients	191
Appendix Ia: Pathological Data for Patients in the SPF Series	202
Appendix II: S Phase Fraction values from Reproducibility Studies	207
Appendix III: Patient & Histogram data for the BUDR series	213
Appendix IV: Kinetic Parameters in the Bromodeoxyuridine series	216
Appendix IVa: Results for c-erbB-2 Staining in BUDR series	219
Appendix V: EGFR Exp ⁿ , Kinetics & Pathological Data for 105 Patients	221

LIST OF FIGURES

	Page
 <u>PART I</u>	
Figure 1: Howard and Pelc model of the cell cycle	2
Figure 2: Checkpoints within the cell cycle	6
Figure 3: Principle of percent labelled mitoses technique	15
Figure 4: Relationship between tumour size and tumour age	18
Figure 5: Summary of thymidine labelling technique	27
Figure 6: Life table for TLI values above and below median	31
Figure 7: Bland-Altman plot for interobserver variation of TLI	33
Figure 8: Theoretical ploidy histogram	36
Figure 9: Diploid ploidy histogram- simulated	37
Figure 10: Screen photographs of ploidy histograms	38
Figure 11: Aneuploid ploidy histogram	37
Figure 12: Rectangular model of S phase fraction	40
Figure 13: Printout of S phase estimation in diploid histogram	41
Figure 14: Principle of determination of T_s from a single sample	46
 <u>PART II</u>	
Figure 15: Flow chart of sample preparation for flow cytometry	61
Figure 16: Fluid dynamics of flow cytometer	62
Figure 17: Detection system of flow cytometer	63
Figure 18: Principle of doublet discrimination	65
Figure 19: Model of background subtraction	69
Figure 20: Principle of estimation of SPF	70
Figure 21: Models of S phase available	72
Figure 22: Statistical methods for comparing two measurements	74
Figure 23: Distribution of DNA indices	77
Figure 24: Life table for diploid versus aneuploid tumours	78
Figure 25: Distribution of values of SPF	79
Figure 26: Life tables for SPF values above and below median	82
Figure 27: Comparison of estimates of SPF obtained by two observers	86

	Page
Figure 28: Types of aneuploid histogram	90
Figure 28a: Screen photographs of aneuploid histograms	91
Figure 28b: Screen photographs of aneuploid histograms (cont.)	92
Figure 29: Printout of S phase estimation in aneuploid histogram	98

PART III

Figure 30: Flow chart of preparation of BUdR labelled samples	105
Figure 31: Example of two parameter histogram	109
Figure 32: Screen photograph of two parameter histogram	110
Figure 33: Method of peak delineation in one parameter histogram	111
Figure 34: Example of one parameter BUdR fluorescence histogram	112
Figure 35: Method for eliminating unwanted diploid G_2/M labelled cells	113
Figure 35a: Screen photograph of method demonstrated in fig. 35	114
Figure 36: Distribution of numbers of labelled undivided cells	118
Figure 37: Distribution of DNA indices	119
Figure 38: Frequency distribution of histogram CVs	120
Figure 39: Distributions of basic kinetic parameters	120
Figure 40: Plot of labelling index versus length of S phase	121
Figure 41: Values of T_s broken down by labelling time	123
Figure 42: Plot of values of ILI against BLI for each tumour	124
Figure 43: Plot of values of BLI against SPF for each tumour	127
Figure 44: Distribution of values of SPF	127
Figure 45: Values of BLI broken down by ploidy	131
Figure 46: Values of T_s broken down by ploidy	131
Figure 47: Values of ILI and \bar{TLI} broken down by ploidy	132
Figure 48: Values of kinetic parameters broken down by erbB-2 status	133
Figure 49: Values of ILI and TLI broken down by erbB-2 status	134
Figure 50: Photomicrograph of radioimmunohistochemistry section	148
Figure 51: Frequency distribution of EGFR levels in tumours	153
Figure 52: Plots of EGFR expression against kinetic parameters	155

LIST OF TABLES

	Page
<u>PART I</u>	
Table 1: Summary of cell kinetic methods	12
Table 2: Relationship between tumour growth and SPF (Arnerlöv et al)	20
Table 3: Summary of results from direct tumour observation	23
Table 4: Relationship between TLI and survival (Meyer et al)	28
Table 5: Relationship between TLI and survival (Silvestrini et al)	29
Table 6: Relationships between TLI and prognostic factors	30
Table 7: Relationship between TLI and survival	31
Table 8: Inter- and intra-observer variation in TLI	33
Table 9: Summary of large studies of ploidy and SPF	44
Table 10: Correlation of calculated and observed growth in cell cultures	49
Table 11: Summary of Mt Vernon group results with BUDR	52
Table 12: Summary of results with BUDR by other groups	54
<u>PART II</u>	
Table 13: Distribution of prognostic factors in the ploidy series	76
Table 14: Relationships between ploidy and prognostic factors	77
Table 15: Relationships between SPF and prognostic factors	80
Table 16: Relationship between quartiles of SPF and survival	81
Table 17: Results of multivariate analysis (pts with all data available)	83
Table 18: Results of multivariate analysis (all data for all pts)	83
Table 19: Comparison of SPF estimated by different models of S phase	84
Table 20: Reproducibility of different models of S phase	85
Table 21: Interobserver variation of SPF (rectangular model)	86
Table 22: Intraobserver variation of SPF (rectangular model)	87

PART III

Table 23: Summary of prognostic factors in the BUDR series	117
Table 24: Ploidies of tumours in the BUDR series	119
Table 25: Summary statistics of kinetic parameters	121
Table 26: Comparison of flow and histochemical labelling indices	124
Table 27: Kinetic parameters in 8 specimens of normal breast	125
Table 28: Comparison of kinetics in tumour and normal samples	126
Table 29: Relationship between BLI and SPF	128
Table 30: Relationships between kinetics and prognostic factors	129
Table 31: Relationships between prognostic factors and ploidy	130
Table 32: Relationship between erbB-2 status and kinetic parameters	134
Table 33: Relationship between erbB-2 status and ploidy	135
Table 34: Reproducibility of kinetic parameters in serial sections	136
Table 35: Comparison of kinetics from segments versus sections	137
Table 36: Interobserver variation of BLI (head and neck cancer)	138
Table 37: Interobserver variation of kinetic parameters (cervix cancer)	138
Table 38: Kinetics of different tumours studied with BUDR	139
Table 39: Grain counts in cell pellet sections	152
Table 40: Grain count ratios for cell pellets	152
Table 41: Grain count example in normal breast	152
Table 42: Grain counts in all normal breast samples	153
Table 43: Grain count example in tumour and control sections	154
Table 44: Rank correlation between EGFR expression and kinetic parameters	155
Table 45: Relationship between EGFR (as +/-) and kinetic parameters	156
Table 46: Relationship between EGFR expression and prognostic factors	156
Table 47: Summary of published results with BUDR in breast cancer	157
Table 48: Comparison of S phase estimates made by different methods	158
Table 49: Reproducibility of different methods for measuring kinetics	159

PART I

BACKGROUND INFORMATION

AND

HISTORICAL REVIEW

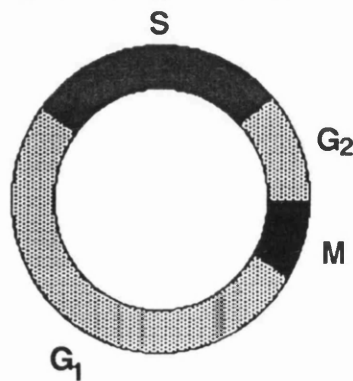
Chapter 1:

Basic Theory of the Growth of Tumour Cell Populations

Section i: Development of models of the cell cycle

Tumours grow because their rate of cell production exceeds the rate at which cells are lost from them. In order to study this process in greater detail, it is necessary to understand the means by which individual cells divide. That this happened in a stepwise manner was established by Howard and Pelc in the early 1950s (Howard and Pelc 1951, 1953), by studying the incorporation of radioactive phosphorus into the nuclei of bean roots. They noted that after pulse exposure to ^{32}P , 16% of meristematic cells were labelled. None of the labelled cells were mitotic figures. If the exposure to ^{32}P was prolonged, however, mitotic figures began to be labelled, until 50% were so identified after 11 hours of exposure. They proposed from this data that there was a period of premitotic DNA synthesis, which they called the S phase, which accounted for some 16% of the total intermitotic interval (ie total cell cycle time), and that there was an 8 hour gap, which they referred to as G_2 , between the end of DNA synthesis and the onset of mitosis. Given that the intermitotic interval of these cells was 30 hours, and the process of mitosis occupied about 4 hours, they further deduced that there was a 12 hour gap, G_1 , between the end of mitosis and the beginning of a new S phase, by subtraction of the sum of S, G_2 and M from the 30 hour total cell cycle time. The model of the cell division cycle which they proposed was thus a progression from one mitosis to the next through the phases G_1 , S and G_2 in that order:

Figure 1: Model of the cell division cycle as derived by Howard & Pelc (1953)



The only subsequent addition to this model came from the work of Lala and Patt (1968), who studied the cellular DNA content of populations of Erlich ascites tumour cells. They showed that whilst the number of cells with a DNA content of G_2 cells (ie twice that of non-dividing cells) was consistent with that predicted from the Howard and Pelc model, the proportion of cells with G_1 content was higher than expected. This gave rise to the concept that there was a compartment of cells with this DNA content which was not contributing to cell proliferation within the population. These came to be called G_0 cells. It is fortuitous in retrospect that Howard and Pelc chose a cell

population in which all cells were dividing so that there were few if any G_0 cells. The concept that cells produced at each mitosis could either commit themselves to a further division (as G_1 cells), or withdraw from the cell division cycle (as G_0 cells) was entirely abstract until quite recently, when the molecular mechanisms driving cell division have begun to be unravelled.

Section ii: Kinetic description of the cell cycle

Having derived a model of the process of cell division, it became possible to describe mathematically the interrelationships between the parameters describing it, and so derive the values for those which are not directly measurable. The following summary is based upon the work of Steel (1977). The very simplest type of cell population is one where every cell is dividing, doing so with the same total cell cycle time (T_c), and where every daughter cell in turn survives to divide. The rate of growth of cell number will be determined by the length of each cell cycle, with the population size doubling with an interval of T_c (that is, the doubling time, $T_d = T_c$). Growth will be exponential, and the number of cells at any given time, N_t , is related to the number at time zero, N_0 , by the equation:

$$N_t = N_0 \cdot 2^{t/T_c} \quad (\text{equation 1})$$

This is a special case of any population growing exponentially, which includes those where the cells do not have the same T_c , where there are a proportion of non-dividing cells, or where cells are being lost from the cell cycle, for which the general growth equation is:

$$N_t = N_0 \cdot \exp(bt) \quad (\text{equation 2})$$

where b is the growth constant ($b \cdot N_t$ is the rate of growth of the population at any given point in time). Equation 1 is given by putting:

$$b = \ln 2 / T_c \quad (\text{equation 3})$$

Tumour populations are subject to cell loss, and not all cells within them are dividing. Populations in which not all cells are taking part in the cell division cycle can be described in terms of the number of proliferating daughter cells produced by each mitosis, α , where the previous case has $\alpha = 2$, or in terms of a growth fraction representing the proportion of dividing cells in the population, which is equal to $\alpha - 1$. Growth is then given by equation 2 with:

$$b = \ln \alpha / T_c \quad (\text{equation 4})$$

The doubling time in this situation is gained by putting $N_t = 2N_0$ and $t = T_d$ in equation 2, which gives:

$$2N_0 = N_0 \cdot \exp\left(\frac{T_d \cdot \ln \alpha}{T_c}\right)$$

Or:
$$T_d = T_c \cdot (\ln 2 / \ln \alpha) \quad (\text{equation 5})$$

Which allows us to rewrite equation 4 as:

$$b = \ln 2 / T_d \quad (\text{equation 6})$$

Accounting for cell loss is more complex, and requires a consideration of the rate of growth rather than just the number of cells in the population. Cell loss can be thought of as the cause of any difference between the actual growth rate of a cell population and the rate at which it would be expected to grow on the basis of the above growth equations, which allow for the fact that not all cells within the population are dividing, but not for cells leaving the population. The rate at which a population would double in size under such conditions, given in equation 5, is referred to as the potential doubling time, T_{pot} , a title presumably chosen to indicate that this represents the 'potential' for the population to grow, were it not subject to cell loss. T_{pot} can also be derived from the cell production rate within the population, K_p . If it is assumed that no cells are being lost in mitosis itself, then this is the same as the rate at which cells are entering mitosis (since each cell entering mitosis can then be assumed to divide into two, so adding one to the total cell population), which gives:

$$K_p = MI / T_m$$

where MI is the mitotic index, the proportion of cells in M phase at any given point in time, and T_m is the length of M phase. The units of K_p are the fraction of cells coming into division per unit of time. If the population is growing exponentially, this implies that the mitotic rate is in constant proportion to the population size. If so:

$$T_{\text{pot}} = \ln 2 / K_p \quad (\text{equation 7})$$

Cell loss is usually expressed as the cell loss factor, \emptyset , the ratio between the number of cells lost per unit time, K_L , and the cells produced per unit time, K_p , that is:

$$\emptyset = K_L / K_p$$

As implied in the first sentence of this section, growth is the result of cell production less cell loss:

$$\text{cell production} - \text{cell loss} = \text{growth}$$

which, in a population of N cells gives:

$$NK_p - N\emptyset K_p = bN$$

Substituting for K_p from equation 7, and for b from equation 6 leads to:

$$\emptyset = 1 - (T_{pot} / T_d) \quad (\text{equation 8})$$

The concept of T_{pot} may seem to be rather unhelpful, but is introduced because it can in fact be estimated in human tumours (vide infra, bromodeoxyuridine), whereas the apparently more concrete parameter T_d is rarely available. Where both are available estimates of the cell loss fraction can be made.

Section iii: Mechanisms of cell loss

It was made clear in Section ii that cell proliferation is only one side of tumour growth, which is also determined by the rate of cell loss from the tumour cell population. In fact, to presage one of the results of the current work, cell loss is far more important in controlling the overall rate of tumour growth than is cell proliferation. We need then to consider at least briefly what we mean by cell loss in this context. In terms of the models of population growth presented above, a lost cell is one which neither enters G_0 or a further round of cell division. It has either left the cell population by migration, or it has lost viability. The latter can happen in two ways- the cell may become necrotic or apoptotic. Necrosis is an ancient pathological entity whereby cells are 'killed' by external forces (eg hypoxia) and digested by a combination of their own enzymes and macrophages. Apoptosis is a more recent concept (Kerr et al, 1994 is a good recent review). It refers to a process whereby the cell apparently 'decides' to die, that is it is an internally determined event, rather than one decided by external forces as necrosis is (Kerr et al, 1972). It occurs in normal as well as tumour tissue, including normal breast (Walker et al, 1989), and its rate in experimental tumours is such that it may represent the predominant mechanism of cell loss in this situation at least (Sarraf & Bowen, 1988). It certainly appears to be important in the cell death that occurs after irradiation (Macklis et al, 1992), chemotherapy (Searle et al, 1975), and hyperthermia (Dyson et al, 1986).

Recent research has explored the molecular mechanisms of apoptosis. At least one gene product, *bcl-2* has been found to specifically protect against apoptosis in lymphoid cells (Hockenbery et al, 1990), but its distribution suggests that it functions in this way in many tissues (Hockenbery et al, 1991). It has also been shown that one function of the p53 tumour suppressor gene is to activate apoptosis (Shaw et al, 1992). Another apparent controller of apoptosis is the oncogene *c-myc*, the first gene to be

implicated in inducing apoptosis (Buttayan et al, 1988). This seems at odds with its oncogenic abilities, but its actions are context sensitive, in that in the presence of growth stimuli, it acts as a proliferation transcription factor, but in the absence of such stimuli it acts to co-ordinate apoptosis (Wyllie 1992).

Section iv: Control of the cell cycle

It appears that regulation is effected at a series of checkpoints within the cell cycle, indicated in the figure below. A specific 'signal' is necessary before the cell can pass any of these points.

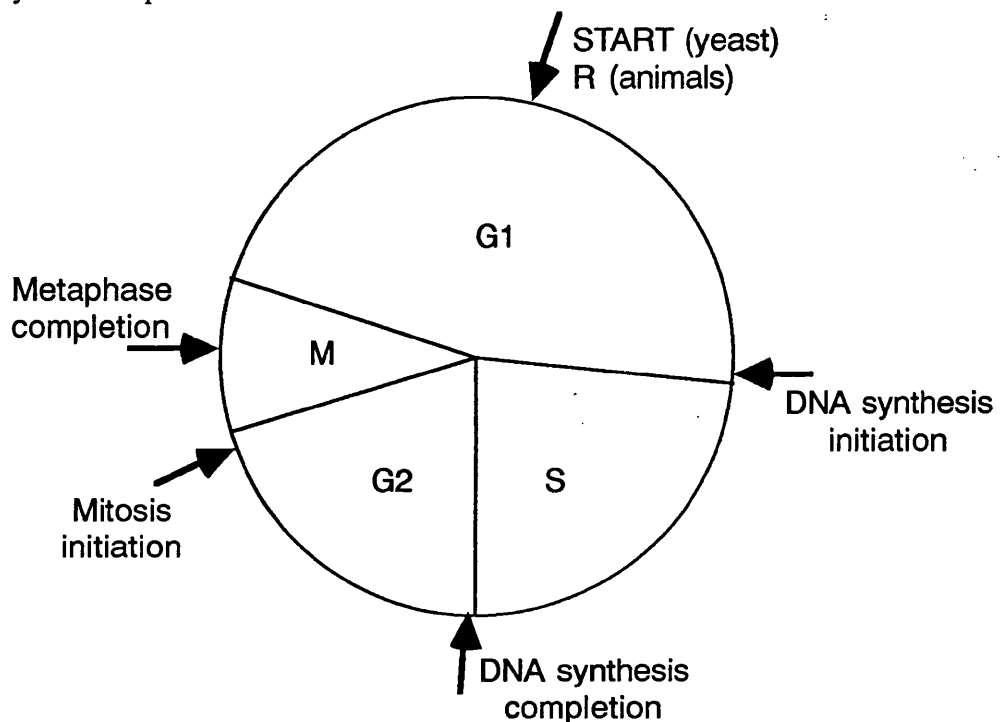


Figure 2: 'Checkpoints' within the Cell Cycle

Passage beyond these checkpoints depends upon phosphorylation of intranuclear substrates, and there exists a class of kinases specifically for this task. This was first discovered in fission yeast, where it was shown that mutations of a gene christened *cdc2* caused cells to stop at two specific points in the cell cycle- at START or at the G2/M boundary (Lew and Reed, 1992). Cloning revealed that *cdc2* encodes a 34kDa serine/threonine kinase, which appears to be the central regulator of cell cycle progression in yeast. *cdc2* is highly conserved in evolution. In animals, however, a number of other *cdc2*-related proteins have been found, the family of cyclin-dependent kinases (CDKs). CDK1 is the member with 100% homology to the kinase domain of *cdc2*.

Self-evidently, CDK *activity* must be cyclical in order to selectively control progress through the cell cycle. This could be achieved by transcriptional control of the kinases

themselves, but in fact their *expression* is non-cyclical. Instead, cyclical activity is the result of three regulators of CDK function: a class of cyclically expressed proteins which bind to the kinases and are essential for their activity, the cyclins (and thus the name of this class of kinases); a group of specific inhibitors of the kinases; and the phosphorylation state of the kinases themselves (at least some cyclins act by causing conformational change when they bind to kinases so as to expose phosphorylation sites). Passage through each checkpoint appears to require some or all of: assembly of a complex of CDK, cyclin and other proteins; CDK phosphorylation; and release of inhibition.

Current indications are that the CDKs and cyclins do not all form strict one-to-one pairings, but rather that some CDKs can bind more than one cyclin, and vice versa. At the time of writing (Nov. 1994), 12 separate proteins with the 100 amino acid cyclin box which contains the binding domain for the CDKs have been isolated, and assigned to 8 classes of cyclin, named A to H, with up to 3 subtypes of each (in the case of the D-cyclins). However, only cyclins A, B, D and E have been assigned fairly definite roles within the cell cycle so far. A similar number of potential CDKs are described, with 7 having at least one known cyclin partner, leading to assignation of a CDK number (CDK7 is unique in not having a cyclin partner. It may act upon the other CDKs, to activate them by phosphorylation of a critical threonine residue (Pines, 1994)).

It was only a year ago that the first indications emerged that CDK function might also be subject to negative control, with the description of two small proteins which appeared to act as CDK inhibitors, p21 and p16 (Serrano et al, 1993; Xiong et al, 1993; El-diery et al, 1993; Harper et al, 1993; Gu et al, 1993; Noda et al, 1993). These have been followed by p15 and p27 (Hannon and Beach, 1994; Polyak et al, 1994; Toyoshima and Hunter, 1994), with no doubt more to follow soon. These molecules appear to act in different ways, and no uniform view of their role has yet been developed, but in each case they bind either to CDK/cyclin complexes to inhibit their activity (eg p27 with the D and E cyclins) or to the CDKs alone preventing complex formation (eg p15 with CDKs 4 & 6). Interestingly, p16 (a negative regulator of D cyclins) appears to be negatively regulated by Rb, which is itself a major target of the cyclin D/CDK complexes. This provides a potential positive feedback loop at the vital R point in the cycle, with D/CDK activation of Rb resulting in reduced p16 inhibition of the D/CDK complex. This class of inhibitors may also represent another point of entry for regulatory signals to the cell cycle control system, p21 having been shown to be transcriptionally upregulated by p53 (El-Diery et al, 1993), and p15 similarly affected by TGF β stimulation (Hannon and Beach, 1994).

Targets for the CDKs are not well characterised other than at the G1/S transition, where CDK2 has been shown to phosphorylate the retinoblastoma protein, pRb, and the closely related p107 (Lees et al, 1991). The role of Rb in controlling cell proliferation has been well studied. It is known to be inhibitory to cell cycle progression in its unphosphorylated form, by binding the transcription factor E2F (Challappan et al, 1991). Phosphorylation by CDK2 leads to dissociation of this complex, with release of E2F and potentially increased transcription from the genes encoding thymidine kinase, *myc*, *myb*, dihydrofolate reductase and DNA polymerase α , among others, which possess E2F binding sites in their promoters.

Section v: Cell cycle response to external stimuli

The ways in which cell surface interactions are transmitted to the nucleus, in order to regulate the cell cycle, have also been elucidated to some extent in recent years. The restriction point in the cell cycle appears to be the major site of entry of signals from the cell membrane. Signalling is currently thought to channel through the mitogen-activated protein kinase (MAPK), which is able to cross the nuclear membrane in its phosphorylated form and acts upon transcription factors such as jun and fos to produce its downstream effects, which include induction of cyclin D (Pines, 1993), and thus passage through the R point. This apparently central role of MAPK may of course simply reflect ignorance of alternative pathways from the cytoplasm to nucleus.

The route from cell surface to MAPK is becoming clear at least in respect of the tyrosine kinase class of cell surface receptors, which are of particular relevance in this thesis. This expanding group of compounds consist of an extracellular ligand binding domain, a short trans-membrane domain, and an intra-cellular domain with tyrosine kinase activity. The paradigm of this group is the receptor for the epidermal growth factor (EGFR). One other member is well characterised, the product of the *c-erbB-2* oncogene (EGFR is also, rarely, known as *c-erbB-1*, and this type I class of tyrosine kinase now extends to *c-erbB-3* & *4*, although these are far less well studied so far). For all of these receptors, ligand binding results in autophosphorylation of the intra-cellular domain. These phosphorylated tyrosine residues create epitopes recognisable by SH2 domains on second messenger molecules (Fantl et al, 1993). These have been shown to include phosphatidylinositol 3-kinase, phospholipase C- γ , and the *ras* complex. *ras* is recruited via the GTP-ase activating protein, which in the setting of EGFR at least seems to join with two other factors, *grb2* and *sos*, in activating *ras*. *ras* then activates the *raf* kinase, which in turn phosphorylates MAPK kinase, the controller of MAPK activity. This apparently linear sequence of events is of course actually taking place in the midst of many other interactions, and does not exist in the splendid isolation suggested by this description.

Chapter 2:

Overview of Methods in Tumour Cell Kinetics

Theoretical understanding of the cell division cycle provides the basis for the rational investigation of the rate of growth of tumour cell populations. The remainder of this introduction considers in detail the theoretical and practical problems associated with the methods developed for this purpose, and reviews the results which have been gained by applying them to the study of human breast cancer. Before going on to this, it is important to ask why it should be of benefit to bother studying tumour cell kinetics at all, and why breast cancer is an appropriate system to use.

Section i: Why Study Tumour Cell Kinetics?

Abnormal growth is a defining, and fundamental, characteristic of a tumour, along with the ability to invade locally and metastasise to distant sites. This alone might be regarded as an adequate reason for wishing to understand the process. In the absence of the ability to intervene in the process of growth, however, the mere capacity to describe it is of limited value. The recent explosion in knowledge about the molecular mechanisms underlying cell division, and about the ways in which tumour cells appear to have subverted the normal controls on division, has opened up the possibility of intervention to obstruct the pathways used by tumours to give them growth advantage over other cells. If this is to be done, it is critical that methods are available to determine which of the many molecular abnormalities within tumours are important in determining their growth rate, as many of the changes seen might be non-functional. What are required are means for determining the rate of cell growth within tumours, to be compared with the abnormalities being studied. Put simply, to determine why tumours grow, you need the means of telling how fast they are doing so.

At a clinical level, even if intervention was not possible, the ability to describe tumour growth might be of some value. It is appealing to hypothesise that rapidly growing tumours will have a worse outlook than those which grow more slowly. That is, prognostic information might be gained by knowledge of tumour kinetics. Prognostication alone is of limited benefit to the patient, but it does make selection of patients for further investigation or therapy somewhat more rational- not inconveniencing patients with very poor outlook who are unlikely to be helped, or conversely not jeopardising the health of people with a very good outlook.

In the case of radiotherapy and chemotherapy, there is a stronger rationale for the use of information about tumour cell kinetics. These therapies are cell cycle dependent in the sense that they target dividing cells by interfering with the process of cell division.

It would seem to be very helpful in planning such treatment to have information as to how many cells within a particular tumour are trying to divide in a given period to time. It is readily apparent that a tumour in which very few cells are dividing is going to be relatively resistant to these modalities, whilst one which provides many targets by having most cells in cycle is likely to be more responsive (and indeed it is an empirical principle that aggressive tumours of poorer intrinsic prognosis respond better to chemo- and radio-therapy). Information as to tumour cell kinetics may be able to help in two ways here- by indicating which patients might be better served by the exhibition of these therapies (McNally, 1989), and also in helping determine what schedules to use in applying them. In this way, cell kinetics might be one way of predicting drug resistance or resistance to radiotherapy.

A good example of the latter point is accelerated radiotherapy protocols (Fowler, 1985; Dische and Saunders, 1990). This form of treatment is based upon the premise that standard radiotherapy protocols, using daily or less frequent fractions, may fail in the case of tumours containing a rapidly dividing cell population because of repopulation of the tumour between fractions. That is, the tumour cells are capable of dividing so rapidly that they are able to make up the cell numbers lost or damaged in each dose of radiotherapy. So-called hyperfractionation involves dividing the total radiation dose into more fractions and giving two or even three fractions per day. The total period of treatment is reduced. The dose intensity is increased, and with it the incidence of side-effects in normal tissues, which repopulate more slowly. The use of this type of therapy therefore depends upon the ability to identify tumours which require this approach, for which the benefits may make this risk worthwhile (Tucker and Chan, 1990). Trials are underway to see if measurement of tumour cell kinetics can indeed predict response to hyperfractionated radiotherapy (Begg et al, 1990; Lochrin et al, 1992).

In summary, there are three major lines of argument to defend the study of methods to measure tumour cell kinetics:

- they are a tool for investigating the biology of tumour growth;
- prognostic information may be gained; and
- they may allow more rational use and scheduling of chemo- and radio-therapy.

Section ii: Why Breast Cancer?

The reasons for using breast cancer as the tumour type in which to explore and extend the application of tumour cell kinetics are also threefold. Firstly, it is now the second commonest non-skin malignancy afflicting females in Western society, having, in the

last few years only, been overtaken by lung cancer. 23,000 cases are diagnosed annually in the United Kingdom, and 13,000 women die of this cause each year in the UK. These figures indicate that assuming a steady state of the disease in the population, 56% of all patients with the disease eventually die of it. Although like most tumours it increases in incidence with age (Haagensen, 1956, p.334), it is by no means rare in young adults, and common in middle-aged women. There is therefore a continuing need to improve our understanding and treatment for this condition.

This is all the more apparent when the prognosis is considered in historical context. If we look at the corresponding figures for incidence and mortality from Haagensen's book (1956, pp. 332-33), in the USA in 1950, there were 18,734 deaths from breast cancer, and the incidence was stated to be 62.2 per 100,000 women. Now there were about 75 million women in the US at that time (Encyclopædia Britannica, World Data Annual for 1992, p. 753), which translates at the given rate of incidence to 46,650 cases per year. The number of deaths is 40% of this, rather than today's 56%. Using historical data of this uncertain provenance is open to many pitfalls, but it does suggest that there has been little if any improvement in the outlook for patients with breast cancer in the last 40 years. It is also worth noting that perhaps as many as 20% of women with *untreated* breast cancer will survive for 5 years anyway (de Moulin, 1989, table 2, p. 90). The quality of life of women with this disease may well have been greatly improved by current treatment, but the quantity may not have increased so markedly.

Finally, and perhaps because of the two points considered already, breast cancer has been widely studied in the past, and most cell kinetic methods have at some stage been applied to it. This provides a substantial body of literature to draw from in assessing the newer techniques which will form the experimental part of this work.

To reduce these arguments to point form, the rationales for the choice of breast cancer are:

- it is a very common tumour;
- the outlook has not improved for many years; and
- it has been well studied in the past.

Section iii: Summary of Methods Available

The techniques available for assessing some aspects of the rate of growth of tumours and/or their constituent cells are listed in table 1. They will be briefly introduced now, and then in the succeeding chapters of the introduction, those which have been applied to the study of human breast cancer will be considered in greater detail.

- 1) *Direct Measurement of Tumour Volume Increase*
- 2) *Measurements of Cell Cycle Distribution*
 - a) Estimation of S Phase
 - thymidine labelling index
 - flow cytometric S phase fraction
 - halodeoxyuridine labelling index
 - b) Estimation of M Phase
 - mitotic index
 - c) Estimation of all In-Cycle Cells
 - Ki-67
 - Proliferative cell nuclear antigen (PCNA)
- 3) *Estimation of Serum Thymidine Kinase activity*
- 4) *Measurements of the Rate of Cell Cycle Transit*
 - a) Halogenated Pyrimidines
 - in vivo halodeoxyuridine labelling
 - dual labelling
 - b) Percent Labelled Mitoses
 - c) Strathmokinetics

Table 1: Classification of Methods used for Studying the Growth of Human Tumours

The most obvious means of studying tumour growth is to simply observe the rate of growth in size of tumours in situ. In order to do this the lesion must be accessible to measurement, and must go untreated for some period of time. These requirements are actually rather stringent, as it turns out.

A rough indication of proliferative activity can be inferred from the proportion of cells in different phases of the cycle. The most readily identifiable phases initially were the S and M phases. If a large proportion of cells are in either of these phases then it is assumed many of the tumour cells are 'in cycle' (ie not in G_0 phase), which will result in an increased rate of cell production if the relative lengths of the various phases are not altered. M phase can be recognised histologically because of the condensation of chromatin at this time, and the formation of a mitotic spindle, although it must be appreciated that these typical appearances are not seen throughout the phase. S phase is recognised by methods which target the process of DNA synthesis that occurs exclusively at this time. This was initially done by the use of a tritiated form of the DNA precursor thymidine, which is incorporated during DNA synthesis or repair through the salvage pathway for pyrimidine bases. Its presence can then be visualised by detection of the emitted radiation. More recently halogenated pyrimidines, which

can substitute for thymidine in the salvage pathway and subsequently within DNA, have found favour instead, as these can be detected using antibodies without the necessity for the use of radioactivity.

S phase cells can also be recognized by their DNA content, which is intermediate between that of non-dividing cells and those in the G₂ or M phases (which have duplicated their DNA). This is achieved by staining cells with fluorescent DNA-binding dyes and flow cytometry, which quantifies the amount of dye bound by each cell nucleus. A frequency histogram of the DNA contents of a large sample of cells is created, and analysed to obtain an estimate of the proportion of cells with the content appropriate to S phase cells. This process is explained in much greater detail in later parts of this thesis, as it constitutes one of the methods examined by this work.

It has only been possible to detect cells in other phases of the cell cycle more recently. This has come about through the development of antibodies to cell cycle specific antigens, that is, to proteins expressed only in cells undergoing cell division (although not necessarily expressed at all times throughout the cycle). The two most widely used antibodies are Ki-67 and PCNA. These can be used as primary antibodies for immunohistochemistry, and the proportion of cells expressing the antigens recognised counted, as a measure of the number of 'in-cycle' cells.

Serum activity of the pyrimidine salvage pathway enzyme thymidine kinase is indirectly related to the amount of proliferative activity of tumours, in that the TK1 isoform of this enzyme is present in high concentration in dividing cells, but is absent in G₀ cells (Bello, 1974). The fact that tumours represent a large mass of dividing cells led to the hypothesis that elevated levels of TK might be present in the serum. This was demonstrated to be the case in animal models (Taylor et al, 1981; Kreis et al, 1982), and extended to human tumours by a group in Northern Ireland (O'Neill et al, 1986, 1987), including breast cancers (McKenna et al, 1988). Although potentially, the level of TK could be a measure of the amount of proliferative activity occurring within a tumour (allowance being made for tumour mass), this does not seem to have been pursued, and initial responses did not confirm the Irish findings (Calvert and Satchithanandam, 1989).

All of these methods are static in the sense that, whilst they provide information as to the cell cycle distribution of cell population, they do not give any indication of the rate of progress of cells through the cycle. Only with this additional information can calculations be made to estimate such parameters as the cell production rate or potential doubling time. The first method developed in an attempt to gain this type of data was the percent labelled mitoses technique (Steel, 1977; chapter 4). To do this, S phase tumour cells were point labelled (this being a historical method, this was done with

tritiated thymidine, the only label available at that time). The tumour was sampled at intervals thereafter, and the proportion of mitotic figures which were labelled with the thymidine counted. Theoretically, if the labelled S phase cohort passed through the cycle in concert, successive waves of labelled mitoses would be seen at an interval which corresponded to the total cell cycle time (figure 3). In reality the labelled cells progress at different rates, and so spread out in the cycle within a few rotations, a process referred to as damping. Mathematical models can be used to estimate the total cell cycle time from the damped graph. The percent labelled mitoses method was never widely used in human tumours *in vivo*, because of the need to administer a radioactive DNA precursor, and has never been used in human breast cancer to my knowledge; it is not discussed in the following chapters for this reason.

Although this problem could now be overcome by using halogenated pyrimidines, this does not get around the need to take many tumour samples. However, a method using halogenated pyrimidines as label, but requiring only a single subsequent tumour sample has since been developed (Begg et al, 1985). This method was developed using the pyrimidine bromodeoxyuridine. After point labelling, it is presumed that all S phase cells will have taken up the agent. A biopsy specimen is then taken some hours later, and stained for bromodeoxyuridine content, and for total DNA content. Flow cytometry allows each of these parameters to be measured in many cells. From the DNA content of the labelled cells, which phase they are in can be assessed, and so their progress in the cell cycle since they took up the bromodeoxyuridine can be measured. This value for 'distance' travelled can be divided by the time between labelling and biopsy to estimate velocity. The actual parameter obtained is the length of S phase in hours. A labelling index is also obtained, and the two can be combined to estimate the potential doubling time. This method is covered in detail in future sections of the manuscript.

It is also possible to obtain dynamic data from a single biopsy by using multiple labels. This can be done by using more than one halogenated pyrimidine, or a combination of one such with tritiated thymidine, since one of the labels can be incorporated *in vitro*. So for instance, bromodeoxyuridine could be administered as just described, and the subsequent biopsy labelled *in vitro* with iododeoxyuridine. The proportion of cells stained with each of the labels alone, and the proportion double labelled are counted. The proportion of S phase cells is given by the iododeoxyuridine labelling index. Presuming that not enough time was allowed for cells to complete a whole cycle and re-enter S phase, the dual labelled cells are those which have failed to complete S phase between the two labelling events. This allows determination of the number of S phase cells and the number which have left that phase in a known period of time, from which the length of S phase is easily calculated (Hoshino et al, 1972; Shibuya et al, 1993).

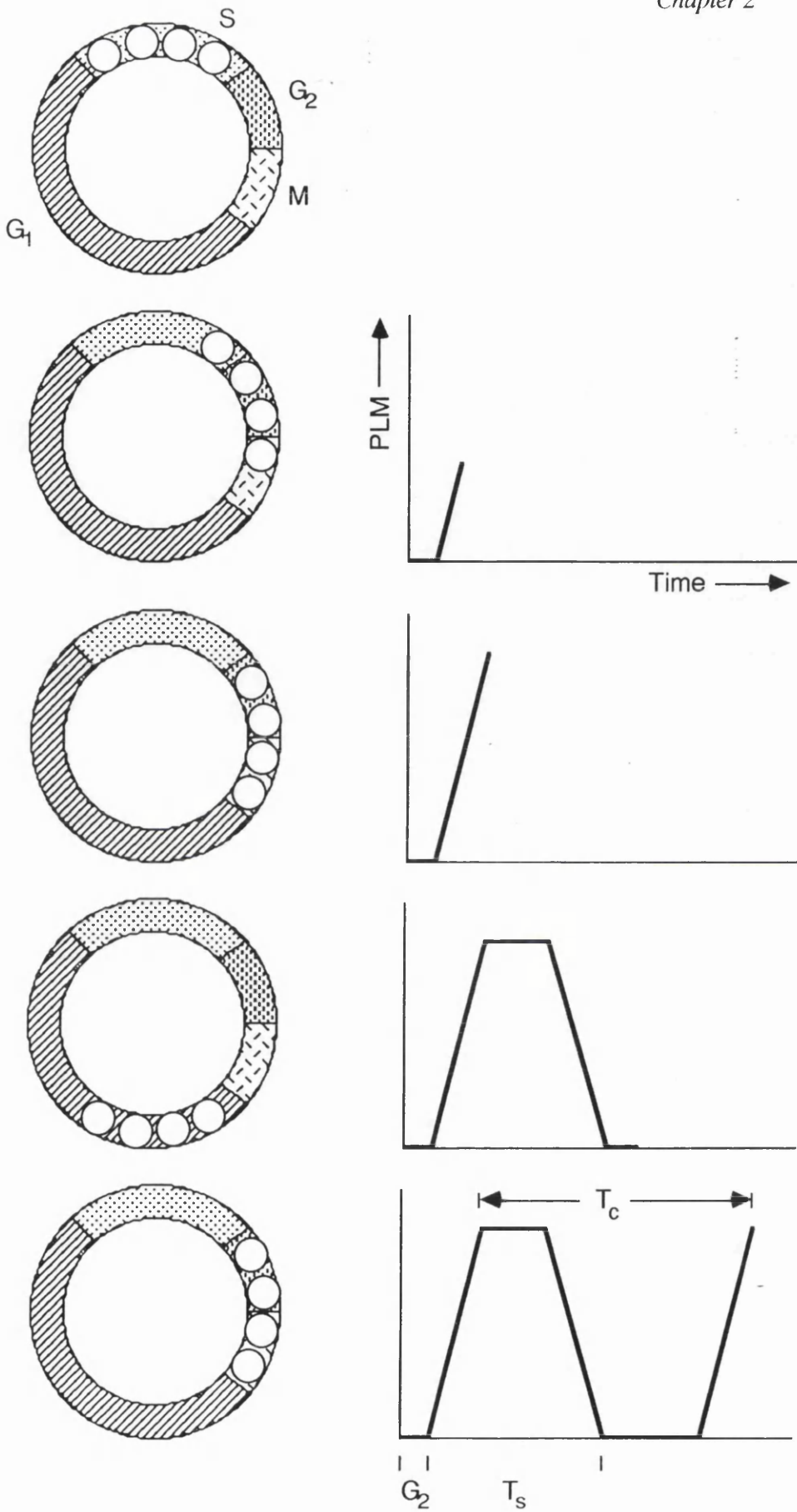


Figure 3: Principle of Percent Labelled Mitoses (PLM) Technique, following the fate of an H3-thymidine labelled cohort of cells (white balls) alongside a plot of the proportion of labelled mitoses at each stage.

A further method for gaining dynamic cell cycle information is the strathmokinetic technique (Steel, 1977, p.88 et seq). This utilises the ability of the vinca alkaloids and colchicine to cause cells to arrest in metaphase, where they are easily recognisable. For the method, vincristine is given, samples are taken at several times thereafter, and the number of mitotic figures in each sample is counted. The number of mitotic figures is plotted against time, and the slope of this line gives the rate of accumulation of cells in M phase. If it is assumed that all cells survive this phase normally, then the rate of entry to M phase is equal to the cell production rate of the population. The problems in applying this to human cancer are familiar- the need to give a mitotic poison, and to take multiple samples, rules it out as an *in vivo* technique. It can be used for tissue samples in culture, and in the study of gastro-intestinal crypts, but like the percent labelled mitoses method, it has not been applied to human breast cancer.

Even dynamic cell kinetic methods still only provide information at one point in time, and are uninformative as to the rate of cell loss from the population (unless the action tumour growth rate is known, when cell loss can be inferred from the difference between potential and actual doubling times). Furthermore, the ability of any cell kinetic measurements to predict patient outcome is limited by the fact that it is metastatic behaviour which ultimately leads to death in nearly all cases, and so kinetics only provide prognostic information in as far as they are linked to the metastatic phenotype. These are still unresolved shortcomings of the current state of the art in measuring tumour cell kinetics. Following on from this overview of cell kinetic theory and methodology, the next section commences the more detailed review of the information gained in the case of breast cancer. We begin with the measurement of *in situ*, whole tumour growth rates.

Chapter 3: Review of Static Methods Applied to Breast Cancer

Section i: Direct Measurement of Tumour Growth

In vivo observation appears to be the simplest and definitive measurement of tumour growth. Unfortunately, this type of information is rarely available. There are at least two reasons for this. Firstly, the calculation of growth rate relies upon at least two measurements being made at different time points, and if the information is to be related to the natural history of the tumour it follows that the lesion must be untreated for the interval between these measurements. Most tumours are not left untreated for a length of time adequate for this purpose. Nevertheless, sometimes this does happen because the patient is unfit for or refuses treatment. Another source of information comes from mammographic studies, where a tumour has been overlooked on one examination (but is visible and measurable in retrospect) and subsequently detected on another. The second reason for the rarity of direct tumour growth measurements is that the tumour needs to be accessible for and amenable to the process of measurement itself. That is, it must be well defined in its extent, superficial and non-tender if it is to be sized by clinical examination, or in a site favourable for radiological delineation.

Quite apart from the difficulty of finding suitable cases, the process by which tumour growth is calculated from clinical or radiological measurements is suboptimal. Obtaining a point estimate of tumour volume is problematic. True volume can of course only be obtained by removing the tumour. *In vivo* estimates are made on the basis of measured diameters. If a tumour were perfectly spherical, then volume could be accurately deduced on this basis from a single diameter, d , as $V = (\pi/6) \cdot d^3$. Tumours are not spherical, unfortunately, and the next best estimate comes by taking 3 diameters at right angles to one another (d_1 , d_2 and d_3) and calculating $V = (\pi/6) \cdot (d_1 \cdot d_2 \cdot d_3)$. Even then, whilst two diameters are often available the depth of a lesion being measured clinically is not easily obtained. Similarly, most imaging investigations are two dimensional, and so unless images at right angles have been taken, only two diameters will be gained. With only two dimensions to work from the calculation of volume is even more approximate.

Accepting the shortcomings of individual volume measurements, accurate calculation of growth rates would best be achieved by multiple observations at different time points, when an appropriate growth curve could be fitted mathematically on the basis that errors will be randomly distributed. In other words, the reliability of growth measurement increases with the number of size determinations upon which it is based (Steel, 1977, p. 41). It will be readily appreciated however that in most cases only two

or three observations are made. Furthermore, it was pointed out in the last section that human tumour growth is not constant, but rather slows with time as a result of increasing cell loss. Calculated doubling time is thus dependent upon the stage of the natural history at which it is being measured. Only if multiple time points are studied can a Gompertz curve be fitted in order to make allowance for this. There is a general point here, in that all observations are being made upon tumours in a very late stage of their natural history, and this applies to all studies of *in vivo* tumour growth. If it is assumed that a single cell weighs about 10^{-9} g, then it requires about 30 doublings before it achieves a clinically observable size of 1g (and tumours in many sites may not be apparent until they are substantially larger than this). Most tumours prove lethal at a total tumour burden of the order of 1kg, which is only 10 further generations. That is, only the last quarter of the lifespan of a tumour is clinically evident, in terms of doublings, although it must be remembered that the doubling time increases with the age of the tumour, so that these last 10 doublings will occupy more than one quarter of the lifespan of the tumour in terms of time:

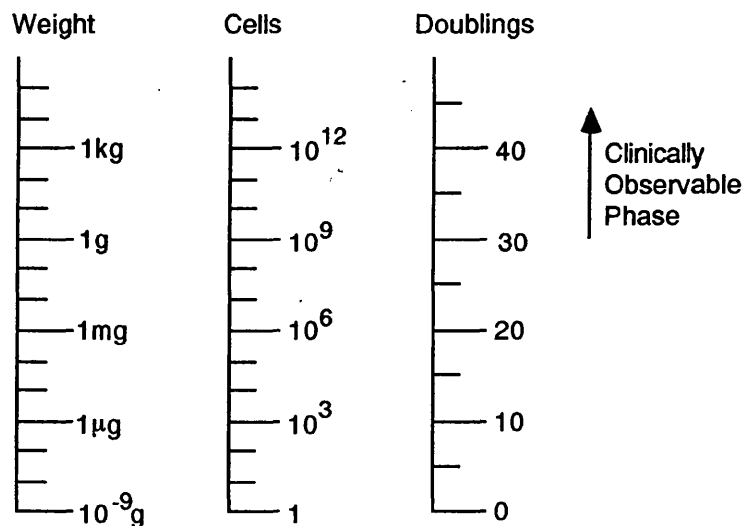


Figure 4: Relationship between tumour age (in terms of number of doublings) and tumour size (in terms of weight and number of cells).

The direct observation of tumour growth can be seen to be neither as simple nor as definitive as first imagined. Nevertheless, there is no other source of information about actual tumour doubling times. The published data for breast cancer is of several kinds—data based upon tumours missed in one mammogram and subsequently detected on another, data based upon the growth of recurrences in the scar from a mastectomy, data based upon serial observations of untreated primary tumours, and data inferred from the history of the illness in the patient.

Gershon-Cohen and his colleagues in Philadelphia, who were strong early proponents of mammography as a diagnostic tool in breast cancer, were also the first to gain

experience of tumours visible in retrospect on previous mammograms of cancer sufferers (Gershon-Cohen et al, 1963). They calculated tumour volumes on two to six occasions, using the area (A) of the tumour on each mammogram and applying the formula $V = 0.75 \times A^{3/2}$. This assumes that the unknown diameter of the tumour is equal to the average of the other two. The interval between observations was from 4 to 54 months, with the not surprising corollary that no growth was observable in one such case with an observation period at the lower end of this range. Tumour doubling times were calculated on the basis of simple exponential growth, which is reasonable for short observation times but not for longer ones where Gompertzian retardation might be significant. The doubling times which they presented were from 23 to 209 days (mean 115 days).

A larger series of 147 cases was published by Fournier et al (1980). They had an observation interval of 2 months to 11 years, with an average of 27 months, during which time the patients had between 2 and 11 mammograms. How many of the observation intervals fell at the lower end of the range is not stated. Derived tumour doubling times were from 44 to 1869 days, with a mean of 212 days. Volumes were calculated from 3 diameters measured from a single view, but the equations used for this transformation are not stated. Doubling times were probably estimated by fitting of a Gompertz curve, but what was done in the half or more of cases with only 2 mammograms is not clear. These authors made the point that the estimation of the size of a mammographic shadow was subjective and interpretation varied from one observer to another. They also discuss the assumption that the visible shadow corresponds to the size of the tumour, since it may be that the margin of the shadow consists of stromal reaction around the tumour, or conversely that the tumour margins extend invisibly beyond the visible abnormality. Details are provided of results obtained from 6 serial mammograms of one lesion over a 5 year period, which resulted in estimates of T_d varying from 80 to 193 days, with no clear trend for doubling time to get shorter or longer over this interval. Rather, this would appear to indicate the imprecision of the method.

Spratt et al (1981) reported the doubling times of 32 tumours based on serial mammography. The observation intervals varied from 3 to 24 months, and doubling times appear to have been based on 2 measurements only, with an assumption of exponential growth. Volume was calculated from 2 diameters on a single view, using a spheroidal model of tumour shape. 9 tumours with relatively short periods of observation did not grow during this study. The remaining 23 tumours were reported as having doubling times of between 109 and 944 days, with a median of 324 days. Only 7 of the 23 tumours with observable growth had a doubling time of less than 200 days, the longest reported by Gershon-Cohen et al.

The only recent study of this type was published by Arnerlöv et al (1992), who made measurements in 158 screen detected cancers which were retrospectively visible on a previous mammogram. Doubling times were calculated on the basis of a single diameter from two films taken 2 to 94 months apart. They state that tumours were presumed to be spherical in shape, but the assumed model of growth is not given. 11 tumours demonstrated no growth during the period of observation, but insufficient data is presented to determine whether these were tumours with a short interval between the two films. In the 147 cases with measurable growth, they found a median doubling time of 9 months, with a range from 0.6 months to 96 months. The modal group was below the median, at 3-6 months. They found that tumours with above median growth rates were more common in stage II tumours than stage I lesions (because this was a study of screen detected cancers, all but one tumour was in these two stages, and in fact 68% were stage I). They also performed DNA flow cytometry upon the tumours in this series, and calculated the tumour S phase fraction (SPF) from the resultant histograms. This is the only attempt among all of the papers looking at actual doubling times to correlate this with any measurement of tumour cell growth rates. They found that aneuploid tumours were significantly more likely to show rapid growth, and that rapidly growing tumours had a significantly higher mean SPF:

Ploidy	Doubling Time (months)			
	0-3	3-9	9-48	48+
Diploid	3	18	24	10
Aneuploid	17	36	39	3

Chi-square = 13.49, df = 3, p = 0.004

	Doubling Time (months)			
	0-3	3-9	9-48	48+
Mean SPF (%)	17.8	11.5	9.0	6.2

p = 0.001 (original authors' t test)

Table 2: Data from Arnerlöv et al 1992) relating tumour ploidy and S phase fraction to observed doubling times

The rate of growth of mastectomy scar recurrences is calculated on the basis that they have presumably arisen from one or very few cells at or about the time of that operation, although Brown et al (1987) have provided complex statistical evidence that the number of initiating cells is of the order of 60,000 (this is still a very small lesion, with a mass of <100µg, but represents 16 doublings of a single cell, sufficient to entirely invalidate this approach). If however the paucicellular origin is accepted, it

provides V_0 for use in a growth equation. In all cases calculation has been based on only one later observation (at the time of extirpation of the recurrence), which means again that only a simple exponential can be fitted, without allowance for Gompertzian growth. It must also be borne in mind in assessing this type of report that the growth of a tumour recurrence is occurring in a different milieu to that of the primary tumour, and represents a self-selected cellular sub-population which may have growth characteristics atypical of the original tumour. Phillippe and Le Gal (1968) calculated growth rates of 78 nodules selected as not being ulcerated or showing histological evidence of necrosis. They found doubling time to range from 3 to 211 days, with a mean of 78 days. The distribution of doubling times was bimodal, with peaks at 25 days and at 93 days, suggesting the possibility of two different types of nodule of fundamentally different biology. This type of distribution is not apparent in other studies. The other study based on scar recurrences (Pearlman 1976) specifically refutes this concept, finding instead that doubling times are log normally distributed (like most biological characteristics). Pearlman studied 82 cases, apparently unselected. T_d was calculated in exactly the same way as Phillippe and Le Gal. The range of calculated values is not stated, but from his figure 3 appears to be from 3 to 170 days with a median of about 26 days.

Anecdotal evidence as to the clinical rate of growth of breast tumours was given by Richards (1948), who stated that the average breast cancer grows by 1cm in diameter every 3 months. What measurements may have led to this statement are not given or hinted at. More assessable data is presented by Kusama et al (1972), who documented the growth of 212 tumours in 199 patients with breast cancer. In 163 cases these observations were made upon primary lesions, and in another 49 cases upon a mixture of local recurrences, involved lymph nodes, pulmonary and other metastases. The interval over which observations were made in each case are not given, but it is stated that if no growth was observed over a period of one month or more, the doubling time was taken to be infinity. Some intervals were very short indeed, and given the inaccuracy of clinical measurement of these lesions, it is not surprising that growth could not be detected. Volume change was calculated from change in a single diameter, and doubling time was taken as one third of the diameter doubling time (in fact $T_d = 3/8 \times$ diameter doubling time, so that this approximates $3/8 = 1/3$). This method assumes that volume doubling is reflected in equal expansion in all dimensions, which is probably reasonable in breast and lung where there is little physical constraint on growth in any direction. They also note that some initial observations were made before referral to their centre, so that the initial and later diameters were measured by different people, which in this distinctly subjective field is clearly not optimal. Lesion by lesion growth rates are not stated, the most basic data provided being a breakdown

of doubling times by intervals of one month, with all tumours having a doubling time of over 10 months being grouped together. The median T_d is given as 3.5 months (105 days) with a range of 0.2 to 18 months (6 to 540 days). They state that there is no significant difference in the median doubling time of primary and secondary tumours, although the median for primary tumours is lower. The raw data to check this are not presented, but from their table 1 it is possible to perform a chi-square test to examine the null hypothesis that there is no difference in the growth rate of primary and secondary lesions within the total study group. Doing so gives $\chi^2 = 14.884$, $df = 4$, $p = 0.0049$, rejecting the null hypothesis, contrary to their assertion. Examination of the distributions indicates that the trend is as they have indicated, in favour of faster growth in secondary tumours.

The final technique which has been used to assess the rate of growth of primary breast cancers is to note the history of the disease in the patient. Commonly, the size of the lesion is correlated with the length of time since any abnormality was first noted by the patient. Those with clinical experience in the area of breast cancer will have met many women with fungating tumours which they claim have only been present for a matter of weeks, and realize that the patient's history is a poor guide to the period that symptoms have been present. Notwithstanding this argument, slower growing tumours as defined in this way have been reported as having a better prognosis (Collins et al, 1956). A similar approach was described by Charlson and Feinstein (1980). This was based on the interval between the first abnormality noticed by the patient and the time of definitive treatment, modified by the occurrence of disease progression during this interval. This could well be considered to represent a measure more of treatment delay than of tumour growth, or equally of a process whereby good prognosis tumours have been self selected by making no demand upon the patient's attention. They demonstrate that what they regard on this basis as slow growing tumours have a better prognosis in a sample of 685 patients with all stages of disease, but this was not subjected to multivariate analysis. A similar study was reported by Boyd et al (1981), who also found that this type of information correlated with prognosis in a series of 756 patients with early breast cancer, slow growing tumours having a better outcome. In this report, auxiometric classification was a less powerful predictor than nodal status, tumour size or histological grade. No multivariate analysis was reported. It is difficult to assess the relevance of these results to a discussion of tumour growth rates.

The information provided in these different ways about the growth of breast tumours is summarised in the following table:

First Author	Method Used	Cases	T_d (days)	
			Mean	Range
Gershon-C. (1963)	Mammography	18	115	23 - 209
Phillipe (1968)	Scar Recurrence	78	40	3 - 211
Kusama (1972)	Direct Measurement	212	105 ¹	6 - 540
Pearlman (1976)	Scar Recurrence	82	26 ¹	3 - 170
Fournier (1980)	Mammography	147	212	44 - 1869
Spratt (1981)	Mammography	23	324	109 -944

Table 3: Summary of information about actual tumour doubling times from various means of observation of *in vivo* breast tumour growth. 1 = median value

From this review we can summarise that there is relatively scant information as to the growth of breast tumours (only 400 primary breast cancers accumulated in the course of over 40 years of study). Estimates of the mean doubling time for primary tumours in their (late) clinically detectable phase vary from roughly 100 to 300 days. The only two studies of secondary lesions, based upon scar recurrences, give doubling times well below this. The growth of local recurrences thus appears to be faster than that of primary lesions. This has to be interpreted with some caution, as it is based on measurements made by a different method from primary tumours. It must also be taken into account that recurrences are growing in a different environment from primaries. Putting these factors aside for a moment, this observation suggests that either tumour populations grow more rapidly as they evolve and acquire genetic abnormalities, that recurrence represents a process of clonal selection of more rapidly proliferating cells, or that proliferation is favoured by lower tumour size (ie is Gompertzian) given that secondaries are being studied at the beginning rather than the end of their growth curve.

Section ii: Use of the Mitotic Index

Mitotic figures are cytologically identifiable on routine histological preparations, and pathologists have often sought to classify tumours by the number of mitoses identified, as being of low or high mitotic index. There are a number of pitfalls to this approach. Firstly, whilst nuclei in metaphase and anaphase are easily recognizable, mitotic figures in prophase and telophase are not so easily discerned (Steel, p. 87). The proportion of cells in a given population counted as mitotic will thus depend upon the quality of the preparation of the specimen and the experience of the observer. This has important consequence for the use of this parameter as a measure of cell kinetics, as the mitotic index depends upon the rate at which cells enter into mitosis (which is the real kinetic measurement being estimated) and the length of time that they spend in it, the

latter depending upon the period for which they are recognisable as being in mitosis. If this varies from one observer to another and from one preparation to another, this undermines the use of the mitotic index to estimate the rate of entry of cells into mitosis, which is based upon the presumption that the length of mitosis is essentially constant.

Secondly, if the process of fixation of the cells is not prompt, then entry into mitosis is arrested before exit from mitosis during warm ischaemia (Bullough 1950). This will reduce the number of cells in M phase. Such delays in fixation are not uncommon in the routine processing of pathological specimens. Thirdly, there is a potential geometric artefact in the assessment of mitotic index, because mitotic nuclei are larger than those in other phases of the cell cycle. The chance of such a nucleus being included in a given tissue section are thus higher than that of its smaller neighbours. If the section thickness is of the same order as the average nuclear diameter, this produces a significant bias in favour of mitotic nuclei in an uncorrected count. This was pointed out by Abercrombie (1946), who provided a correcting formula based upon the section thickness and the diameter of the respective types of nuclei, but this has very rarely been applied since. The final problem with the mitotic index is that because very few cells are observed at any point in time to be in mitosis, a very large number of cells need to be counted in order to obtain a statistically reliable estimate of the index. It has been shown for the counting of S phase cells that the measured index of cells in that phase becomes stable at about 2000 cells counted (Going, unpublished observations). This was done by plotting the estimated index after each 100 cells counted, and seeing how long it took for the initially large variations to settle down to a stable value for the proportion of labelled cells. Since the length of S phase is four times that of M phase, one would predict that 8000 cells would be required for a valid estimate of the mitotic index. This would represent a wearisome task indeed, especially whilst maintaining a rigorous system for assuring the at least semi-random choice of fields to be counted, so as to avoid any selection bias (there is an innate tendency to choose fields with a high proportion of labelled cells). Notwithstanding all of this, the mitotic index has been shown by many authors to be a statistically significant, independent, prognostic factor in breast cancer (Stenkvist et al, 1982; Baak et al, 1985; le Doussal et al, 1989; Joensuu et al, 1990; Clayton, 1991; Aaltomaa et al, 1992).

Section iii: Staining for Cell Cycle Specific Antigens

Only cells in the mitotic phase of the cell cycle are recognisable as such in routine histological sections. The problems due to the different size, and relative rarity of M phase cells have just been discussed. Stains which recognise cells in other phases have been sought for some time, and this ambition has in the last decade been realised. These use immunohistochemistry to identify the presence of proteins whose

expression is cell cycle dependent. The two commonly used sets of antibodies are not specific for cells in any one phase of the cell cycle, but rather the proteins recognised are expressed from G₁ through to M phase. They provide an estimate of the growth fraction of the tumour, that is the proportion of cells which are actively engaged in the cell division cycle, as opposed to those in G₀ phase. These two antibody groups are directed at antigens which have been named Ki-67 and PCNA.

Ki-67 was raised from mice immunized with nuclear extract from lymphoma cells (Gerdes et al, 1983), and found to recognize an epitope expressed from mid/late G₁, through S and G₂, to M phase (Gerdes et al, 1984). It proved to be difficult to clone the gene for the Ki-67 product in full although this has now been achieved in part (Gerdes et al, 1991). A major drawback with the initial antibodies to Ki-67 was that they only recognised the epitope in unfixed tissue sections. Newer antibodies have overcome this problem, and work in formalin-fixed, paraffin-embedded sections (Key et al, 1992).

PCNA has the same ability to recognise its epitope in fixed and embedded sections, and so was initially used as a Ki-67 substitute when this was the available material for study. The PCNA antigen is better characterised, and has been cloned in full (Almendral et al, 1987) and is known to be a 36kDa auxiliary protein to DNA polymerase δ (Bravo et al, 1987). It is in fact the autoantibody produced by patients with systemic lupus erythematosus (Miyachi et al, 1978). Although cell cycle regulated, it has been shown the PCNA gene can become deregulated in human solid malignancies, specifically including breast cancer (Hall et al, 1990). This could result in non-cell cycle related expression under these circumstances, such that the antigen was no longer a marker of cell proliferation. Certainly it has been noted that there is marked variability of data related to the fraction of PCNA positive cells in human tumours (Lipponen and Eskelinen, 1992), who suggested that this might be the result of variable sensitivity of detection systems used by different groups, or the use of different scoring systems; another suggestion has been that different antibodies to PCNA give different results (Leonardi et al, 1992). These are arguments which apply equally well in comparing data from different groups using Ki-67 as well. In addition, whilst the use of these antibodies avoids the two problems with mitotic index referred to in the first paragraph of this section- the size bias, and the paucity of M phase cells, some of the other problems associated with that method remain. In particular, the selection of random fields, and counting of an adequately sized sample of nuclei are not always indicated in reports of tumours studied in this way.

A large number of reports show staining indices for both Ki-67 and PCNA to be predictive of outcome in breast cancer, and to correlate with pathological prognostic

factors for the disease (eg in respect of Ki-67 Barnard et al, 1987; Bouzabar et al, 1989; Wintzner et al, 1991; and Veronese et al, 1993; and for PCNA Dawson et al, 1990; Shrestha et al, 1992; and Aaltomaa et al, 1993). It must be noted that in the case of PCNA not all authors have been able to achieve such results, finding no evidence of such correlation (Leonardi et al, 1992; Noguchi et al, 1993), or conflicting results (Betta et al, 1993). The majority of authors who have looked at both in the same tissues have concluded that the two give well correlated results. Assessing this claim more closely, Dervan et al (1992), for example, studied 46 tumours and normal tissues and achieved a Pearson correlation coefficient of 0.8. If we take the raw data from table 1 of their paper, and divide the tissues as above or below the median value for each index, then 6/46 (13%) appear in different groups with respect to the two stains (ie they are above median for one and below median for the other). If the distributions are divided into quartiles, then 13/46 (28%) are classified differently by the two antigens. This is not as good as the simple rank correlation value alone would lead one to believe. This bears out the recent statistical belief that the correlation approach is not an appropriate one for this type of problem (vide infra, Statistical Methods section in chapter 5).

Section iv: Thymidine Labelling Index

Identifying S phase overcomes some of these problems, as S phase is relatively longer, the nuclear size is the same as other phases (except M phase), and because methods have been developed which more clearly identify these cells. The first such method to be developed involves the incorporation of tritiated thymidine, which is taken up and incorporated into DNA by cells in S phase (although thymidine is a normal component of DNA, it is not a normal component of the DNA synthetic pathway, but the enzymes for its use are universally distributed). Due to the long half life of tritium and the potentially damaging effect of radiation upon DNA, it has not often been accepted as ethical that tritiated thymidine be given to patients in order to study its *in vivo* incorporation by tumour cells. Instead, tumour explants are incubated in short term tissue culture in the presence of thymidine and hyperbaric pressures of oxygen (which maintains the metabolic activity of the outer 500 μ of the explant, Fabrikant et al, 1969). Uptake is detected by taking tissue sections of the explants after incubation and coating these with photographic emulsion (figure 5). These are exposed for a period of several weeks, and nuclei which have taken up the thymidine (that is, those which were in S phase during the incubation) are recognised by the presence of developed silver grains overlying them. The number of such nuclei as a proportion of all tumour nuclei is counted. This figure is termed the thymidine labelling index (TLI).

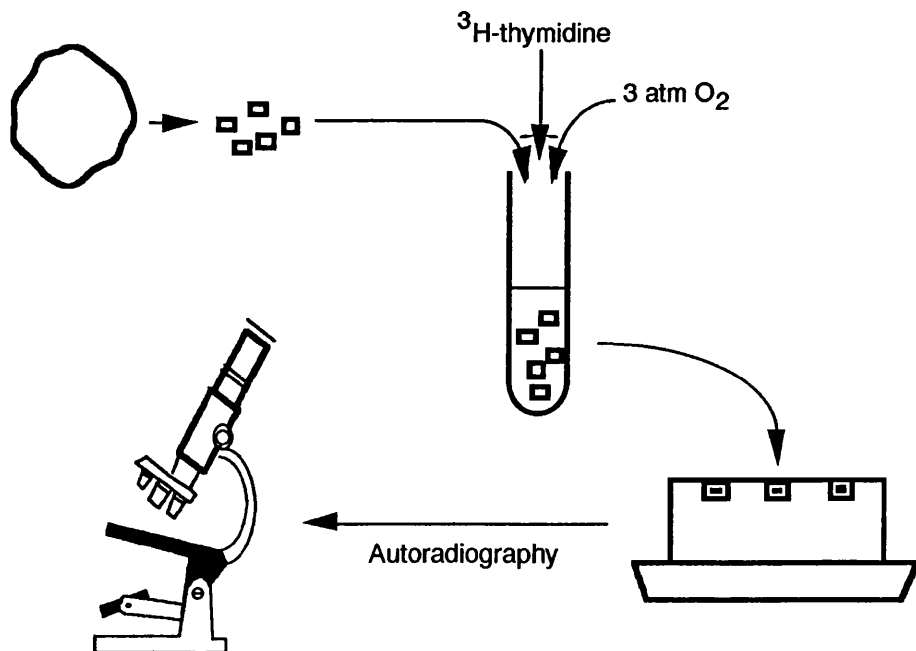


Figure 5: Summary of the thymidine labelling technique

Whilst this measurement overcomes some of the problems associated with mitotic indices, it must be remembered that in contrast to them it is based on the behaviour of tumour explants in short term tissue culture. The results for an individual tumour may

not represent the kinetic behaviour of that tumour when it was in situ. It is also important to ensure that counting is performed in a truly random fashion, as otherwise there is a tendency for the observer to count on well labelled fields. This is best achieved by the use of a grid system, counting randomly chosen grid locations, but this is difficult to apply in a situation where not all of the section is suitable for counting because some of it will represent anoxic areas. This means that a degree of subjectivity is required in determining which regions have been adequately incubated, and this can easily introduce counting bias.

TLI was first applied to breast cancer by Johnson and Bond (1961), and since then several groups have published the results of large studies of its prognostic significance. Meyer's group in St Louis was one of the first to embrace this technique. They have now studied tumours from over 500 women followed for a mean of 4.1 years (Meyer and Province, 1988). The median value of TLI in their hands was 5.2%. They have divided the patients into three groups using the tertiles of the TLI distribution (3% and 8%). Actuarial 5 year survival rates (% of patients) in the three groups were:

TLI	Nodal Status	
	Negative	Positive
≤ 3%	89	79
3-8%	64	71
> 8%	66	52

Table 4: Actuarial 5 year survival rates (as % survivors) for 500 breast cancers studied by Meyer et al, sub-divided by nodal status and TLI

This result was independent of nodal status, grade, size and oestrogen receptor status in multivariate analysis. It is unfortunate that longer term survival data are not available from this group, and odd that in node negative patients the survival curves for mid level and high TLI nearly overlap, whilst in the the node positive group it is the curves for low and mid level groups which do so. This may indicate that the TLI is less discriminating than such a division suggests, and that a simple cutoff at the median value, as they used in an earlier report (Meyer et al, 1983) is all that is justified.

Tubiana and Koscielny (1988) have reported upon long term follow up (median 15 years) of their 128 patients. They also divided the patients into three groups by TLI, and observed a large and statistically significant survival advantage to patients with tumours having a low TLI. Interestingly, they too demonstrated no survival difference between tumours of intermediate and high TLI (as in Meyer's node negative patients), bearing out the point that TLI appears to be relatively non-discriminating in the sense that it supplies only a high-low answer effectively.

The most active proponents of the introduction of TLI into clinical decision-making have been Silvestrini's group at the Italian National Cancer Institute at Milan. They have now analysed the prognostic value of TLI in nearly 900 patients with breast cancer (Silvestrini et al, 1989, 1990). The median labelling index in their hands is 2.8%, and patients are divided into two above and below this value. Overall 5 year survival figures (%) for each group are:

TLI	Nodal Status	
	Negative	Positive
≤ 2.8%	95	85
> 2.8%	81	73

Table 5: Overall 5 year survival rates for 900 breast cancers studied by Silvestrini et al, sub-divided by nodal status and TLI

These results are statistically significant, and independent of degree of nodal involvement, tumour size, and oestrogen receptor status. However, the survival rate for this group of patients is surprisingly good, with nearly three quarters of women still alive at five years even in the worst prognostic group (node positive, high TLI). This suggests that they may be a selected good prognosis group, and that these results are not necessarily applicable to the general run of breast cancer patients.

Thymidine labelling was also carried out on patients within the Liverpool Breast Cancer Series, from which series the material studied in part II of this thesis was derived. Long term prognostic data were recently published (Cooke, Stanton et al, 1992). Analysis was carried out in January 1st 1990, when the minimum follow up of surviving patients was 93 months. The TLI was measured in 185 tumours by the method of Meyer (Meyer and Bauer, 1975). Fresh tumour was divided into five 2mm cubes, which were added to tubes containing 5 ml of RPMI and 0.2 ml of ³H-thymidine (25 fCi/ml ; SA 44 Ci/mmol). Tubes were incubated in a shaking water bath for two hours at 37°C, at 3 atm produced by addition 10 mls of a 95% O₂/5% CO₂ mixture. Tissue was then fixed in formalin and wax embedded. Five micron sections were mounted on histological slides and Kodak AR stripping film applied. Autoradiographs were exposed at 4°C for 28 days, and counterstained with haematoxylin and eosin.

Labelling was assessed in 2000 nuclei per tumour, four separate areas of 100 nuclei on each of 5 slides. Nuclei were considered to be positive if there were more than 10 reduced silver grains over them, although negative nuclei never demonstrated more than 3 grains. TLI was related to other variables by the Mann-Whitney U test and the Kruskal-Wallis one-way analysis of variance. Univariate survival analysis was performed using the life-table method, expressed as the log rank probability. Patients

alive at the close of the study, or dead of unrelated causes, were treated as censored observations. Multivariate survival analyses were performed with the Cox proportional hazards model, using both forward and backward selection of variables.

Values of TLI ranged from 0.3% to 19.1% (median 3.2%). The relationship between TLI and other data is indicated in the table on the next page. There is a tendency for higher values of TLI to be associated with indicators of poor prognosis, but this is statistically significant only in respect of tumour grade.

Variable		n	%	TLI (%)		
				Mean	Median	
Tumour Size	T1	8	5	3.4	2.4	p = 0.529
	T2	119	73	4.5	3.2	
	T3	37	23	4.7	4.2	
Nodal Status	N0	57	43	4.4	2.6	p = 0.407
	N1	76	57	5.0	3.4	
Hist. Grade	I	37	33	3.4	3.0	p = <u>0.032</u>
	II	46	41	4.5	3.1	
	III	30	26	6.2	5.1	
ER Status	ER+	93	58	3.9	2.7	p = 0.123
	ER-	68	42	5.5	3.3	
Menopausal	Pre	55	38	4.9	3.8	p = 0.168
	Post	91	62	4.1	2.1	
ErbB-2 Status	Neg	129	78	4.0	2.8	p = 0.266
	Pos	37	22	4.8	3.1	

Table 6 : Distribution of prognostic variables, and comparison of TLI between groups within each variable. Analysis using Mann-Whitney test (2 subgroups), and Kruskal-Wallis test (3 subgroups). The result significant at the 5% level is underlined.

Univariate survival analysis based on TLI values above or below the median shows a trend to improved survival in the latter group, but this is not statistically significant (figure 6). Analysis dividing the patients into 4 groups based on the quartiles of the TLI distribution was also carried out. Although this demonstrates a difference in the outcome for the extreme groups, there is no statistically significant trend (table 7). Multivariate analysis of survival was carried out in a model containing node status, size, erbB-2 staining and TLI. Data were available for 164 patients. Within this group, nodal status is far the strongest variable, and tumour size is also independently prognostic. TLI does not show a statistically significant influence on survival.

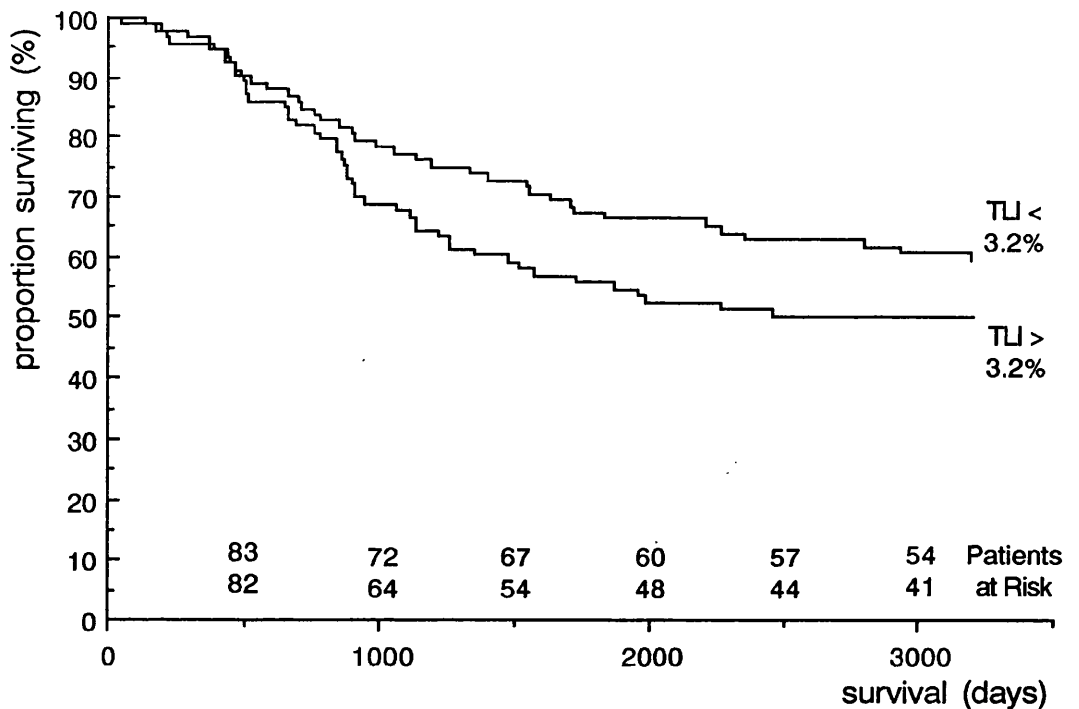


Figure 6: Life table for patients within Liverpool Breast Cancer Series in whose tumours TLI was measured, divided into those with TLI above and below the median value of 3.2%. Log rank probability of difference between survival in the two groups = 0.14.

The observed survival difference at 6 years in our population is 13% in favour of tumours with below median TLI. This accords with Silvestrini's figures of 12% for node negative and 14% for node positive patients. As noted above, Meyer's group presented their results by dividing TLI into three groups. The survival advantage for those in the lowest TLI band over those in the highest is 23% for node negative and 27% for node positive patients at five years. Our own observed difference at that stage between the uppermost and lowest quartiles of TLI is 27%, as shown in the table below:

	Thymidine Labelling Index (%)			
	<1.4	1.4 - 3.15	3.2 - 6.25	≥6.3
Survival (%)	73.3	61.7	65.2	46.6

Table 7: 5 yr actuarial survival for 185 patients within the Liverpool Breast Cancer Series, subdivided into quartiles of the thymidine labelling index of their tumours.

Although we have not reproduced the statistical significance of these studies, our data are very similar. Why then has the TLI not entered into routine clinical practice? Primarily, this is for logistical reasons, in that the autoradiographs need to be exposed for several weeks; taken with the very arduous task of counting at least 2000 cells for each tumour, the process becomes both time consuming and labour intensive. The time

delay also means that the information obtained this way is available too late to influence therapy in the early postoperative period, when decisions about the use of adjuvant therapy need to be taken.

The question of reproducibility also becomes a very important one if these measurements are to become the basis of clinical decisions. This was addressed within the Liverpool series, as it has been by both Meyer and Silvestrini. Meyer's group report the labelling indices calculated by three different observers using the same autoradiographs from five tumours (Meyer and McDivitt, 1986). They used the coefficient of variation of each tumour (the standard deviation of the three values as a percentage of the mean of the three) as the measure of variability, not a very accurate tool because of the relative inadequacy of a standard deviation derived from such a small sample. The five CV's derived were 2, 13, 19, 22 and 50%, for a mean value of 21%. Since about 95% of values lie within 2 standard deviations of the mean in a normal distribution there is a 95% chance that a second estimate will be within $\pm 42\%$ of the first. Another approach to this problem is to normalise all estimates as a ratio to the mean estimate for that tumour. Since the overall mean ratio will be one, the CV becomes 100 times the standard deviation of the ratios, a figure based upon all 15 estimates rather than only 3. Doing this with Meyer's data gives a slightly higher overall CV of 23%. It is also apparent from Meyer's data that one of the three observers gets values consistently below the mean and another observer gets values above the mean in 4 of the five cases. The variability observed may relate predominantly to inherently different counting by the three observers.

Silvestrini (1991) provides more substantial data that addresses this distinction between interobserver variation and reproducibility by the same observer on two occasions. The results of 240 cases counted by two observers are presented (they are a little worryingly referred to as a "representative series"), showing a Spearman correlation coefficient of 0.96. A CV of 12% is quoted. The means of calculation of this figure is not given, but presumably it has been done in the same way as Meyer, based on the two estimates in each case. As indicated already, this is not a very accurate means of evaluation, but it does appear that the results for this group are better than those of Meyer. It is worth noting that even these apparently good results include such pairs of estimates upon the same slides as 3% and 6%, and 1.2% and 2.5%, reading off figure 1 of this paper, so that variation of a factor of 2 is present within the data. 50 tumours were evaluated at two institutions in this study, with a correlation coefficient of 0.93. The CV for this data is not given.

Within the Liverpool series, 18 autoradiographs were counted by one observer on two occasions, and by a second observer. The raw data is shown in the following table:

Case	SH1	SH2	RC	Case	SH1	SH2	RC
1	8.20	7.00	3.50	10	8.70	3.42	4.10
2	3.50	6.30	4.50	11	11.90	7.19	8.25
3	20.70	16.70	13.40	12	0.60	1.40	1.20
4	6.80	7.05	8.30	13	4.80	7.60	5.05
5	2.80	3.00	3.70	14	3.50	4.50	3.70
6	3.70	1.90	4.17	15	8.70	9.50	8.20
7	2.40	4.85	2.95	16	3.80	6.75	6.40
8	5.60	5.60	4.70	17	5.80	9.30	6.95
9	6.90	7.75	6.90	18	7.96	9.95	8.04

Table 8: Estimates of thymidine labelling index (%) made upon the same 18 sections by one observer on two separate occasions (SH1 and SH2), and by a second observer (RC).

The correlation coefficient for the intra-observer variation is 0.87, and for the estimates of the two observers is 0.85. The ratio of each estimate to the mean of the three estimates for that tumour was calculated in order to compute the CV in the the same way as was done with Meyer's data, coincidentally giving the same value of 23%. One observer obtained values higher than the mean by an average of 8%, so that there was a systematic difference in interpretation between the observers, again as noted in Meyer's data. The degree of variation can be appreciated from a plot of the ratios of each estimate to the mean, against that mean value:

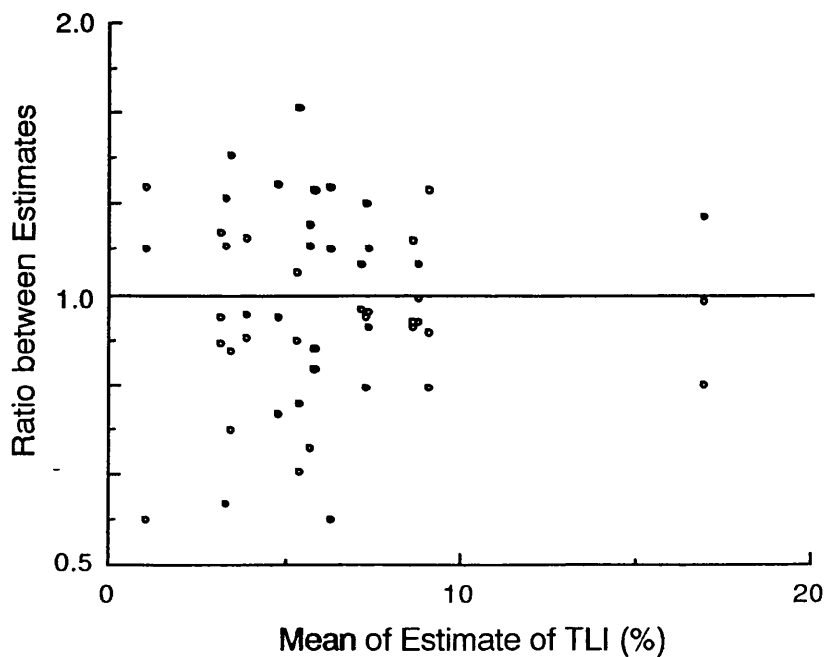


Figure 7: Variability in the estimation of TLI. 18 slides were counted by two observers, one doing so twice, to give 3 estimates for each slide. The ratio between each of these 54 values and the mean value for that slide is plotted against that mean. The ratios vary from the ideal of 1.0 by up to a factor of 2.

To summarise the results of studies of reproducibility of TLI, the use of a correlative approach suggests that the counting process is highly reproducible between different observers and different timepoints. Closer analysis reveals that the 95% 'confidence interval' for estimates of TLI is of the order of $\pm 25\%$ at best (Silvestrini) or 40% in other hands (Meyer, current study). This is small in comparison to the overall range of values of TLI which is from less than 1% to 20%. It is a level of uncertainty which is more important if measurements of TLI are to be used to divide patients into prognostic groups upon which treatment is to be based. It is salutary that the median value of TLI found by different groups varies from 2.8% (Silvestrini) to 5.2% (Meyer), suggesting that substantial interlaboratory variation in methodology exists. This would impose a burden of standardisation upon any laboratory that wished to provide this service.

Section v: Flow Cytometric S Phase Fraction

Release from the time-consuming and labour intensive nature of calculating thymidine labelling index came with the application of flow cytometry to the study of cell kinetics. This technology provides a means for very rapidly studying a large number of cells. In essence, a flow cytometer is a machine which runs a series of small particles through a highly focussed laser beam, and records the amount of light of different wavelengths scattered or given off by each particle during its passage through the beam. Usually, the particles are treated in some way to make them fluorescent, and it is this fluorescence which is measured. The application of flow cytometry to cell kinetics arises from the ability to measure the DNA content of particles in this way. To do this, a suspension of cells or nuclei is created, and stained with a fluorescent dye specific for DNA which binds stoichiometrically- that is, binding is in linear proportion to the amount of DNA present. The amount of fluorescence given off during passage through the laser beam will be in linear proportion to the amount of DNA in the nucleus. If the suspension is run through the flow cytometer, the amount of DNA in each nucleus can be counted as the amount of emitted light of the particular wavelength at which the dye emits given off as that nucleus runs through the exciting beam. In this way, a frequency histogram is created which reflects the distribution of DNA contents within the nuclei constituting the suspension. A flow cytometer is capable of counting 10,000 particles per minute accurately, and so a statistically valid sample is very rapidly achieved.

The frequency histogram built up in this way is referred to as a ploidy histogram. Its characteristic shape can be related to the distribution of cells through the cell cycle. Consider a small cell population where at a certain point in time 50 of the total of 100 cells are in the G_0 phase having differentiated after their previous cell division, 30 cells are in G_1 phase having committed themselves to a further cell division, 10 cells are in S phase synthesising DNA for their ensuing mitosis, 5 are in G_2 phase after completing that process, and 5 are actually undergoing mitosis. Although they are doing different things in cell kinetic terms, the G_0 and G_1 cells have the same DNA content, that which is normal for non-dividing cells of whatever species and tissue they belong to (what the geneticist refers to as diploid DNA content). Those cells which have completed the process of DNA synthesis and have not finished the subsequent division (ie those in G_2 and M phases) will have exactly twice this amount. The S phase cells will have DNA contents intermediate between these two, the amount in each cell depending upon how far it has progressed with synthesis at the moment of observation. The frequency histogram for the distribution of DNA content then looks like this:

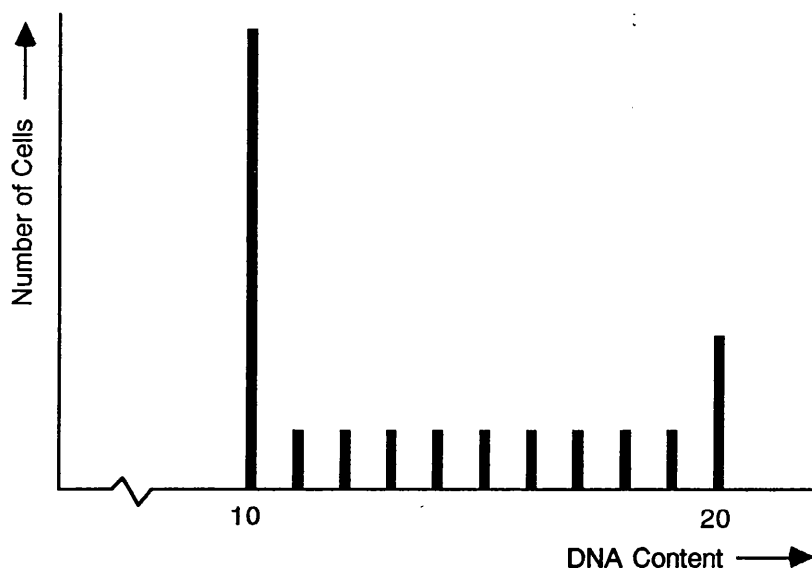


Figure 8: Theoretical frequency histogram of DNA contents in a population of normal cells undergoing cell division.

When this population of cells is run on a flow cytometer, small variations in the recorded fluorescence of cells having the same DNA content, by virtue of variation in binding of the dye and within the machine itself, will result in a frequency histogram with peaks which are not single lines. An actual ploidy histogram for such a population will look like the one in figure 9 (which has for clarity been drawn. This is *not* an actual flow cytometer generated histogram. Where used for illustrative purposes, such synthetic histograms have been used throughout, as indicated in captions. A screen photograph of such a histogram is shown in fig. 10a). If a population of tumour cells is run through the flow cytometer after DNA staining, a histogram like this may indeed be obtained. In about two thirds of cases, a histogram like that in figure 11 will be seen instead (also simulated ease of understanding, with photographic example in fig. 10b).

In this histogram there are two overlapping cell populations having a different G_0/G_1 DNA contents. In order to interpret this, it is necessary to realise that the population of cells within a tumour comprises not only the tumour cells themselves, but also a large number of other elements such as lymphocytes, macrophages, fibroblasts and endothelial cells. These non-tumour cells are non-transformed, and so will have a DNA content that is normal for their species and tissue type. The fact that there are two different populations in the above histogram indicates that some at least of the tumours cells do not have this same DNA content. A tumour of this type, where the cells have a different DNA content from normal, is referred to as DNA aneuploid. Tumours giving a ploidy histogram like figure 9, where only one population is seen such that tumour and non-tumour cells must have the same DNA content, are referred to as DNA diploid. This division into DNA diploid and aneuploid is the so-called tumour ploidy,

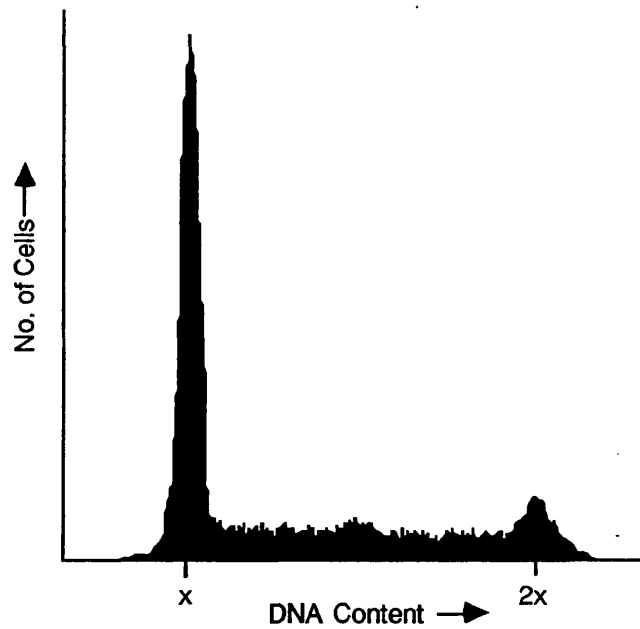


Figure 9: Simulated flow cytometric frequency histogram of DNA contents of a cell population undergoing cell division.

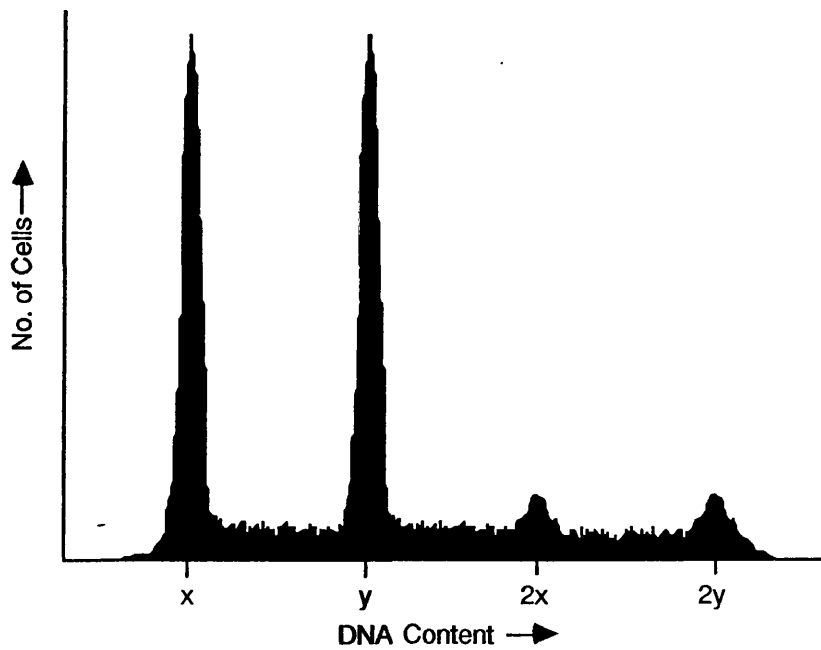


Figure 11: Aneuploid DNA content frequency histogram, as seen in some tumours. For explanation see text. Simulated histogram.

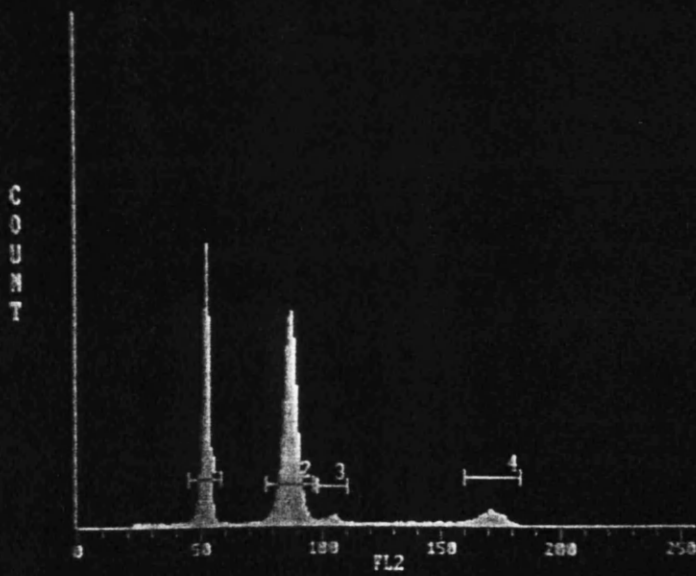
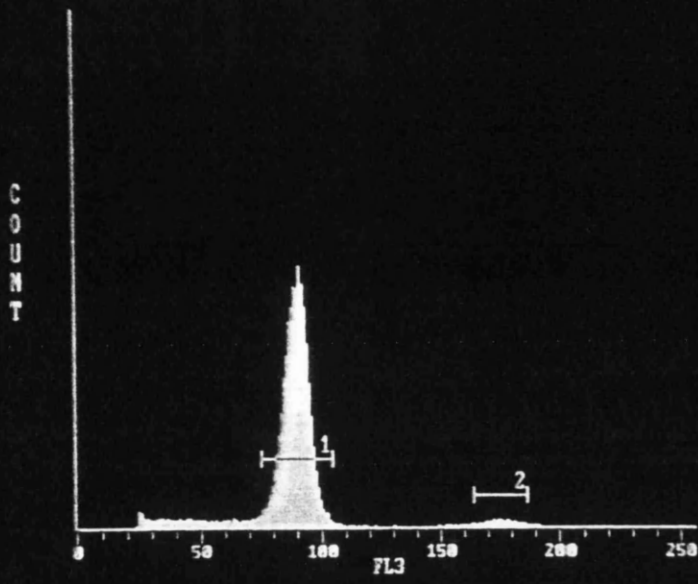


Figure 10: Screen photographs of diploid (upper) and aneuploid histograms

and it is for this reason that the particular form of frequency histogram produced by a flow cytometer under these conditions is designated a ploidy histogram. The terms DNA diploid and DNA aneuploid are used to avoid confusion with the genetic meaning of diploid as the normal G_0/G_1 DNA content of a cell type. In this thesis, since this genetic usage will not appear any further, and for the sake of brevity, the terms diploid and aneuploid will subsequently be used instead of DNA diploid and DNA aneuploid respectively.

Tumour ploidy is only one piece of information which can be gained from the ploidy histogram. The relative DNA content of the tumour cells with respect to normal cells can be more exactly expressed in terms of the DNA index. This is the ratio between the DNA content of the tumour G_0/G_1 cells and the normal G_0/G_1 cells. Thus the DNA index of a diploid tumour is 1.0. Most aneuploid tumours have a DNA content greater than normal (hyperdiploid), and so a DNA index of greater than 1, extending up to about 3 in highly aberrant cases. It is important in the context of this thesis to realise that neither the tumour ploidy nor the DNA index are cell kinetic measurements per se—they are items of information about the tumour biology gained incidentally in the course of obtaining an estimate of the S phase fraction of the tumour. Because ploidy and SPF are parameters derived from the same source they are almost universally considered together, and this convention is continued in the following experiments.

The spatial separation of cells in different phases of the cell cycle in the ploidy histogram allows an attempt to be made to estimate the proportion of cells within each of these phases. By this means alone, neither G_0 and G_1 cells, nor G_2 and M cells can be distinguished from each other, since they have the same DNA content. The S phase cells stand isolated between the two combined peaks, and this has been extensively studied, usually using offline analysis software in order to fit a compartment simulating S phase to the histogram as in figure 12 (with real example in figure 13).

The size of this compartment is then measured, and this is taken as the flow cytometric S phase fraction, abbreviated henceforth as SPF. Whilst this looks straightforward in the example above, it will immediately be apparent that this process is not so in the majority of aneuploid histograms, where the S phases of the diploid and aneuploid cell populations overlap, and the G_0/G_1 and G_2/M peaks intrude upon the S phases. Whilst the software used does allow for these problems, it must always be borne in mind that the process can only ever be one of approximation, however sophisticated.

A further advance was made with the publication of a protocol for the use of paraffin embedded tissue as the starting material for creating ploidy histograms by flow cytometry (Hedley et al, 1983). They recognised that the quality of the histograms

obtained was not as high as that from fresh tissue, and that the stoichiometry of dye binding was dependent upon the method of fixation and embedding used, so that external standards could not be added as a guide to the diploid DNA peak, but the advantage gained by opening up the possibility of using archival material for analysis was considerable. This was especially so in the case of breast cancer given the very long lead time before the outcome of a group of patients is known. Since the advent of this protocol, many investigators have studied the utility of ploidy, DNA index and SPF in human breast cancer. The following review is not intended to be comprehensive, but concentrates upon larger and better conducted studies, and upon some methodological problems which limit their interpretation. Reviews of the area have been published by Friedlander, Hedley and Taylor (1984), McGuire and Dressler (1985), Hedley (1989), Merkel and McGuire (1990), and Frierson (1991).

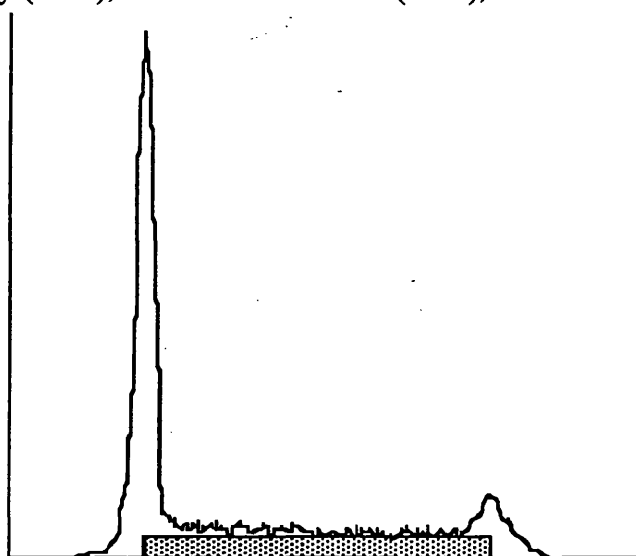


Figure 12: Example of S phase compartment (dotted box) fitted by computer analysis to a simulated diploid histogram, as a means of estimating the proportion of cells in S phase. Real example in figure 13.

Ploidy analysis was possible before the advent of flow cytometry using the method of microscopic densitometry (static cytometry). Nuclear smears, or tissue sections stained by the Feulgen technique, by virtue of which the optical density of the nuclei become proportional to their DNA content, are scanned nucleus by nucleus in order to build up a frequency histogram analagous to the ploidy histogram. This can be further analysed to obtain an estimate of SPF, although only a minority of reports appear to have done this, the validity of such measurements based upon the very small sample sizes obtained by static cytometry being questionable. The technique was first applied to breast carcinomata almost 40 years ago (Atkin and Richards, 1956), and prognostic data were presented 20 years ago, showing better survival in diploid and near-diploid than other aneuploid tumours in a sample of 67 cases (Atkin, 1972). This is a very small study by the standards of flow cytometric ones, which reflects the comparatively

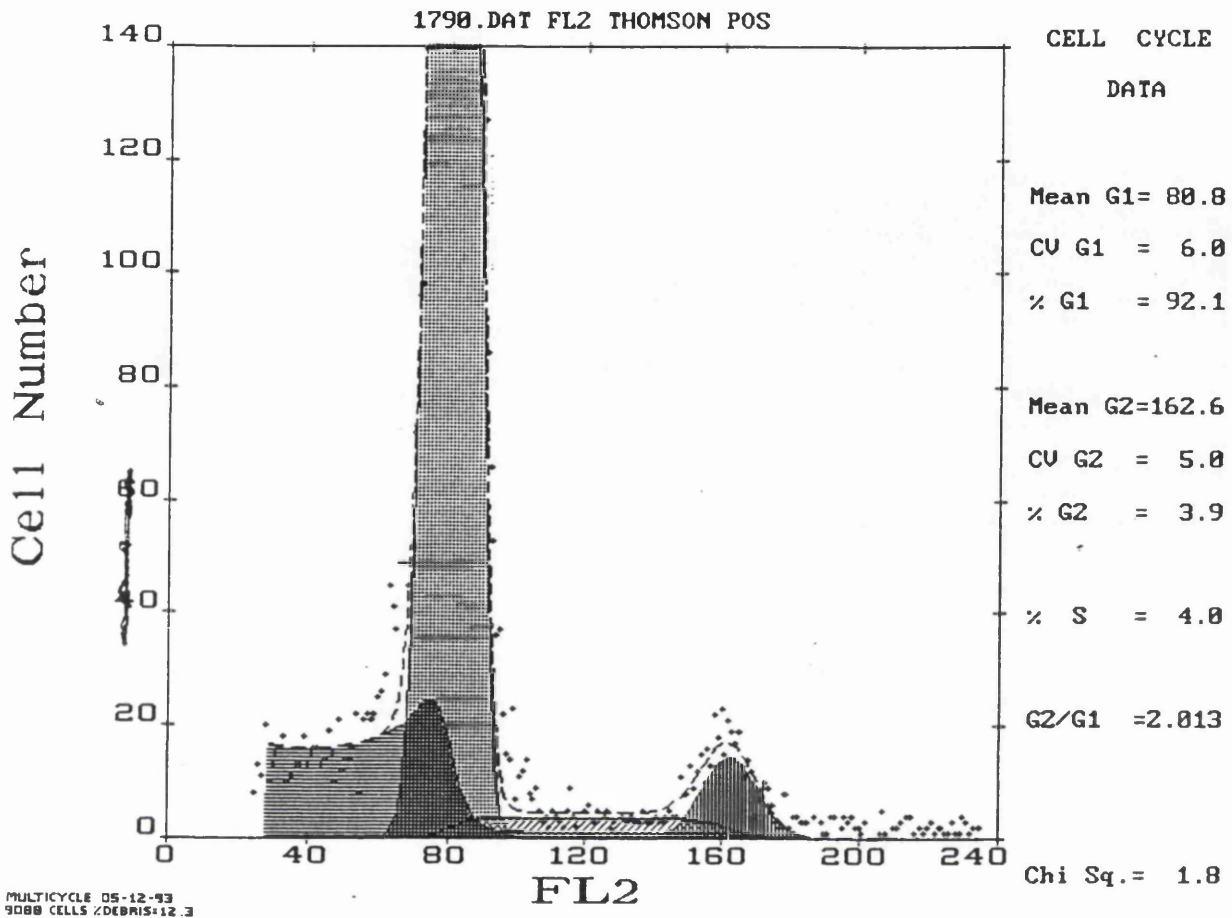


Figure 13: Printout of SPF estimate by the Multicycle package (as used latterly for SPF analyses). The fills for the areas of interest are: dotted- G0/G1; vertical stripe- G2/M; background counts- horizontal stripe; S phase- oblique stripe.

time-consuming nature of this method. Auer et al (1984) reported results based upon a similar analysis of 78 cases. They compared 36 tumours associated with >15 yrs survival and 42 tumours where the patient died in less than 2 yrs, and found aneuploid tumours to be more common in the latter group, and in those in the long term survival group who had suffered local recurrence or metastasis. By 1989, this group were able to present updated results based upon ploidy profiles from 464 tumours, confirming the prognostic power of ploidy, for node negative cases only. In contrast, Hatschek et al (1989) in studying 117 tumours found that ploidy did not predict prognosis, and although SPF did so, this was no longer the case when other clinico-pathological variables were allowed for by multivariate analysis.

The large number of flow cytometric studies have used different patient groups and end points, making direct comparison difficult. Of this plethora of papers, only seven reports which are based upon studies of more than 300 patients, followed for a median of at least 5 years, and analysed using multivariate techniques have appeared. These are worthy of individual consideration. Cornelisse et al (1987) studied 565 patients with all stages of disease, for up to 10 years, and found DNA aneuploidy to be an independent adverse prognostic factor. In a series of 472 tumours with a minimum of 6 years of follow-up studied by Stål et al (1989), conversely, ploidy was not an independent prognostic variable. Tumours with a low SPF showed improved survival independent of tumour size, nodal status and ER content, although this was not broken down by ploidy status. They noted that the relationship between disease recurrence and SPF was not significant over the entire follow-up period while controlling for other variables, suggesting that the prognostic value of SPF was reduced by the multivariate analysis.

Toikkanen et al (1989) reported upon the very long term follow-up of 351 patients in whom both ploidy and SPF were measured. Although ploidy predicted strongly for survival at 25 years, this result was not borne out in multivariate analysis. SPF did show independent prognostic significance with low SPF predicting for survival, but SPF was entered as above or below a figure of 7%, chosen on the basis that this provided the greatest distinction between low and high figures. That this figure was selected from the data and then applied back to it, and not validated upon a separate data set weakens the findings in this study. The same criticism can be levelled at Clark et al (1989), who found ploidy alone to be of independent prognostic significance in a group of 345 patients with node-negative breast cancer, DNA diploid tumours showing an 11% survival advantage at 7 years in univariate analysis which remained significant upon multivariate analysis. They found SPF to be of no additional value in DNA aneuploid patients, but that it was a univariate predictor of survival in DNA diploid patients at cutoffs between high and low SPF of 5.0 - 9.0%, with a survival

advantage to those falling below the cutoff. This effect remained in multivariate analysis using the figure of 6.7%, again not validated upon data from which it was not derived, and furthermore a figure which put 87% of cases into the low SPF group.

Hedley et al (1987), the originators of the technique for utilising paraffin-embedded material for flow cytometry, performed flow cytometry upon 490 node-positive tumours, with 6 or more years of follow-up. In their series, patients with DNA diploid tumours showed improved survival in univariate analysis, but this effect was no longer evident in multivariate analysis. Tumours with a low SPF showed a survival advantage, using a cutoff very near the median, but this was not evident in multivariate analysis, predominantly due to a strong association with tumour grade.

Kallioniemi et al (1988) followed 308 patients for 8 years, and found a large univariate survival disadvantage for aneuploid tumours (relative risk 3.0), which was not, however, borne out in multivariate analysis. Ploidy and SPF could be combined to create three prognostic groups which were independent predictors of survival, although once again this relied upon cutoffs determined by examination of the data. Finally, Fisher et al (1991) have reported upon results from the NSABP-04 trial in 398 patients. This represented only 54% of available tumour blocks, the remainder failing to provide adequate histograms. In this series, ploidy did not predict 10 year survival in univariate analysis. SPF was divided at the median appropriate to that tumour's ploidy, with low SPF tumours having a survival advantage at 10 years of 14%. This result was remained significant in multivariate analysis, although they noted that low SPF tumours still had only a 53% survival at this length of follow-up.

A large study by Beerman et al (1990) reported upon the outcome in 690 patients with stages I-III disease, but looked only at tumour ploidy. They found that this parameter did predict survival in both univariate and multivariate analysis, with a median follow-up of 7 years. Conversely, another large series reported by Hatschek et al (1990) found that ploidy did not significantly predict for outcome in multivariate analysis, although follow-up was only 4 years in this study. Within this group, SPF was found to be independently prognostic. In a separate paper based upon the same series of patients (Hatschek et al, 1989), these workers assessed the ability of ploidy and SPF to predict survival after first recurrence. Ploidy did not do so, even in univariate analysis, but SPF again held independent significance, with a survival advantage to tumours with low SPF. Blanco et al (1990) looked at this same end-point in 226 patients, and also found that ploidy did not predict for outcome. This group did not report upon the value of SPF.

There are many other smaller series, often with shorter periods of follow-up, included in the reviews referenced above, but little if anything is to be gained by further consideration of these papers here. The consensus from the larger and better conducted studies (table 9) could reasonably be stated as: diploid tumours are often found to have a survival advantage over aneuploid tumours in univariate analysis, but only a minority of studies find this effect to be independent of existing prognostic factors; whilst most studies find that tumours with low SPF carry a true survival advantage over those with high SPF.

Author	year	n	FU (yrs)	Ploidy	SPF
Cornelisse	(1987)	565	3-12	yes	ND
Stål	(1989)	472	>6	no	yes
Toikkanen	(1989)	351	27	no	yes
Clark	(1989)	345	5	yes	yes ¹
Hedley	(1989)	490	>6	no	no
Kallioniemi	(1988)	308	8	no	yes
Fisher	(1991)	398	10	no	yes
Beerman	(1990)	690	7	yes	ND
Hatschek	(1990)	430	4	no	yes
Blanco	(1990)	226	>4	no	ND

Table 9: Summary of results from larger studies of the prognostic significance of tumour ploidy and S phase fraction in breast cancer. n = number of patients studied; FU = years of follow up (x-y: range; >x: minimum; x: median); last two columns give significance in multivariate analysis. ND = not done. 1 = effect restricted to diploid tumours

Chapter 4:

Review of Dynamic Methods Applied to Breast Cancer

The methods so far discussed give information about the distribution of cells through the cell cycle, but provide no indication as to the rate at which cells are progressing through the cycle. The technique of *in vivo* labelling with bromodeoxyuridine has made this information available for the first time. Bromodeoxyuridine (more fully 5-bromo-2'-deoxyuridine; henceforth abbreviated BUDR) is a thymidine analogue, which is stably incorporated into DNA, inter-changeably with thymidine. It has been used sporadically as a radiosensitizing agent for the treatment of cerebral tumours. The potential for using BUDR for the study of cell kinetics arose with the development of a monoclonal antibody which recognises it within DNA. This was achieved by Gratzner (1982), and created a mechanism by which cells which took up the BUDR could be identified, as is possible with tritiated thymidine, but without the necessity for the use of a radio-isotope. Because BUDR itself is non-toxic to the cells which take it up in low doses, it can be given to patients (doses used for cell kinetic studies are an order of magnitude lower than those used therapeutically without side-effects). This allows the labelled cells to progress through the cell cycle, and it is the study of that process which gives the 'dynamic' information as to the rate of cell cycle transit. The theory and practice of the determination of cell cycle kinetics in this way were developed by Adrian Begg and his colleagues at the Mt Vernon Laboratories in London (Begg et al, 1985).

Section i: Theoretical Basis of the use of Bromodeoxyuridine

Looking at this first in descriptive terms, if BUDR is given intravenously to a patient with a tumour, it should be taken up by all cells synthesising DNA at that point in time (its half life is so short, of the order of a few minutes, that it is effectively a point label). It follows from this that if a tumour biopsy were taken at that time, and stained so as to demonstrate not only the DNA content of each nucleus (with propidium iodide, just as if creating a ploidy histogram), but also the BUDR content (using an appropriately labelled anti-BUDR), then the BUDR labelled nuclei should occupy S phase. If instead the biopsy is delayed for some hours, the labelled cohort of cells will continue through the cell cycle, toward and into G₂ and subsequently M phase, thereby dividing into two labelled G₀/G₁ cells. Multi-parameter flow cytometry allows us to perform such double labelling, and identify the position of the labelled cells within the ploidy histogram (figure 14). We assume the position of the labelled cells in the histogram at the time that they took up the BUDR (distributed throughout S phase alone, as in fig. 14a), and can measure their position at the time of biopsy, the

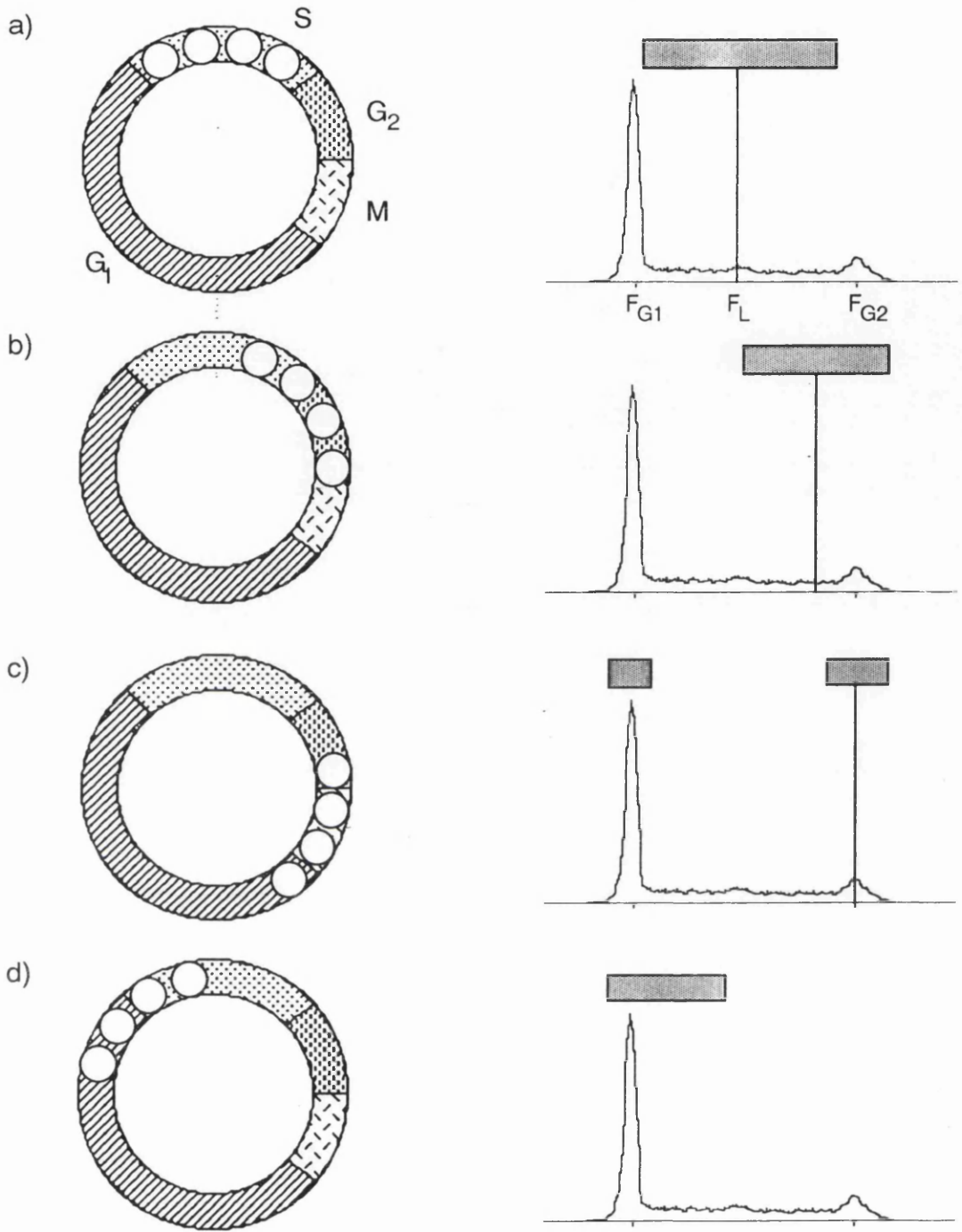


Figure 14: Principle of the Determination of T_s from a single sample. On the left of each figure, a model of the cell cycle showing as white balls cells which have taken up BUdR given at time zero (a), and are progressing through a single cycle (b,c,d). On the right, the position these balls is shown as a box above a ploidy histogram of the cell population. The mean position on the x axis of the G0/G1 peak, the G2/M peak, and the balls is shown in a) only as F_{G1} , F_{G2} and F_L , respectively.

'distance' which they have moved can be worked out. Since the time since labelling is also known, it is possible by dividing distance by time to obtain an estimate of the velocity of this movement, in this case the length of S phase, T_s . The proportion of cells within the histogram which are labelled can also be calculated, which provides a labelling index analogous to the thymidine labelling index. The two measurements can be combined in an equation derived by Steel (1977, p.69):

$$T_{\text{pot}} = \lambda \cdot (T_s / \text{LI}) \quad (\text{equation 9})$$

where lambda is a factor dependent upon the relative lengths of the phases of the cell cycle, discussed further below.

In mathematical terms, the rate of cell cycle transit in the form of the length of S phase (T_s) is derived by defining a measure of the average position of the labelled cells within the histogram. This was termed the relative movement by Begg et al (1985). Consider the ploidy histogram where the labelled cells are indicated above the ploidy histogram, and enclosed in the box (figure 14). The average channel number for these cells (that is, their average position on the x axis) is shown as F_L . The relative movement is calculated from this value, and the average channel numbers for the G_0/G_1 and G_2/M peaks, which we will call F_{G_1} and F_{G_2} respectively, as:

$$\text{RM} = \frac{F_L - F_{G_1}}{F_{G_2} - F_{G_1}} \quad (\text{equation 10})$$

The numerator here represents the average distance between the labelled cells and the G_0/G_1 peak, the denominator the distance between the means of the G_0/G_1 and G_2/M peaks (theoretically, $F_{G_2} = 2F_{G_1}$, and so the denominator can be approximated by F_{G_1} . To use the equation in the original form is more accurate). If we ignore the cells which have divided, we can consider the labelled cohort to be moving as a group toward the G_2/M peak. Initially, given the assumption that they are evenly distributed through S phase, their average position will be exactly half way between the two peaks. F_L will therefore be half way from G_0/G_1 to G_2/M , and so RM will be 0.5 at the time of labelling under this model. This is the situation shown in figure 14a. Still ignoring the divided cells, at the time when the last labelled cell from S phase (presumptively the one which had only just entered S phase at the time of labelling) reaches the G_2 phase, all labelled and undivided cells will be in the G_2/M peak, and so F_L will equal F_{G_2} , and RM will be 1. Note that this time corresponds to the length of S phase (T_s), as this last cell has traversed that phase from start to finish during the period of observation. As the length of time from labelling to biopsy increases from zero to T_s , the RM thus progresses from 0.5 to 1.0. It is possible to calculate T_s from time and RM in this way:

$$T_s = \frac{0.5}{RM - 0.5} \times t \quad (\text{equation 11})$$

where t is the time between labelling and biopsy. The numerator now indicates the distance which the RM has to move from its initial to its final positions (between $t=0$ and $t=T_s$), and the denominator the distance which it has actually moved.

A number of assumptions were made in deriving the above equations. It was explicitly stated that the labelled cells were evenly distributed through S phase at the time of labelling. It was on this basis that the 'starting' position of the labelled cohort was taken to have an RM of 0.5. In the terms of S phase analysis as discussed in the previous chapter, this amounts to an assumption that S phase is rectangular. It was noted then that although this is the simplest and most reproducible model of S phase for the purposes of offline analysis, a number of other models have been proposed on theoretical grounds. These do not assume even distribution of cells through S phase, the deviations being due to the process of cell loss in and subsequent to this part of the cell cycle (Steel, 1977, p.79). It seems likely that such loss does occur, and that as such the rectangular model is an oversimplification.

It is also assumed that all cells in S phase take up the bromodeoxyuridine, but it has been observed for both thymidine and bromodeoxyuridine that some cells in S phase do not incorporate these pyrimidine bases (Allison et al, 1985; Wilson et al, 1985). This could be the result of arrest of cells in S phase, such that they have a DNA content greater than the G_0/G_1 content of the population but are not synthesising DNA (de Fazio et al, 1987), but it also seems to be the case that some cells simply do not incorporate these bases despite carrying out DNA synthesis. The reason for this is not known. The failure of this assumption has two consequences for the process of calculating T_{pot} . The first is that it leads to underestimation of the labelling index, and so to overestimation of the value of T_{pot} , in an unpredictable way since it cannot be assumed that the proportion of unlabelled S phase cells is constant from one sample to the next. Secondly, it creates a biased sample of cells used in the determination of T_s , as it cannot be assumed that all of the unlabelled cells are non-contributory to tumour growth, nor that they are cycling at the same rate as the labelled cells which are amenable to analysis. As in the case of the assumption about the shape of S phase, it is impossible to theoretically account for this deviation within the calculation of T_{pot} .

The mathematics of the calculation of RM also assumes that G_2/M is negligibly short. Consider a simplified sample in which there are 100 labelled S phase cells initially evenly distributed through S phase and moving toward M phase at the same rate as each other, but then failing to go through mitosis (that is, G_2/M is infinitely long). The initial rate of movement of each cell is the same, and so the average velocity of

movement is that of each cell, which we may refer to in flow cytometric terms as x histogram channels/unit time. Once 50 of the cells (those which constituted the second half of S phase initially) have reached arrest in M phase, then only 50 cells are still moving (with velocity x), whilst the arrested cells have velocity zero. The average velocity is thus only $x/2$. That is, the rate of change of F_L (and so of RM) has halved, because fewer of the observed cohort of undivided labelled cells are contributing to it. The model thus assumes that each labelled cell divides as soon as it reaches the end of S phase, as at this stage it ceases to contribute to increase of F_L , that is that G_2 and M phases are vanishingly short. The longer that these two phases are, the greater will be the extent to which the rate of change of RM slows with time. Fortunately, G_2 and M are indeed relatively short in the cell cycle of human tumours, but not negligibly so, and so the plot of RM against time is not linear as assumed, but is convex superiorly (figure 4 in the Begg paper). The linear relationship assumed in equation 11 is thus only an approximation to this curve. Begg et al did consider this problem in their original description, and suggested that the linear equation $T_s = [0.6/(RM - 0.4)] \times t$ may better fit real data, given the length of G_2 and M phases in human tumours. In fact, observations upon cultured cell lines using the bromodeoxyuridine method to determine cell kinetics indicate that the uncorrected model provides adequate data. These unpublished experiments were performed in Liverpool by Prof Cooke's group prior to my own involvement with this work. Cell cultures in exponential growth were briefly exposed to bromodeoxyuridine and harvested at time points thereafter. Manual cell counts and calculation of T_{pot} by the Begg method were performed. In the situation of exponential growth, cell loss is theoretically zero, and so the actual and potential doubling times should be the same. Comparing the last two columns in the table below, it can be seen that this is in fact very nearly the case, showing that in this situation at least, the technique of Begg et al provides an adequate approximation to real values. That the T_d in this experiment is consistently longer than the T_{pot} might arise from the fact that even in these ideal conditions the cell loss fraction is not in fact zero.

Cell line	T_s (hrs)	LI(%)	T_{pot} (hrs)	T_d (hrs)
HT29/5	12.5	44	22	24.3
HMY	9	36	20	21.9
HSN	5	37.8	11	12.6

Table 10: Observed doubling times for cell lines (T_d) compared to potential doubling times (T_{pot}) calculated by BUDR labelling.

The calculation of T_{pot} from the values of LI and T_s introduces the variable lambda, a concept described initially by Steel (equation 9). It is needed because the calculation of

T_{pot} is based upon observations made solely upon cells in the S phase of the cell cycle. If the distribution of cells through the cycle were even, that is, that there were equal numbers of cells at any given point in the cycle, observations upon any point or area of the cycle could be generalised to the whole. However, because each cell divides into two at one point, there will always be more cells in the early part of the cycle beyond this point, whether or not the extra cells are being lost as in a stable population size, or are continuing through the cycle to expand the population. Whereabouts in the cycle we make our observations will now make a difference to the data which we obtain about the number of cells in the population. Lambda is the means by which correction is made for the position of S phase within the cycle with respect to the division point (the end of M phase), and depends upon the relative lengths of the various phases of the cycle:

$$\lambda = \frac{T_{pot}}{T_S} \left[\exp \left[\frac{\ln 2}{T_{pot}} [T_{G_2M} + T_S] \right] - \exp \left[\frac{\ln 2}{T_{pot}} T_{G_2M} \right] \right]$$

The theoretical limits to the value of lambda are $\log_e 2$ and $2\log_e 2$. Since the observations made upon each tumour indicate only the length of S phase, the value of lambda cannot be calculated individually. Fortunately, in human tumours the lengths of G_2 and M phases are relatively short compared to those of G_1 (especially) and S phases, and so the value of lambda lies well toward its lower asymptote ($\log_e 2$, or 0.693). The value which was assumed by Begg et al in describing the bromodeoxyuridine based determination of T_{pot} , and which we have used, is 0.8. It must be recognised that this is only an approximation, and is not actually a constant as assumed.

The desire to avoid this assumption as to the value of lambda led White et al (1990) to use further information as to the length of G_2 and M phases contained within the two dimensional histogram in order to calculate T_{pot} without reference to any external constant. Whereas Begg et al exclude from consideration any cells which have divided since labelling, ie labelled cells in the G_0/G_1 peak, White et al use both the fraction of labelled undivided cells, f^{lu} and the fraction of labelled divided cells, f^{ld} , to define the function v :

$$v = \ln \left[\frac{1 + f^{lu}(t)}{1 - f^{ld}(t)/2} \right]$$

They then show that for $T_{G_2M} \leq t < T_S + T_{G_2M}$ (where t is the interval between bromodeoxyuridine labelling and biopsy),

$$T_{pot} = \ln(2) \frac{T_S}{v}$$

The labelling times used do indeed fall within these constraints (roughly 2 to 12 hours). Note that whilst this method avoids the assumption as to the value of lambda, T_s is calculated in the same way, with all of the assumptions which that involves. Given the values of LI, T_s and using the value of T_{pot} arrived at by this method, it is possible to calculate the implied value of lambda, by simply rearranging equation 9:

$$\lambda = \frac{LI \cdot T_{pot}}{T_s}$$

If this is done using the data from patients in the current study, then lambda is consistently estimated at 0.7. This supports the assumption that it is a constant, albeit with a different value to that assumed. In this situation there would seem to be little to tell between the methods of Begg and of White. In this study, values of T_{pot} have been calculated by both methods, but analyses are based on those obtained using the original description by Begg.

Section ii: Application of the Bromodeoxyuridine Method

The Mt Vernon group applied their method in a number of different tumour types. Their initial report (Wilson et al, 1988 and then with several additional patients Riccardi et al, 1989) dealt with results obtained from 112 tumours. 50 of these were acute non-lymphoblastic leukaemias, and these were compared with 10 specimens of normal bone marrow from patients with non-haematological malignancies. The normal marrow specimens all showed higher labelling indices than any of the tumours, the values of T_s being similar in the two groups. Subgroup analysis of the leukaemic patients showed that response to therapy was associated with lower labelling index. These data suggest that the marrow of patients with leukaemia is proliferating more slowly than normal, and that the more slowly the marrow proliferates, the more likely it is to respond to chemotherapy. This is contrary to the *a priori* assumption that response to cell cycle related treatment modalities is a characteristic of faster growing, 'more aggressive' tumours.

In the same series, 42 gastric cancers were analysed, and compared with histologically normal gastric mucosa from 7 of the cases. Here, the tumours showed substantially higher labelling than normal (median tumour LI 10.7% cf normal 5.9%), but with a significantly longer median T_s (tumour 14.4hrs, normal 10.9hrs), such that median T_{pot} in the two groups was not significantly different. Advanced stage tumours had a higher LI than earlier tumours. The other 20 tumours reported upon by Riccardi et al were a variety of types of brain malignancies. It was noted solely that no differences in clinical behaviour were associated with kinetic data for these tumours. In their study of 100 colon tumours (Rew et al, 1991), the median labelling index was relatively similar to that for gastric malignancies, at 9.0%. There was no comparison with normal tissue

presented in this report. Kinetic parameters were found not to be correlated with Dukes' classification or histological tumour grade.

From 75 breast tumours (Rew et al, 1992), they could obtain no data from 6, and labelling index alone in a further 18. The median value for labelling index was 4.2%, rather lower than that for colon cancers in the previous report. Median T_s , 8.7hr, was shorter, but despite this the median potential doubling time was twice as long (8.2 days). There were no statistically significant differences in kinetic parameters when tumours were stratified by nodal status, tumour size, histological grade, or menopausal status. It is worth comparing the results of *in vivo* labelling with bromodeoxyuridine in different tumours as carried out by the Mt Vernon group, on the basis that the same methodology can reasonably be assumed to have been used regardless of tumour type. The table below combines data from the four studies just discussed:

Tumour Type	n	LI (%)	T_s (hrs)	T_{pot} (days)
Leukaemia	50	6.1	12.7	8.8
Gastric	21	10.7	14.4	8.4
Colorectal	100	9.0	13.1	3.9
Breast	69	4.2	8.7	8.2
Brain	20	6.4	14.8	12.1

Table 11: Summary of results reported by Mt Vernon group, using *in vivo* bromodeoxyuridine labelling in a variety of human tumours (all values are medians).

Four other groups have used bromodeoxyuridine labelling for the study of breast cancers, but have used it to obtain static data only. Meyer et al (1993) labelled 450 tumour biopsies *in vitro*, using a technique exactly analogous to their method for thymidine labelling, but simply substituting bromodeoxyuridine for the thymidine in the incubation mixture. Immunohistochemistry was then carried out with a primary antibody to bromodeoxyuridine, and the proportion of positive nuclei in a sample of 2000 was counted. The median value of the bromodeoxyuridine labelling index was 3.9%. This parameter was positively correlated with tumour size, nodal involvement and aneuploidy, and negatively correlated with patient age and oestrogen receptor status. The same type of experiment was performed by Lloveras et al (1991) on 148 breast cancers. The median labelling index for BUdR in their hands was 3.0%, and they found the same positive correlation with tumour size, and inverse relationship with oestrogen receptor status, but failed to find any relationship between labelling index and patient age, nodal status or histological grade. They also examined 21 benign breast lesions, among which were 13 fibroadenomata, which had a mean labelling index of only 0.65% with none higher than 1.5% (for comparison the corresponding mean value of labelling index for the tumours was 4.6%).

Sasaki et al also used *in vitro* labelling, in a group of 18 cancers, finding a markedly higher median index of 10.9%, based on counts of only 1000 cells (though this is less of a problem with such a high labelling index). In such a small series, it is possible that these are non-representative patients. Little information is provided that enables us to check this, but it may be relevant that 81% of the tumours which they studied were aneuploid, which is certainly higher than usual. Goodson et al (1993) labelled 109 women with bromodeoxyuridine, and subsequently performed immunohistochemistry on tumour biopsies in order to calculate a labelling index in the same way as Meyer's group. The median labelling index was 10.3%. Since it is impossible to correct for division of cells which have taken up the bromodeoxyuridine into two labelled cells in this type of experiment, it would be appropriate to administer the bromodeoxyuridine immediately prior to surgery. Whether this was the case or not is not stated in this article. These labelling indices may for this reason have an inherent tendency to over-estimate the proportion of S phase cells. The mean labelling index for these tumours, 11.1%, was very close to the median figure. This is very different to the findings of the other workers, where the mean value is markedly higher than the median, which is much more what one expects for biological parameters, which so often have a long upward tail in their distribution. The data from Goodson et al need to be treated with some circumspection. This is a pity, as they made an interesting comparison between the labelling index in primary tumour and involved lymph nodes, a unique study in terms of bromodeoxyuridine labelling. They found the two to be highly positively correlated, that is primary tumours with high labelling index tended to have highly labelled secondaries. This would argue against a clonal selection model of metastasis, but given the doubtful nature of the basic data it is probably unwise to give much weight to this particular experiment.

There have been disparate reports of the application of *in vivo* bromodeoxyuridine labelling in tumour types other than breast cancer over the last 2 years. As with the two studies just considered, most of these have failed to make use of the capability of this methodology to provide dynamic data, and have calculated a tumour labelling index only. This is bromodeoxyuridine used simply as an alternative to tritiated thymidine, its only advantage being that *in vivo* labelling is theoretically more satisfactory than *in vitro*. All have reported their results in terms of mean values of labelling index, which ignores the fact that this parameter almost certainly has a non-normal distribution. They will not be discussed individually, but a brief summary of results is given in the following table:

Author	Year	Tumour	Type	n	LI	T _S	T _{pot}
Tinnemans	1993	lung	vivo	27	9.9	10.0	7.8
Tachibana	1993	bladder	vitro	81	10.0	-	-
Popert	1993	bladder	vivo	19	7.9	-	-
Roncucci	1992	colorectal	vivo	43	20.3	-	-
Ito	1992	medullobl.	vivo	26	11.7	8.0	-
Yousof	1991	colorectal	vivo	7	25.8	18.7	-

Table 12: Summary of results published by various authors using bromodeoxyuridine labelling in human tumours other than breast. Type refers to whether labelling was carried out *in vivo* or *in vitro*. All kinetic values are means.

This brings us up to date with the current state of play in the measurement of tumour cell kinetics. The relative impracticality of measuring actual doubling times, and the labour-intensive, time-consuming nature of thymidine labelling have precluded them from establishing themselves as routine techniques. The same might have happened with the counting of mitotic figures and of staining with Ki-67 and PCNA, but at least the preparation here is simple and quick. What is at risk of happening though is routine users taking the short cut of not counting an adequate sample of cells. This is the attractive element of flow cytometry- the ability to automate the counting, and furthermore to do it very quickly. What is lost is the ability to see what is being counted, and the last two sections indicate only too clearly just what assumptions are made in the process of interpreting flow cytometric output. Reduced to its barest essentials, this is what this thesis seeks to examine- do the benefits of flow cytometric techniques outweigh their disadvantages? This question is formalised and broken down to some extent in the following statement of aims, after which we turn to the description of the experimental work undertaken.

STATEMENT

OF

AIMS

The preceding review indicates that all methods for the study of tumour cell kinetics have technical limitations. The application of flow cytometry to this area has huge potential advantages in terms of time saving, and the ability to measure dynamic kinetics. This thesis is intended to assess that potential, and the way that these data might best be used to further our understanding and treatment of breast cancer. The general aim may be stated in the following terms:

The purpose of the current programme of experiments is to to critically evaluate the potential use of flow cytometric methods for the determination of tumour cell kinetics, particularly in the study of human breast cancer.

This is effected by the study of :

a retrospective series of 293 breast cancers in which S phase fraction is measured

a prospective series of 89 breast cancers labelled with bromodeoxyuridine

The individual experiments address a more specific group of questions:

what are the validity and reproducibility of flow cytometric S phase fraction and bromodeoxyuridine-based kinetics?

what are the prognostic power of tumour ploidy and flow cytometric S phase fraction?

what are the dynamic kinetics of breast cancer, their relationship to traditional prognostic factors, and to the kinetics of other human malignancies and normal breast tissue?

do in vivo labelling and flow cytometry offer any advantage over static methods of assessing tumour cell kinetics?

can tumour cell kinetics help assess the significance of molecular abnormalities in breast cancer, specifically aberrant expression of type I growth factor receptors?

PART II

S PHASE FRACTION

AS A

PROGNOSTIC FACTOR

IN

HUMAN BREAST CANCER

Introduction to the Experimental Parts of the Thesis

To address the aims of the thesis, experiments have been performed in the two major areas of application of flow cytometry to the field of tumour cell kinetics- the estimation of S phase fraction by analysis of ploidy histograms, and the calculation of dynamic kinetics by multiparameter flow cytometry after administration of bromodeoxyuridine. The following two parts of the thesis describe these investigations. In Part II, the results of the examination of over 300 tumours with long follow up, to determine ploidy and S phase fraction are described. Part III looks at the application of bromodeoxyuridine-based technology in an ongoing series of about 90 cancers.

Overview of Ploidy Studies

This Part begins with a brief description of the patient base for the Liverpool Breast Cancer Series, and what tumour material from this cohort we were able to access for ploidy studies. There follows a detailed description of the process by which nuclear suspensions were prepared from this tissue and subsequently stained for DNA content. Technical details as to how these were run on a flow cytometer are then covered. This section continues on from the theoretical account of flow cytometry in section v of chapter 3. The means by which the flow cytometric output was interpreted to provide data as to tumour ploidy and S phase fraction are discussed, and this again follows on from the theory presented in chapter 3. The final section of the methodological chapter sets out experiments assessing the sources of variation in measurements of S phase fraction.

The results, and discussion of them, focus on two questions, encompassed within the specific aims of the thesis: firstly, what prognostic information is given by tumour ploidy and by flow cytometric S phase fraction; and secondly, how reproducible are the measurements themselves?

These experiments formed the basis for the paper: Lack of prognostic significance of ploidy and S phase fraction in human breast cancer. Stanton PD, Oakes SJ, Murray GD, Winstanley J, Cooke TG, George WD. *Br J Cancer* 1992; 66: 925-9.

Chapter 5: Patients and Methods

Section i: Patients Studied

This study used archival, formalin-fixed, paraffin-embedded tissue from patients who were part of the Liverpool Breast Cancer Series. This series was established in 1979 by Mr T G Cooke, to assess the prognostic significance of oestrogen receptor expression in early breast cancer. 749 patients under the care of 16 surgeons in four hospitals were recruited to the study. It was hoped to include all consenting patients with TNM stages T_{0-3} N_{0-1} M_0 breast cancer treated in the Liverpool area, and prospective audit of operating lists suggested that this was very nearly achieved throughout the period of recruitment. The absence of metastatic disease was based on full blood count, liver function tests, serum electrolytes, chest X-ray and skeletal survey with isotope bone scan in the case of equivocal X-ray results, in line with the limited availability of nuclear scanning at that time, especially in peripheral hospitals.

Patients were treated at the discretion of individual clinicians, with operative procedures ranging from simple to radical mastectomy. Some form of axillary lymph node sampling procedure was a requirement of the study, many patients having a full axillary dissection. Patients who had been given prior systemic therapy were excluded, as were patients given adjuvant chemotherapy (eleven patients). Subsequent treatment was again entirely at the discretion of the individual surgeons involved, as was follow-up. The patients were flagged with the regional Cancer Registry, so that the only deaths potentially not recorded were those of patients dying outside of Britain. Recurrence data from clinical follow-up are not nearly so complete as mortality data, as two of the four participating hospitals have since been closed, so that death is the only satisfactory endpoint for statistical analysis in this series.

Patient details recorded on a standard proforma at the time of entry to the study included age and menopausal status. Tumour size was assessed clinically, nodal involvement histologically by the respective hospital pathologists. Tumour grade was allocated by a single pathologist according to the criteria of Bloom and Richardson. Oestrogen receptors (ER) were assayed by the dextran coated charcoal technique at the Tenovus Institute in Cardiff, and the cut off between ER positive and negative tumours was taken as 5 fmol/mg cytosol protein. The thymidine labelling index was measured in 196 of the tumours as described in the previous section.

452 of the tumours were stained immunohistochemically for the erbB-2 oncoprotein using the 21N polyclonal antipeptide antibody developed at ICRF by Dr W Gullick.

This work was performed by Mr J Winstanley. Tumours were classified as positive for erbB-2 if any positively stained tumour cell groups were identified.

Section ii: Tissue Available

Formalin-fixed, paraffin-embedded material was sought from all cases in the series from the archives of the contributing hospitals' pathology departments. Due to the closure of two of the hospitals involved, the blocks produced by the hospital pathologist at the time could not be found in many cases. In some of these cases, the blocks used for measuring the thymidine labelling index were available and were used in place of original pathology specimens to provide material for flow cytometry. One or more samples were available from these sources for 329 of the total of 749 patients within the series.

Section iii: Preparation and Staining of Nuclear Suspensions

Suspensions were made by a slight modification of the technique published by Hedley et al (1983), summarised in figure 15. 50 μ sections were cut from each block with a standard microtome. Although this exceeds the calibrations on the instrument, accurate sections of this thickness were obtained by marking the ratchet within the instrument (which simply advances the block by 1 μ per tooth) at intervals of 25 teeth, and manually turning the ratchet two such markings. Two sections were cut to allow a repeat/duplicate section without further recourse to the block, in order to preserve the available material. Before taking the thick sections for flow cytometry, a standard 4 μ section was cut for H&E staining in order to verify the presence of tumour within the sectioned tissue. All of these sections were reviewed by the author, with the assistance of Dr J Going in the Department of Pathology, GRI in cases of any dubiety. Hedley's original description was of the use of 30 μ sections, but it was subsequently shown that increasing the thickness of the sections reduced the proportion of debris attributable to nuclei divided by the blade on the surfaces of the section (Stephenson et al, 1986). These authors demonstrated that there was no significant diminution of debris using sections of greater than 50 μ in thickness. The subsequent use of the thin and thick tissue sections is summarised in the following flow chart:

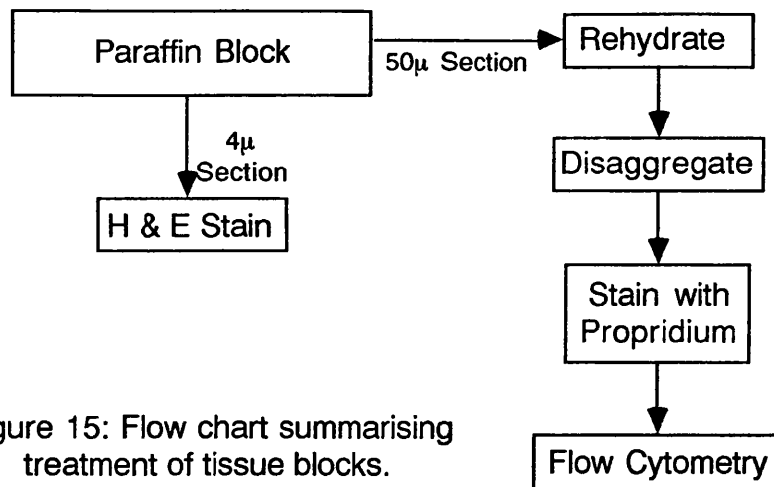


Figure 15: Flow chart summarising treatment of tissue blocks.

The thick sections were dewaxed in graded alcohols. To do this they were individually wrapped in 50µ nylon mesh and placed in steel cages which were then processed in groups of up to 30 on a tissue processor. The stages and times in each were:

Xylene	60mins
Xylene	30mins
100% Ethanol	15mins
100% Ethanol	15mins
90% Ethanol	15mins
70% Ethanol	15mins
40% Ethanol	15mins
Water	15mins
Water	15mins

The cages and mesh were then opened and the usually still intact, rehydrated tissue section transferred with metal forceps to a 5ml plastic test tube.

The sections were then disaggregated by the addition of 1ml of 0.5% pepsin in water at pH 1.5, with incubation at 37°C for 30min. The tubes were centrifuged at 2000g for 5 minutes at 4°C, and the supernatant aspirated manually using a glass Pasteur pipette. 1ml of phosphate buffered saline pH7.4 (PBS) was added to the tubes as a wash solution, and the centrifugation and aspiration repeated. Each sample was then passed through a 25g hypodermic needle by aspiration with a 1ml syringe three times, to achieve additional, mechanical disaggregation, and the suspension passed through a 50µ nylon mesh into a fresh tube. These were again centrifuged and the supernatant aspirated and replaced with a staining solution of 30µg/ml propidium iodide in PBS for 30 minutes at room temperature. After a final spin and resuspension in PBS samples were ready for flow cytometry.

Section iv: Flow Cytometry

All samples were run on the Coulter Epics Profile II benchtop flow cytometer in the University Department of Surgery at the Glasgow Royal Infirmary. This machine has a single, air-cooled, 15mW argon laser emitting at 488 nm, collimated into a beam of elliptical cross section. The sample of between 25 and 200 μ l is injected at a rate of 10 to 100 μ l/second into an outer fluid stream. The combination of sample flow rate and sheath pressure maintains the sample as a very narrow fluid stream such that the contained nuclei progress single file through the beam:

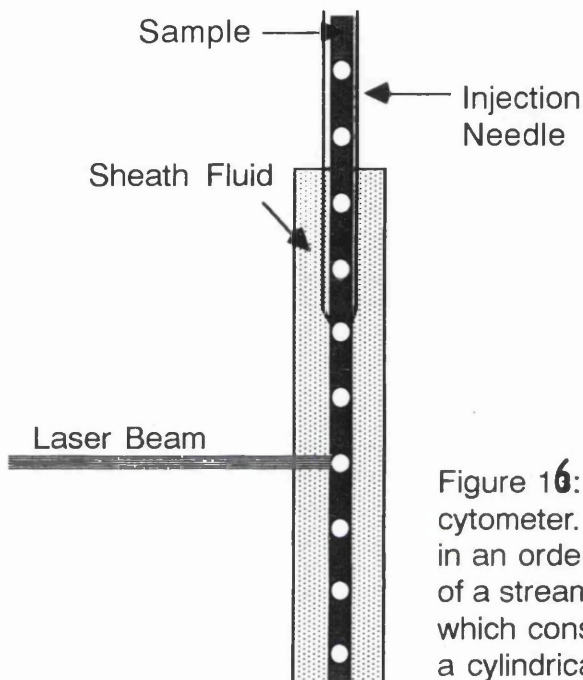


Figure 16: Fluid dynamics of Coulter flow cytometer. Cells are presented to laser beam in an orderly array by injection into the middle of a stream of sheath fluid, the pressure of which constrains the sample fluid to maintain a cylindrical form.

This occurs not in open air as in many cytometers but in a quartz block. Light scattered or emitted by each nucleus is collected directly in front of the beam, and at 90° to its direction where the fluorescence pick up lens recollimates the scattered and emitted light. The side of the quartz block opposite the fluorescence pick up lens is mirrored to direct light scattered away from the sensors back toward them. Within the sensor system are four photomultiplier tubes to which the collimated light is distributed by a system of filters (figure 17). The sensitivity of these detectors can be adjusted by controlling the voltage supplied to them. The signals from each detector are individually amplified using either a linear or log amplification, and displayed and stored by the cytometer until the end of the run. In this machine most parameters can be changed in real time as the run progresses.

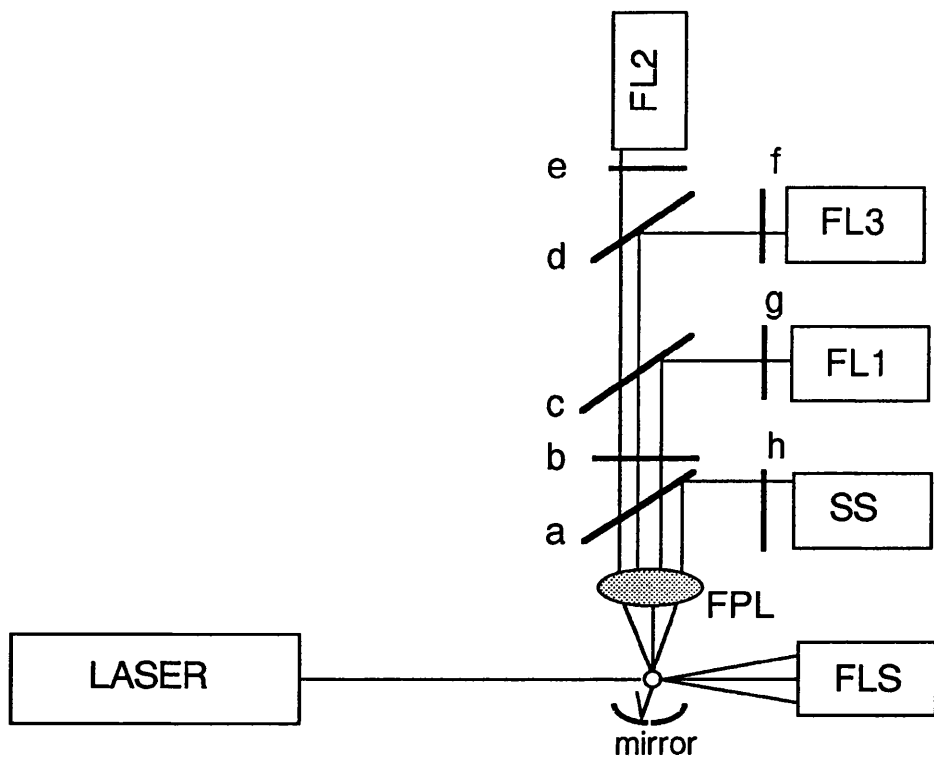


Figure 17: Detection system of the Coulter Epics Profile II flow cytometer. Light scattered from the sample is collected by the fluorescence pick up lens (FPL), and directed by numbered filters to the 4 sensors (FL1,2&3 for various wavelengths of emitted light, and SS for side scatter of laser light). Scattered laser light is also detected by the forward light scatter (FLS) sensor.

In the current study, a 100 μ l sample from each nuclear suspension produced as in the previous section was run at a rate of between 100 and 200 nuclei per second passing through the beam, to a total of 10,000 nuclei. If a suspension proved to be too concentrated for this to be achieved even at the minimum rate of sample flow of 10 μ l/second, it was diluted with further PBS and rerun. If the suspension was too dilute to achieve an adequate flow rate, it was centrifuged and resuspended in a smaller volume of PBS. The sample sheath pressure was set throughout at 7.5psi.

Parameters collected for each nucleus were: forward light scatter (FLS), peak red fluorescence (FL2P) and total red fluorescence (FL2). The filter set up used to achieve this was a 488nm dichroic mirror to split off the scattered laser light (filter a in figure 17) followed by a 457-502nm laser blocking filter (filter b), a 550nm dichroic mirror (filter c, no filter was used in the d position), and 635nm band pass filter in front of the FL2 detector (filter e). In fact filter c is not necessary for this work, but was present as the machine was simultaneously being used for two colour fluorescence work requiring discrimination between green and red fluorescence, which this filter is designed to separate.

The photomultiplier tube voltage was set such that the cell populations lay centrally within the histogram, leaving an adequate number of channels on either side to be used for the estimation of background counts when this was subsequently done in the process of estimating S phase fraction (vide infra, section 7). Usually it was possible to include both diploid and aneuploid populations in the case of aneuploid populations, but with some tumours of very high DNA index (the G_2/M DNA content of which might be 6 times diploid G_0/G_1 content) this was not possible, in which case priority was given to the aneuploid population, upon which S phase fraction estimation was to be performed.

Three histograms were created from these parameters:

a) peak red fluorescence versus total red fluorescence. This histogram is used solely to select the desired population for analysis in the ploidy histogram (histogram c in this list), and to gate out debris and clumped nuclei in doing so. In order to understand the means by which it does so it is necessary to consider the time course of a G_0 phase nucleus passing through the laser beam. The contained propidium iodide will emit fluorescence whilst any part of the nucleus is in the beam. Thus a fluorescent signal (in FL2 in this case) will be detected as soon as the 'leading edge' of the nucleus enters the beam (figure 18(a)). When the entire nucleus is in the beam momentarily later, a larger signal will be detected as more propidium iodide is now being exposed (figure 18(b)). As the nucleus leaves the beam, the detected fluorescence will fall back off (figure 18(c)). The consequent shape of the signal emanating from the photomultiplier is shown in the figure.

It is the area under this curve which is used as the indicator of total propidium content for the purpose of building a ploidy histogram. The figure compares the sequence of events as two objects pass through the beam- firstly the nucleus just considered, and secondly one which consists of two nuclei of exactly half that content clumped together (viewed by the cytometer as a single object). Both have the same propidium content but note that the peak height of the signal given off by the clump is lower than that of the G_2 nucleus, so long as the clump is longer than the height of the beam as illustrated and passes through the beam in a lengthwise orientation (which it will tend to be constrained to do by the fluid dynamics of the flow cell).

In a histogram of the peak signal against the total signal, the two objects will be separate, although they would not be in a ploidy histogram based on the total signal alone. The presence of doublets in such a histogram would artificially inflate the population of G_2/M cells. On the two parameter histogram however, an area of interest can be drawn around those objects having a peak signal 'appropriate' to their total signal, and the ploidy histogram drawn from these objects only, a process referred to as doublet discrimination.

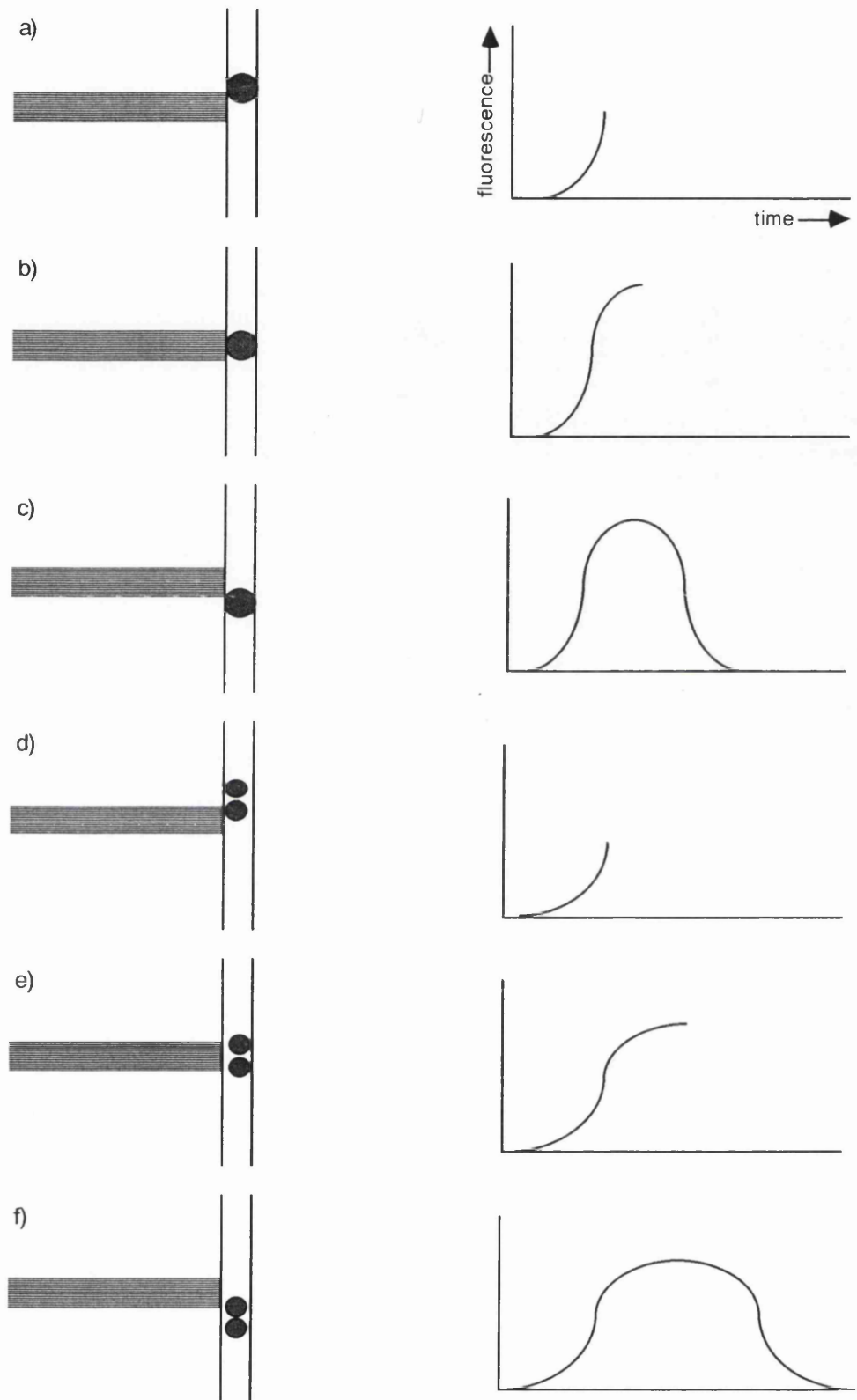


Figure 18: Principle of doublet discrimination, exemplified by the time course of the fluorescence signal recorded as a single object (a-c) and two clumped objects of the same total size (d-f) pass through the laser beam.

b) Forward light scatter versus number of counts. The amount of laser light scattered in the forward direction by each object is related to its size. This histogram is theoretically a frequency histogram of the distribution of nuclear sizes within the sample. At least one previous group have reported that this parameter is of some prognostic significance separate from that of ploidy and SPF (Stål et al, 1989). They used fresh tumour material with added trout and chicken red blood cells, against which nuclear size could be standardised. Our own experience was that FLS was highly variable between samples, and in the absence of any means of standardisation because of the use of paraffin embedded material, it proved to be impracticable to obtain reliable measurement of size in this way.

c) Total red fluorescence versus number of counts, which is the ploidy histogram. It was produced only from counts which fell within an area of interest drawn on histogram a, a process referred to as gating. The area of interest is drawn with a touch sensitive pad attached to the cytometer, and is done in real time while run is in progress (it can be altered subsequently if necessary). It is drawn so as to exclude doublets in the manner discussed above.

Section v: Data Storage

Data from each sample was stored in two ways. The ploidy histogram produced during the run was stored as such onto the hard disc within the machine at the end of the run, and at the end of each session these histograms were downloaded to floppy discs. These discs were then used to transfer the histograms to the separate personal computer on which offline analysis was performed in order to calculate SPF.

The cytometer's data list, containing the raw data from each photomultiplier tube, was also copied onto floppy discs at the end of each run. It is bulky in storage terms (each data list amounts to some 100 kilobytes of disc space), but allows most run parameters to be altered and the histograms to be recreated in the light of the modifications, which cannot be done with the histogram data alone. The list mode data was not used in this study, but was transferred to storage tape in case future reanalysis is indicated.

Section vi: Allocation of Tumour Ploidy

Ploidy histograms were classified simply as diploid or aneuploid, using the population of non-tumour cells within the sample as a standard. If the tumour cells have the same DNA content as the non-tumour cells, then only a single population will be seen in the histogram (diploid), if not then two or more populations will be seen (aneuploid). Matters are not always as clear cut as this would suggest. For instance, does a histogram with very broad peaks represent poor quality, or is it so because there are

two populations very close to one another such that they are not resolved into separate peaks? How large does a putative aneuploid peak have to be before it is accepted as such? Is a substantial peak in the G_2/M position for the diploid population an indication that there are many cells in those phases of the cycle, or does it suggest that there is an overlying aneuploid population with exactly twice the diploid DNA content? There is an element of subjectivity to the allocation of ploidy for some histograms, since different observers will interpret answer the above questions differently in specific instances. This has been demonstrated by Kallioniemi et al (1990) as a cause of interlaboratory variation.

Two means have been used to limit this problem in the current investigation. Firstly, all histograms were reviewed and discussed jointly by a panel of at least three people experienced in this area, and the interpretation of each histogram determined by consensus. In cases of uncertainty, a further section was processed and run, and the two histograms considered together. Secondly, objective (although arbitrary) criteria were used to answer two of the queries in the paragraph above:

a) Histograms were only considered interpretable if the coefficient of variation (CV) of the putative diploid G_0/G_1 peak was less than or equal to 10%. This provides a means of excluding histograms of poor quality, and those with near-diploid populations which cannot be resolved from the diploid peaks (which would wrongly be classified as diploid). This concept of the CV of a peak requires explanation. All of the G_0/G_1 cells of a given cell population have exactly the same DNA content, certainly in the case of normal cell populations. They should therefore all demonstrate exactly the same amount of fluorescence in the flow cytogram, and be counted in a single channel. In reality there are minor variations in the staining of each nucleus, and in the signal detected by the cytometer even given exactly the same emitted fluorescence, as explained above. As a result, the cells are not counted in one channel, but rather in several. The more the variation due to technical factors, the wider the peak. Such variation is greater for peaks with a high mean amount of fluorescence, as a 1% 'error' for a cell of theoretical fluorescence of 50 units will only be half of that resulting from the same error for a cell with 100 units of fluorescence. The CV is the ratio between the standard deviation and mean channel of a peak. It expresses the peak width in relationship to its position in the histogram, and so takes account of this 'magnifying' effect of a stronger mean signal.

b) A putative aneuploid peak overlying the diploid G_2/M peak (a so-called tetraploid peak) was only considered to exist if the proportion of total histogram events contained within that peak exceeded 15%. In respect of such peaks, the acceptable range for the DNA index (DI, see Ch.3, Sect. v) was taken to be 1.85-2.10. Obviously, the DI of

the G_2/M population should theoretically be 2.0, but varies from this is a result of non-stoichiometry in dye binding, and non-linearity of the machine response to increasing signal strength. The range stated was based upon that observed in diploid histograms. The reason for having such a criterion was that if the mean channel of a putative G_2/M peak fell outside of this range, it was presumed that the peak must actually represent a small G_2/M peak merged with a larger aneuploid G_0/G_1 peak of DI outside of the range. In this circumstance, the presence of the aneuploid population would be accepted without the need to fulfill the 15% criterion.

Section vii: Estimation of S Phase Fraction (SPF)

SPF was calculated using the Cytologics software package provided by Coulter Electronics, run on an IBM compatible, 386-based PC. All histograms were assessed by the author. With this software, the histograms are read off the floppy discs on which they were stored by the cytometer at the end of each session. The area of the histogram containing the population of interest is then indicated by the placement of cursors in channels either side of that population. Only counts within these cursors were then further considered by the software.

An option is then provided for the subtraction of background counts due to debris and machine 'chatter'. Within the Cytologics package, this is done using an exponential model (that is, with an assumption that the number of background counts falls off exponentially from left to right in the histogram). This model was found by Feichter et al (1988) to provide the best of correlation of SPF with TLI. In this study, background subtraction was always attempted, although in a minority of cases, it was not felt that an adequate estimate of background counts was produced by the software, and so the uncorrected histogram was used for the estimation of SPF. The estimate of background counts is produced by the placement of cursors around channels on either side of the population of interest, felt to represent background counts only, that is, to the left and right of all populations within the histogram. The fact that this will need to be done has to be borne in mind when the samples are run on the cytometer, so that the PMT voltage is set such that adequate areas are deliberately left at the margins of the cell populations. The number of counts in the indicated channels is then used by the software to calculate the putative background counts in the channels in between, that is in the area of interest. This curve is drawn onto the screen superimposed onto the histogram (figure 19), and an option is provided to accept or reject the estimate. If rejected, an option is provided to try again using different channels to indicate the background counts, and the method is very sensitive to changes of even a single channel on some occasions. Whether an estimate is accepted is purely a matter of subjective assessment on the part of the operator. In the current study, the major criterion was whether the background curve paralleled the top of the S phase

component of the histogram- that is, converted this compartment into a rectangle, this being the presumed shape of S phase for this investigation.

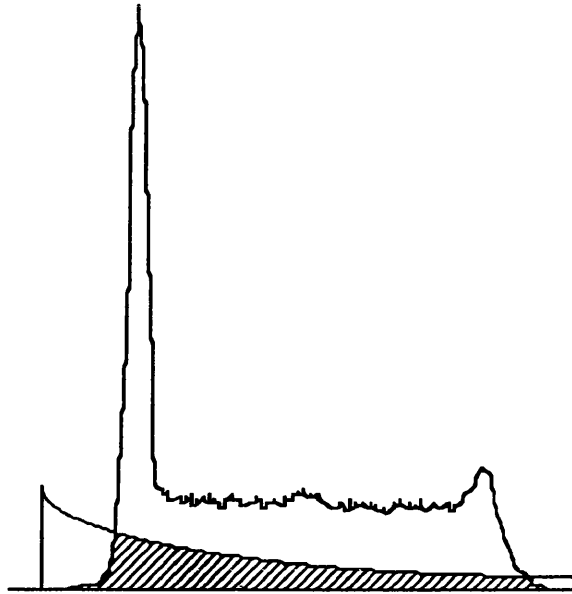


Figure 19: Exponential model of background counts used by the Cytologics analysis software. The counts regarded as due to debris are included in the shaded box.

The programme next detects what it regards as the G_0/G_1 peak, and places cursors to mark it. The operator is given the chance to move these cursors, and this option was always exercised. The reason for doing so is that the software looks for the top of the peak, its sharpest and most symmetrical part. It then assumes that the peak is Gaussian in shape and extends this top down in both directions to form the full peak, rather than following the actual shape of the peak. Any surplus of counts when this theoretical peak is subtracted from the actual peak are counted as events outside of G_0/G_1 . On the right hand side, these are regarded as S phase cells. Now the presence of S phase cells with DNA contents down as low as the mean channel of the G_0/G_1 peak is undeniable, and these will produce a non-Gaussian distortion of this side of the peak, but the fact that such variation is often seen to just the same extent on the left side of the peak indicates that this is not the predominant source of this phenomenon. As such, allowing the software to make this interpretation will inflate the apparent S phase fraction, and this is borne out by the fact that the compartment as fitted with the Gaussian assumption visibly exceeds the interpeak size of the S phase fraction. Subjectively more satisfactory estimates are obtained by moving the cursors indicating the top to the G_0/G_1 peak to encompass the entire peak. This process of identification and modification is then repeated for the G_2/M peak. An option is now provided to exclude any extraneous peaks overlapping the S phase. In the most common aneuploid tumour, with a DNA index of between 1.5 and 1.8, the G_2/M peak of the diploid cells

will do just this. If any such peak requires identification, this is done in just the same way as the G_0/G_1 and G_2/M peaks.

The software now subtracts from each channel in the area of interest the calculated background counts and the counts attributed to any peak, and takes the remaining counts between the G_0/G_1 and G_2/M peaks to be due to cells in S phase (figure 20). In an aneuploid histogram, S phase is divided into two separate compartments either side of the intervening diploid G_2/M peak: If this peak is too close to either of the aneuploid population peaks, there may be no net counts in the channels in between, and so the computer will fit no S phase to this area. This is one reason why histograms with lower CVs (narrower peaks) are more readily analysable.

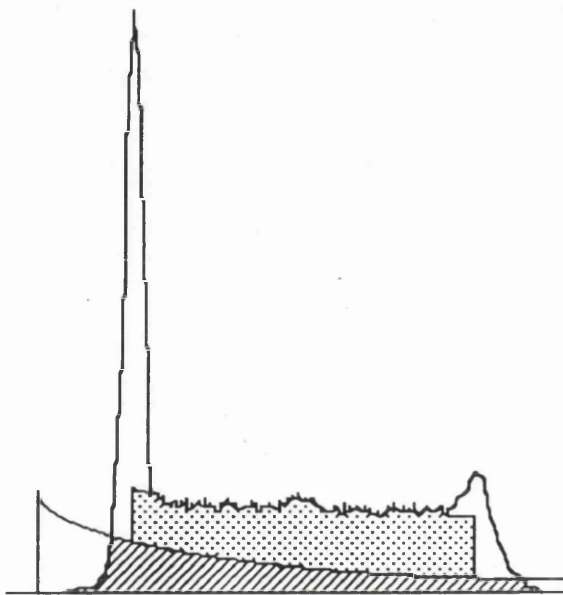


Figure 20: Estimation of SPF (dotted region) as the net counts remaining after subtraction of the background counts (shaded area), extending from the middle of the G_0/G_1 peak to the middle of the G_2/M peak.

Four models are provided within the software for converting the net S phase counts in each channel into an estimate of the S phase fraction. That used here and in nearly all other series is a rectangular model, owing originally to Baisch et al (1982). To use this model, the computer simply sums the net S phase counts and divides by the number of channels between the mean channels of the G_0/G_1 and G_2/M peaks to give the average number of S phase counts per channel. The S phase fraction is then represented as a box stretching between the means of the G_0/G_1 and G_2/M peaks, with a height equal to the mean S phase counts per channel. In numerical terms, the SPF is the sum of the net counts, expressed as a percentage of the total counts (less background) in that population. The fitted compartment is displayed on screen, and its suitability assessed, which is a purely subjective assessment on the part of the operator as to whether it fits

over the S phase component of the histogram in the way illustrated in figure 20.

The other three models provided by the software were used only in the reproducibility studies in this experiment. All four are illustrated on a blown-up histogram in figure 21. The trapezoid model fits a compartment analogous to the rectangular, but instead of a horizontal line on top of the compartment (created by averaging the counts in each channel), uses a straight line of any slope (calculated by least squares regression of the counts). The rectangular model is a special case of the trapezoid with the slope of the line restrained to be zero. The quadratic model fits the counts with a second order quadratic, such that the top can now have a varying slope. The three models so far discussed fit a single compartment extending from the middle of the G_0/G_1 peak to the middle of the G_2/M peak. The fourth model, the multiple broadened rectangles, takes a different approach, by dividing S phase into up to 9 compartments (the number is user selectable). Gaussian curves are then fitted to each compartment and the areas under these summed. Unfortunately the Cytologics package implements this model poorly, as it often fits negative compartments, which is of course a theoretical nonsense.

Section viii: Statistical Methods

The distribution of values of SPF was not statistically normal, and so non-parametric methods have been used. For description, medians and either full or interquartile ranges are given, whilst for comparison of the SPFs of sub-groups the Mann-Whitney (where there are only two groups) or Kruskal-Wallis (for three or more groups) have been applied. In analysing ploidy differences between sub-groups, the chi-square test was used. The only parametric statistic employed was the two sample t test, for comparing the, normal, age distributions of patients with aneuploid and diploid tumours. Differences between groups were regarded as statistically significant if the null hypothesis had a probability <5%.

Survival analyses were carried out to relate survival to ploidy, SPF, lymph node status (positive or negative), tumour size (T1, T2, T3), oestrogen receptor status (positive or negative), and *c-erbB-2* staining (positive or negative). Patients known to be alive at Jan 1st, 1990 or who were known to have died from causes unrelated to cancer, were treated as censored observations. Univariate analysis was performed using Kaplan-Meier estimates and log rank tests. In light of the differences between SPF as calculated in DNA diploid and DNA aneuploid tumours, the effect of this variable was analysed separately for the two ploidy groups. A combined analysis using a common median was also done, on the grounds that this was the method used in other reports. Multivariate analyses used the Cox proportional hazards regression model, using both forward and backward selection of variables. The tests sought interactions within a

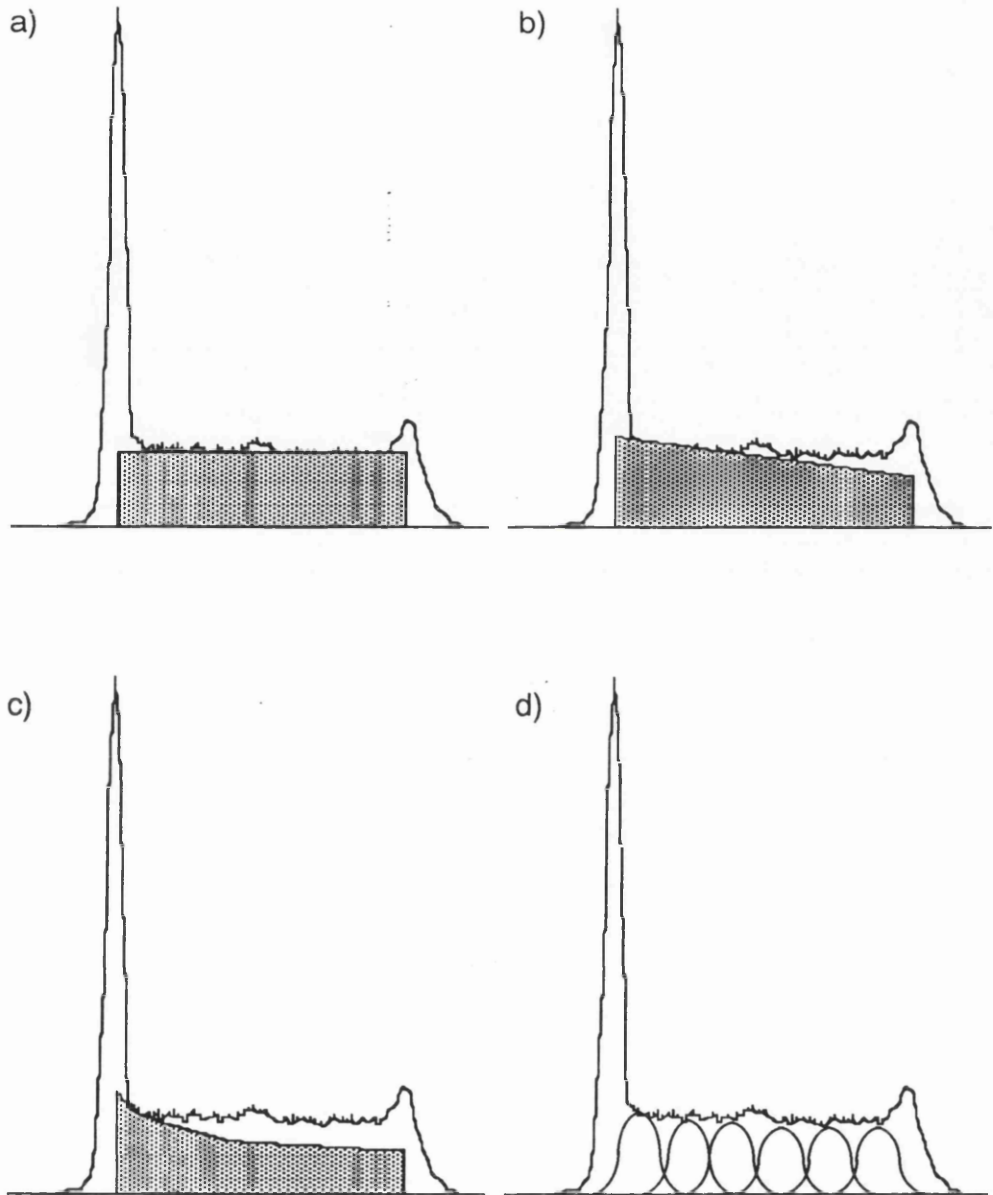


Figure 21: Models of S phase available in the Cytologics analysis package. a) rectangular; b) trapezoidal; c) quadratic; d) multiple broadened rectangles. In a) - c) the estimated S phase fraction is shown by the dotted region (background counts are ignored). In d) the SPF is the combined area under the Gaussian curves.

model containing the effects of six prognostic variables - ER status, node status, size, *c-erbB-2* status, ploidy and SPF. SPF was analysed as a binary variable, above or below the median appropriate to the ploidy of that particular tumour.

Inter- and intra-observer variation, and the comparison of different models of S phase were carried out by the method of Bland and Altman (1986), who pointed out that the correlative approach used up to that time to compare two means of measuring the same thing was not ideal, in that this statistical process is designed to test the hypothesis that two samples are not independent. If the samples represent two measurements of the same thing, then perforce they are not independent, and the existence of a correlation is almost preordained. Bland and Altman suggested that it was more appropriate to describe the differences between estimates of the same thing, rather than the similarities. The method which they developed was to take the difference between each pair of observations upon the same patient or specimen. Statistical description of the distribution of these differences then provides two items of information:

a) the mean of the differences indicates whether there is any tendency for one set of observations to consistently exceed the other, and if so by how much. This follows from the fact that however widely the pairs of observations may vary in individual cases, if neither has an intrinsic tendency to give a higher answer than the other, then observation A will be higher than observation B just as often as the contrary holds, and by the same average amount. The difference of the mean from the null expectation that it will be zero can be tested with a one sample t test, but this can be approximated by considering the 95% confidence intervals for the mean as lying 2 standard errors on either side. If zero does not lie between these intervals, then a significant difference exists, and the limits of the probable size of this are indicated.

b) Even if the mean difference is zero, the differences between the two observations or measurements in individual cases may be large. The magnitude of the individual differences is indicated by the standard deviation of the distribution. Since the distribution of differences will tend toward a normal distribution (Bland, 1987, p.172), it is reasonable to state that 95% of differences will be less than 2 standard deviations from the mean.

This method of analysis can be displayed graphically by plotting the difference between each pair of observations against the mean of the two. In the medical sphere, the differences often tend to be proportional- that is, the difference increases as the value of the measurement gets larger. In such cases it may be more appropriate to describe the ratio between each pair, rather than the absolute difference, a suggestion made by Murray and Miller (1990). This will then be independent of the value of the measurement, for if this criterion is not met it would really be necessary to give a mean

difference (or ratio) and standard deviation (SD) for each value or range of values of the original measurement, rather than one overall mean and SD. The modification of Murray and Miller is more often used for the analyses in this study because ratios did indeed demonstrate greater independence.

In light of the novelty of this method of analysis, it is worth examining an example in more detail, for which we will use some of the data from part III. In chapter 9, section xi (b), the following results are given for calculating a labelling index by two methods in the same 19 tumours. In each case the difference between the two values is also given:

Method 1:	0.4	2.9	9.5	0.6	5.0	1.3	2.2	1.9	1.8	0.6
Method 2:	1.1	3.2	8.9	0.5	3.2	1.2	1.6	1.2	0.8	4.1
Difference:	-0.7	-0.3	0.6	0.1	1.8	0.1	0.6	0.7	1.0	-3.5
Method 1:	7.1	2.2	8.2	8.3	8.3	9.9	3.7	8.0	1.2	
Method 2:	5.1	1.9	7.9	4.8	5.1	7.9	3.6	6.4	0.8	
Difference:	2.0	0.3	0.3	3.5	3.2	2.0	0.1	1.6	0.4	

The respective median labelling indices are 2.9% and 3.2%, not significantly different on a Mann-Whitney test ($W=391.5$, $p=0.55$). The pairs of values are plotted against each other in fig 22(a) below, showing clear correlation. The Spearman coefficient, $\rho=0.86$, $p<0.0005$. This would lead conventional analysis of these results to conclude that the two methods gave similar results. All it actually shows is what it says- that there is a correlation between the values obtained by the two methods. This is hardly surprising, and tells us nothing about the results in individual cases.

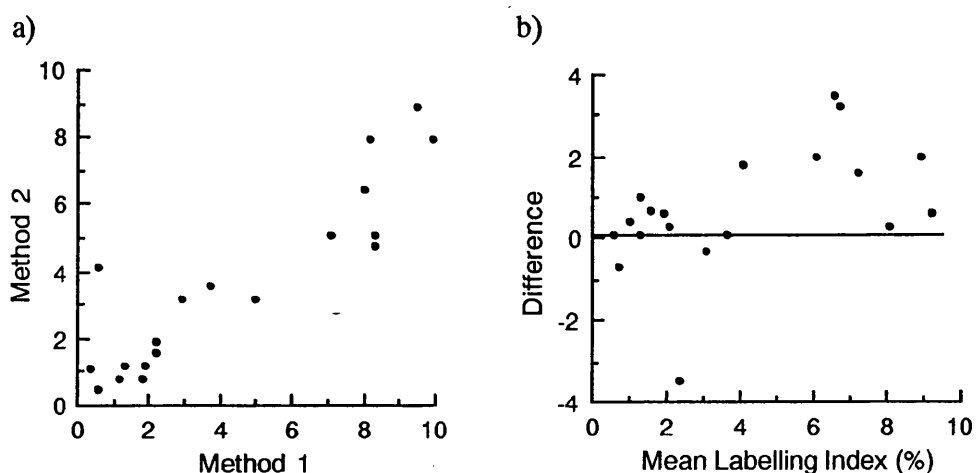


Figure 22: Two ways of comparing results from two methods for measurement.

a) correlative approach b) Bland-Altman approach. See text for details.

We see pairs like 0.6% vs 4.1%, and 8.3% vs 5.1%. If we take the difference between the pairs in each case, and plot these against the mean value for each pair (because this

is the best guess as to the 'real' value), we get the graph in fig 22(b). Now ideally the differences will all be on the zero line (both methods the same), but we can see firstly that most points are above this line, and that some are quite distant from it. This indicates that method 1 tends to give higher values than method 2, and that large differences occur in some cases.

We can summarise this using descriptive statistics for the distribution of differences. The mean difference is +0.73%, with a standard error of 0.35%, and a standard deviation of 1.52%. This confirms that method 1 gives larger estimates, since the mean is above zero. Since this mean (0.73) is more than two standard errors (0.35) from zero, this trend is probably statistically significant at the 5% level, which can be confirmed by performing a t-test of $\mu=0$ for the 19 differences, which gives $t=2.08$, with $p=0.05$. With a standard deviation of 1.52%, the 95% confidence interval for the difference is 3.04% (2×1.52) either side of the mean difference. That is, in 95% of cases we would expect the difference between the two to be no more than $0.73 \pm 3.04\%$, or from -2.31 - 3.77%. That sort of difference is large in relationship to the labelling indices themselves (up to 10%, but with a median of around 3%). It can be seen from fig 22(b), that the differences get larger as the mean value increases, and for this reason in the Chapter 9, when these data are analysed, this is done in terms of the ratio of the two estimates, rather than the difference between them as here.

Section ix: Reproducibility Studies

Because of the subjectivity in the measurement of S phase fraction in terms of defining peaks and background subtraction (section 7), experiments were carried out to assess the inter- and intra-observer variation for this measurement. These were not carried out upon histograms from tumours in the Liverpool Breast Cancer Series. They were however performed upon breast cancers, from a series of lumpectomy specimens collected by Mr C S McArdle at the Glasgow Royal Infirmary between 1983 and 1986, for the purpose of looking at predictors of local recurrence after breast conserving cancer excision. Blocks were obtained for all 119 of these tumours, which were processed for flow cytometry in exactly the same way as described in section 3. The ploidy histograms were then analysed to obtain estimates of SPF as explained in section 7. This was done by the author on two separate occasions two months apart, using each time all four models available within the Cytologies software and not just the rectangular method used for the prognostic analyses above. Independent measurements of SPF using the same histograms were also performed at two times, using the rectangular method, by another worker within the laboratory (Ms S J Oakes). A total of ten estimates of SPF for each of the 119 histograms was therefore made (or at least attempted). These data sets have been analysed using the Bland-Altman method to assess the reproducibility of this endeavour.

Chapter 6: Results

Section i: Patient Characteristics

Paraffin blocks were found for 329 tumours from the original series total of 749 patients, for the reasons given in section ii of the previous chapter. Histological review indicated that 36 of these blocks examined showed no remaining tumour. The study population for the current series consisted of the 293 remaining specimens. The distribution of prognostic factors is available for the 224 from whose tumours SPF could be gained (vide infra, Section iv), and is indicated below:

Variable	Groups	n	%
Nodal Status	N0	130	59
	N1	91	41
Tumour Size	T1	19	9
	T2	152	71
	T3	43	20
Grade	1	41	34
	2	39	33
	3	39	33
ER Status	Pos	128	59
	Neg	88	41
<i>c-erbB-2</i> Status	Pos	52	24
	Neg	163	76
Menopausal Status	Pre	49	24
	Post	159	76

Table 13: Distribution of prognostic factors among the 224 patients from whom both SPF and ploidy were available

Section ii: Basic Ploidy Data

Histograms meeting the criteria enunciated in the methods section were obtained in 281 cases (96% of those with tumour-containing blocks). Appendix I gives the following raw data for each of these tumours- CV of the G₀/G₁ peak, ploidy, DNA index, SPF, and (in Appendix Ia, in respect of patients for whom SPF is available) the menopausal status of the patient, tumour size, nodal status, histological grade, oestrogen receptor and *c-erbB-2* status. 179 (64%) of histograms were classified as DNA aneuploid, and 102 were DNA diploid. The median CV for the G₀/G₁ peak was 5.6% (interquartile range 4.6 - 7.0%). The distribution of DNA indices is shown:

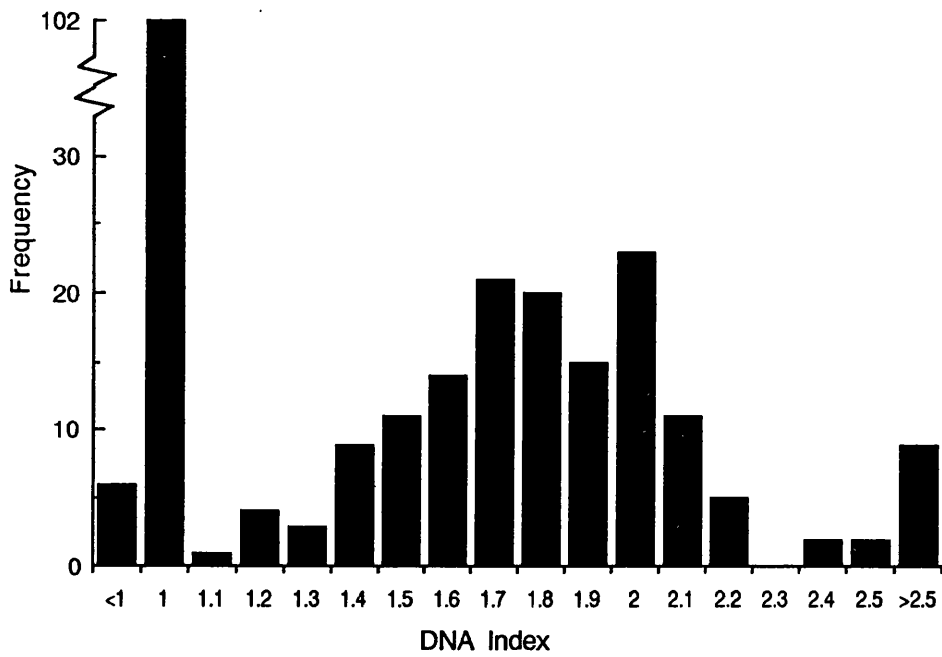


Figure 23: Distribution of DNA indices for 281 tumours in which interpretable histograms were obtained, excluding the 18 polyploid tumours.

The relationships between ploidy and other prognostic factors recorded for each patient are analysed in table 14. There is no statistically significant difference in the distribution of subgroups for any factor when cases are divided by ploidy. There is a trend for erbB-2 positive tumours to be aneuploid, but in the case of tumour size, nodal status, menopausal status and expression of oestrogen receptors there is really no suggestion of a relationship with ploidy in this group of patients. Mean age of patients with diploid tumours was 58.4 years, and for patients with aneuploid tumours was 58.1 years, there also being no statistically significant difference between these two ($t=0.15$, $df=191$, $p=0.88$).

	Menopausal Status		Tumour Size		
	Pre	Post	T1	T2	T3
Diploid	43	42	42	41	37
Aneuploid	57	58	58	59	63
	Nodal Status		Histological Grade		
	N1	N2	G1	G2	G3
Diploid	42	41	39	49	38
Aneuploid	58	59	61	51	62
	Oestrogen Receptor Status		ErbB-2 Expression		
	ER+	ER-	erbB2-	erbB2+	
Diploid	44	36	45	33	
Aneuploid	56	64	55	67	

Factor	χ^2	df	p
Menopausal Status	0.028	1	0.867
Tumour Size	0.268	2	0.875
Nodal Status	0.017	1	0.896
Estrogen Receptor Status	1.178	1	0.278
erbB2 expression	2.607	1	0.106
Histological Grade	1.072	2	0.585

Table 14: Relationship between tumour ploidy and various prognostic factors. In the upper part of the table, tumours are subdivided by each factor, and the percentage of diploid and aneuploid tumours in each subgroup is given (ie all figures are column percentages). The chi-square statistics for each comparison (using the raw data rather than percentages given in the lower part of the table). Raw data in Appendices I and Ia.

Section iii: Prognostic Power of Tumour Ploidy

Univariate analysis of survival stratified by ploidy is shown in figure 24. There is a survival advantage in favour of DNA diploid tumours of 4% at five years and of 3% at 10 years, but this result is not statistically significant. Expressed in terms of a hazards ratio, the relative hazard for patients with DNA aneuploid tumours is 1.20 with 95% confidence limits of 0.81 - 1.76.

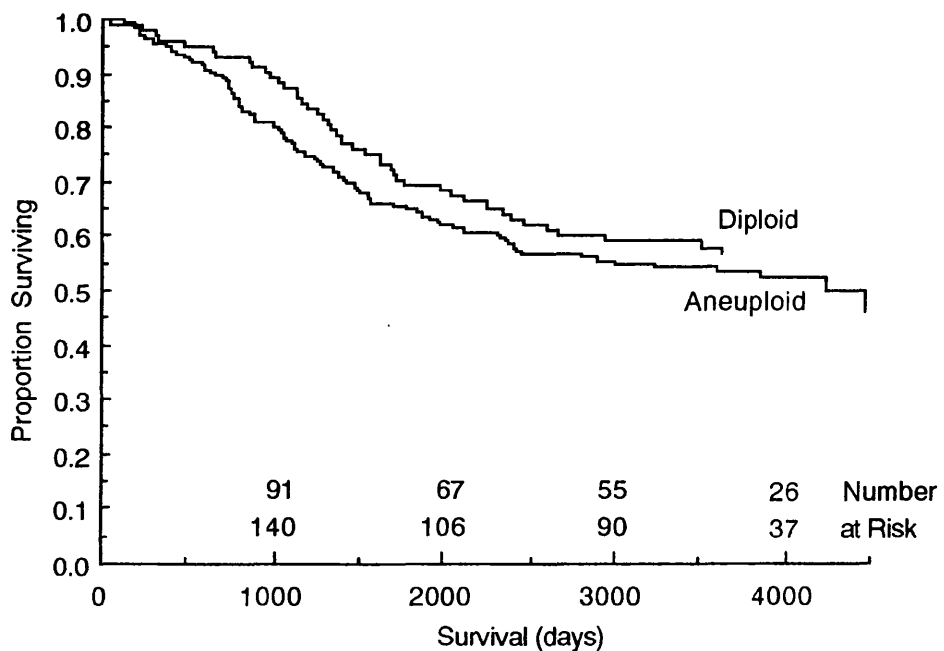


Figure 24: Life table for 281 patients subdivided by the ploidy of their tumours. Probability of difference between the groups (log rank χ^2) = 0.23.

Section iv: Basic Data on S Phase Fractions

Estimates of SPF were obtained in 224 cases (80% of those from which ploidy was interpretable). The median value of SPF was 7.25% overall, 4.5% in DNA diploid tumours and 10.9% in DNA aneuploids. The distribution of values of SPF is shown:

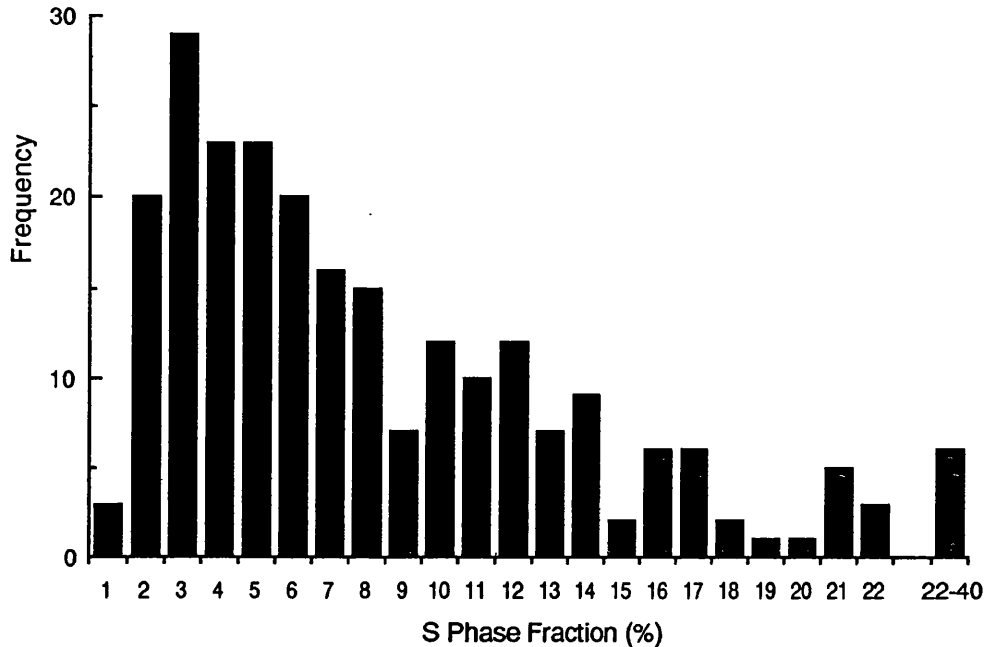


Figure 25: Frequency distribution of SPF in the 224 cases in which it was available. Values along the x axis are midpoints, that is 3 represents values 2.50 - 3.49.

No attempt has been made to compare the distributions of values for DNA diploid and DNA aneuploid tumours statistically, because of the different nature of the measurement in the two types of histogram (see discussion). The relationship between SPF and other prognostic factors has also been analysed separately in the two ploidy groups, as otherwise the comparisons would be based on a combination of ploidy and SPF. This is because a subgroup with a higher proportion of aneuploid tumours would tend to have a higher mean SPF for this reason, so that a difference in SPF between groups could be due to a ploidy imbalance alone. The relationships between SPF and other prognostic factors, looked at in this way, are shown in table 15. Analyses were performed using the Mann-Whitney test where 2 groups are being compared and the Kruskal-Wallis test when 3 groups are involved (tumour size, histological grade). Results significant at the 5% level are underlined. Node positive, high grade, and oestrogen receptor negative tumours had significantly higher values for SPF. In the case of nodal status and ER status, this was only the case for aneuploid tumours, but with a trend in the same direction for diploid tumours. This may simply reflect the fact that there are twice as many aneuploid as diploid tumours. The only other positive finding is that pre-menopausal women had tumours with higher SPF than postmenopausal women.

Factor	Ploidy	Subgroup	Median SPF	p
Nodal Status	diploid	N0	4.05	
		N1	4.50	<u>0.674</u>
	aneuploid	N0	9.90	
		N1	12.55	<u>0.003</u>
Hist. Grade	diploid	G1	3.10	
		G2	4.40	
		G3	4.80	<u>0.035</u>
	aneuploid	G1	10.50	
		G2	12.85	
		G3	11.95	<u>0.039</u>
Menopausal Status	diploid	pre	5.60	
		post	4.15	<u>0.05</u>
	aneuploid	pre	11.7	
		post	10.5	0.397
erbB-2 expression	diploid	neg	4.1	
		pos	4.1	0.968
	aneuploid	neg	10.3	
		pos	11.3	0.15
Tumour Size	diploid	T1	4.35	
		T2	4.10	
		T3	5.15	0.381
	aneuploid	T1	9.4	
		T2	11.3	
		T3	11.9	0.199
Estrogen Receptor Status	diploid	pos	4.3	
		neg	4.65	0.532
	aneuploid	pos	9.55	
		neg	12.2	<u>0.019</u>

Table 15: Relationship between prognostic factors and S phase fraction. Analyses using Mann-Whitney and Kruskal-Wallis tests. Significant results underlined.

It should be stressed that these results are not independent; for instance there may be more node positive tumours among the premenopausal women. This type of analysis does not address the question as to which of the prognostic factors if any is functionally associated with SPF, and which are associated secondarily.

The relationship between tumour size and SPF is potentially interesting. A large tumour may have become so either because it has grown faster, or because it is further along in its natural history; in this case, if Gompertzian conditions apply, it may actually be growing more slowly than an earlier tumour. Although there is no statistically significant difference in this series, the trend in both diploid and aneuploid tumours is for an increase in SPF with tumour size. This supports the former hypothesis, that large tumours are so because they are intrinsically faster growing. This assumes that tumours do not grow in an 'inverse Gompertzian' fashion and speed up as they enlarge, but there is no evidence that this is the case.

Section v: Prognostic Power of S Phase Fraction

Life tables for survival for these populations split at the respective medians, and at the overall median, are shown in figure 26. None of these analyses show a statistically significant survival effect of SPF. Analysis was also performed within each ploidy group using quartiles of SPF, to assess whether there was an effect restricted to extreme values, but this provides no evidence that this was the case (table 16). The relative hazard for all tumours with above median SPF, regardless of ploidy, is 1.31 with 95% confidence intervals 0.87 - 1.98.

Ploidy	Survival	Q1	Q2	Q3	Q4
Diploid	5 yr	67	78	58	75
	10 yr	54	65	53	55
Aneuploid	5 yr	71	69	60	58
	10 yr	59	57	49	45

Table 16: Percentage survival at 5 and 10 years in subgroups defined by tumour ploidy, and quartiles of SPF within each ploidy group.

Section vi: Multivariate Analysis

Multivariate analysis using the Cox proportional hazards model was carried out in the 201 cases where all prognostic variables were available for the tumour (table 17). This represents 72% of tumours for which ploidy was measured, and 89% of those for which SPF was available. In a stepwise procedure with all terms starting out of the model, only nodal status is found to be independently prognostic. The same result is

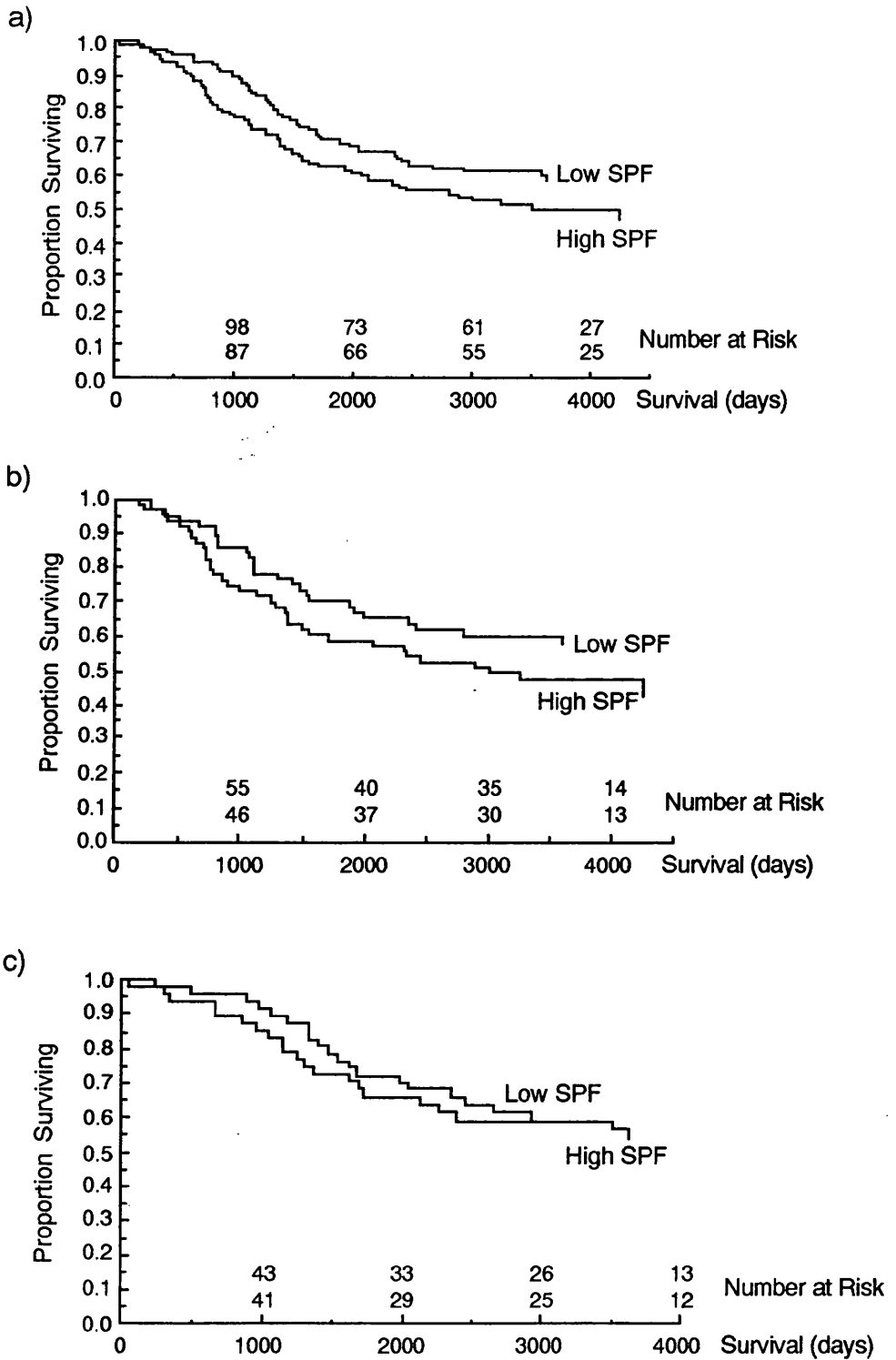


Figure 26: Life tables for tumours divided by SPF above or below median value. a) all tumours (median 7.25%, $p=0.11$) b) aneuploid tumours (median 10.9%, $p=0.33$) c) diploid tumours (median 4.5%, $p=0.33$)

obtained with a model where all terms start in. The relative hazard for aneuploid tumours was 1.17, and for high SPF 1.28, but both have very wide confidence intervals, are not statistically significantly different from 1.0.

Because this excludes almost a third of cases for which ploidy was available, the prognostic effect of the two study variables was also analysed using all data available for each patient (table 18). The results were very similar to the preceding analysis; no independent prognostic effect for ploidy or SPF was observed.

Variable	Coeff.	SE	$e^{\text{coeff.}}$	$e^{\text{co.-2SE}}$	$e^{\text{co.+2SE}}$
Nodes	0.6457	0.2199	1.9073	1.2286	2.9609
ER	-0.0766	0.2281	0.9263	0.5870	1.4617
erbB-2	0.0445	0.2570	1.0455	0.6253	1.7480
T1	-0.7860	0.5010	0.4557	0.1673	1.2411
T2	-0.4902	0.2528	0.6125	0.3694	1.0155
Ploidy	0.1568	0.2264	1.1697	0.7438	1.8397
SPF	0.2495	0.2225	1.2834	0.8224	2.0027

Table 17: Multivariate analysis 201 cases in which all variables available. The column $e^{\text{coeff.}}$ gives the relative hazard for that variable, and the following two columns are the lower and upper limits of the 95% confidence intervals for the hazard. Nodal status is the only significant predictor of survival in this model, as it is the only variable for which a hazard of 1.0 is not included within the confidence intervals.

Variable	n	Coeff.	SE	$e^{\text{coeff.}}$	$e^{\text{co.-2SE}}$	$e^{\text{co.+2SE}}$
Nodes	728	0.7699	0.1139	2.1595	1.720	2.712
ER	714	0.2289	0.1149	1.2572	0.999	1.582
erbB-2	449	-0.3407	0.1677	0.7112	0.508	0.995
T1 v T2	574	0.3471	0.2086	1.4150	0.932	2.147
T1 v T3	220	0.7778	0.2271	2.1768	1.382	3.428
Ploidy	273	0.1792	0.1926	1.1963	0.814	1.758
SPF	220	0.2698	0.2063	1.3097	0.867	1.979

Table 18: Multivariate analysis using all data available for each patient. Columns correspond to those in table 17 (ie relative hazard and confidence intervals in the last three columns).

Section vii: Reproducibility Studies

Two or more estimates of SPF could be made from histograms obtained from 91 of the 119 blocks (76%) analysed in this experiment. This is very similar to the rate of interpretability seen in the main series. 7 of the blocks were found upon histological review not to contain tumour, but these have been retained within the current analyses, as the question here is not one necessarily specific to tumour histograms. In respect of these 91 cases, Appendix II gives for each histogram the half peak coefficient of variation (CV), ploidy, and each SPF estimate made. The median CV for these histograms was 4.5%. 45% of histograms were aneuploid (49% of tumour histograms). More than half of all estimates made with the multiple broadened rectangles model (model 4) were negative, presumably because of poor implementation of the model by the software. Since this is theoretically ludicrous, results given by this model were not further considered in analysis.

a) Comparison of different models of S phase

Let us start by comparing the results given by each to the three remaining models (rectangular, trapezoid, quadratic) on the same histograms. In my first analysis of the series, an estimate for the SPF was gained with the rectangular and trapezoid models in 87 cases each, and for the quadratic model in 80 cases. Results are shown for analysis by the Bland-Altman technique. For each histogram, the estimate of SPF obtained by one method had been divided by the estimate obtained by another. The distribution of these ratios is summarised in the table below, to provide the information discussed in section 8 of the Methods chapter.

Comparison	n	Mean Ratio	SE Mean	SD Ratios
Rectangular/Trapezoid	87	1.114	0.021	0.193
Rectangular/Quadratic	80	0.917	0.053	0.472
Trapezoid/Quadratic	80	0.846	0.047	0.424

Table 19: Comparison of estimates of SPF made by analysing the same histograms using different models. In each row, the answer obtained using the first named model has been divided by the answer obtained using the second named model. The summary statistics describe the distribution of these ratios. Raw data in Appendix II.

This reveals that the quadratic model gave the highest answer on average, followed by the rectangular model and the trapezoid in that order. The low standard deviation of the rectangular vs trapezoid comparison indicates that in this case the rectangular model tends to relatively consistently give an estimate higher than the trapezoid by the mean ratio (ie, by 11%); that is, these two models give consistently similar results with one a little higher than the other. The two comparisons involving the quadratic model both

have much higher standard deviations, which shows that although it gives on average a higher estimate of SPF than either of the other two models, it is sometimes much higher, and sometimes a lot lower. This method is less consistent judged against the other two. It is also possible for fewer of the histograms (80 of 87 for the other two).

Let us now turn to the reproducibility of each of the models, when I repeated the analyses upon the same histograms two months later. Here, the estimate of SPF obtained at the first sitting has been divided by the estimate using the same model from the second sitting to give the ratios summarised in the table:

Model	n	Mean Ratio	SE Mean	SD Ratios
Rectangular	80	1.025	0.024	0.219
Trapezoid	78	1.052	0.026	0.227
Quadratic	69	1.201	0.111	0.919

Table 20: Comparison of estimates of SPF made on two occasions by analysing the same histograms with the same model. In each row, the answer obtained the first time has been divided by the answer obtained the second time. The summary statistics describe the distribution of these ratios. Raw data in Appendix II.

There is little to tell between the rectangular and trapezoid models in these terms. Estimates were gained in 2 more cases with the former, and the mean ratio is nearer to zero, which shows it to be slightly more consistent between the two sittings, reinforced by the fractionally lower value for the standard deviation. The huge value for SD for the quadratic model indicates that there were some very large differences between the estimates made at the two time points. This makes this model much less suitable than the other two for routine use. The rectangular was used in the prognostic series because of its small advantage in reproducibility over the trapezoid, as well as its widespread adoption in previous studies. Ideally it would be desirable to use all models in the multivariate analysis of results, as the best model is that which gives the most prognostic information, regardless of its reproducibility.

b) Inter-Observer Variation

In light of the above results, inter-observer variation was assessed using only the chosen, rectangular, model. In the table below, my estimate of SPF for each histogram has been divided by that of the second observer (Ms Oakes), in each case using the values obtained at our respective first sittings. The second line of the table looks at the results of dividing the average of my two estimates upon each histogram by the average of her two estimates, to see if this improved agreement.

Comparison	n	Mean Ratio	SE Mean	SD Ratios
PS1/SO1	66	0.842	0.028	0.229
PSave/SOave	64	0.843	0.027	0.214

Table 21: Comparison of SPF estimates by two observers analysing the same histograms using rectangular model. In each row, the answer I obtained has been divided by the answer obtained by the other observer. The summary statistics describe the distribution of these ratios. The first row compares single estimates, the second compares the averages of two estimates by each observer. Raw data in Appendix II.

It can be seen that the mean ratio in each case is significantly below one, indicating that I tend to get a lower estimate of SPF by 16%, which gives an indication of the degree of subjective influence which the operator can have with this software. Putting the value of SD into context, this shows that in 95% of cases, the ratio of my estimate to the second observer's lay between 0.38 and 1.30. That is, if my value for a given histogram was 10%, then we could statistically guess hers to be from 3.8% to 13% with 95% certainty. This is not terribly encouraging, and is not much altered by using the average of two estimates by each observer. In light of this it is instructive in this one case to illustrate the simple plot of our estimates against one another (fig. 27). The seductive appearance of this graph (the value of r is 0.945) belies the poor reproducibility just demonstrated, and this was the rationale for the development of the Bland-Altman approach.

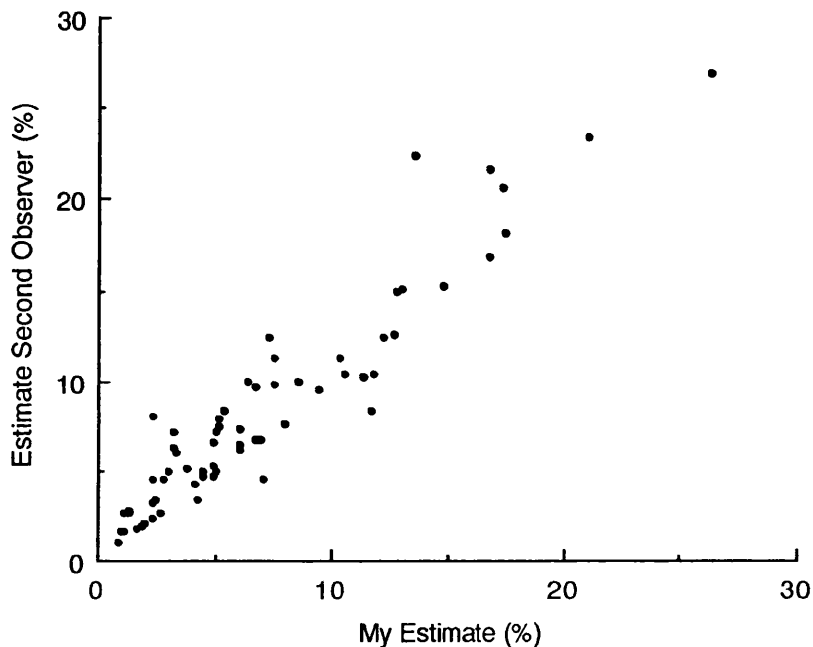


Figure 27: Results of analysis of the same histograms by two observers using the rectangular model of S phase, plotting the two estimates against each other. Line of best fit is $y = 1.058 + 1.024x$.

c) Intra-Observer Variation

Finally, we compare the results at the two sittings by the two observers, using the chosen model. My results are of course, presented already in table 20, as the results for the rectangular model. Once again, the earlier estimate is divided by the subsequent one:

Observer	n	Mean Ratio	SE Mean	SD Ratios
The Author	80	1.025	0.024	0.219
Ms Sarah Oakes	66	1.026	0.026	0.212

Table 22: Comparison of estimates of SPF made on two occasions analysing the same histograms with the rectangular model, by each of two observers. In each row, the answer obtained the first time by that observer has been divided by the answer obtained the second time. The summary statistics describe the distribution of these ratios. Raw data in Appendix II.

The results are similar. Neither of us tends to get higher or lower results at the second sitting, and the standard deviations are very close. This measure of agreement is very similar to that seen when comparing the two of us (previous table), suggesting that the range of variation for a second estimate is about the same whether the analysis is repeated by the same observer or another (but I get a higher answer on average).

Chapter 7: Discussion and Conclusions

These results provide evidence of only a very limited prognostic effect for tumour ploidy. There was an observed survival difference by univariate analysis of 3% at 10 years of follow up, in favour of patients whose tumours were classified as diploid. This was not statistically significant, nor did it become so with multivariate analysis. This is in keeping with the previous studies presented in chapter 3, where there was an overall a trend toward better survival for patients with diploid tumours, which was statistically significant in only a minority of those reports. There are a number of technical reasons which may well act to limit the usefulness of ploidy data.

It must firstly be recognised that all tumours are aneuploid in the sense that cytogenetic analysis shows that they have both quantitative (Remvikos et al 1988) and qualitative (eg point mutations) chromosomal abnormalities. Flow cytometry is a less sensitive tool for measuring DNA content, and so there is a 'threshold' below which a tumour is not recognised as different from normal, because the difference in DNA content is not large enough to be recognised by the technique. This threshold is arbitrary, depending upon the quality of the nuclear suspension gained from a particular tumour, of the process of staining and running that suspension on the flow cytometer, and the characteristics of the cytometer itself. We can compare this series with others in this respect by looking at the overall proportion of tumours classified as diploid, since if the distribution of ploidies is the same in different series, then the higher the technical threshold, the higher will be the proportion of diploid tumours. The figure of 36% diploid tumours for the current population is comparable with the other series discussed (eg 36% Kallioniemi et al, 1988; 37% Stål et al, 1989; 43% Fisher et al, 1991).

Another index of quality is the coefficient of variation (CV) for the ploidy histograms. The intrinsic CV of the Coulter Epics Profile II flow cytometer is of the order of 1.5% using calibration beads. The best histograms using paraffin embedded material achieve CVs within 1% of this figure. At the upper end, once peaks become too broad they run together and it becomes impossible to accurately interpret the histogram in terms of the ploidy of the sample. The arbitrary level taken as the upper level of acceptability was taken as 10% in this study, and only 3% of the original 293 histograms fell beyond this level. The median CV for the study population of 281 cases was 5.6%.

The ploidy of a tumour sample can only be established by comparison with cells with a known DNA content. When using fresh tissue, standards such as trout or chicken red blood cells are often added to nuclear suspensions. These have a DNA content of 80%

and 33% of normal human DNA content, respectively, and so allow identification of the diploid G_0/G_1 peak. Unfortunately the staining characteristics of formalin fixed, paraffin embedded tissue are not uniform, and appear to depend upon the original fixing and embedding conditions (Hedley et al, 1985). The stoichiometry of DNA staining is maintained, but the amount of dye bound by a given quantity of DNA is variable under these circumstances. As such, external standards which have not been fixed and embedded with the tissue are unhelpful for the type of sample used in this study. The assessment of ploidy in this situation relies instead upon the presence of a population of normal cells within the sample. These are present in all tumours, in the form of lymphocytes, fibroblasts, endothelial cells, fat cells, and in some cases non-tumour breast epithelium. These cells provide an internal standard against which to measure the DNA content of the tumour cells. If only one cell population is apparent in the histogram, then it is presumed that the two different populations must be overlying one another, that is that the tumour cells have the same DNA content as the non-tumour cells, indicating that the tumour is diploid. Where two or more populations are apparent, they are presumed to arise because the tumour cells have a different DNA content from the non-tumour cells, so that the tumour is aneuploid. In this situation it is not possible to definitively identify which of the populations represents the tumour cells, and which the non-tumour cells. Cytogenetic experience indicates that the majority of aneuploid tumours have a DNA content greater than that of normal cells, and so in this situation the peaks with higher DNA content are presumed to represent the tumour population. External standards overcome this problem when using fresh tissue as the starting material for flow cytometry, as the position of the diploid peaks can be inferred.

Some authors have sub-classified aneuploid tumours into up to five groups (figure 28):

- a) hypodiploid;
- b) those with DNA content between once and twice normal (the majority);
- c) those with twice normal DNA content, where the G_0/G_1 peak overlies the normal population G_2/M peak, referred to as tetraploid;
- d) those with more than one aneuploid population, referred to as polyploid or multiploid; and
- e) those with greater than twice diploid DNA content.

It has been proposed that tetraploid tumours may have a better, and polyploids a worse, prognosis than other aneuploid tumours. The incidence of polyploid tumours in the current series is so low (18/281, or 6%) that it is impossible to make any separate comment about them. The definition of a tetraploid tumour is problematic, because it overlies the diploid G_2/M peak, which itself may account for 10% of the events within the that population. If the population of tumour cells is small compared to that of non-

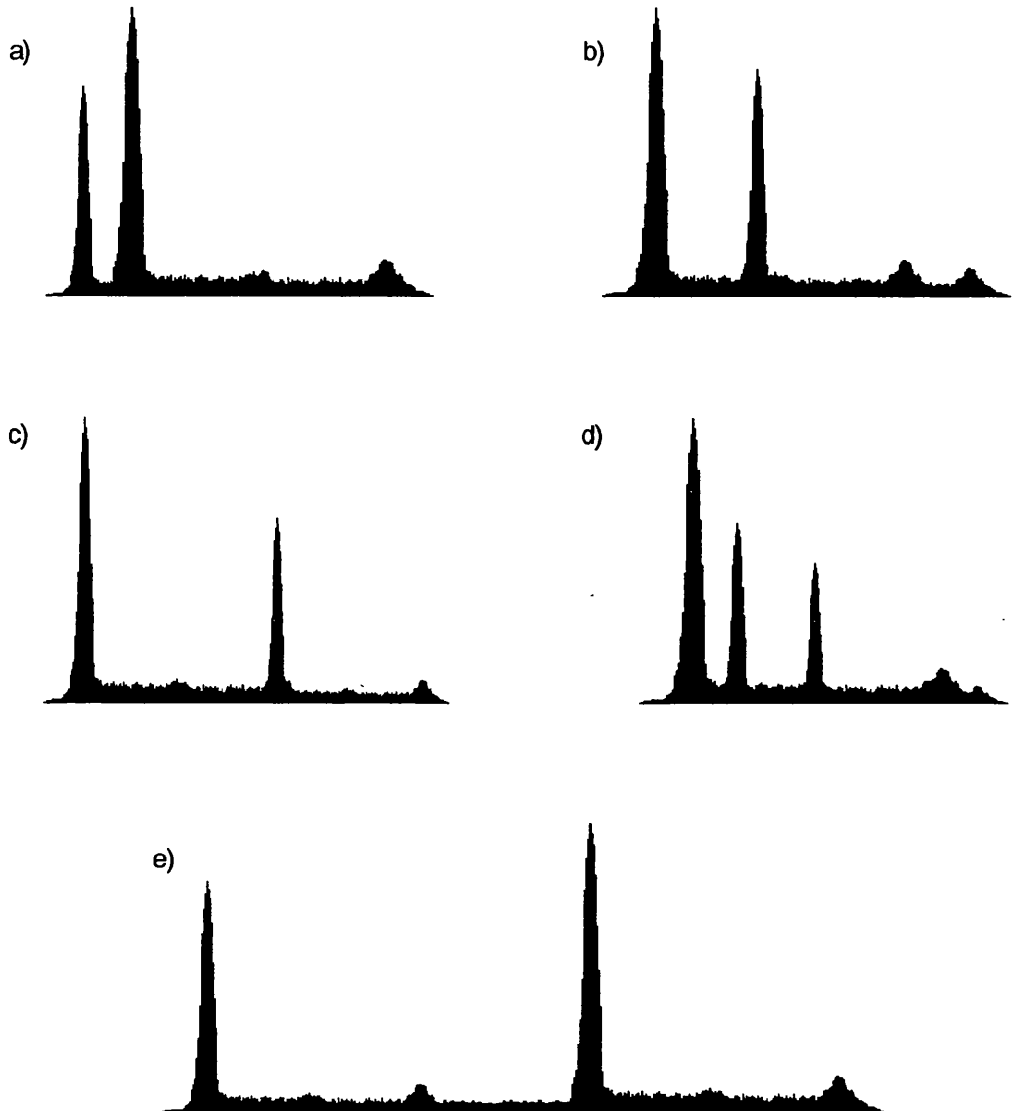


Figure 28: Types of aneuploid histogram. The identifying letters correspond to the text descriptions.

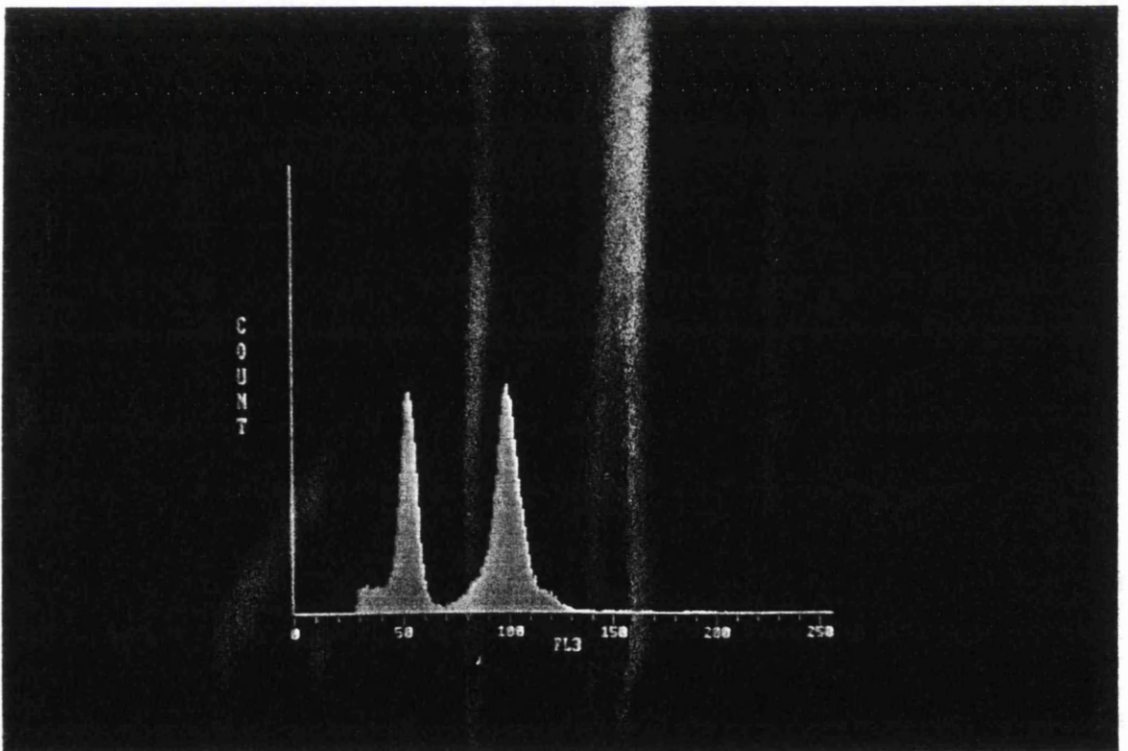
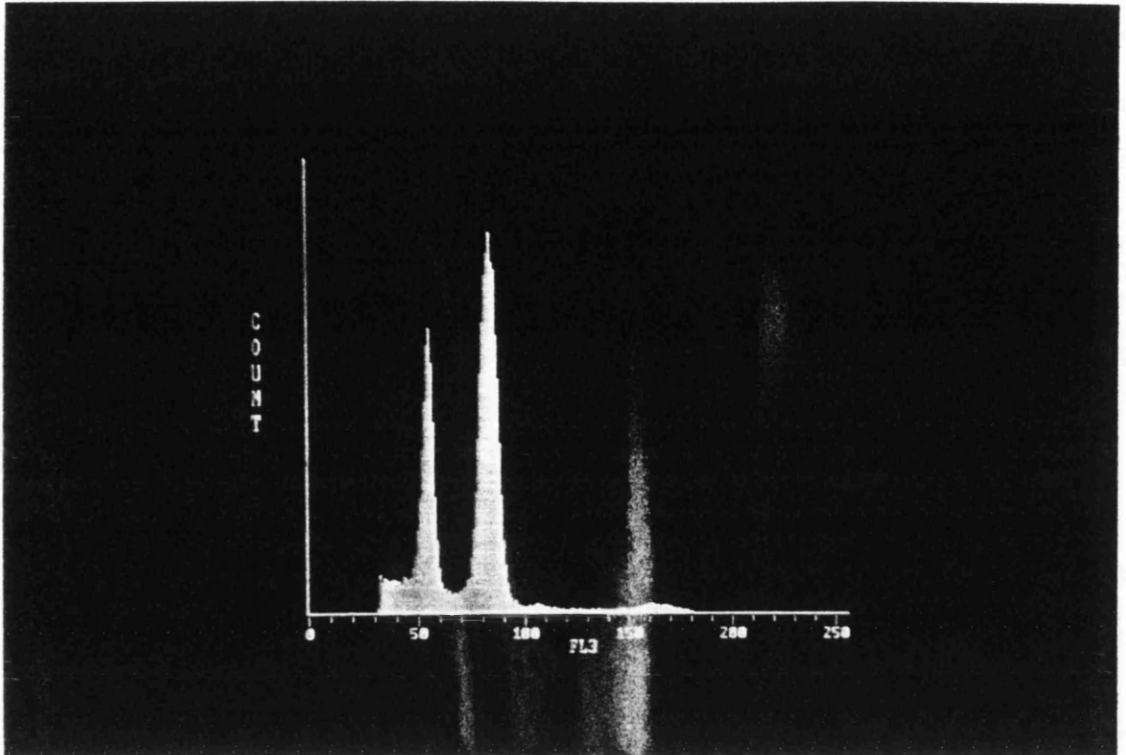


Figure 28a: Screen photographs of different types of aneuploid histograms, corresponding to those in figure 28. Above, classic hyperdiploid; below, tetraploid.

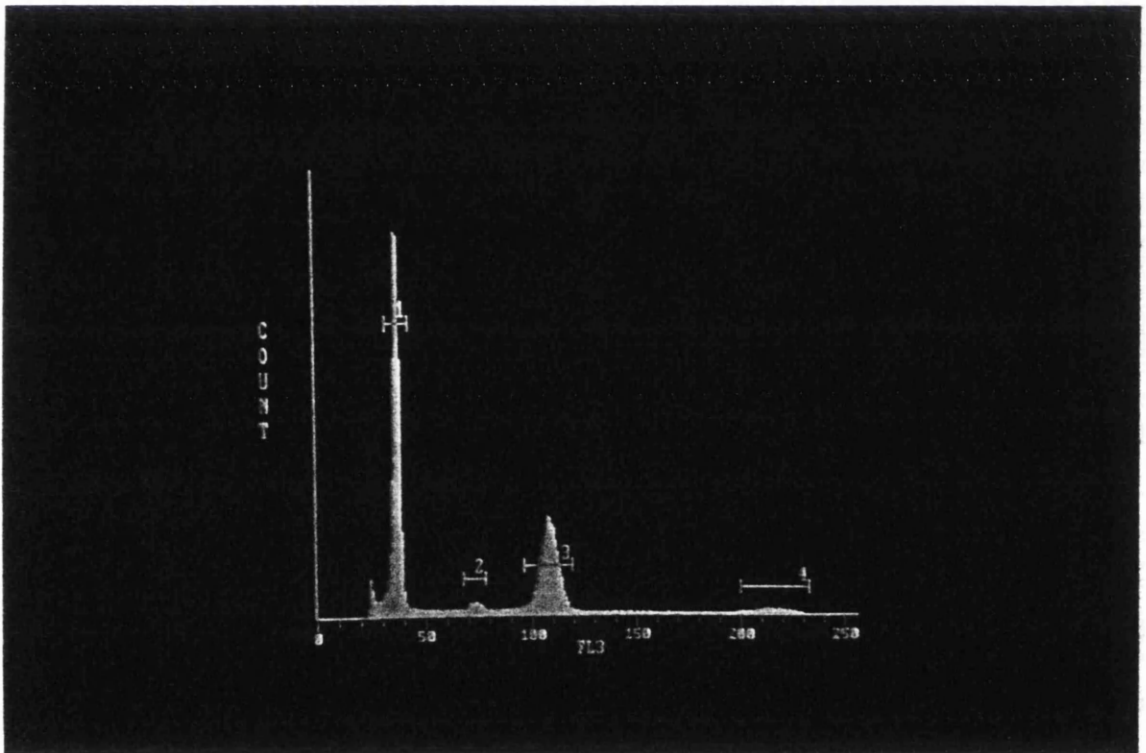
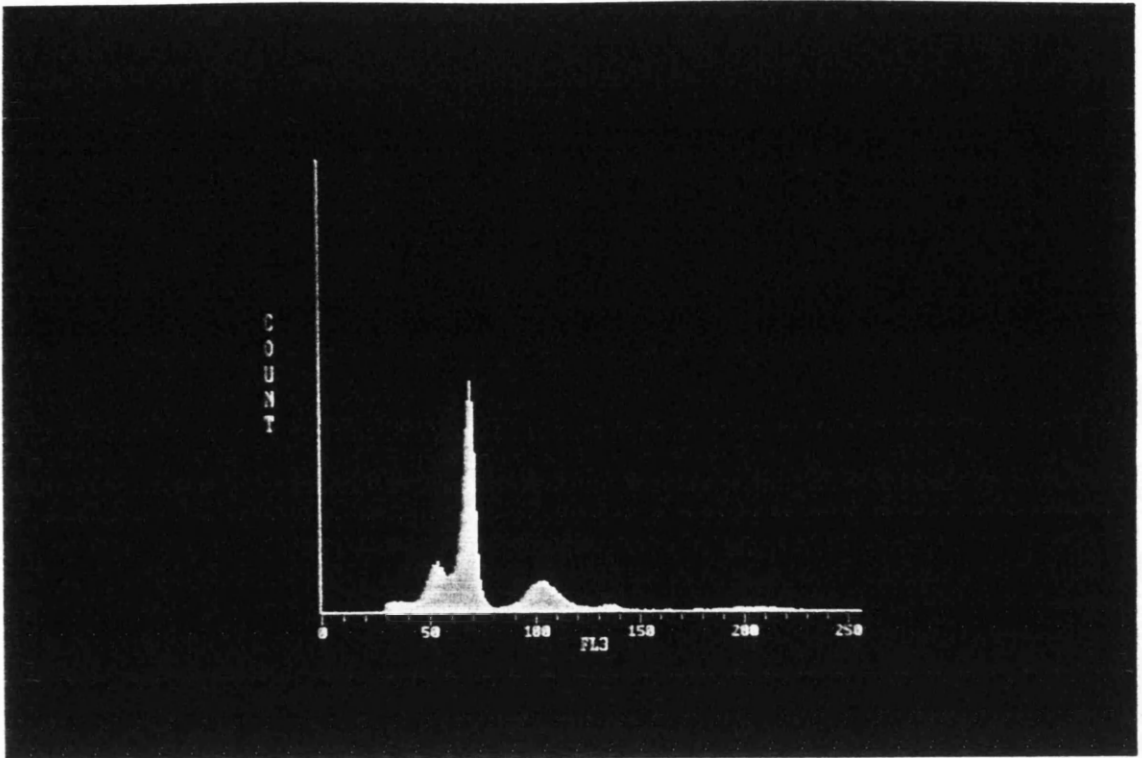


Figure 28b: Screen photographs of different types of aneuploid histograms, corresponding to those in figure 28. Above, multiploid; below, hypertetraploid.

tumour cells- the aneuploid population rarely accounts for more than 50% of total events in the histogram, and often substantially less, then the aneuploid G_0/G_1 peak may be no larger than this. Its corresponding G_2/M peak will be even smaller, and more difficult to identify. In this situation, it is only possible to use an objective cutoff, and that which has been employed in this series is that any G_2/M peak which accounts for more 15% of total events within the histogram indicates the presence of a tetraploid population at this position. Others have applied a cutoff of 10% of total events, and this will result in the classification of a higher proportion of histograms as tetraploid. Note that such histograms would be classified in the current series as diploid. There is a further problem as to just what range of DNA indices are to be regarded as tetraploid. Theoretically, the tetraploid tumour has a DNA index of 2.0. However, the vagaries of the preparation and running of the samples, referred to already, result in some variation from this figure for the index of G_2/M peaks to their own G_0/G_1 peaks. From the experience of analysing many histograms where the G_0/G_1 and G_2/M peaks of individual populations were clearly distinguished, the range of ratios was found to be from 1.85 - 2.10. This was taken as the range in which aneuploid peaks would be taken as tetraploid. Other reports do not so clearly indicate the criteria applied in the definition of tetraploid tumours. All of the above would seem to render impracticable the reliable subclassification of aneuploid histograms, and no separate analysis of subtypes has been carried out.

The final technical problem in the analysis of ploidy is that of tumour heterogeneity. The assignment of tumour ploidy by the analysis of flow histograms assumes that the DNA content of tumour cells throughout the tumour is consistent, in that a single small sample is used in order to categorise the entire lesion. In fact, as with most tumour characteristics, this parameter does indeed vary from place to place within at least some tumours. Two papers in the literature report the analysis of more than one sample from the breast tumours. Fuhr et al (1991) analysed multiple samples from different areas of fresh breast cancer biopsies. They found that 14 of 74 aneuploid tumours (19%) produced at least one sample which was diploid. Curiously, the overall rate of aneuploidy in this report was only 52% (cf 64% for the current series), when one would have expected multiple sampling to have 'exposed' more aneuploid tumours. Kallioniemi (1988) looked at 1394 biopsies from a number of tumour types (breast cancer accounted for 37%). Two samples were processed, from fresh and paraffin-embedded material respectively. 10% of breast tumours were aneuploid in one sample and diploid in another, and in a further 10% of tumours the DNA index was different between samples, but both were still classified as aneuploid. It is possible that some or all of the variation in this study arose from a difference between the types of starting material (fresh vs paraffin-embedded), but the findings do concord with Fuhr's, and with those from other tumour types (Hiddeman et al, 1986; Ljungberg et al, 1985; Quirke et al, 1985; Vindeløv et al, 1980)

Not only will variation between distant areas within the tumour be missed by the single sample approach, but variation within the small segment used for analysis may also be obscured. A small proportion of aneuploid tumours show more than one non-diploid population, and as noted in the previous paragraph, these are referred to as polyploid or multiploid. Here the presence of variation in DNA content within the sample is recognised, but if one population of tumour cells were aneuploid and another diploid then this variation within the sample would not be seen. It is also possible that very small aneuploid populations can be missed because they are obscured by background counts within the histogram. Thus variation in tumour DNA content both within and outside of the studied sample can be missed in flow cytometric analysis of tumour ploidy. This leaves the whole approach open to the criticism that the allocation of ploidy is arbitrary. In answer to this it must be realised that the majority of tumours are not heterogeneous in their ploidy, as indicated by the work of Fuhr and of Kallioniemi. In those which are heterogeneous, an alternative approach is that given a certain distribution of ploidies within a total tumour cell population, the probability of obtaining a sample of a given ploidy is related to the proportion of that population having that ploidy. That is, if in a given tumour 75% of tumour cells are aneuploid and 25% diploid, then these are the odds of obtaining a sample giving those two answers as to the tumour ploidy. The most likely ploidy to be assigned is that of the majority population, and this is one reasonable answer to the philosophical problem as to the 'appropriate' ploidy of a heterogeneous tumour. Other answers to this query are that the presence of any aneuploid population is adverse, or that the presence of variability itself is prognostically bad. If either of these hypotheses were true, then the flow cytometric approach applied to a single sample will not allocate the appropriate ploidy in some heterogeneous cases. Neither this study nor any other provide any information upon which to base an answer to this, and so the problem of heterogeneity must remain an open question in relationship to this type of investigation.

All of the foregoing indicates that the assignation of tumour ploidy is not as straightforward as it first appears, and that in terms of prognostic information there are a number of circumstances in which a tumour could be assigned to the 'wrong' group on the basis of the type of data derived in this study. This may explain the apparent lack of prognostic information given by tumour ploidy in this analysis.

In respect of SPF, our results are compatible with the trend toward improved survival in the low SPF tumours found by most previous studies, with an observed survival advantage to this group of 5% at 10 years in DNA diploid tumours, and of 11% at that stage in DNA aneuploid tumours. That these results are not statistically significant may represent a type II statistical error. The extent of this potential error can be assessed from the broad confidence intervals for the relative hazards calculated for ploidy and

SPF. The relatively low observed level of risk in high SPF tumours may also reflect our decision to divide SPF at the median rather than at a level chosen from the data as in other studies, a process which is open to criticism as stated previously.

The method of calculation of SPF is fundamentally different in diploid and aneuploid tumours, such that SPFs from tumours of different ploidy cannot really be compared. In a diploid tumour, the single population present in the ploidy histogram is a mixture of tumour and non-tumour cells, as already discussed. When the SPF of this population is measured, it reflects the SPF of both of these components. If we assume that the SPF of the non-tumour cells is lower than that of the tumour cells, then their admixture will lead to a falsely low estimate of the SPF of the tumour cells by this method, due to the dilutional effect of the non-tumour cells. In an aneuploid histogram, the tumour cell population is separate, and is analysed on its own. That is, the SPF of an aneuploid tumour is that of the tumour cells themselves, whereas the SPF of a diploid tumour is that of all the cells in the tumour. In some cases this difference could be overcome by measuring the SPF of both diploid and aneuploid components of an aneuploid histogram, and taking an appropriate weighted average of the two, in order to give an answer which approximates to that which would have been obtained if the tumour cell population had been diploid rather than aneuploid. However, in most aneuploid histograms the two populations overlap to a degree that precludes SPF calculation upon both, and furthermore, since it is the aneuploid histogram which gives us the purer measurement, it seems intrinsically undesirable to adulterate that answer for the sake of comparability alone. The dilutional effect of non-tumour cells upon the calculated SPF in diploid tumours creates an inbuilt tendency for diploid tumours to have a lower SPF than aneuploid tumours, if we accept that the non-tumour cells themselves have a lower rate of proliferation than the tumour cells (which is indeed the case in those histograms where both components can be separately analysed). This is the reason that the two tumour types cannot directly be compared. Few previous studies have attended to this problem, and most have analysed SPF of all tumours together. If this is done, the figure becomes not solely one of SPF, but a compound measure of ploidy and SPF. Whilst this may be a valuable variable, it must be recognised that it does not fairly assess the prognostic value of SPF itself. In this study, therefore, results are presented both separately for diploid and aneuploid tumours, as well as combined together.

The use of offline analysis packages for the calculation of SPF from ploidy histograms has technical limitations which result from the necessity of fitting a real histogram to a mathematical model. The source of the width of peaks within the histogram has already been considered- all nuclei of a given peak have exactly the same DNA content, but variability in dye binding and measurement of emitted fluorescence result in small

apparent deviations from this figure. These variations should be random, and so the shape of the peak should be Gaussian, which is the universal assumption made within software analysis packages. On this basis, when the software searches for a peak it looks for its top, and then rather than following its actual outline down to the baseline, it extends the top down as a Gaussian curve. The assumption is then made that any deviation of the actual shape from the Gaussian is the result of other elements within the histogram, ie S phase cells. This is not necessarily so, as is apparent from the fact that the deviations occur on both sides of the peaks. This problem can be overcome by overriding the computer definition of the peak, and instead defining its full extent manually, which involves indicating between which channels the peak shall be taken to lie. Whilst this avoids the previous source of inaccuracy, it introduces an element of subjectivity which undermines the rationale for computer analysis that it is algorithmic and thus objective and repeatable. There is a further manner in which subjectivity enters into the analysis, which is in the subtraction of background counts from the histogram. These arise from any contamination of the nuclear sample, or from the presence of nuclear fragments. Such fragments are numerous in specimens prepared by the disaggregation of fixed tissue sections, where they arise by division of nuclei situated on the margins of the section. Since nuclei in the body of the section should not suffer in this way, the proportion of divided nuclei will diminish as the thickness of the section increases, and this is one of the ways in which the current protocol varies from Hedley's original, in that he used 30 μ sections whereas we and most others now use 50 μ thickness.

The process of background subtraction involves the identification of areas either side of the cell population itself, wherein all counts represent background. The pattern of background counts within the cell population channels is then inferred by mathematical extension of these areas, and these counts are then subtracted from each channel to leave the estimated 'true' count for that channel. The type of mathematical model used varies from programme to programme. The Cytologics software used here assumes an exponential falloff of background counts within the histogram from left to right. This is the simplest model, assuming that the smaller the nuclear fragment (which is what these spurious counts are assumed to represent), the more likely it is to occur. More sophisticated background subtraction algorithms, which allow for the presence of sliced nuclei and clumps, and take account of the frequency distribution of nuclear sizes within the histogram, are not implemented by this software. The estimate of background is very sensitive to the areas used for definition, with variations of only a single channel markedly affecting the outcome. It is up to the operator to assess the accuracy of fit of the background counts, and further subjectivity is thus introduced.

Once the peaks and background counts have been defined, the computer measures the number of counts in the remaining S phase compartment, and expresses this as a proportion of total counts within the cell population under study. The problem of which mathematical model of the shape of S phase to use was referred to in the methods section of this chapter. These models are based upon different assumptions as to the distribution of cells throughout the cell cycle. The previous literature has established the rectangular model of Baisch as the norm, and we have also found this to be the most consistent model.

Overlap between the tumour and non-tumour cell populations in an aneuploid histogram may further complicate S phase analysis, and is a major problem in the analysis of this, the most common pattern of histogram. An illustrative example is shown in figure 29. Given the most frequent DNA index of 1.5 - 1.7, the G₂/M peak of the non-tumour cells lies over the S phase of the tumour cell population. The software allows for the identification and subtraction of confounding peaks, although this involves yet further operator intervention with its reduction in objectivity, but the rectangular model requires the identification of a flat segment of S phase between each pair of peaks (if there is a confounding peak, S phase is divided into two components by the software). If the peaks are too close, then no flat segment of S phase can be distinguished between them, and so one of the components of S phase is simply not estimated. In this type of histogram the size of S phase will be underestimated with respect to other aneuploid tumours. Whatever model is being used, the complexity created by the overlap of two separate S phases, along with the intrusion of peaks into each, makes this a more demanding exercise for the fitting program.

In view of these technical and theoretical problems, the findings with regard to reproducibility are not surprising. The good correlation of repeated estimations does suggest that in general, taking a group of tumours, most will be assigned to the same part of the range of SPF each time. We can explore this using my own two series of estimations using the rectangular method upon 119 histograms. Values were assigned both times for 80 tumours. If tumours were assigned simply into those above or below the median value, then 5 out of the 80 (6%) would have changed group depending upon which series of estimates was used. If tumours were divided into three groups based on the tertiles of the two series, then 13 tumours (16%) would have changed group. That this attempt starts to break down with even such a blunt classification as low, medium or high SPF is a consequence of the finding that the actual value of SPF is subject to large variation in individual tumours, such that the 95% confidence interval for a single estimate is of the order of $\pm 40\%$. How we assess the usefulness of SPF as a prognostic indicator, or as a parameter of tumour biology, depends upon the situation. If we are considering a series of tumours, as here, then it is a tool capable of dividing them into broad categories of proliferation. But in the context of trying to

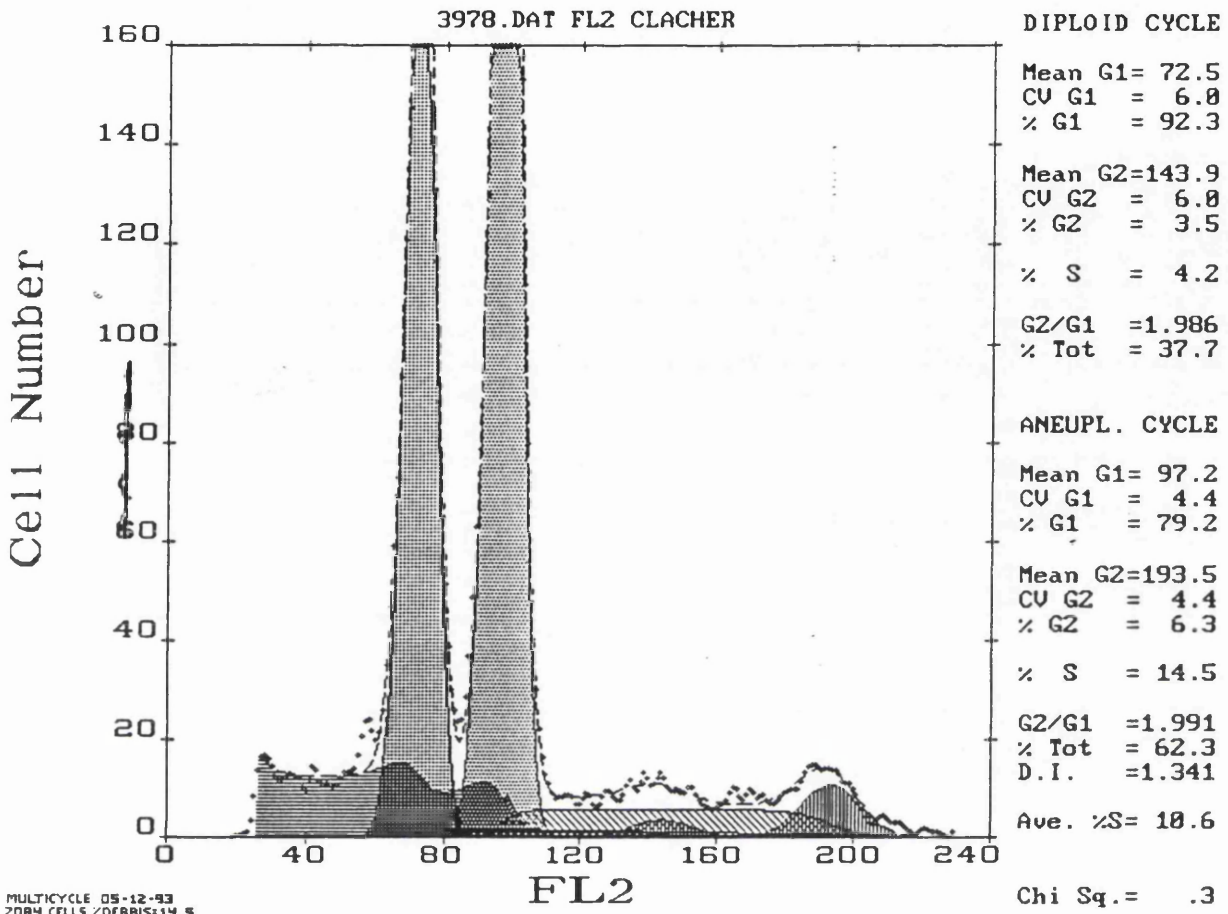


Figure 29: Printout of actual analysis of an aneuploid histogram by the Multicycle package. Both G0/G1 peaks are stippled (the aneuploid peak is the right hand one . Note that the y axis scale has been expanded so that the top of these peaks is lost, in order to demonstrate the S phase); the aneuploid G2/M peak has vertical bars; the diploid G2/M peak is in the middle of the aneuploid S phase, which has oblique bars; background counts are shown with horizontal shading. This well demonstrates the complexity of the modelling used to separate out the aneuploid S phase.

apply this to the individual case, the degree of uncertainty about a single measurement makes this an unsatisfactory method.

The artificial constraints imposed by the use of analysis software have led one group to eschew their use entirely (O'Reilly et al, 1990). These workers use a very simple manual method of calculation, drawing a rectangular S phase component between the means of the G_0/G_1 and G_2/M peaks at what they assess to be the height of the compartment. The number of counts within S phase is then readily calculated as the height of the box multiplied by the number of channels between the two peak means. Although this seems very subjective, it has been clearly demonstrated above that the supposedly objective method of algorithmic analysis is anything but, and is furthermore hampered by its inability to assess the histogram in other than mathematical terms. In support of this, the method is very reproducible in their hands.

The S phase fraction may be expected to show the same heterogeneity as tumour ploidy. There has been no published experimental work on this topic, but given the known information about the heterogeneity of tumour ploidy presented above, the assumption seems reasonable, and poses a corresponding problem- what is the 'true' value of SPF. The possible answers are the same, and there is likewise no way of resolving the matter. All of the foregoing make it no great surprise that tumour ploidy and SPF have provided only limited prognostic information despite the fact that they represent fundamental aspects of tumour biology.

PART III

in vivo ADMINISTRATION

OF

BROMODEOXYURIDINE

IN

HUMAN BREAST CANCER

Overview of Bromodeoxyuridine Studies

This second experimental part of the thesis takes cognizance of the largely negative results from the last part, and asks: can we improve upon this with the use of *in vivo* labelling with bromodeoxyuridine? This has been addressed by studying an ongoing series of patients, 91 at the time of production of this manuscript. The layout of this Part is similar to the previous one. I begin by describing the patients we have recruited, the means by which they were labelled, and the specimens obtained from their tumours. Once again the most detailed sections deal with the protocols for preparation of samples for flow cytometry, and the way in which the cytometer was set up and used to analyze them. Histogram interpretation is also examined in depth, following on from the theoretical discussion of this subject in section i of chapter 4.

The results chapter is somewhat different in style from the corresponding chapter in Part II, reflecting the more developmental nature of the bromodeoxyuridine-based technique. More basic questions about the parameters measured are examined first: are the dynamic data independent of the static component; is the length of time between patient labelling and biopsy critical; can the flow cytometric counts be validated by reference to tissue sections; and what is the relationship between the kinetics of breast cancer and those of normal breast and of other tumours? Since follow-up is still too short for prognostic information to have emerged, this question is approached instead by looking at the relationships between the kinetic data and existing pathological factors known to predict outcome. As in the previous part, there is an examination of the reproducibility of the methodology. We then look beyond the simple area of prognosis, to examine the biological significance of kinetic measurements by their correlation with tumour ploidy and with expression of oestrogen receptors, *c-erbB-2*, and EGFR. In the case of the last, a relatively novel, quantitative immunohistochemical method has been used. In view of the need to describe this in greater detail, a separate chapter is devoted to this comparison.

Chapter 8:

Patients and Methods

Section i: Patients Studied

Patients were selected from among those being treated on the academic surgical unit of the Glasgow Royal Infirmary (GRI) and under the care of Mr D Smith at the Victoria Infirmary (VI). All stages of disease were considered, including patients with known distant metastatic disease at the time of surgery. Only postmenopausal patients and those who had previously had a hysterectomy were entered, in view of the unknown embryotoxicity of bromodeoxyuridine. Other selection criteria were that a firm cytological or histological diagnosis was available preoperatively (so that bromodeoxyuridine was not administered to women who turned out not to have breast cancer), and that the tumour was clinically of such a size that adequate tissue seemed likely to be available for analysis once diagnostic needs had been met (about 2cm diameter). Because of these constraints, the labelled population is not representative of the total population of breast cancers treated in the two units.

Patients who fulfilled these criteria were asked to give written informed consent to taking part in this study. Only about 5% of interviewed patients refused consent. Approval for the project was given by the Ethical Committees of the Eastern (covering GRI) and Southern Units (VI) of the Greater Glasgow Health Board. The way in which the patient was treated formed no part of this study, and was entirely at the discretion of the surgeons involved. Patients having breast conservation or mastectomy were included, as were those having adjuvant radiotherapy or chemotherapy.

Section ii: Bromodeoxyuridine Labelling

Bromodeoxyuridine from two sources was used in the course of this study. Initially, a commercial product provided in 200 mg ampoules by Takeda Chemical Company was purchased. When this ceased to be made, pharmaceutical grade bromodeoxy-uridine was packaged by the CRC Drug Formulation Unit at the University of Strathclyde specifically for CRC funded research. The ampoule size for this product was 250mg. Bromodeoxyuridine was administered in one of two ways, depending upon the time of day at which the patient was scheduled to have their operation. Where possible, the co-operation of clinicians was gained such that operations were performed in the middle of the day. If this was the case, bromodeoxyuridine was given as an IV bolus in the morning. This was made up by the addition of 10ml of normal saline to the ampoule. Either the entire solution (Takeda product) or 8ml of it (Strathclyde product) were drawn up and administered, noting the time at which this was done.

In the case of patients being operated on early in the morning, an alternative method of administration was used. Once again 200 mg of bromodeoxyuridine was drawn up, but diluted to 25ml with saline in a 50ml syringe. This was done the evening before operation, and the syringe labelled and stored in the ward refrigerator. An IV line was established before the patient retired for the night. The order for the administration of the bromodeoxyuridine was placed on the IV fluid chart, and at the indicated time the syringe was sidelined through the infusion by agency of a Vickers infusion pump at maximum rate (100ml/hr). This resulted in administration of the bromodeoxyuridine as an infusion over 15 minutes. This was timed to be done roughly 4 hours before the anticipated time of biopsy.

Section iii: Specimen Collection

In nearly all cases I attended the operations upon these patients when performed in the Royal Infirmary, in which case I received the operative specimen directly, and transected the tumour. A 5mm thick section off the face of the tumour was removed and placed into 70% ethanol as fixative. If the tumour was large enough, a further specimen was taken and placed into liquid nitrogen. For cases at the Victoria Infirmary, one pathologist (Dr Morag McCallum) agreed to receive all labelled specimens, and removed a sample into 70% ethanol from them. All alcohol fixed biopsies were stored at 4°C pending subsequent analysis.

Section iv: Patients and Tumour Data Noted

The following details were noted on a proforma at the time of bromodeoxyuridine labelling - unit record number

- age
- menopausal status

Subsequent course was followed by casenote review at intervals, noting the following:

- pathology department number
- type of operation, mastectomy or breast conserving
- macroscopic tumour size (maximal diameter) as recorded by the reporting pathologist. For the purposes of analysis, this was coded in accord with the TNM classification as T1- tumour less than or equal to 20mm in diameter, T2- tumour greater than 20mm but no more than 50mm in diameter, T3- tumour greater than 50mm in diameter. There were no T4 tumours in this study.
- involvement of ipsilateral axillary lymph nodes (number of involved/number of uninvolved nodes) as determined histologically by the reporting pathologist. For the purposes of analysis, this was coded as N0- no nodes involved, N1- one or more involved nodes, NX- no nodes available to pathologist.

- oestrogen receptor status (fmol/mg protein, dextran coated charcoal technique), where tumour was sent for this assay by the pathologist. For the purposes of analysis this was treated as a binary variable with a cut off of 5 fmol/mg protein.
- adjuvant therapy given, if any
- clinical course, including results of investigations

Section v: Specimen Preparation

This was done by using an adaptation of the Hedley method for ploidy studies upon paraffin embedded tissues described in the previous chapter. This adaptation was developed in the laboratories of the Departments of Surgery at the Royal Liverpool Hospital and then the Glasgow Royal Infirmary by Ms G Forster.

After at least 24 hours fixation in 70% ethanol at 4°C, segments from the tumour biopsies were paraffin embedded, and a 50µ section taken and dewaxed in the same way as for the ploidy studies in the previous chapter. A consecutive 5µ section was taken for H&E histology to confirm the presence of tumour in the section being used for cell kinetic studies. All histological material was reviewed with Dr J Going, Senior Lecturer in the Department of Pathology at the Royal Infirmary.

The subsequent treatment of the specimens is as follows:

- place dewaxed sections in 5ml plastic test tubes
- disaggregate the sections by addition of 1ml of 0.5% pepsin in water brought to pH 1.5 with 2M HCl. Incubate the tubes in a water bath at 37°C for 30min.
- centrifuge for 5min at 2000rpm (all subsequent spins were the same)
- using a glass Pasteur pipette, pipette off and discard supernatant
- wash off remaining pepsin by adding 1ml PBS, pH 7.4 (made up from Sigma tablets)
- centrifuge and remove supernatant
- resuspend with 1ml PBS
- aspirate and expel sample 3 times using a 1ml syringe and a 26g hypodermic needle. This provides mechanical disaggregation.
- push into a fresh tube through a 50µ nylon mesh, thereby removing any large aggregates remaining in the suspension. The surviving sample consists of mostly intact nuclei, as well as small membrane and cytoplasmic fragments.
- centrifuge and remove supernatant
- add 1ml of 2M HCl whilst rotamixing, and leave for 30min at room temperature. This partially denatures the nuclear DNA in order to expose the contained bromodeoxyuridine to the monoclonal antibody used to detect it.
- centrifuge and remove supernatant

- neutralise remaining acid with 1ml of 0.1M Borax at pH 8.5 for 5min at room temperature
- centrifuge and remove supernatant
- wash by addition of 1ml of PBS
- centrifuge and remove supernatant
- wash again, with 1ml of PBS with 0.5% bovine serum albumin (Sigma, to block non-specific antibody binding) and 0.05% Tween 20 (Sigma, a detergent to permeabilise the nuclear membrane). This solution will be referred to as PBT.
- centrifuge and remove supernatant
- add 100 μ l of a 1/30 dilution in PBT of anti-BUDR antibody (Dako, mouse monoclonal IgG1). Rotamix gently and incubate at room temperature for 1hr.
- add 1ml PBS
- centrifuge and remove supernatant
- add 1ml PBS, centrifuge and remove supernatant; repeat
- detect anti-BUDR by addition of 100 μ l of rabbit anti-mouse IgG conjugated with FITC (Dako), diluted 1/40 with PBT, and incubate for 30min at room temp.
- add 1ml PBS
- centrifuge and remove supernatant
- add 1ml PBT
- centrifuge and remove supernatant
- add 1ml PBS
- stain total DNA by adding 10 μ l of 10mg/ml propidium iodide (PI, Sigma), giving a final concentration of 100 μ g/ml PI.
- incubate for 30min at room temperature
- centrifuge and remove supernatant
- add 1ml of PBS. The sample is now ready for flow cytometry

This is summarised in the flow chart below:

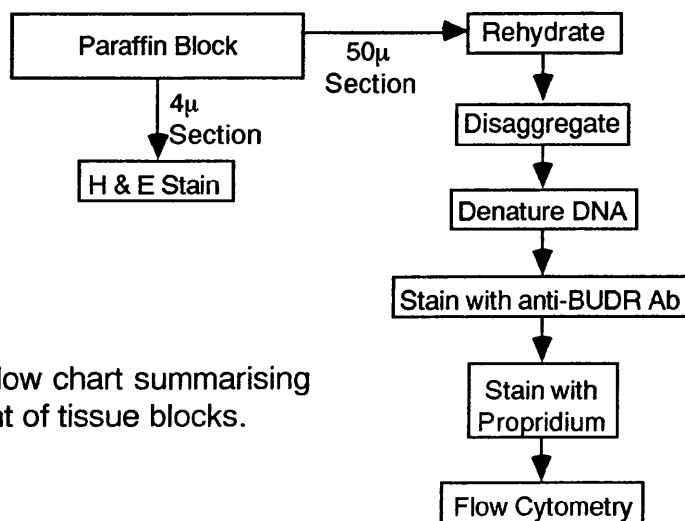


Figure 30: Flow chart summarising treatment of tissue blocks.

The procedure was often carried out over 2 days, the samples being stored over-night after the pepsin was washed off. The first day consisted of dewaxing and disaggregation of the specimens, and the second of their staining. The final samples were also often stored at 4°C overnight before being run on the cytometer. It was in fact observed that after they were run the samples could be stored at 4°C for at least a week and rerun with the same results.

Section vi: Flow Cytometry

The cytometer was set up as for the ploidy studies. The filter set up was described in the last chapter, where it was noted that filter d (in figure 14) was not necessary for that study. In the current investigation, this dichroic mirror separates the green (fluorescein isothiocyanate, that is BUDR) fluorescence, which being of shorter wavelength is reflected by the mirror, from the red (propidium iodide, that is total DNA content) fluorescence, which passes the mirror. Green fluorescence is then collected in FL3, through a 525nm band pass filter (filter f in figure 14), and red fluorescence in FL2 through a 635nm band pass filter. The propidium iodide signal is much the stronger, but the strongly positive FITC positive cells do make a small contribution to the measured signal in FL2. Because of the strength of the PI signal, even the lower limit of its emission spectrum provides enough emitted light to add noticeably to the signal in FL3. This has the effect of adding apparent strength to the BUDR signal as the PI signal increases- that is, nuclei with high DNA content show a spuriously higher BUDR content, and so may be counted as positive when they are not. This is dealt with by the cytometer by what is termed colour compensation, whereby a percentage of the signal from one channel is subtracted from that registered in another. The machine allows each of the six potential crossovers between the 3 fluorescence channels to be dealt with. In this case, the crossover from red to green channels can be negated by subtraction of 2-5% of the FL2 (red) signal from the FL3 (green) signal. The amount of FL3 - FL2 colour compensation was individually set for each sample. FL2 - FL3 compensation of 1 or 2% was normally adequate to prevent strongly FITC positive cells from showing a spuriously high DNA content.

The amount of compensation required on any given day was largely determined by the sensitivity of the photomultiplier tubes (PMTs), which is determined by the voltages supplied to them. These voltages were set to be appropriate for the first run of the day. The voltage for FL3 was rarely altered for the rest of that day's specimens. That for FL2 was often altered in order to position the ploidy histogram optimally. The ploidy histogram was positioned so that the population of interest (that is, that upon which calculation was to be carried out, the one containing the tumour cells) was as far to the right in the histogram as possible. This was done so that it occupied the maximum number of channels, thereby increasing the statistical accuracy of the positional

measurement which underlies the estimation of relative movement. In some cases a change in the PMT voltage for FL2 carried out to achieve this was large enough to significantly alter the crosstalk into FL3, such that a change in colour compensation was required. The FL3 PMT voltage was set at the highest level at which the bulk of negative nuclei continued to register as having a zero fluorescence, unless this resulted in positive nuclei giving a reading at the very top of the scale, in which case a lower voltage was used to ensure that no positive nuclei were lost off the top of the histogram. Even so, there is a very large difference in the signal from positive and negative nuclei such that to encompass them both on the same axes, log amplification of the FL3 output was used. This provides progressively less amplification the stronger is the original signal, so that a single histogram axis can encompass a range of values covering about 3 orders of magnitude. Using the linear amplification used for instance for red fluorescence, only 1 order of magnitude is covered.

Events were collected at 200 counts per second if possible, by manipulation of the sample flow rate. If the final nuclear suspension was too concentrated for this to be achieved at minimum flow rate (10 μ l/sec), then the sample was diluted with further PBS. If the suspension was too dilute, then it was centrifuged and resuspended in a lower volume. The minimum volume used was 0.5ml, but even in this volume some samples gave lower counting rates than the desired 200/sec at the maximal flow rate of 200 μ l/sec. Such samples were counted at the maximal achievable rate.

At least 50,000 nuclei were counted if possible, although this total was not achieved in dilute samples. In concentrated samples, counting was allowed to continue until terminated by the cytometer, which has an inbuilt limit to the number of counts accumulated in any one channel of any histogram. The bulk of events were recorded in the zero channel of the green (BUDR) fluorescence, and so the machine automatically cut out in most cases at about 70,000 events. Such a sample size is obviously well above what is required to give a reliable estimate of the ploidy, S phase fraction or proportion of BUDR labelled cells in the suspension. The process which may require this number of nuclei counted is the measurement of the relative movement of the BUDR labelled cells, since here the sample size is that of the labelled undivided cells. If we consider a sample of 50,000 nuclei with a labelling index of 1%, then only 500 nuclei will be BUDR labelled. If one third of the labelled cells have moved into G₀/G₁ between labelling and biopsy, then the eventual sample for the estimation of RM is 333. In order to gain a statistically adequate sample, a lower limit of 100 BUDR labelled, undivided cells was set, and if at all possible, 200 such events were accumulated by running a second, double specimen (ie two sections were disaggregated and stained together).

The following histograms were created at the time, in order to allow calculation of labelling index and relative movement from the machine printout without offline analysis:

a) Peak vs Total Red Fluorescence

As with the ploidy study, this histogram was used to select the desired cell population(s) for further analysis, and to carry out doublet discrimination and exclude some debris at the lower end the histogram.

b) Red vs Green Fluorescence

This is the main analysis histogram for the determination of cell kinetics. DNA content (red fluorescence) is represented on the x axis and BUDR content (green fluorescence) on the y axis

c) Red Fluorescence vs Number of Counts

This is a ploidy histogram, as used in the investigation described in the previous chapter. It is used firstly to clearly demonstrate the tumour ploidy (although with experience it is nearly always possible to do this from either of the above histograms), secondly to set more accurately the areas of interest in histogram b by defining the extent of the various peaks, and thirdly for offline analysis of S phase fraction as described in Part II.

d) Green Fluorescence vs Number of Counts

This histogram portrays the range of values of BUDR content, which is essentially bimodal, with negative cells set to be very close to zero, and positive nuclei in the upper half of the histogram even with log amplification which is applied to this signal. This demonstrates that this separation has been achieved, and as with histogram c allows accurate determination of the optimal position for setting boundaries between different areas of interest in histogram b.

Section vii: Data Storage

Both histogram and list mode data were stored on floppy disc for offline analysis. Due to a bug in the system software of the cytometer, only about 25% of the full data list was transferred to disc in each case.

Section viii: Determination of Cell Kinetic Parameters

In order to determine the bromodeoxyuridine labelling index and the relative movement of the labelled cells, three sub-populations of cells within the total tumour cell population must be identified and characterised- firstly the cells which are not labelled with bromodeoxyuridine, secondly those which are labelled and have not divided since

labelling (that is, those which are still in S, G₂ or M phase), and thirdly those cells which are labelled with bromodeoxyuridine and have divided since prior to biopsy (those now in G₀ or G₁ phase). With the system software of the cytometer, this is done by drawing rectangular areas of interest (boxes) onto the two parameter plot of red versus green fluorescence (histogram b in section vi). These areas are used to encompass the three groups of cells described above, as shown in figure 31. The software indicates the number of events in each box and the mean position of those events on each of the axes.

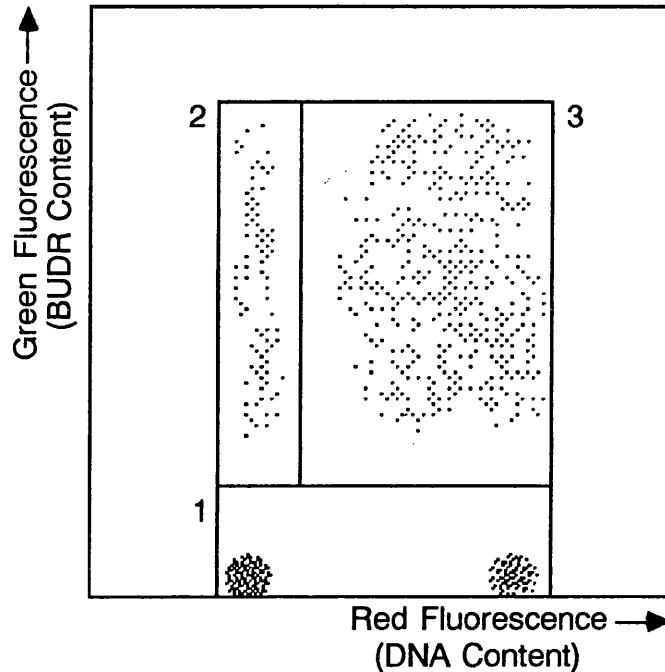


Figure 31: Example of two-parameter histogram, showing analysis boxes. Box 1 includes cells not labelled with BUDR, with concentrations of cells representing G₀/G₁ (left) and G₂/M (right) peaks. Box 2 encompasses labelled cells which have divided, and Box 3 labelled undivided cells. An actual example is shown in figure 32.

To work out the kinetic parameters by the method of Begg et al (1985), let us call the number of events in boxes 1-3 in the figure N₁, N₂ and N₃ respectively. Because each of the cells in box 2 has divided into two since taking up the bromodeoxy-uridine, to calculate the number of cells which were in S phase at the time of labelling we must count each of these cells as only one half. Thus the labelling index is the number of labelled undivided cells (box 3) plus half of the labelled divided cells (box 2), divided by the total number of cells, or:

$$LI = [N_3 + (N_2/2)] / [N_1 + (N_2/2) + N_3]$$

The mean position on the x axis of the events contained in box 3 will be seen to be the quantity referred to in the derivation of equation 10 (Chapter 4) as F_L . The values F_{G1} and F_{G2} from that equation can be gained from histogram c, by putting cursors across

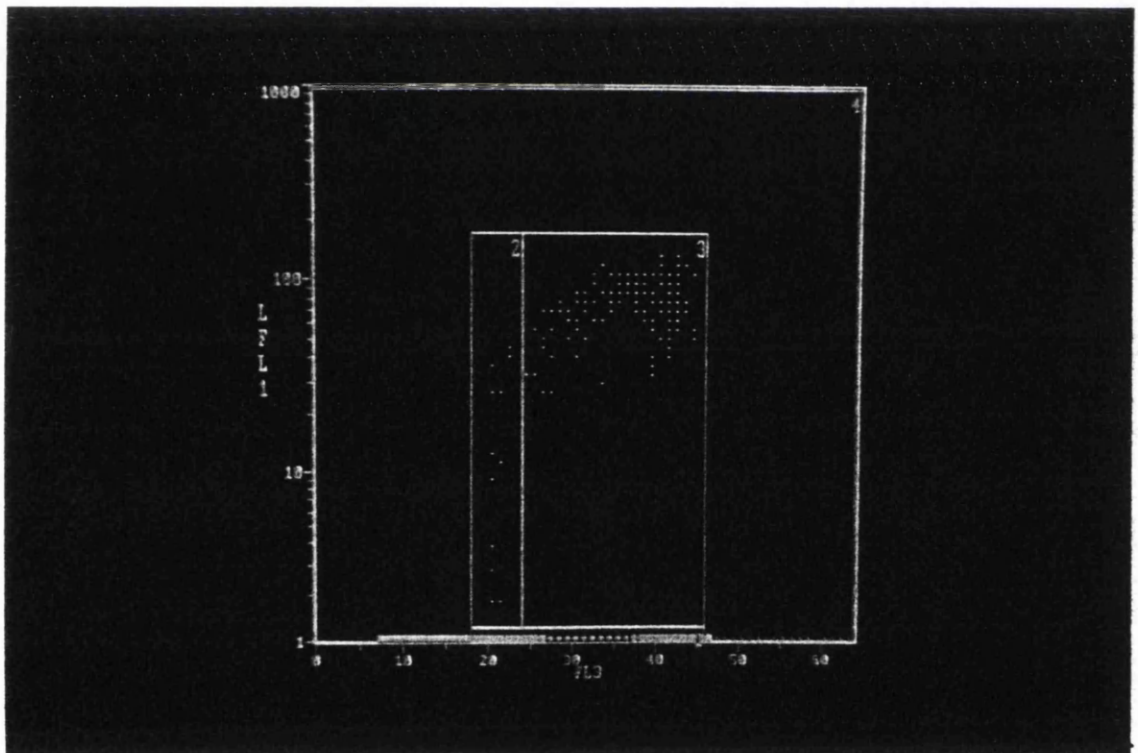
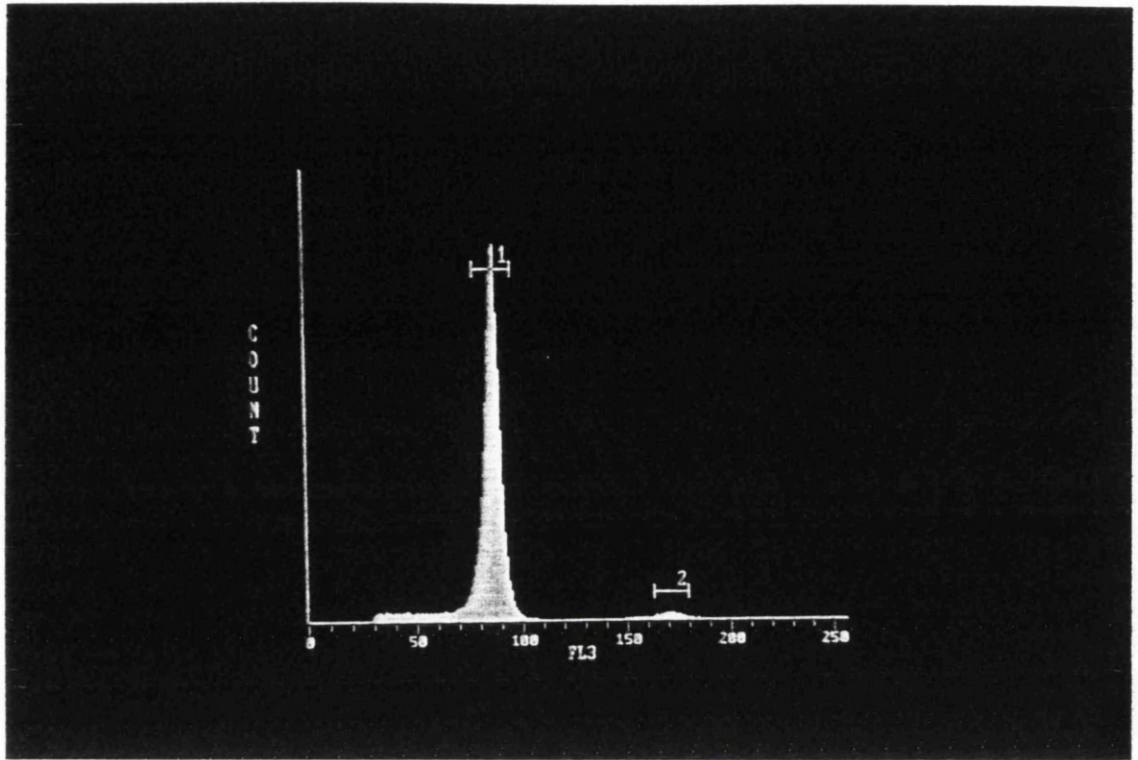


Figure 32: Screen photograph of two parameter histogram for analysis of dynamic cell kinetics as simplified in figure 31 for illustrative purposes. Ploidy histogram for this tumour above.

the respective peaks and thereby obtaining the mean channel number for the peak in each case (in transferring this result to a calculation made in histogram b, it is necessary to divide the obtained values by 4, as histogram c has 256 channels whereas histogram b has only 64 on the x axis). All of the terms required for the calculation of RM are now available, and so given the time between labelling and biopsy it is possible to obtain the estimated value of T_s from equation 11 (Chapter 4). T_{pot} can then be arrived at given the values of LI and T_s , making the assumption as to the value of lambda already discussed.

To estimate T_{pot} by the method of White et al requires the fractions of labelled divided and labelled undivided cells (f^{ld} and f^{lu} in equation 12), which are given by N2 and N3 as proportions of the total number of cells respectively. T_s is calculated in the same way as for Begg's method, n from equation 12 and T_{pot} from these two (equation 9).

The degree to which these calculations reflect the theory outlined in the introduction depends upon the accurate delineation of subpopulations by the boxes drawn onto the histogram. To place these requires answering two questions- firstly in which channels do the G_0/G_1 and G_2/M peaks start and finish, and secondly where is the cut off between unlabelled and labelled cells? Question 1 is answered by referring to the ploidy histogram (histogram c), on which areas of interest are defined by cursors. These take the form of horizontal bars with upright cross bars at either end, placed over the relevant peaks with the cross bars in the channels felt to represent the limits of the each peak (figure 33). The numbers of these channels are then given by the system software of the cytometer, and these can be transferred to histogram b by dividing by four as previously mentioned. The left hand edge of boxes 1 & 2 is the lower channel of the G_0/G_1 peak, the junction between boxes 2 & 3 is the upper channel of that peak, and the right hand edge of boxes 1 & 3 is the upper channel of the G_2/M peak.

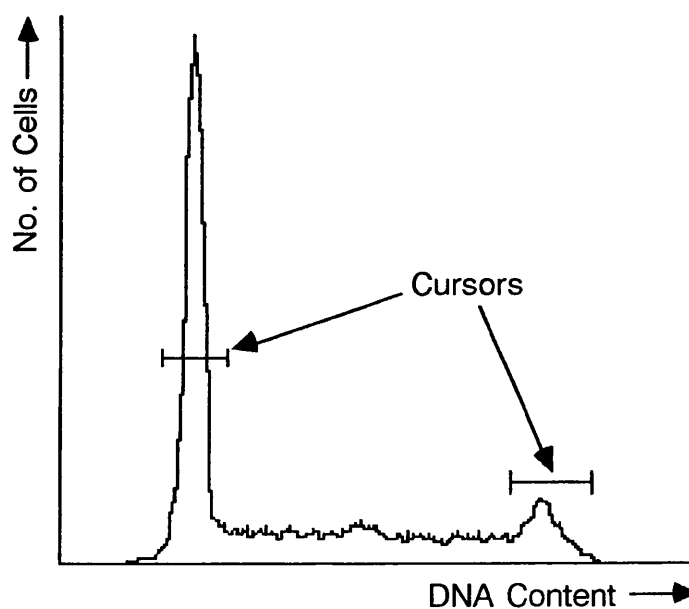


Figure 33: Method for delineating peaks in one-parameter histograms, showing placement of cursors from lower to upper channels of each peak.

The second question is answered by referring to histogram d, identifying there the nadir between the unlabelled cells (which take the form of a descending exponential curve from the left hand margin) and the labelled cells (which should constitute a distinct peak to the right of this, figure 34). The channel number is identified by placing a cursor, and can be transferred without correction to the y axis of histogram b. This defines the upper limit of box 1 and the lower limit of boxes 2 & 3.

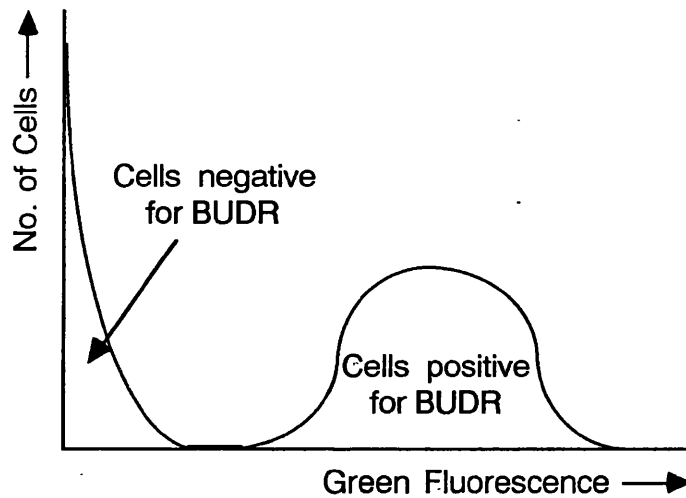


Figure 34: Example of a single parameter histogram of BUDR content, indicating the position of labelled and unlabelled cells.

The above calculations are demonstrated upon a diploid histogram. The situation in analysing an aneuploid histogram is complicated by overlap between the diploid and aneuploid populations. The usual situation is that the diploid G_2/M peak lies in the first half of the S phase of the aneuploid population. The number of diploid cells in late S phase and the G_2/M peak is usually small compared to the total aneuploid population, and as such should have little effect upon the calculated labelling index even if they were ignored. This is not necessarily the case with the estimation of relative movement, as the number of cells upon which this is based can be quite small as already discussed. Even a small number of labelled diploid G_2/M cells lying in the lower reaches of the aneuploid S phase may markedly drag down the mean channel number of the cells in box 3, the more especially because they most often lie well toward the left hand size of the box.

In some histograms, the cohort of labelled diploid G_2/M cells is quite distinct from the labelled aneuploid cells (the divided cells to its left in the histogram, the undivided cells to its right). This occurs where the time between labelling and biopsy is long enough that the labelled cells have had sufficient time to move out of the early part of S phase, but not so long that the divided cells have yet entered a new S phase. The situation is not so unlikely as it may sound, and if so it is possible to exclude the labelled diploid

G_2/M cells by leaving box 3 'short' on its left hand side, so that there is a gap between the two, the diploid cells lying in this gap (figure 35). Note that there remain labelled diploid S phase cells admixed with the aneuploid G_0/G_1 peak, and no attempt has been made to exclude the unlabelled diploid cells which overlap, in both cases because the cells involved are not distinct from the aneuploid component. The process just described is thus only a partial correction for this problem, but does probably deal with the area where the overlap causes greatest error. It is not possible where the labelled diploid cells are not distinct in the histogram, in which case any attempt to exclude them would inevitably also leave out the labelled aneuploid cells in lower S phase and bias the estimate of relative movement to the right.

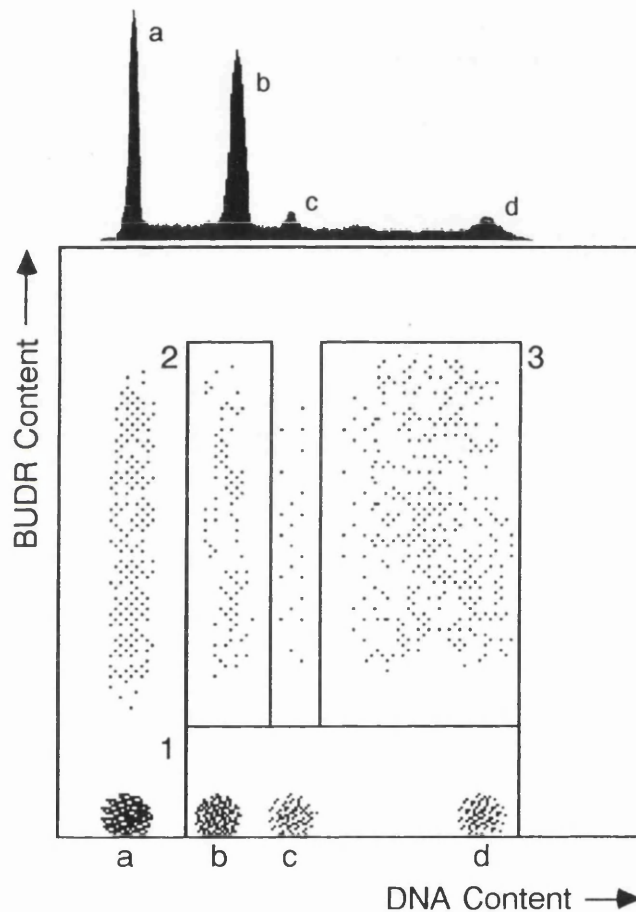


Figure 35: Example of two-parameter histogram in an aneuploid tumour, showing placement of analysis boxes so as to exclude labelled diploid G_2/M cells. The ploidy histogram for this tumour is overlaid at the top to aid in interpretation. Peaks identified in both components are a) diploid G_0/G_1 , b) aneuploid G_0/G_1 , c) diploid G_2/M , d) aneuploid G_2/M .

It is implied in the above discussion that in an aneuploid tumour the population of tumour cells can be distinguished from the population of normal cells to at least some degree. This is obviously impossible in a diploid tumour, where the two populations overlaid each other. The implications for cell kinetic measurements were discussed in

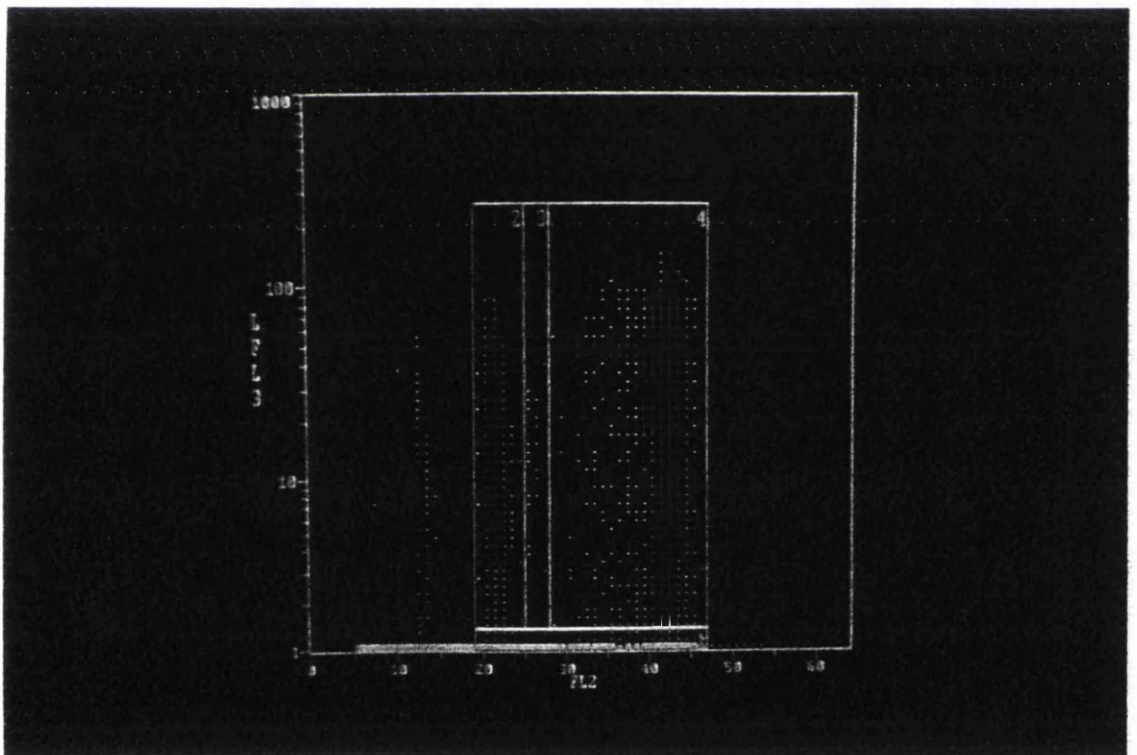
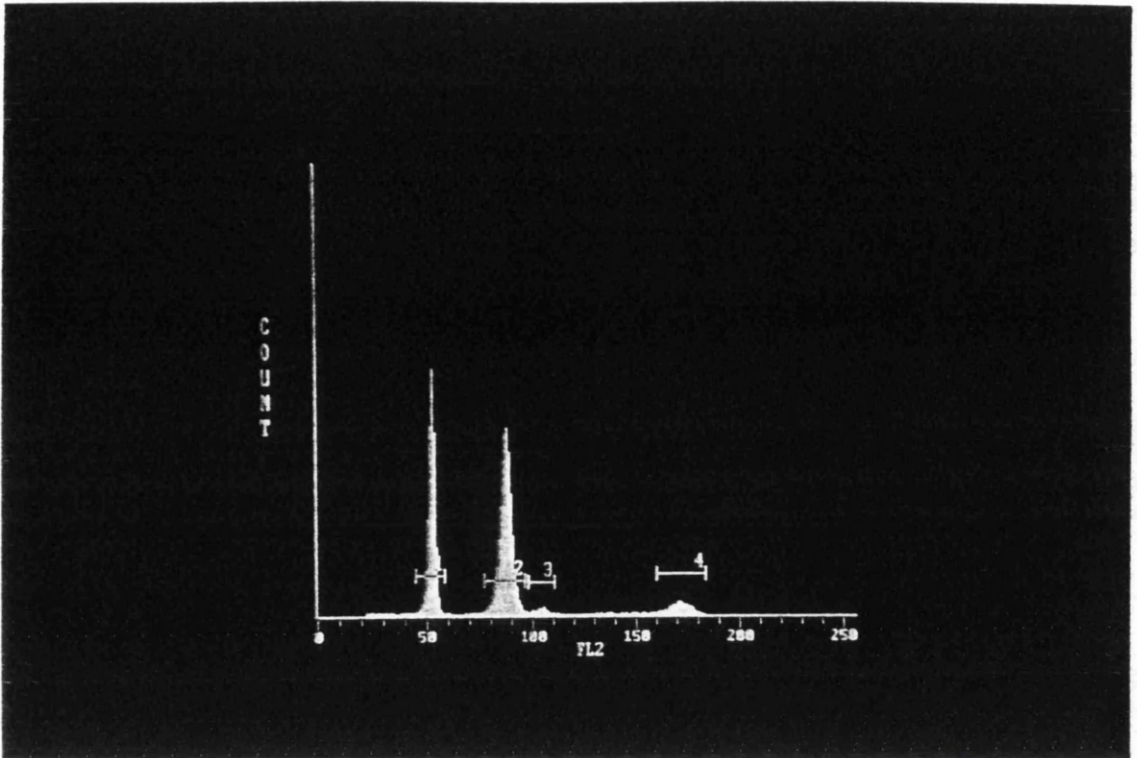


Figure 35a: Screen photograph of a two parameter histogram for analysis of dynamic cell kinetics in an aneuploid tumour, using the method demonstrated in figure 35 for excluding labelled cells in the diploid G2/M population. Ploidy histogram for this tumour above.

the previous chapter. An attempt has been made in this study to level this playing field by defining the total labelling index (TLI). The TLI is an attempt to make LI measurements comparable for aneuploid and diploid tumours by 'handicapping' aneuploid tumours. To make the measurement, all labelled cells in the histogram are taken as a proportion of all cells (labelled or unlabelled). Thus aneuploid tumours are 'watered down' in the same way as diploid ones are normally. No correction is made for the fact that cells in G_1 must have arisen by division since the time of taking up bromodeoxyuridine, and their numbers thus halved, as is done in calculating the normal LI. Thus the TLI for a diploid tumour (G_1 population not halved) will be slightly higher than normal LI (G_1 population halved). Given that the LI of the normal cells is presumptively lower than that of the tumour cells, the TLI of an aneuploid tumour should be substantially lower than the normal LI.

Section ix: Other Data

a) Immunohistochemical Counts of Labelling

50 of the tumours within the series were counted manually on histological sections after immunohistochemical staining for bromodeoxyuridine by Dr James Going, Senior Lecturer and Honorary Consultant, Department of Pathology, Glasgow Royal Infirmary, in order to determine the labelling index in the tumour. Whilst time consuming and unable to provide information as to the rate of cell cycle transit, such immunohistological study has the advantage that tumour cells can be identified by their cytological and histological characteristics. By contrast, with flow cytometry even in an aneuploid tumour it is rarely possible to analyse the tumour cells in total isolation from overlapping normal cells, and in a diploid tumour the two become indistinguishable. The two methods are important adjuncts to one another in determining cell cycle kinetics with bromodeoxyuridine, and the immunohistological labelling indices provide a valuable quality control for the flow cytometry.

3-4mm specimens for immunohistochemistry were fixed overnight in 10% neutral buffered formalin, and processed for paraffin histology. 4 μ sections were immunostained for bromodeoxyuridine by an ABC method. The primary anti-bromodeoxyuridine antibody (Becton-Dickinson) was diluted 1:20 and applied after acid hydrolysis with 0.7M HCl for 1 hour at room temperature, followed by trypsin digestion for 1 hour.

Counting was performed on random fields selected with an 'England' field-finding stage graticule. The only field exclusion criterion was the absence of viable tumour cells. Labelled and total tumour cell counts were recorded for every field, with the help of a 10x10-square eyepiece graticule. Successive fields were used until a minimum of 2000 cells had been counted.

b) Expression of c-erbB-2

4 μ sections from the alcohol-fixed, paraffin-embedded blocks used for kinetic studies were stained immunohistochemically by Ms S Oakes to determine expression of c-erbB-2. The 21N anti-peptide polyclonal antibody developed and supplied by Dr W Gullick at the Imperial Cancer Research Fund laboratories was used at a concentration of 2 μ g/ml as the primary antibody. Endogenous peroxidase was blocked by prior incubation with hydrogen peroxide/tris buffered saline, and non-specific binding reduced by use of normal swine and human serum. Antibody binding was demonstrated by incubation with biotinylated secondary antibody (swine anti-rabbit), followed by streptavidin-horseradish peroxidase developed with diaminobenzidine. Control sections for every tumour were run with non-immune rabbit serum as primary antibody, and previously established positive and negative controls were included with each batch.

Stained sections were assessed by two observers (Ms Oakes and Dr Going), and regarded as positive for expression of c-erbB-2 if any groups of membrane stained tumour cells were present. Cytoplasmic staining alone was classified as negative. In any cases of dubiety, repeat sections were stained and scored.

Section x: Statistical Methods

As with SPF in the previous section, the distributions of the kinetics parameters were not normal, and so non-parametric statistics have been used throughout this section. Distributions are described by median and range (or interquartile range), and inter-group comparisons are made with the Mann-Whitney or Kruskal-Wallis methods as appropriate. Labelling index and length of S phase were correlated using the Spearman rank method. Ploidy variations between groups were analysed using the chi-square statistic, and comparisons of like with supposed like were performed with the Bland-Altman approach, generally using ratios. For a detailed description of this technique, see the methods section of the previous chapter.

Chapter 9: Results

Section i: Patient Characteristics

88 patients with 91 tumours were given bromodeoxyuridine between October 1989 and October 1992, 80 at the Royal Infirmary and 11 at the Victoria Infirmary. Specimens for determination of kinetic parameters were obtained in all but two of these tumours. In a further two cases, no invasive tumour was present in the specimen, as determined by examination of H&E sections. In three other tumours, no cell kinetic data could be gained by analysis of the specimen, as explained in the next section. The age, menopausal status, pathological tumour and nodal stage, and oestrogen receptor status of the remaining 81 patients and 84 tumours, who constitute the study population for this investigation, are given in Appendix III.

Summaries of each of these prognostic variables are given in table 23. The high median age of the patients is a result of the deliberate selection of postmenopausal women for this study. Oestrogen receptor status is unfortunately available for only a minority of cases, due to a change in the arrangements for carrying out this assay within the hospitals involved over the period of the study.

Variable	n	Subgroups	
Nodal Status	52	N0	31
		N1	21
Tumour Size	57	T1	22
		T2	25
		T3	10
Hist. Grade	68	GI	13
		GII	23
		GIII	32
ER Status	28	pos	16
		neg	12
Age	77	mean 62 years range 36-90 years	

Table 23: Summary of prognostic factors. Column 2 gives the total number of patients for which information about the variable is available. Raw data in Appendix III

Section ii: Basic Cell Kinetic Data

Of the 87 tumours from which specimens for flow cytometry were obtained, 3 repeatedly failed to give adequate numbers of cells from disaggregation for histograms to be built. No kinetic data could be ascertained from these specimens. The other 84 samples could at least be used for the calculation of the labelling index, which requires only the separation of nuclei positive for BUDR from the remainder. If T_s (and so T_{pot}) are to be determined, then the population of labelled undivided cells must be large enough and clearly enough defined to be reliably distinguished in the histogram. This involves an objective criterion (number of such cells), but also a subjective assessment of the quality of the 2 parameter histogram. The distribution of the number of labelled undivided cells in each case is shown in figure 36, with 2 cases falling below the cutoff at 100 cells. The median number of labelled undivided cells counted was 501.

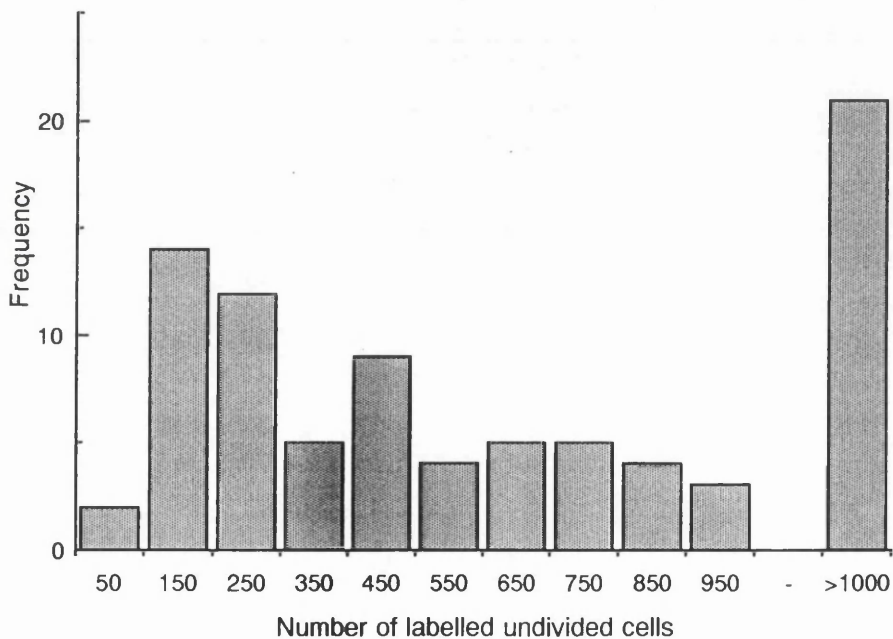


Figure 36: Frequency distribution of the number of labelled undivided cells in the 84 cases interpretable for labelling index. Column labels are midpoints, that is, 50 means 1-100 cells. Raw data in Appendix III.

A further 15 cases were regarded as being unsuitable for interpretation of T_s , either because the population of labelled undivided cells was indistinct, or because the tumour was polyploid in which case multiple such populations are present and overlapped. From the original 91 cases given BUDR, this leaves 67 in which full kinetic data were determined. A breakdown of the reasons for loss of the others is given:

No specimen obtained	2
No tumour in specimen obtained	2
Inadequate yield of nuclei from sample	3
Inadequate labelled undivided cells	2
Labelled undivided cell pop ⁿ not distinct	15

The following parameters for each histogram are given in appendix III- the number of labelled undivided nuclei counted, the half peak coefficient of variation (CV) of the diploid G_0/G_1 peak, and the DNA index of the tumour. A frequency histogram of the DNA indices is shown in figure 37, and a breakdown of the ploidy distribution is given in table 24. The frequency distribution of CVs is shown in figure 38. The median CV was 5.0% (interquartile range 3.0%-7.0%).

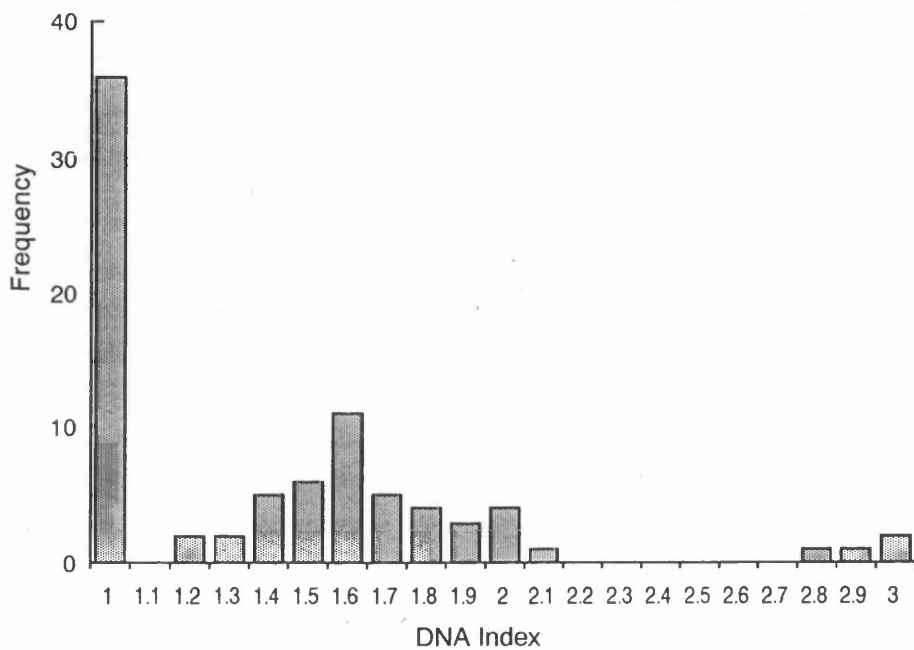


Figure 37: Frequency distribution of DNA indices for all cases which gave at least some kinetic data, excluding the one polyploid tumour (83 cases). Column labels are midpoints, that is 2 means 1.95-2.04. Raw data in Appendix III.

Ploidy	No.	%

Diploid	36	43
Aneuploid	48	57
DNA index 1.1-1.85	35	42
Tetraploid	7	8
Hypertetraploid	5	6
Polyploid	1	1

Table 24: Summary of ploidies of the 84 tumours which gave kinetic data.

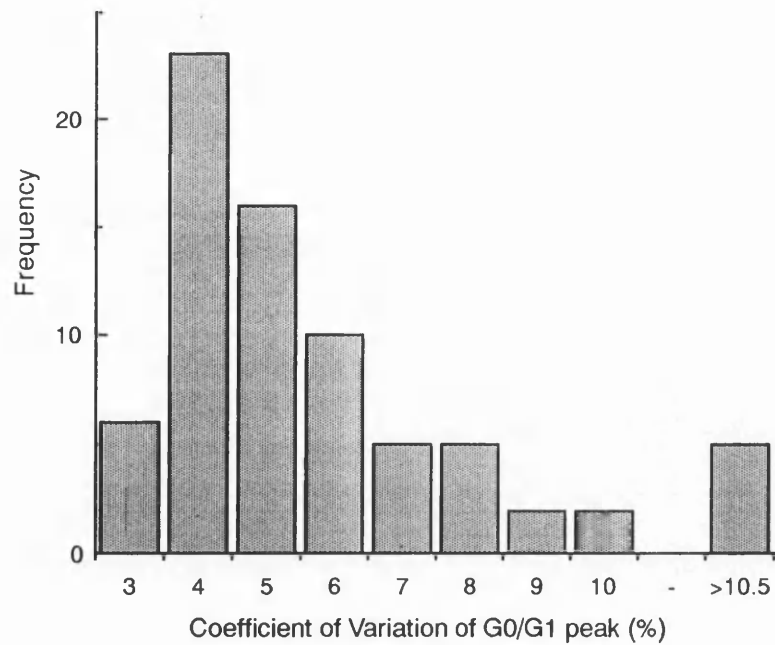


Figure 38: Frequency distribution of half-peak coefficients of variation of the diploid G0/G1 peaks in each histogram. Column labels are midpoints, that is 4 means 3.5-4.4. Raw data in Appendix III.

To summarise, LI could be calculated in 84 cases, and all three kinetic parameters in 67. Appendix V gives these data case by case. Frequency distributions of each are represented in figure 39, and summary statistics in table 25. It can be seen that there is greater variation of labelling index than the length of S phase, the LI varying by a factor of over 30, whilst T_s ranges only over a factor of 6 with a narrow interquartile range between 10 and 16 hours. These two combine to give values of T_{pot} varying from 3 days to over 60 days.

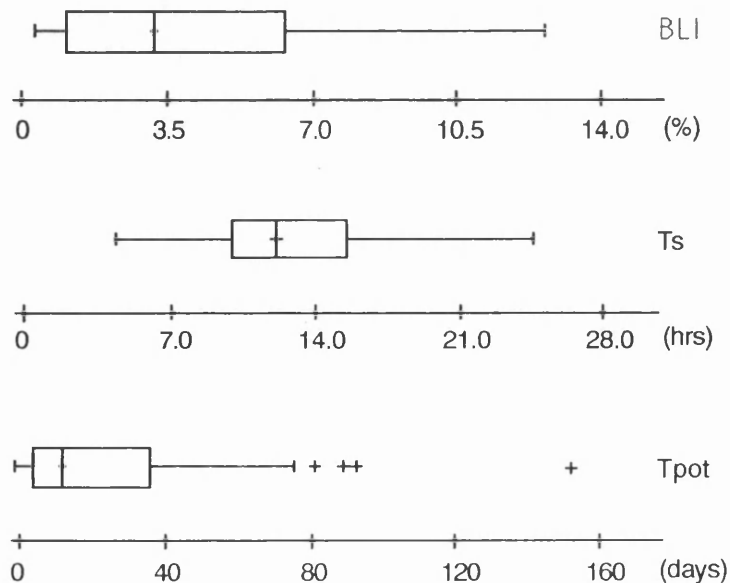


Figure 39: Distribution of kinetic parameters in all cases. Raw data in Appendix IV.

Parameter	n	Median	IQ Range	Range
BLI (%)	84	3.2	1.2 - 6.4	0.4 - 12.9
Ts (hrs)	67	12.7	10.3 - 16.5	4.8 - 32
Tpot (days)	67	14.6	8.0 - 37.5	3.7 - 153

Table 25: Summary of kinetic parameters in all cases in which they were measurable.

IQ Range = interquartile range. Raw data in Appendix IV.

Section iii: Independence of Labelling Index and Length of S Phase

If the dynamic information provided by *in vivo* labelling with bromodeoxyuridine is to provide any advantage over existing static methods, the speed of cell cycle transit must be independent of labelling index so that it provides additional information. It is possible, for instance, that the tumours with high labelling indices are also those in which the rate of cell cycle transit is high, in which case little is being gained by measuring the latter. In figure 40, the labelling index for each individual tumour is plotted against the length of S phase for that tumour, for each of the 67 cases where both parameters were calculated. It is apparent from inspection of this graph that there is no strong trend for one to vary with the other, the points lying in a nearly horizontal band across the chart. This is borne out by statistical analysis, with Spearman rank correlation coefficient $r = -.010$ ($p = 0.93$). The length of S phase for a particular tumour is therefore independent of the labelling index of that tumour within this series, and represents a novel item of information about the lesion. This does not presuppose any significance for this additional data.

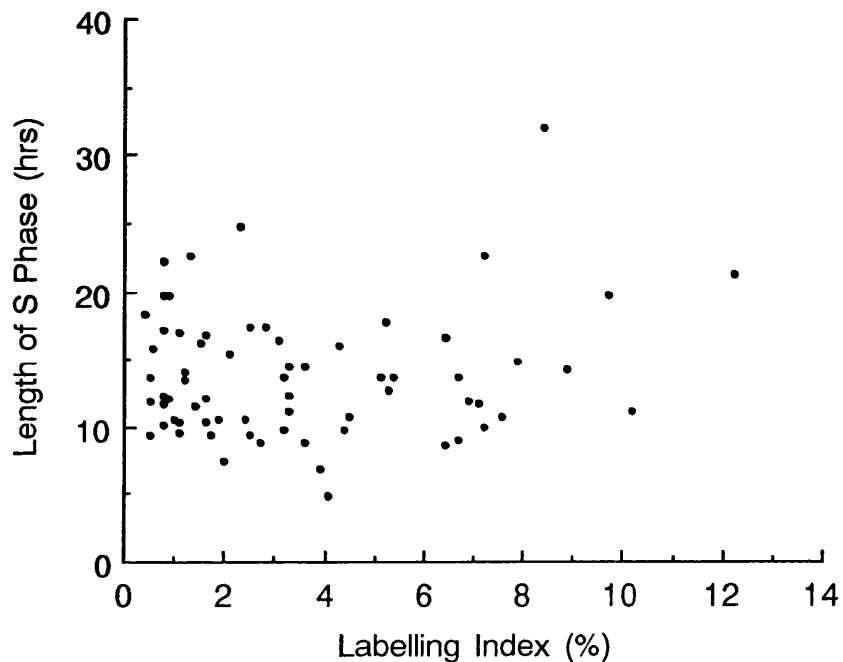


Figure 40: Plot of bromodeoxyuridine labelling index against length of S phase in tumours for which both are available ($n=67$). Raw data in Appendix IV.

Section iv: Relationship of Length of S Phase to Labelling Time

The mathematical model used for the calculation of T_s from data derived from the bivariate histogram assumes that labelled cells are initially evenly distributed through S phase, and progress at uniform rate toward tetraploid DNA content. If these conditions are not met then the relative movement will not vary linearly with time, and the estimate of S phase made from the histogram will partly depend upon the labelling time.

In order to obtain an accurate estimate of RM it might also be necessary for the labelled cells to have progressed some distance through S phase. This is a result of the fact that the DNA content of each cell is reduced to a channel number within the histogram. Each channel covers a range of values of DNA content, and this range is larger in the 64 channel two parameter histogram than the 256 or 1024 channel one parameter ploidy histogram used for calculating SPF. This uncertainty about the position of each point in the histogram is fixed, and so it is proportionally greater at low DNA contents, or small differences between two points of interest. As an extreme example, if the labelling time were very short indeed, each labelled cell might have moved less than one channel within the histogram. Some would have crossed a channel boundary even in making this small movement, but many will not have, and so will appear not to have moved in the histogram at all. If the labelling time were longer, such that the average movement was of six channels this error of one channel is proportionally less (only 16% rather than 100%). So the calculation of relative movement becomes statistically more accurate the longer the labelling time. This is counterbalanced at long labelling times by the loss to the calculation of cells which have divided, but this is another reason why T_s may be dependent upon the labelling time used.

To examine the effect of these points upon the estimation of T_s , figure 41 shows this parameter broken down by labelling time. It can be seen that as anticipated from the second argument above, T_s does have a different distribution at very low labelling times. Encouragingly, for labelling times above 4 hours (80% of all tumours), T_s is independent of labelling time, suggesting that the mathematical model for calculation is appropriate within the current setting.

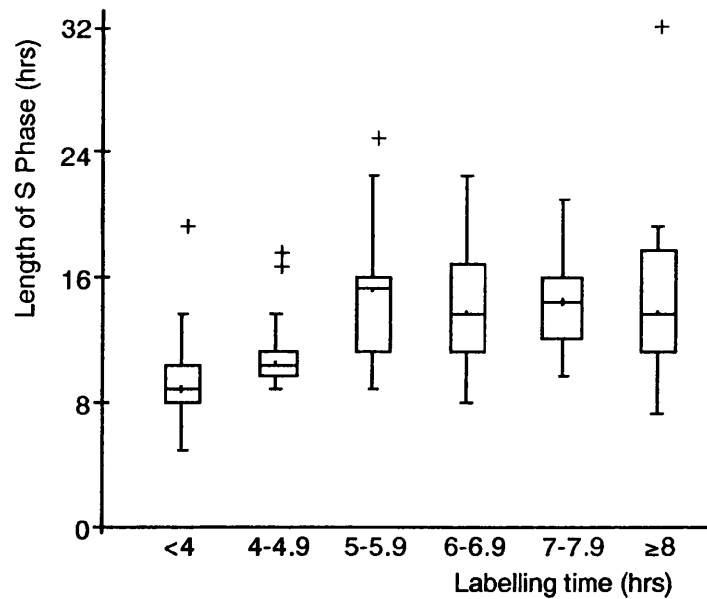


Figure 41: Variation of T_s with time between bromodeoxyuridine labelling and tumour biopsy. For each interval indicated on the x axis, the distribution of values of T_s for the tumours which had this labelling time is given. The line inside each box indicates the median value, the box itself encloses the central two quartiles of the distribution, and the whiskered lines show the full range. + indicates outlying values.

Section v: Flow versus Immunohistochemical Labelling Indices

The labelling index as determined from the bivariate histogram could be compared to that calculated by counting at least 2000 cells on a suitably stained tissue section (the immunohistochemical labelling index, ILI; see methods, section ix) in 50 cases. As discussed in the previous chapter, the calculation of bromodeoxyuridine labelling index (BLI) is ploidy dependent, being inherently higher in aneuploid tumours. An attempt has been made to overcome this bias by calculation of the total labelling index (TLI), which includes all cell populations within the tumour, and makes no correction for cells which have divided since taking up the label. Since the immunohistochemical counts cannot make allowance for cells which have divided, the TLI might theoretically accord better with the ILI, in diploid cases at least. Counting on the sections does only include tumour cells, and so in an aneuploid tumour the BLI, which also only includes tumour cells, would theoretically be expected to be the more appropriate figure for comparison.

Appendix IV includes the tumour ploidy, the bromodeoxyuridine and total labelling indices, and the immunohistochemical counts for each case. The first two are plotted against each other below.

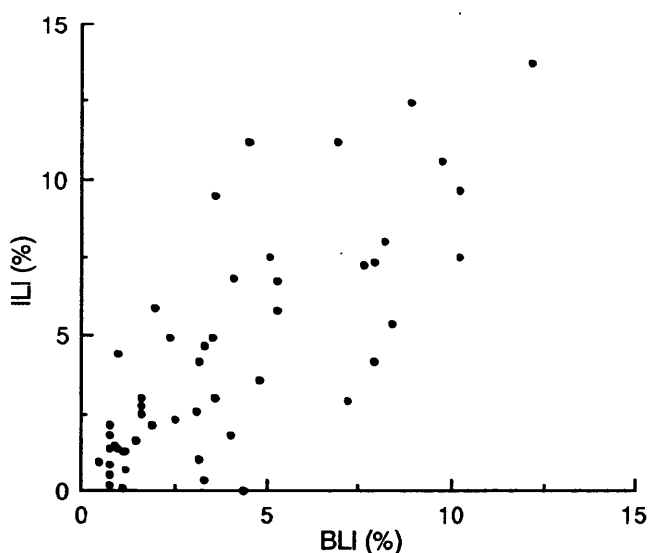


Figure 42: Plot of bromodeoxyuridine labelling index (BLI) against immunohistochemical labelling index (ILI) in 50 cases for which both are available. Line of best fit is $y = 0.799 + 0.896x$ ($r = 0.777$). Raw data in Appendix IV.

In table 26 the degree of agreement between the flow and histochemical methods is presented as analysed by the Bland-Altman technique. Cases are considered all together, and also broken down by ploidy, with mean differences more than two standard errors different from zero underlined. In all cases the ILI is slightly higher than the flow cytometric indices, giving a negative result for the difference as calculated. As predicted theoretically, agreement is better with the BLI for aneuploid tumours, and with the TLI for diploid tumours. For these two comparisons, there is no significant difference between the flow derived and immunohistochemical labelling index overall. The degree of divergence in individual cases can be judged from the standard deviations for the differences, given in the final column of the table. The SDs of just over two percent indicates that 95% of differences were less than about 4.6%. This is a substantial figure in relationship to even the highest labelling indices of the order of 10%, indicating that the good overall agreement does not preclude relatively large differences in individual cases.

Comparison	n	Mean Diff	SE Mean	SD Diff
BLI - ILI (all)	50	-0.389	0.325	2.30
TLI - ILI (all)	50	<u>-1.279</u>	0.388	2.74
BLI - ILI (dip)	22	-0.597	0.505	2.31
TLI - ILI (dip)	22	-0.285	0.503	2.31
BLI - ILI (an)	28	-0.354	0.429	2.27
TLI - ILI (an)	28	<u>-2.034</u>	0.546	2.89

Table 26: Comparison of labelling indices calculated by flow cytometry (BLI & TLI) and immunohistochemistry (ILI), for all 50 cases counted immunohistochemically, and separately by ploidy groups. Bland-Altman analysis using differences. Mean differences significantly different from zero are underlined. Raw data in Appx. IV

One further point to be made from these results follows from the observation that the TLI in aneuploid cases is lower than the other two labelling indices. This indicates that the labelling index in the non-tumour component is indeed lower than that in the tumour itself, as assumed in talking of the 'dilutional' effect of this component. This is in keeping with the following result.

Section vi: Comparison of Kinetics in Tumour and Normal Breast

In patients being treated by mastectomy, an attempt was made to obtain a specimen of breast tissue from a site distant from the tumour. In many cases, histological examination showed this to consist of fatty stromal elements only. In eight cases specimens of normal breast parenchyma were obtained, and these were processed for multivariate flow cytometry in the same way as tumour samples. The values of BLI, T_s and T_{pot} for each of the 8 cases are listed in table 27. One of these samples came from one of the two patients in whom there was no tumour in the 'tumour' sample taken for analysis of cell kinetics. The distributions of the kinetic parameters in all 8 specimens have been compared to the values for all 84 tumours; in the 7 cases where there was a corresponding tumour sample, the normals have been compared with the tumours from the same patients. The results of this analysis are summarised in table 28.

Tumour	BLI	T_s	T_{pot}
1	1.2	14.3	33.8
2	0.6	10.4	46.9
3	0.2	11.8	168.0
4	0.3	11.9	104.7
5	0.5	27.7	163.4
6	0.3	17.7	163.0
7	0.2	16.6	308.1
8	0.9	13.7	43.1
median	0.4	15.5	128.9

Table 27: Kinetic parameters in 8 specimens of normal breast

The bromodeoxyuridine labelling indices of the normal samples were significantly lower than those of all tumours, and also lower than those of the 7 tumours from the same patients. Length of S phase was no different with either type of comparison. As might be expected from these results, the potential doubling time was significantly longer in the normal tissues than the tumours. All normal specimens were diploid. Of the 7 corresponding tumours, 6 were aneuploid. Not for the first time, we run into the problem that ploidy biases the kinetic values obtained, so that direct comparisons such as the foregoing are potentially misleading. Comparison of the bromodeoxyuridine

labelling index in the normals with the total labelling index for the tumours should address this problem, and it is for this reason that the results of this analysis are also presented in the table. The normal samples have also been compared to all diploid tumours as a further check. It can be seen that the finding of lower labelling in the normal tissues is unchanged by removing the ploidy bias in these ways.

Comparison	n norm	n tum	median normal	median tumour	95%CI (t-n)	p
BLI, all normal vs all tumours	8	84	0.4	3.2	0.9 - 4.9	<u><0.0001</u>
Ts, all normal vs all tumours	8	84	15.5	12.0	0.8 - -5.0	0.14
Tpot, all normal vs all tumours	8	84	129	12.5	-35 - -153	<u>0.0001</u>
BLI, normal vs corr. tumours	7	7	0.3	4.8	0.2 - 6.2	<u>0.011</u>
Ts, normal vs corr. tumours	7	7	14.3	12.7	4.7 - -7.6	0.90
Tpot, normal vs corr. tumours	7	7	163	7.6	-25 - -161	<u>0.015</u>
BLI, normal vs diploid tumours	8	36	0.4	1.25	0.4 - 2.1	<u>0.0009</u>
BLI normal vs TLI all tumours	8	84	0.4	2.65	0.85 - 3.48	<u>0.0001</u>
BLI normal vs TLI corr tumours	7	7	0.3	2.89	0.18 - 4.4	<u>0.015</u>

Table 28: Comparison of kinetic parameters in tumour and normal breast. The first column indicates the parameter(s) being compared and the cases being used for the comparison. Column 6 gives the 95% confidence intervals for the difference between the two groups (tumour - normal). Significant differences are underlined in the last column.

Section vii: Comparison of Labelling Index and S Phase Fraction

The ploidy histograms obtained in the course of running these specimens were analysed offline to calculate the value of SPF, as used in the section II save only that here this was done using updated software (Multicycle, Phoenix Systems). Theoretically this is the same measurement as the bromodeoxyuridine labelling index, since the label is supposedly taken up by all S phase cells, and only by S phase cells. The corresponding values of BLI and SPF have been compared for each tumour.

Calculation of SPF using the objective criteria employed in Part II was possible in 74 of the 84 cases (88%) for which BLI is available. The higher success rate in obtaining values for SPF compared with the series reported in Part II is probably the result of two factors, firstly the greater number of nuclei counted for each histogram (about

50,000 here, but only 10,000 in the earlier series), and secondly because the newer software is more capable than the Cytologics programme used in Part II. The data on SPF for each tumour are included in Appendix IV. The 74 pairs of values of BLI and SPF are plotted in fig. 43, and the distribution of values of SPF is shown in fig. 44.

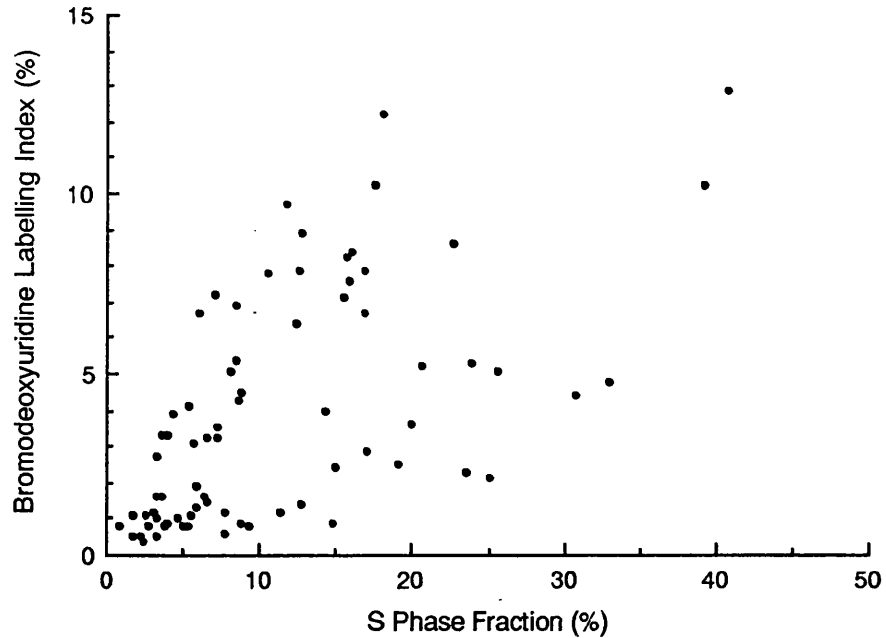


Figure 43: Plot of bromodeoxyuridine labelling index against S phase fraction for each of the 74 tumours in which both could be measured. Raw data in Appendix IV.

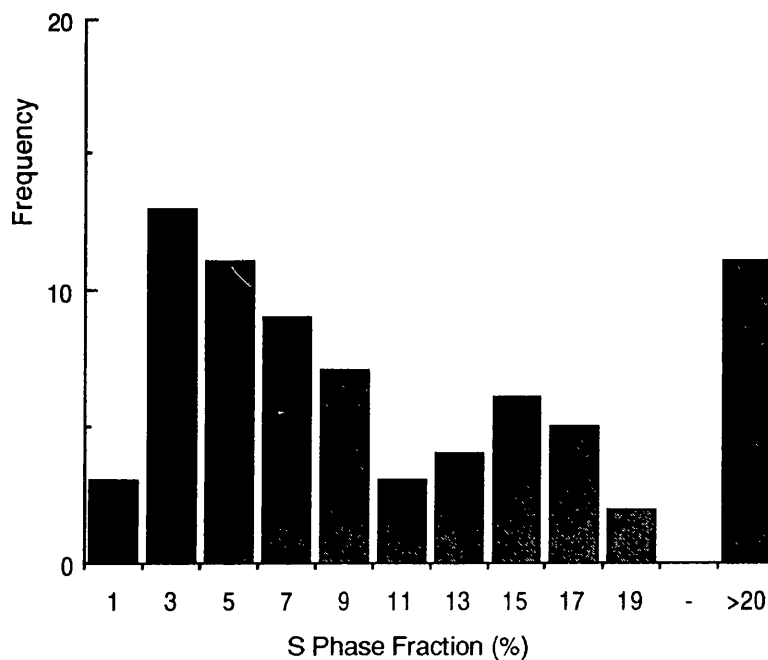


Figure 44: Frequency distribution of values of S phase fraction in the 74 tumours in which it could be measured. Column labels are midpoints, that is 3 means 2.5-3.49. Raw data in Appendix IV.

Spearman rank correlation of the two distributions gives $r = 0.667$, $p < 0.0005$. Since the two are supposedly measurements of the same thing, this finding is not surprising, and in order to assess the association between the two, Bland-Altman analysis has again been used. Examination of the data showed that disagreement increased with increasing mean value, and so the analysis was performed using the ratio between the two figures in each case:

Mean Ratio	SE Mean	SD Ratios
4.11	0.374	3.2

Table 29: Summary of the distribution of the ratios SPF / BLI in the 74 cases in which both could be measured. Raw data in Appendix IV.

It can be seen that the value of SPF tends to be higher than that of BLI for the same tumour (there are only three examples where this is not the case), on average by a factor of 4. Given the standard error of this figure, this is highly significantly different from the ideal ratio of 1. The fact that the standard deviation is so high in relationship to the mean indicates that very large variations are observed, and indeed the highest ratio between the two is 16.4 (SPF = 14.8%, BLI = 0.9%). Although there is close rank correlation between these two measurements of the proportion of S phase cells in the tumour population, SPF almost uniformly gives a higher estimate, by a very variable factor. If we accept that the two are theoretically measurements of the same biological parameter by different means, they cannot both be right. Is the SPF tending to overestimate the true proportion, the BLI to underestimate, or both? Although the updated computer software is a great improvement upon the original, most of the caveats about the use of such packages discussed in Part II remain. It has also already been stated that not all cells synthesising DNA take up thymidine or its analogues, so that there is some rationale for suggesting that BLI might underestimate the true S phase percentage. The answer to the query above is probably both. Even so, the good correlation between S phase fraction and bromodeoxyuridine labelling index is encouraging in the sense that if we are not too concerned with the actual value for the number of cells in S phase at a point in time, but rather with the relative values for different samples, then the two techniques provide comparable answers. In terms of determining prognosis, or guiding therapy, or exploring tumour biology, it is just this type of relative information that is needed. In this sense, the two methods do tend to bear each other out.

Section viii: Relationship of Kinetics to Pathological Prognostic Factors

Follow-up of these patients is still too short to assess the prognostic significance of the kinetic parameters themselves. Some indication can be gained by studying the degree of correlation between these variables and other tumour characteristics known to predict outcome. These interrelationships are summarised in table 30.

None of the three kinetic parameters are significantly associated with nodal status, the single strongest predictive factor for outcome, or with size of the primary tumour. Histological grade is very strongly related to labelling index, grade 3 tumours having a median labelling index 5 times higher than that of grade 1 tumours. This result is not altered by the use of total labelling index or immunohistochemical labelling index as the basis of comparison, indicating that it is not the result of ploidy bias. Grade is not related to length of S phase, but the effect upon labelling index is carried through into potential doubling time, which is significantly shorter in high grade tumours.

Factor		n (LI)	LI	Median Values of:		n (T _s & T _{pot})
				T _s	T _{pot}	
Nodal Status	N0	31	3.2	12.1	16.15	24
	N1	21	4.8	13.7	14.2	17
	p		0.83	0.12	0.60	
Tumour Size	T1	22	4.05	11.3	13.45	16
	T2	25	2.0	13.6	25.1	21
	T3	10	4.2	11.7	10.5	9
	p		0.58	0.41	0.18	
Tumour Grade	1	13	1.0	13.5	37.5	13
	2	23	2.4	13.6	17.7	19
	3	32	5.1	11.9	8.6	23
	p		<u><.001</u>	0.60	<u><.001</u>	
Estrogen Receptor Status	ER-	12	4.0	14.35	11.35	10
	ER+	16	1.2	12.85	36.5	14
	p		<u>0.026</u>	0.77	0.14	

Table 30: Relationship between kinetic parameters and prognostic factors. The second and last columns give the numbers of patients in that subgroup for whom LI and T_s, respectively, are available. Probability values are based on Mann-Whitney (nodal and ER status) or Kruskal-Wallis analysis (size and grade). Results significant at the 5% level are underlined. Raw data in Appendices III & IV.

The prognostic factor most strongly associated with labelling index independent of ploidy, the histological grade, is also the factor which predicts ploidy to some degree in cross tabulation. In this analysis the proportions of aneuploid and diploid tumours in

subgroups defined by each prognostic factor were compared by the chi-square method (table 31). High histological grade is associated very strongly with an increasing proportion of aneuploid tumours, with only 2 of 13 grade 1 tumours being aneuploid compared with 22 out of 32 grade 3 lesions.

	Nodal Status		Tumour Size		
	N0	N1	T0	T1	T2
Diploid	42	40	38	48	30
Aneuploid	58	60	62	52	70

	ER Status		Hist. Grade		
	Neg	Pos	G0	G1	G2
Diploid	27	50	85	45	31
Aneuploid	73	50	15	55	69

Factor	χ^2	df	p
Nodal Status	0.019	1	0.90
Tumour Size	1.079	2	0.58
Hist. Grade	10.60	2	<u>0.005</u>
ER Status	1.395	1	0.24

Table 31: Relationship between tumour ploidy and prognostic factors in the BUDR labelled tumours. The upper part of the table gives the proportion of aneuploid and diploid tumours in each subgroup (that is, all figures are column percentages). The tables for each factor have then been analysed by the chi-square method, using the actual numbers in each cell rather than the percentages, and the results are shown in the lower part of the table. The only result significant at the 5% level is underlined. Raw data in Appendix III.

Section ix: Relationship of Kinetics to Ploidy

The fact that kinetic parameters are measured upon different populations within the histogram in aneuploid and diploid tumours has already been explained. This creates an inherent tendency for aneuploid tumours to appear to have higher labelling indices, and this is indeed reflected in the current sample. When the values of BLI are simply broken down by ploidy status of the tumour as in figure 45, the median labelling index for the aneuploid tumours, 5.2%, is significantly higher than that for diploid tumours, 1.25% (Mann-Whitney, $W = 905.5$, $p < 0.00005$).

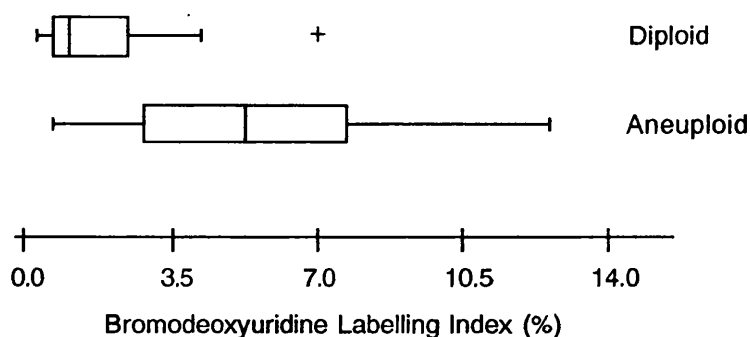


Figure 45: Box and whisker plot of values of bromodeoxyuridine labelling index broken down by tumour ploidy. The line within each box indicates the median, the boxes enclose the central two quartiles of the distribution, and the whiskers span the full range of values save for outlying values indicated with a + symbol. Raw data in Appendix IV.

Although the same problem exists for the calculation of T_s , it is not so clear *a priori* that the rate of DNA synthesis in tumours will be any different to that in normal tissue. Values of T_s broken down by ploidy are shown in figure 46; there is no significant difference between the two groups (aneuploid median 13.6hrs, diploid median 11.7hrs; Mann-Whitney, $W = 1024.5$, $p = 0.14$). There are two possible explanations for this. The simpler is that there is no difference in the length of S phase between either diploid and aneuploid tumours, or between tumour and non-tumour cells. It is also possible that there is a difference between aneuploid and diploid tumours, which is being counterbalanced by difference in the opposite direction between tumour and non-tumour cells. If, for instance, diploid tumour cells have a shorter T_s than aneuploid tumours cells, but the non-tumour cells with which they are mixed in the histogram have a longer T_s than either, then the mixture of diploid and non-tumour cells seen in a diploid histogram may give the same net value of T_s as the pure tumour cell population of an aneuploid population. This is an inherently less likely explanation on Occamite grounds, but it does demonstrate that a difference in the rate of DNA synthesis between diploid and aneuploid tumours cannot be excluded on the basis of this result alone.

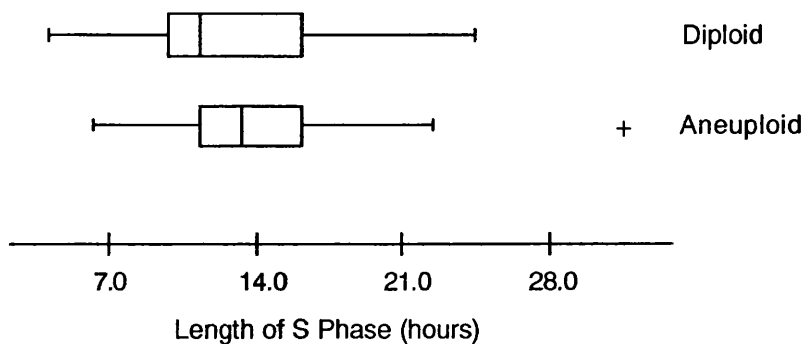


Figure 46: Box and whisker plot of values of length of S phase broken down by tumour ploidy. Symbols as in figure 38. Raw data in Appendix IV.

The same arguments can be made in respect of labelling index, but in this case it is possible to eliminate the bias in favour of aneuploid tumours and establish whether the observed difference in labelling index is real. This has been looked at in two ways- by the use of a corrected labelling index (the TLI); and by the use of immunohistochemical counting (the ILI), which ignores non-tumour cells. Figure 47 illustrates the relationships between these indices and tumour ploidy:

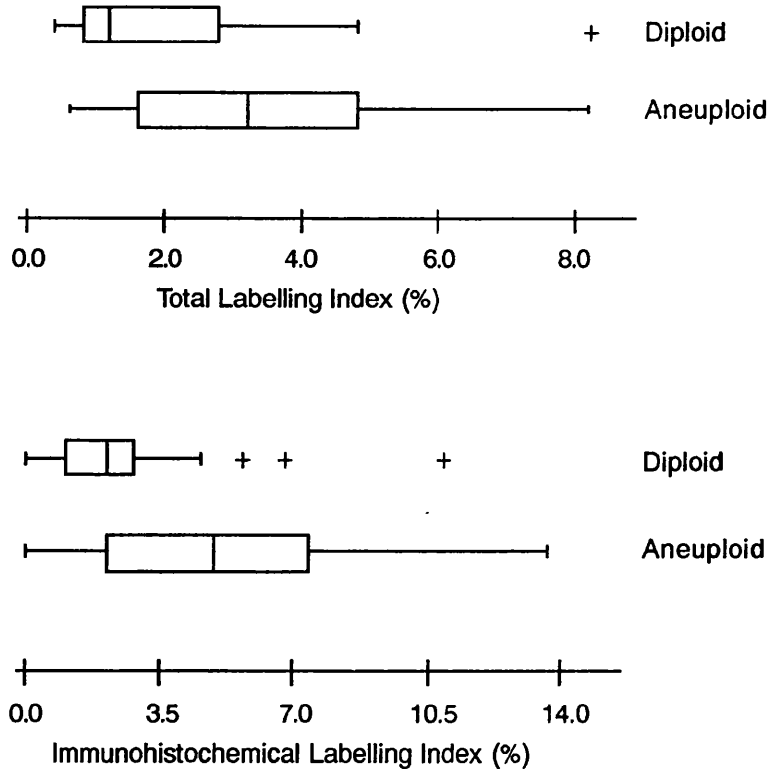


Figure 47: Box and whisker plot of values of TLI (above) and ILI (below) broken down by tumour ploidy. Symbols as in figure 38. Raw data in Appendix IV.

In each case, the statistically higher labelling index in aneuploid tumours persists (Mann-Whitney, $p = 0.001$ for TLI, $p = 0.01$ for ILI). Within this series then, aneuploid tumours have a higher labelling index than diploid lesions. Given the absence of any difference in length of S phase between the two ploidy groups, this would be expected to lead to lower values for T_{pot} in the aneuploid tumours, and this is indeed the case (diploid median $T_{pot} = 33.35$ days, aneuploid median $T_{pot} = 8.9$ days, Mann-Whitney $W = 1475$, $p = 0.0001$).

Section x: Relationship of Kinetics to *c-erbB-2* Expression

Expression of the growth factor receptor oncoprotein *c-erbB-2* has been associated with a poor prognosis in breast cancer (Winstanley et al 1992, Slamon et al 1987, Clark and McGuire 1989). It is not unreasonable to hypothesise that this might be because overexpression of such molecules conferred a growth advantage upon such

cells. If so it might be possible to observe that rates of cell growth were more rapid in tumours exhibiting overexpression than in those not doing so, and this has certainly been the finding of some groups using SPF or TLI as measures of cellular proliferation (Anbazhagan et al 1991, Barnes et al 1991, Kallioniemi et al 1991, Tommasi et al 1991). This question has been approached here by immunohistochemical staining for the presence of the *c-erbB-2* protein, as described in the methods section.

74 of the tumours for which kinetic data were available were assessed for this marker. 29 of these (39%) were found to be positive. The result for each tumour is given in Appendix IVa. Figure 48 shows each of the three kinetic parameters broken down by the *c-erbB-2* status of the tumour, and table 32 gives the results of statistical comparison of the two groups in each case.

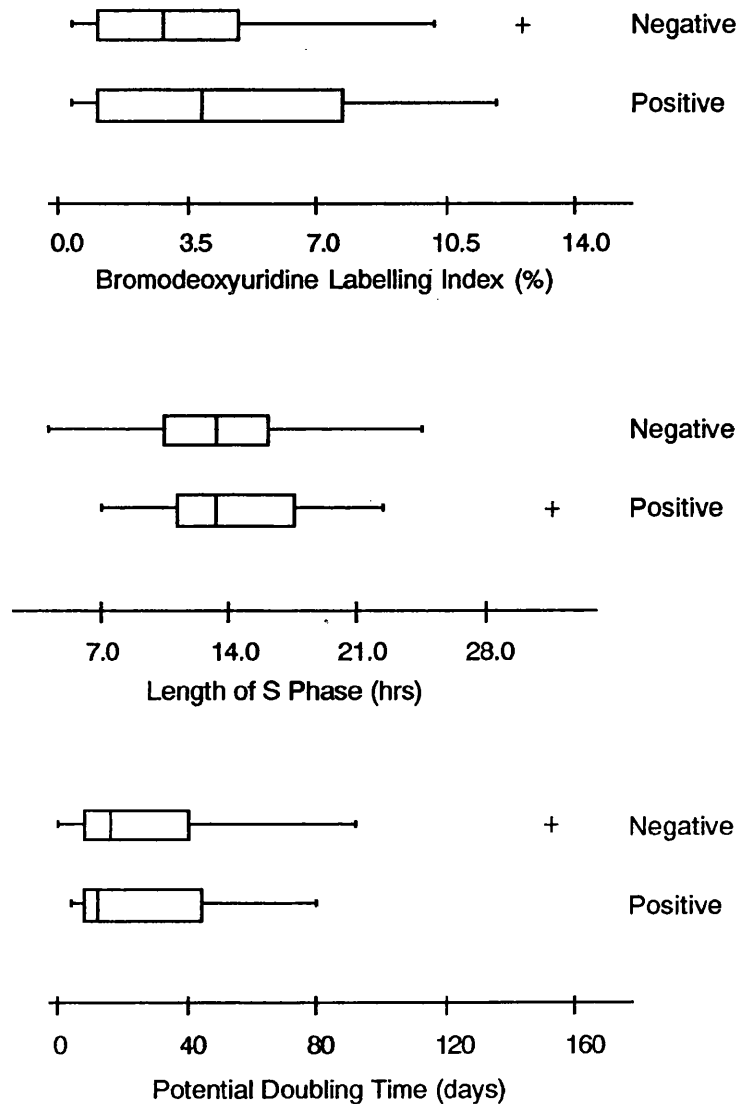


Figure 48: Box and whisker plot of values of kinetic parameters broken down by expression of the *c-erbB-2* oncoprotein. The line within each box indicates the median, the boxes enclose the central two quartiles of the distribution, and the whiskers span the full range of values save for outlying values indicated with a +. Raw data in Appendices IV&IVa.

Parameter	number		median		95%CI	p
	neg	pos	neg	pos		
BLI(%)	45	29	2.8	4.0	-2.4 - 0.40	0.28
T _S (hrs)	38	20	13.6	13.55	-3.4 - 1.7	0.48
T _{pot} (days)	38	20	19.6	13.65	-6.8 - 12.9	0.77

Table 32: Comparison of kinetic parameters in tumours which do or do not express *c-erbB-2*. The first two columns give the numbers of negative and positive tumours for which that parameter is available. Mann-Whitney test, including the 95% confidence interval for the difference in medians. Raw data in Appendix IVa.

Within this series, there is no difference between the cell kinetics of tumours which do or do not express *c-erbB-2*. It has been noted by previous authors that expression of *c-erbB-2* is more common in aneuploid tumours, and a ploidy imbalance between any two groups of interest will bias their comparison because of the difference in the method of calculating labelling index in aneuploid and diploid tumours. It is therefore important to look at the relationship between the ploidy-independent labelling indices TLI and ILI in the two *c-erbB-2* groups, and this is done in figure 49. In table 33 tumour ploidy and staining for *c-erbB-2* are cross tabulated. Chi-square analysis using this data shows that in keeping with previous reports, aneuploid tumours are more likely to express *c-erbB-2*, but allowing for this does not reveal any hidden relationship with labelling indices (Mann-Whitney, $p = 0.63$ for TLI, $p = 0.19$ for ILI).

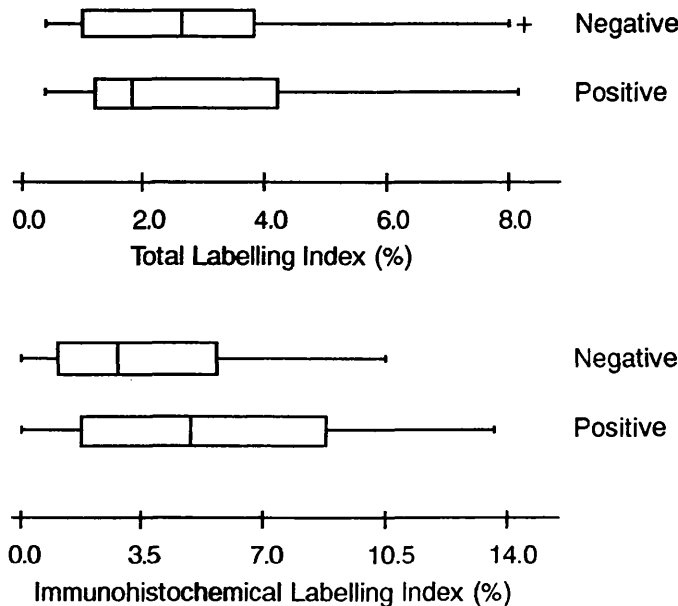


Figure 49: Box and whisker plot of values of total and immunohistochemical labelling indices broken down by expression of *c-erbB-2*. The line within each box indicates the median, the boxes enclose the central quartiles of the distribution, and the whiskers span the full range of values (outlying values indicated with a +). Raw data in Appendices IV&IVa.

	<i>c-erbB-2</i>	
	Negative	Positive
Diploid	24 (75%)	8 (25%)
Aneuploid	21 (50%)	21 (50%)

Table 33: Comparison of ploidy in *erbB-2* positive and negative tumours.

Figures in brackets are row percentages. $\chi^2 = 4.76$, 1 df, $p = 0.03$. Raw data in Appendices IV&IVa.

Section xi: Reproducibility Studies

The validity of the parameters measured by this methodology has been tested in a number of ways. Since there is no gold standard against which to check the absolute values obtained, testing has concentrated on establishing the limits of consistency and reproducibility of the method. This has been done by:

- running duplicate sections of the same tumour at different times;
- comparing the results obtained by disaggregation of dewaxed tissue sections, as used in this study, with the method of Begg et al involving disaggregation of non-embedded tumour; and
- multiple analysis of derived histograms at different time-points and by different individuals to establish the inter- and intra-observer reproducibility of the subjective process of histogram interpretation.

This work has been carried out in association with other workers within the laboratory performing similar investigations in cancers of the cervix and head and neck. Some of the results use data from these series rather than this one.

a) Results from Serial Sections

This was done by Ms G Forster using material derived from head and neck cancers, processed in exactly the same way as in the current series. A new 50 μ section from 12 previously studied tumours was processed and the kinetic values obtained were compared to those gained from the original section. Analysis was by the Bland-Altman method, using the ratio between pairs of results (that is, the distribution of the quotient 'first observation / second observation'). This form of analysis is used throughout this section. The data and results are given in the table:

Patient	Labelling Index (%)		Length of S Phase (hrs)	
	Section1	Section2	Section1	Section2
1	8.0	8.6	16.9	14.8
2	7.1	8.0	13.2	12.8
3	14.6	13.2	18.6	16.1
4	9.3	9.1	10.5	10.3
5	10.0	10.2	17.6	16.3
6	9.4	9.9	14.9	14.8
7	11.2	8.5	22.6	20.4
8	1.4	1.6	16.4	14.9
9	9.3	8.7	20.3	17.1
10	15.8	13.3	28.8	29.7
11	14.4	12.3	19.3	21.5
12	1.8	1.6	15.0	16.6

	Mean Ratio	SE Mean	SD Ratios
LI	1.05	0.038	0.13
Ts	1.05	0.027	0.09

Table 34: Comparison of results obtained from two sections of the same tumour, run separately. Raw data above. For the lower table, the first result has been divided by the second for each tumour, and the columns describe the distribution of these ratios.

The mean value of the quotient did not vary significantly from unity in respect of either kinetic parameter, indicating no overall tendency for the second series of sections to provide either higher or lower answers than the first series. The size of the standard deviations means that 95% of the second estimates for each parameter were within 25% of the original estimate for that parameter upon that tumour. For biological data with this degree of variability from tumour to tumour, this is a very acceptable degree of variation using this demanding form of analysis. Contiguous sections could be expected to be very similar in the nature of the contained cell population, and so tumour heterogeneity should contribute little of the observed variability. This is one of the advantages of using sections for study, rather than unembedded tumour samples.

b) Results from Tumour Segments

In 19 cases, a second sample was analysed from a previously studied tumour, but using nuclei obtained by disaggregation of an unembedded tumour sample rather than a repeat 50 μ section. This work was performed on breast cancers from the current series, and raw data are shown in table 35, below which are the Bland-Altman summary statistics.

Patient	Labelling Index (%)		Length of S Phase (hrs)	
	Segment	Section	Segment	Section
4	0.4	1.1	16.2	17.0
13	2.9	3.2	10.8	9.8
16	9.5	8.9	20.4	14.2
17	0.6	0.5	13.1	13.7
30	5.0	3.2	16.4	13.6
36	1.3	1.2	6.4	14.0
37	2.2	1.6	9.5	12.0
46	1.9	1.2	24.3	16.2
56	1.8	0.8	22.7	11.8
60	0.6	4.1	6.2	4.8
61	7.1	5.1	14.1	13.6
62	2.2	1.9	13.3	10.5
63	8.2	7.9	14.7	9.4
65	8.3	4.8	4.0	11.1
67	8.3	5.1	24.6	12.0
68	9.9	7.9	19.8	14.9
70	3.7	3.6	12.7	8.8
73	8.0	6.4	18.1	8.5
79	1.2	0.8	12.9	17.1

	Mean Ratio	SE Mean	SD Ratios
LI	1.238	0.108	0.469
T _s	0.991	0.134	0.584

Table 35: Comparison of results obtained from a section and a segment of the same tumour, run at separate times. Raw data above, and below the result obtained from the section has been divided by that gained from the segment. Columns describe the distribution of these ratios.

Neither mean ratio differs significantly from 1, indicating no trend for either type of sample to give higher or lower values for either labelling index or length of S phase. In this respect, the result is the same as that obtained when the repeat specimen was a further section (a, above). The striking difference between the two sets of results is that the standard deviation of the distribution of ratios for both LI and T_s is much higher here, where the repeat specimen is a separate tumour sample, than in the previous experiment when the repeat specimen was a further section from the same sample. This increase in variability almost certainly reflects the degree of tumour heterogeneity with respect to cell kinetics. Whilst this must cause some disquiet as to the validity of any measurement based upon a single tumour sample, it is also encouraging technically in the sense that far the smaller component of the overall

variation, as reflected in the standard deviations in this experiment, is provided by the run to run variation as tested in the previous experiment.

c) Inter- and Intra-Observer Variation

We have so far considered the variation from one run to another of the same tumour arising in the many steps of sample processing, in the degree of error inherent in any measuring system such as a flow cytometer, or due to variation of the measured parameters within the tumour itself. We need also to consider the potential for variation from the subjectivity of the interpretation of the derived histograms. The values of both LI and especially T_s depend upon the precise situation of the boxes defining the subgroups of labelled undivided, labelled divided, and unlabelled cells. The criteria used for placing these boxes are covered in the Methods chapter. The reproducibility of the calculation of kinetic parameters from histograms has been tested by two experiments in which the same histograms were analysed by two observers. In the first of these, 37 histograms from head and neck cancers were analysed by Ms Forster and myself. This experiment looked at labelling index only, the results being shown below:

	Mean Ratio	SE Mean	SD Ratios
LI	1.13	0.056	0.160

Table 36: Comparison of results obtained from 37 histograms analysed by two observers (myself and Ms G Forster). My result has been divided by hers. Columns describe the distribution of these ratios.

In the second series, Mr B Bolger and I analysed 23 histograms derived from cervical carcinomata. Here the reproducibility was expressed using the difference, My result - His result, in respect of labelling index, length of S phase and potential doubling time:

	Mean Diff	SE Mean	SD Diffs
LI	0.177	0.087	0.417
TLI	0.235	0.062	0.298
T_s	-0.497	0.126	0.604
T_{pot}	-0.265	0.062	0.298

Table 37: Comparison of results obtained from 23 histograms analysed by two observers (myself and Dr B Bolger). His result has been subtracted from mine. Columns describe the distribution of these differences.

In both series, there are indeed differences in the answers obtained by the two observers, from the same histograms. In the first series, I estimate labelling indices 13% higher on average than Ms Forster (ie I use a lower cut off between labelled and

unlabelled cells in terms of amount of green fluorescence). This means that if I obtained an estimate of LI of 3.2% (the median value) for a given histogram, then the most likely value for Gill's estimate for that histogram would be 2.8%. Given the standard deviation of 0.16 for the distribution of ratios, the 95% confidence intervals for her estimate of the labelling index are plus or minus 0.32 times the mean of our estimates (ie $0.32 \times 3\%$) or 1.8 and 3.8%. Compared to the range of values of LI across the 84 tumours of 0.4 to 12.9%, this interobserver error is small in relationship to the variability of the parameter being measured, but of considerable size nevertheless.

In comparing my results to Mr Bolger's, it needs to be emphasised that these are expressed not in terms of ratios, as in the previous experiment, but rather as absolute differences between the two sets of data, these showing less tendency to vary with the size of the parameters being measured. Whilst this is not directly comparable to the results above, it allows us to examine the interobserver variation in terms of magnitude rather than proportion. As was the case in the previous comparison, I obtain on average higher estimates of labelling indices, and in this case lower estimates of the length of S phase, both of which tend to make my estimates of potential doubling time shorter. But here the amplitude of these differences is very small in relationship to the values of the parameters themselves, with my measurement of LI being on average 0.18% higher (mean LI for the 23 histograms was 11.1%), and of T_s 0.50hrs shorter than his (mean T_s for the 23 histograms 10.9 hrs). The analyses for this experiment were performed over a year later than those for the previous one, and this may explain the greater concordance of interpretation.

Section xii: Comparison with Kinetics of Squamous Tumours

As the above section makes clear, other workers within the labs at the Royal Infirmary have been using the bromodeoxyuridine methodology which we have developed, for the study of other tumour types. It would seem to be worthwhile to present at least the briefest summary of those data, in order to look at the differences between tumours:

Tumour	n	% aneup.	LI(%)	T_s (hrs)	T_{pot} (days)
Breast	84	57	3.2	12.7	14.6
Cervix	120	71	10.9	13.2	5.3
Head & Neck	105	72	8.0	13.7	6.2

Table 38: Summary of cell kinetic data for three tumour types studied by *in vivo* bromodeoxyuridine labelling in our laboratory. All kinetic values are medians.

Breast cancers are seen to have cell kinetics quite distinct from those of the two squamous tumour types, with a much lower median labelling index and longer median potential doubling time. The squamous tumour types are themselves fairly similar in their proliferative characteristics. Note that the values of T_s are very much the same for all three cancers, as has been the case in all other comparisons of T_s between groups in these results.

It is tempting to suggest that this finding is in keeping with the clinical observation that breast cancer is a relatively slow growing tumour. Indeed it is, but without information as to the relative rates of cell loss from the different tumour types, it is theoretically perfectly possible that breast cancers, despite their slower cell production rate, have a faster volume growth rate than the squamous tumours.

Chapter 10:

Relationship between EGFR Expression and Cell Kinetics

Section i: Introduction

The epidermal growth factor receptor is the oldest known member and exemplar of the type I receptor tyrosine kinases, of which *c-erbB-2* is also a member. Several ligands are now recognised, and monoclonal antibodies to the receptor have been available since 1984, so that it has been possible to study the occurrence of this molecule *in vivo*. This has been done by many groups for breast cancer. Two types of method have been used. Ligand binding techniques involve the creation of a membrane preparation by centrifugation of ground whole tumour. Aliquots of this preparation are then assayed for their ability to bind EGF, for which there are no other known specific binding proteins. The binding capacity per weight of membrane protein is taken as the measure of the number of EGFR receptors present within the tumour. This is generalised to represent the tumour cells on the assumptions that these will predominate in the sample, and provide most if not all of the binding sites, the other elements of the tumour (benign breast epithelium, lymphoid cells, and stromal cells) not contributing significant numbers of EGFR to the total pool.

The other technique which has been used is immunohistochemistry, in which tissue sections are stained with a primary antibody to the antigen of interest. Binding of the antibody is then demonstrated by amplification and chromogen systems, of which there are many types. The situation of the detected receptors can be ascertained histologically using this type of method, but it is non-quantitative in that it deliberately uses non-linear amplification systems in order to visualise antibody binding. Its sensitivity is unknown and probably variable from one technique to another, and interpretation is at least partially subjective. Having different strengths and weaknesses, ligand binding and immunohistochemical methods would seem to complement each other in the study of EGFR distribution in breast cancer.

The most influential study in this field was probably that by Adrian Harris and his colleagues using ligand binding, with a cut-off of 20fmol EGFR/mg membrane protein. Their latest publication (Fox et al, 1994) gives results for 370 tumours, 175 of which (47%) expressed EGFR at or above this level. They found EGFR expression to decline with increasing patient age and with increasing oestrogen receptor expression, but to be unrelated to tumour size or grade or axillary nodal involvement. In univariate analysis EGFR expression did not significantly effect overall survival (OS) in the total patient

group, although overall and relapse-free survival (RFS) were worse in node negative patients expressing EGFR. This persisted, for RFS only, in multivariate analysis. This comes down to one of only 4 combinations of OS and RFS against EGFR positive and negative, in an analysis with good numbers of patients, and a favourable distribution of EGFR (nearly 50/50, the ideal split for statistical power). This suggests that the prognostic power of EGFR is limited in comparison to existing factors (especially nodal status), a conclusion borne out by the review of published series included in this same paper. They identified 16 reports involving 3009 patients (a mean of 188 patients per study), only 4 of which showed EGFR expression to be independently prognostic in multivariate analysis. None of these series yet have long follow-up (longest survivors in the Harris series are still only at about 7 years, and median follow-up for the series reported was only 18 months), so that longer term survival may yet turn up a greater significance for this factor.

The other series looking at EGFR in breast cancer are broadly in line with Harris in respects other than survival as well. A review of 40 studies comprising 5232 cases (Klijn et al, 1994) found the overall rate of EGFR positivity to be 45% (although with a range from 14-91% positive). The finding that EGFR expression is inversely related to ER expression is an almost universal finding where it has been sought (Toi et al, 1994; Castellani et al, 1994; Railo et al, 1994; Nicholson et al, 1994; Klijn et al, 1994; Charpin et al, 1993; Bellantone et al, 1993; Bolla et al, 1992; Bilous et al, 1992; Umekita et al, 1992). Likewise, most authors have agreed with Harris that expression of EGFR is not related to tumour size (Toi et al, 1994; Minckwitz et al, 1993; Klijn et al, 1994; Charpin et al, 1993; Gasparini et al, 1992), nodal status (Toi et al, 1994; Minckwitz et al, 1993; Klijn et al, 1994; Charpin et al, 1993; Bellantone et al, 1993; Gasparini et al, 1992; Umekita et al, 1992), or histological grade (Minckwitz et al, 1993; Charpin et al, 1993; Gasparini et al, 1992; Umekita et al, 1992). A smaller number of workers have found such associations, EGFR positive tumours being associated with larger tumour size (Bellantone et al, 1993), presence of nodal metastases (Castellani et al, 1994), or poor tumour differentiation (Castellani et al, 1994; Bolla et al, 1992). Three other groups at least have looked at the relationship to patient age, and have been unable to confirm Harris's finding in this respect, establishing no relationship of EGFR expression to age (Klijn et al, 1994; Charpin et al, 1993; Bellantone et al, 1993).

A number of papers have included some measure of cell proliferation, with a consensus that EGFR positive tumours show more rapid proliferation. Most commonly, this comparison has been performed using Ki-67 staining as the index of proliferation

(Gasparini et al, 1994; Toi et al, 1994; Nicholson et al, 1994; Charpin et al, 1993; Nicholson et al, 1993; Bilous et al, 1992, with Gasparini et al, 1992 and 1991 dissenting from this view and finding no relationship). Single reports have used PCNA staining (Shrestha et al, 1992), confirming this direct relationship, and mitotic index (Umekita et al, 1992) in which case no correlation was found.

There is less information in the literature about the expression of EGFR in normal breast, with very few of the studies above using this for comparison or as a control tissue. What information there is comes predominantly from immunohistochemical studies, but at least one report using ligand binding has shown similar binding characteristics for EGFR in benign and malignant breast tumours, with significantly lower concentrations in malignant tissue (Dittadi et al, 1993). Ozawa et al (1988) found the converse, that ligand binding capacity was higher in malignant than benign breast tissue, and for completeness Barker et al (1989) found no difference between the two. The last study used normal tissue from mastectomy specimens, as opposed to benign breasts used by the other two. Immunohistochemical studies cannot perform this quantitative comparison, but have consistently noted that EGFR is readily stainable in normal breast lobules (particularly in the myo-epithelial cells) and ducts (Damjanov et al, 1986; Möller et al, 1989; Tsutsumi et al, 1990), which would suggest that expression in the normal is at least higher than that of the 55% of tumours which are EGFR negative in the previously discussed ligand binding studies. The lower rate of detection of EGFR by immunohistochemistry in breast carcinomata compared to benign breast tissue was confirmed by a number of groups (Möller et al, 1989; Tsutsumi et al, 1990; Tauchi et al, 1989). This is supported by the report of Travers et al (1988) that EGFR mRNA can be detected in all non-malignant breast tissues studied, but in only 42% of tumour samples examined.

As mentioned earlier in this section, both methods for the study have advantages and weaknesses, and are complementary in the the study of EGFR expression. The way in which ligand binding is carried out makes the cytogenetic origin of the detected receptors uncertain. By this I mean that the membrane preparation created by homogenisation of tissue for the assay derives from all cells present within the tumour. The heterogeneity of this population has already been discussed in relationship to flow cytometry, and consists not only of tumour cells but also potentially elements of insitu tumour, normal breast, fibroblasts, myoepithelial cells, endothelium, macrophages and lymphocytes. In using ligand binding for EGFR in squamous tumours, which express large numbers of receptor per cell, and have a relatively small stromal component, this is not necessarily an important problem. It might be so in breast cancers for these very reasons.

Immunohistochemistry (IHC) lacks the ability to quantify receptors as ligand binding can do. Additionally, the sensitivity and specificity of IHC depends upon the methods used for fixation and detection of antibody binding. A technique which combined the quantitation of ligand binding, and the localisation of IHC might be more valid for either alone. With this in mind, for this project I have used a quantitative immunohistochemical method pioneered in squamous tumours by Fred Hendler in Dallas and latterly Louisville. This is done by using a radiation based detection system, quantified by emulsion autoradiography, which we have termed radio-immunohistochemistry (henceforth RIHC). The details of the method as used for the breast tumours is given in the following section.

Section ii: Patients and Methods

a) Patients studied, and Material available

The antibody used for this study was the R1 IgG2 mouse monoclonal originally described by Waterfield et al (1984), provided by Dr B Ozanne of the Beatson Institute for Cancer Research. The antibody, which recognises an epitope in the extracellular domain of the EGFR molecule close to the membrane, is not effective in fixed sections. Accordingly, the assay was performed upon frozen sections of tumour. As stated earlier, a sample of tumour was kept in liquid nitrogen where possible, but priority was given to gaining material for flow cytometry. Frozen tumour was available for 53 of the cases who were bromodeoxyuridine labelled. In fact the assay has been performed on a total of 105 tumour samples, and the results for all of these are presented where this is appropriate, using the 53 overlapping results for the exploration of the relationship between EGFR expression and cell proliferation. All 105 patients are listed in Appendix V, with pathological prognostic data, identifying separately those who are part of the bromodeoxyuridine series.

b) Antibody iodination

The R1 antibody was radio-iodinated for use in the assay by the iodogen method as follows. Reaction tubes were prepared by pipetting 100 μ l of 0.5mg/ml iodogen (1,3,4,6-tetrachloro-3 α ,6 α -diphenylglycoluril, Sigma) into 13x100mm glass test tubes, and allowing this to evaporate in a fume hood overnight. Tubes were then stored in a dessicator. For each iodination, 50 μ g of antibody in PBS was pipetted into one of these tubes. 250 μ Ci of I-125 (Amersham) in a volume of 2.5 μ l was mixed with 25 μ l of PBS, added to the tube and incubated for 10min. The reaction was stopped by the addition of 1ml of a 1:1 mixture of PBS and foetal calf serum to the tube. The contents of the tube were then added to a NAP-10 column, equilibrated with 10ml of PBS, and

eluted with 1.5ml of PBS. The eluent was assayed as below, and then divided into 100 μ l aliquots in micro-Eppendorf tubes for storage at -20°C.

Radioactivity of the iodinated antibody, and absence of unbound iodine, was assayed by counting an 5 μ l aliquot before and after trichloroacetic acid (TCA) precipitation. To achieve this, a 5 μ l sample of the antibody solution was counted directly. Another 5 μ l aliquot was diluted to 1ml with PBS and precipitated with 100 μ l of TCA. The reaction mixture was centrifuged and a 100 μ l aliquot counted. This allowed calculation of the activity of the iodinated antibody as bound (ie precipitable) counts per weight of antibody. High activity is not necessary or desirable for this assay (shelf life is lower due to disruption of antibody molecules by decay, and saturating amounts of antibody need to be added to each slide anyway, so that high activity antibody would need to be diluted with cold antibody). Levels achieved were of the order of 100MBq/mg (100counts per second per ng of antibody). Antibody was used as soon as possible after iodination, to a maximum of one month after iodination, activity at the time of use being calculated from a standard decay table for I-125.

c) Incubation

3 sections were used for each tumour, duplicate test sections and a negative control section incubated with the iodinated antibody in the presence of a 100 fold excess of unlabelled antibody. 4 μ m thick frozen sections on silane coated slides were obtained, and a parallel section stained with H&E to confirm the presence of tumour. All sections were placed well to one end of the slide. With each batch of tumours a set of standards were run, consisting of sections of one particular normal breast from a reduction mammoplasty, and sections of pellets of three cell lines (ZR-75-1, EJ, A431).

The sections to be assayed were pre-fixed in acetone for 10min, washed twice for 5min in normal saline, and circled with an oil pen without allowing them to dry. Sections were then placed on racks in a closed box with well moistened tissues in the bottom of the box to maintain humidity. 100 μ l of preincubation solution was added to each section. This consisted of a 1:1 mixture of PBS and foetal calf serum (FCS), to which was added, for the negative control sections only, cold antibody to 100x the amount calculated to be used as hot (iodinated) antibody for each section (see below). Preincubation was carried out for 1hr, and at the end of this time, hot antibody was added to each section and mixed by pipetting.

The amount of hot antibody per section used was calculated to provide 2×10^5 disintegrations/min. Given the specific activity of the antibody of 100MBq/mg, this amounts to roughly 30ng per slide of hot antibody when it is fresh. The appropriate

volume of hot antibody solution for all slides was made up to 10 μ l/slide with 1:1 PBS: FCS, and 10 μ l added to the pool of preincubation mixture on each slide.

Incubation went on for 3 hours, in the middle of which time the solution on the slide was mixed by pipetting with a Gilson. At the end of the time the incubation solution was tapped off, the slides washed 3 times for 1min each in PBS, post-fixed with 4% formol saline, washed once more, and then dried on a heated plate.

d) Film Autoradiography

Once the sections were thoroughly dry, they were taped into an radiographic cassette, and a sheet of Kodak R-PE film laid over them. This was exposed at 4°C for 24hrs. This was used to indicate the approximate level of activity on each section, in order to indicate how long each trio of sections from a particular tumour should be exposed once coated with autoradiographic emulsion. This is basically to ensure an appropriate grain density for counting, and is dealt with in more detail in that section. The judgement was subjective.

e) Emulsion Autoradiography

Sections were now coated with Kodak NTB-3 autoradiographic emulsion. This procedure was carried out in a darkroom with the use of a Kodak No.2 safelight. The emulsion was melted into an equal volume of distilled water at a temperature of 43°, created by sitting the dipping vessel (a standard 4 slide vertical histochemistry staining container) in a water bath. Once this had been done, blank slides were dipped in the emulsion until this emerged free of bubbles. The experimental slides were then dipped in the emulsion, stood on end to dry in grooved perspex racks, and placed in standard metal slide-staining racks (note that the lighting provided by this type of safelight is very dim, in deference to the sensitivity of the emulsion. Racking slides in this light is the most difficult part of this procedure). The racks were then stacked in a metal tin with freshly dessicated silica gel in the base. The tin was sealed, wrapped in a thick, black plastic bag, and placed at 4°C.

It is to economise at this stage that the sections were placed at one end of each slide originally, since they can then be dipped that end first into the emulsion. This reduced the volume that needed to be made up for each batch, since that was determined by the height needed to be covered on each slide in order to coat over the section on it. The emulsion is the most expensive consumable item in this procedure.

Once the sections had been exposed to the emulsion for the period of time determined by the autoradiographic film to be appropriate, the emulsion was developed. This interval varied between 3 hours (the time taken for the emulsion to dry), and 1 week.

Slides were placed in the staining racks after dipping, as stated above, and those due to be developed at the same time were obviously racked together.

Before developing slides the water bath in the darkroom was filled with an ice/water slurry, and 4 staining dishes placed in this. These were filled with photographic developer (Kodak LX24) diluted 1:1 with distilled water, distilled water (2 dishes), and photographic fixer (Champion Super Amfix). The dishes were allowed to equilibrate for at least fifteen minutes before use. At the appointed time, the darkroom was re-entered, safelight conditions resumed, the tin opened, and the appropriate rack removed. It was passed through the dishes as follows:

- developer 4 min
- water 1 min
- fixer 5 min
- water 1 min

Slides were then taken out of the darkroom in the last staining dish for counterstaining.

f) Counterstaining

Sections were stained 'through' the emulsion with 0.12% Safranin O, a red nuclear dye, for a period of about 5 min, before being briefly washed in tap water and mounted in DPX. The Safranin was made up as a 0.2% solution in distilled water, and mixed with 0.1M acetate buffer (9vol 0.1M Na acetate + 1vol 0.1M acetic acid) in the ratio 3vol Safranin to 2vol of buffer. The solution was buffered in this way as it is unstable in neutral solution, and precipitates in a matter of days. Shelf life could be prolonged by buffering. Fresh stocks were made monthly, but even within this period of time it was necessary to use longer staining intervals as the solution aged. This dye also washes out very rapidly, and stains the emulsion, so that washing needed to be brief and carefully monitored, in order to adequately clear the excess dye, whilst preserving adequate staining for tissue identification. This was further complicated by the need to obtain a rather light stain so that the counterstain did not produce sufficient opacity to appear as grains in the course of image analysis, a problem dealt with in detail below. In practice, the sections were barely more than 'dunked' in the water, examined, and the immersion repeated as necessary. If eventual microscopic examination revealed the end result to be unacceptable, the slides were immersed in xylene until the cover slips could be removed, destained with water, and the procedure repeated.

An example of the finished product, at the magnification used for counting, is shown in figure 50.

g) Grain Counting

Measurements of the number of grains per field of view for the tumour tissue (see Figure 49) were made using a Leitz-Ortho-Mikroskop (Leitz, Wetzlar, Germany) attached to an Olympus III-2 camera. The following procedure was used:

1. The tumour tissue was divided into regions of approximately equal area.

2. The number of grains in each region was counted and averaged.

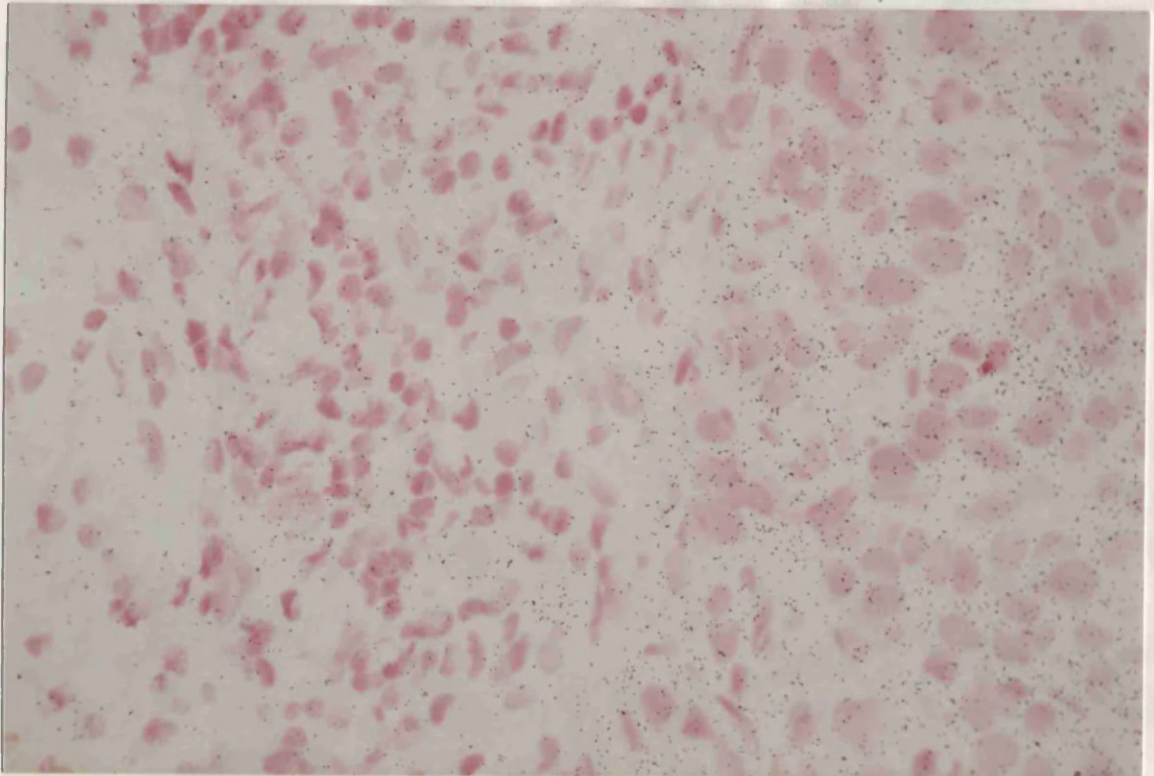


Figure 50 shows the results of the grain counting procedure. The tumour tissue (right side of the field) shows a moderate grain density, while the lymphoid elements and stroma (left and center) show low density background counts. The grain density is also moderate over isolated tumour cells centrally in the field.

The procedure described here is a simple and rapid method for the detection of all tumour cells in a tissue section. It is suitable for the detection of all tumour cells in a tissue section. The method is suitable for the detection of all tumour cells in a tissue section. The method is suitable for the detection of all tumour cells in a tissue section.

Figure 50: Photomicrograph of a counterstained radio-immunohistochemistry section with moderate grain density over tumour to the right (and over isolated tumour cells centrally in the field), and low density background counts over lymphoid elements and stroma to the right and centre.

g) Grain Counting

Measurement of the number of silver grains developed within the emulsion over the tumour areas was carried out using a Joyce-Loebl Mini MagiScan system, attached to an Olympus BH-2 microscope. Basically, the procedure consisted of the following steps:

- establishment of lighting conditions on the microscope, and appropriate thresholds for detection of grains by the system under these conditions
- examination of the section histologically to identify the tumour elements
- capture of the microscopic image (40x objective) by the image analysis system
- outlining areas of tumour cells on screen by the operator
- automated measurement of the area outlined
- automated count of the number of grains in the indicated area
- storage of these data by the system
- repeat image capture and counting, for at least ten screens per section

The automated counting system works by measuring the optical density of each screen pixel in the captured image (the screen is divided into 512 pixels horizontally and 512 pixels vertically. Since the overall image area is $6.67 \times 10^{-3} \text{mm}^2$, each pixel represents only $2.54 \times 10^{-8} \text{mm}^2$ on the section). Grains appear as dense objects on a light background. The background is darkened only by the counterstain (thus the need for a light stain), an effect enhanced by the use of a red filter, which almost abolished the visibility of the counterstain, and so increased the density variation between grains and background, and by the fact that the grains are in a different focal plane to the counterstain at this high power. Obviously this could only be done once the area to be counted on the screen had been identified. Once the screen had been captured, the system identified each pixel with a density greater than a certain threshold (this varied with each session, depending on the exact microscope setup being used, for example the system is extremely sensitive to the lamp voltage which is set with a slide control, and so was never quite the same from one session to another).

The positive pixels are then divided into discrete objects, that is all touching pixels are regarded as being part of a single object, and the number of these objects is counted. This is taken as the number of grains present. Since even the grains are not all exactly focussed in the same plane, the number of pixels occupied by one grain varies from one to several (an effect enhanced by the fact that even a grain of one pixel size lying at the junction of 4 pixels might put all four over the density threshold). This thresholding and counting is visible on screen, and so can be monitored by the operator. This description hopefully makes it apparent why different sections need to be exposed to emulsion for varying lengths of time. This is a compromise between the need for

enough grains to have developed to create a statistically satisfactory sample, and the necessity that the grains remain discrete, so that adjacent grains are not perceived by the analysis system as a single object (leading to underestimation of the grain count). There is thus an optimum density for counting, and it is to create this that the exposure times are judged. Negative controls were exposed for the same time as their test sections, the appropriate interval being judged on the basis of the latter, self-evidently.

The counting of the area of the screen occupied by tumour has to be approached quirkily using this particular analysis system. The area of interest is drawn around using a mouse. Rather than simply measure the area enclosed, it is necessary to threshold the enclosed area with a minimum threshold, which means that all pixels within it are identified as positive. The area which these cover can then be measured by the system. For each section, a file is created in which the system stores the area counted, and number of grains counted within that area, for each screen captured. The totals for area and grains for all screens for that section is also available, and were recorded as the final result.

h) Calculation of EGFR Expression

Counts were calculated as grains per unit of section area per hour of emulsion exposure, averaged over a minimum of 20 fields on the 2 sections of each tumour, and less the counts (per area per time) on the negative section, taken to represent non-specific binding and grain development. They were expressed as a percentage of that in one of the standards run with each batch, the A431 cell pellet, and subsequently as a % of the counts normal breast based on the average count in the 9 normal breast samples (see results, Counts in normal breast). It is also possible to construct a standard curve from the counts in the cell lines, and so convert the grain counts to receptors per cell, but this involves the assumption that cell density is the same in the tumours and cell pellets. For this reason I have not done this, and the standards were only used to check the linearity of the assay in each batch. I also felt that the absolute levels of EGFR expression were of less clinical importance than their relativity to their tissue of origin.

Appendix V gives the counts per unit area per hour, and count relative to normal breast for each of the 105 tumours.

i) Controls

It has already been stated that sections from pellets of three cell lines and normal breast were run in all batches. Pellets were created as follows. A large cell culture flask of cells in sub-confluent growth was washed three times with normal saline, the cells scraped and suspended into a universal container. They were centrifuged at 2000rpm

for 5 minutes, the universal snap frozen in liquid nitrogen, and the pellet in the conical base of the container tapped out. This pellet was then wrapped in foil and returned to liquid nitrogen. It was stored at -70°C until required, at which juncture $5\mu\text{m}$ frozen sections were taken from it for use in the assay.

Pellets were made in this fashion from the following lines: ZR-75-1 (a breast cancer cell line with $2\text{-}3 \times 10^3$ receptors/cell), EJ (a bladder cancer cell line with 1.3×10^5 receptors/cell), and A431 (a vulval cancer cell line with 1.5×10^6 receptors/cell). The RIHC method assumes that the amount of antibody bound to each section is in proportion to the number of EGFR molecules present, and that in turn the number of grains developed in the emulsion is in proportion to the number of antibody molecules bound. If saturating amounts of hot antibody are present, then the first assumption is reasonable, and likewise the second if the response of the emulsion is linear with time (that is, that 1000 disintegrations per hour for 3 hours of exposure gives the same grain count as 100 disintegrations per hour for 30 hours. The decay of the I-125 can be ignored within the time frame used, up to one week of exposure, given that it has a half life of 60 days). If this is the case, then the grain counts for the cell pellets should be in proportion to the known receptor density in these cell lines. The ZR-75-1 line lies below the sensitivity of this assay, but the ratio EJ:A431 should be 1:10-12. This ratio was calculated for each batch to test the underlying assumptions, and the appropriateness of the counting procedure.

Samples of normal breast were obtained from 9 specimens from reduction mammoplasty procedures. These were dissected to seek areas of breast parenchyme (large areas consist macroscopically of fat alone), which were frozen in liquid nitrogen and stored at -70°C . In fact 12 specimens were obtained but no macroscopic breast parenchyme could be identified in 3 of these. All samples were subsequently checked histologically for the presence of breast lobules. Whether this type of sample is truly normal breast is open for debate, a point pursued in the discussion.

Section iii: Results

a) Counts in cell pellets

Sample counts are given in the table below for the cell pellet sections used for one of the batches. In this example the ratio EJ:A431 is 1:11.6, and this was similar for all batches, with ratios consistent with the known ratio of receptors per cell in these lines, demonstrated in the lower table, giving the EJ and A431 counts for each batch.

Cell Line	Grains	Control	Area (10^{-2}mm^2)	Exposure Time (hrs)	Net Grains /Area/Time
EJ	3903	30	13.3	23	12.7
A431	7884	42	13.3	4	147

Table 39: Example of Grain Counts in Cell Pellet Sections

A431 Count	EJ Count	Ratio
135	13.8	9.8
147	12.7	11.6
212	20.0	10.6
140	11.4	12.3
121	11.1	10.9
206	18.7	11.0
170	13.5	12.6
190	18.8	10.1
144	12.2	11.8
148	14.2	10.4

Table 40: Grain counts per 10^{-2}mm^2 per hour of emulsion exposure for cell pellet standards in each batch with which tumours were run.*b) Counts in normal breast*

Results from duplicate sections from one the normal breast samples are given in the table below, along with the A431 counts from that batch, as an example of the method of calculation of EGFR expression:

Slide	Area counted	Grains
Hot1	3.40	890
Hot2	2.94	946
Cold	3.22	232

Total area counted = $6.34 \times 10^{-2}\text{mm}^2$. Total grains = 1836

Exposure time was 17.5hrs.

\therefore Grains/ 10^{-2}mm^2 /Hr = $1836/6.34/17.5 = 16.55$

For cold section (control), grains/ 10^{-2}mm^2 /hr = $232/3.22/17.5 = 4.12$

Net counts = $16.55 - 4.12 = 12.43$ grains/ 10^{-2}mm^2 /hr

For this batch the A431 count was 190 grains/ 10^{-2}mm^2 /hr

\therefore % normal breast to A431 = $12.43/190 \times 100 = 6.54\%$

Table 41: Grain counts in sample of normal breast, and example of calculation from this of the net counts and relativity to cell pellet standard.

Results for all 9 normal breast samples are given in the table below. The mean value is 7.2% of A431 counts, and this is the figure used in normalising the results in the tumours to expression as a % of normal breast.

Sample	1	2	3	4	5	6	7	8	9
%A431	6.54	5.21	6.61	9.45	8.79	9.70	5.30	7.70	5.28

Table 42: Grain counts in the 9 samples of normal breast.

c) Counts in breast cancers

Counts in the 105 tumours are given in Appendix V. The frequency distribution of these counts is shown in the figure below. Note that the x axis for this is the count as a percentage of that in normal breast lobules, that is 100 on the x axis is 100% of normal. It is immediately apparent that nearly all of the tumour samples lie below this level, with only 3 above, that is that virtually all show downregulation of EGFR compared to normal breast. The largest number of tumours lie in the very lowest group, below 10% of normal breast.

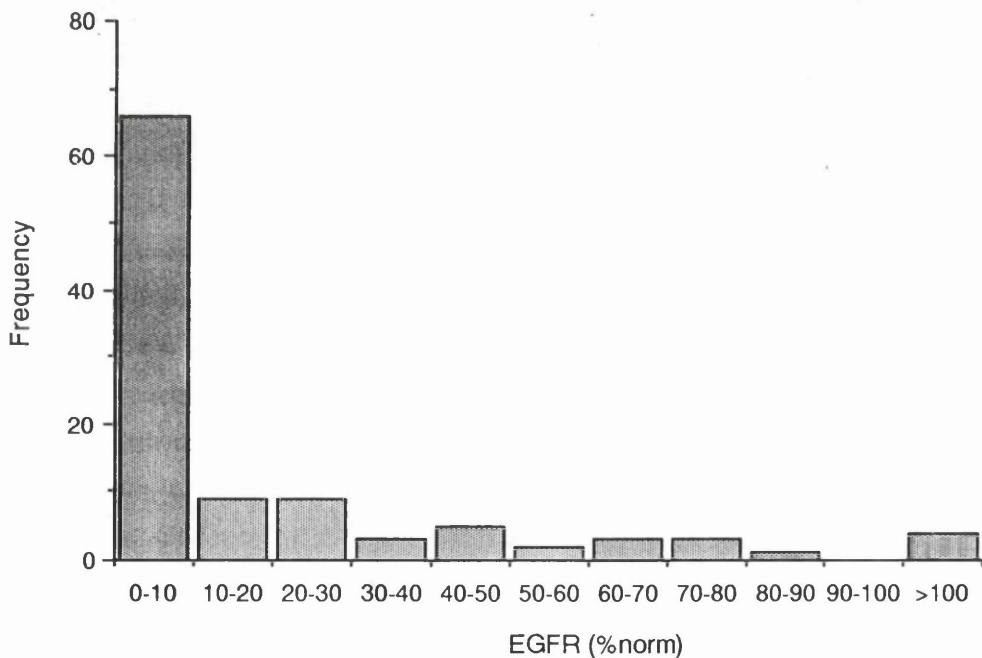


Figure 51: Frequency distribution of values for EGFR expression in all 105 tumours

d) Lower limit of sensitivity

This was ascertained by using a one sided t test on the counts per unit area of the test sections, compared with those on the corresponding negative section. When this was not statistically significant the count for that tumour could not be regarded as above zero. This depends principally upon the area of tumour counted, since however small

the difference between background and specific counts, if enough grains are counted this will become significant. It is a problem of sample size. An example is given below. For this tumour, the level of expression is 9.2% of normal breast. Comparing the two sets of grains per unit area on a one sided t test (experimental slide > control) gives $t = 3.60$, $df = 17$, $p = 0.0011$, that is, the counts on the test slide are statistically higher than those on the control, and so this level of activity is above the sensitivity threshold of this method. It becomes insignificant at below 5% of normal breast, so this is the lowest level of EGFR expression that can be regarded as not zero using the number of fields that I have counted for each slide.

	1	2	3	4	5	6	7	8	9	10
Grains	51	87	72	83	54	101	54	74	81	89
Area	.612	.710	.719	.996	.507	.869	.581	.851	.687	.551
Grains/Area	83	123	100	83	107	116	93	87	118	162
	1	2	3	4	5	6	7	8	9	10
Grains	40	82	51	67	71	48	56	64	41	46
Area	.612	.865	1.13	1.34	.750	.806	1.09	.781	.428	.607
Grains/Area	65	95	45	50	95	60	51	82	96	76

Table 43: Grain counts on a tumour slide (upper panel) and its negative control (lower panel). Area is $\times 10^{-2} \text{mm}^2$. See text for analysis.

e) Relationship to cell proliferation

53 of the 105 cases have cell kinetic data available. It is possible to look at this differently to the way in which I analysed the *erbB-2* data, because in this case EGFR levels are a continuous variable. It is also quite possible to create an arbitrary cut-off, and so divide levels into positive and negative, in order to perform the same type of comparison as used previously, and this has been done as well. For this purpose, tumours with EGFR expression less than 10% of that in normal breast were regarded as EGFR negative, and those above this level as positive. This creates a roughly equal division of tumours, the distribution not being bimodal so as to suggest a more appropriate cut-off. It is worth emphasising again that the great majority of positive tumours still have lower EGFR levels than normal breast.

Looking first at EGFR as a continuous variable, each of the kinetic parameters is plotted against EGFR expression (the latter on a log scale because of the wide spread of values) in figure 52. Since none of the distributions is remotely normal, the appropriate statistic here is a rank correlation, and the results of this analysis are given in the following table:

Parameter	Spearman coeff	Probability
LI	0.321	<u>0.019</u>
T _s	0.072	0.64
T _{pot}	-0.308	<u>0.039</u>

Table 44: Rank correlation between EGFR expression and kinetic parameters using EGFR as a continuous variable

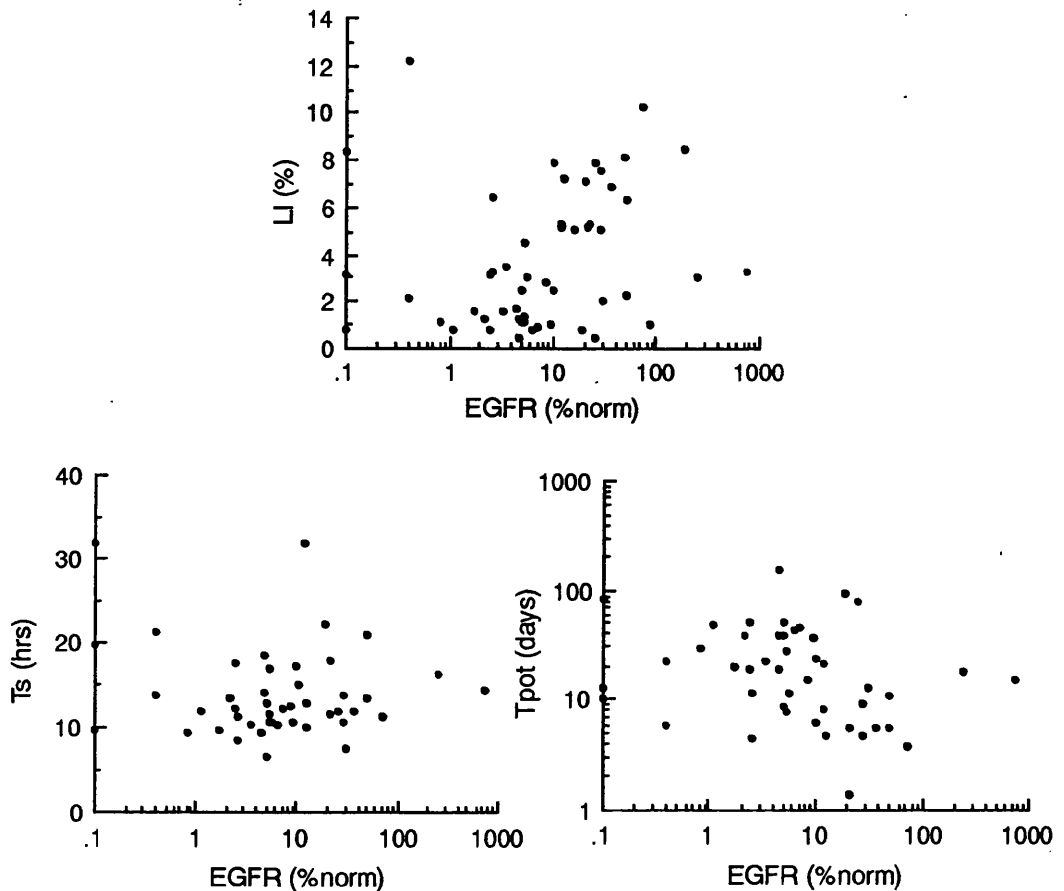


Figure 52: Relationships between EGFR expression and kinetic parameters. EGFR is in each case expressed as % of the mean expression in normal breast, on a log scale (because so many of the values are otherwise crowded at the left side of the plot. Values of zero are represented as 0.1%. T_{pot} also log scale because of the few very large outlying values.

It can be seen that labelling index is indeed directly related to EGFR expression, and that once again T_s shows no variation, resulting in an inverse relationship between T_{pot} and EGFR. The raw data plots, however, show that there is marked variation from tumour to tumour, with the very highest labelling index being in a case with very low EGFR level. The extent of the overall relationship is, however, reinforced by the

analysis using EGFR classified simply as positive or negative, where the median LI in the positive tumours is more than 3 times as high as that in the negatives. The results of this analysis are given in the table below:

	n (LI)	LI	Median values of		n (T_s/T_{pot})	
			T_s	T_{pot}		
EGFR	Pos	23	5.3	13.3	8.9	17
	Neg	30	1.6	11.95	22.3	28
	p		<u>0.001</u>	0.206	<u>0.004</u>	

Table 45: Relationship between EGFR expression and kinetic parameters, using EGFR as a binary variable (below or above 10% of normal breast expression). Medians are expressed as % of normal breast. p values based on Kruskal-Wallis tests.

f) Relationship to pathological variables

The median values of EGFR expression in subgroups defined by nodal status, tumour size, histological grade, and oestrogen receptor status are shown in the table below. As was the case for cell proliferation, it is tumour grade and ER status which are strongly related. In the case of grade, it is apparent that high grade tumours have significantly higher levels of EGFR expression, as do ER negative tumours (that is, there is an inverse relationship between these two factors).

Factor		n	Median EGFR
Nodal Status	N0	51	5.3
	N1	42	7.2
	p		0.46
Tumour Size	T1	28	5.5
	T2	61	5.2
	T3	7	4.2
	T4	6	7.0
	p		0.96
Tumour Grade	1	7	6.3
	2	13	3.5
	3	24	21.7
	p		<u>0.006</u>
Oestrogen Receptor Status	ER-	21	11.6
	ER+	28	2.9
	p		<u>0.018</u>

Table 46: Relationship between prognostic factors and EGFR expression. EGFR is given as % of normal breast. p values- Kruskal-Wallis tests.

Chapter 11: Discussion and Conclusions

Much of the technical discussion of these results has deliberately been included with the presentation of the results themselves. In this section, I intend only to complete the process by comparing them with previous work, and then seeing to what extent bromodeoxyuridine represents an advance over static methods for measuring tumour cell kinetics.

Five previous reports of the application of bromodeoxyuridine to the study of tumour cell kinetics of human breast cancer were identified in the literature review. The table below summarises the results from those studies, alongside the current one:

Author	n	LI (%)	T _s (hrs)	T _{pot} (days)
Current Series	84	3.2	12.7	14.6
Rew (1992)	69	4.2	8.7	8.2
Lloveras (1991)	148	3.0	na	na
Sasaki (1992)	21	10.9	na	na
Meyer (1993)	450	3.9	na	na
Goodson (1993)	109	10.3	na	na

Table 47: Summary of results from previous studies which have used bromodeoxyuridine in breast cancer. All values are means.

The current results are very much in line with three of these previous reports, in terms of labelling index. This agreement is backed up by the good correlation with the immunohistochemical counts in tumours from this series. Of the other two, Sasaki's is a very small and possibly unrepresentative group (see chapter 4). The methodological queries about the Goodson series would not be expected to create so large a difference, though, and so this must remain partly unexplained.

There is only the one other study which has sought dynamic data among these, which makes it difficult to assess the importance of the difference in median values of T_s between us and the Mt Vernon group, although it is this which is responsible for most of the variation in potential doubling times between the two data sets. Given our inability to find any alteration in T_s between subgroups, it seems unlikely that the explanation is that the tumours are biologically different. This would imply that there is methodological variation- in the histogram interpretation, which could lie either in the analysis software or the investigators themselves; or in the sample preparation, and this could be an inherent difference between samples created by direct disaggregation as

opposed to tumours embedded, sectioned and then disaggregated, as we have done. When the two methods of sample preparation were directly compared in our lab though, no difference in derived parameters was found (Forster et al, 1992). It must also be noted that neither series was complete, in the sense that a proportion of tumours were completely (no LI or Ts) or partially (no Ts) non-informative in both centres. It cannot be assumed that the uninformative tumours have the same kinetic behaviour as those from which data were obtained. Therefore the results cannot be generalised to the population of all breast cancers. Furthermore, it is possible given the different methods of sample preparation used, that a different type of tumour was uninformative in the two labs, and this could account for the difference in Ts between the series, given that data for Ts is missing in nearly 25% of the total cases.

The present results can also be considered in the context of our own previous work using thymidine labelling and flow cytometric S phase fraction, presented earlier in this thesis. The results, for S phase estimation only, are summarised in the table:

Method	n	S Phase (%)
Bromodeoxyuridine	84	3.2
Flow Cytometric SPF	224	7.2
Thymidine Labelling	185	3.2

Table 48: Summary of results from studies of the proportion of cells in S phase in breast cancers, using different methods, in our laboratory.

The two methods which rely upon functional identification of cells synthesising DNA show absolute agreement using this crude measure. The higher median value for SPF fits with the finding in the BUDR series that SPF was higher than BUDR labelling index in 70/74 cases. These methods seem fairly conclusively not to be measuring the same thing. The difference may be the result of technical limitations in either or both methods, but it must be understood that the nature of the two measurements is not the same. SPF counts all cells with a given DNA content, whether or not they are actively synthesizing DNA. A proportion of these cells, of unknown extent, may in fact be unable to complete S phase, and have arrested there. By contrast, BUDR and thymidine identify only cells actively incorporating pyrimidines into DNA, although it has been shown for tritiated thymidine that not all cells doing so are labelled (Allison et al, 1985), and this may also apply to BUDR (Wilson et al, 1985). The label may also be incorporated by cells undergoing DNA repair rather than synthesis. That this is infrequent is suggested by the observation that with short labelling times few labelled G_0/G_1 cells are seen. Both methods will label cells undergoing DNA replication but subsequently unable to mitose by virtue of abnormality of the synthetic process, or deficiencies of the cellular mitotic infrastructure. These theoretical considerations are

not adequate to explain the very large difference between the results for the various methods. The more functional techniques, using labelling with DNA precursors, are the more soundly based. This puts SPF in a rather poor light, if these are taken as the gold standard.

It is also worthwhile at this stage bringing together some of the data gathered on the reproducibility of interpretation of the various methods. We have studied breast tumours using thymidine labelling, flow cytometric SPF and bromodeoxyuridine. The inter-observer variation for each is summarised in the table:

Method	n	Mean Ratio	SE Mean	SD Ratios
Bromodeoxyuridine (LI)	37	1.13	0.06	0.16
Flow Cytometric SPF	66	0.84	0.03	0.23
Thymidine Labelling	20	1.01	0.13	0.55

Table 49: Summary of results of reproducibility studies we have carried out on the different methods of measuring S phase fraction.

Thymidine labelling emerges as the method where the two observers got the same answers on average, but also the one where the variation in individual cases was the largest. The other two both show constitutional difference in histogram interpretation by the two observers, but greater concordance when this is allowed for (that is, lower SD), with bromodeoxyuridine labelling index the least variable by this measure. It is worth remembering that this is a very rigorous test of reproducibility, and whilst it would certainly be desirable to avoid the constitutional difference between observers, the level of variation for individual cases using bromodeoxyuridine is quite low.

The other major potential advantage of using bromodeoxyuridine, though, was the ability to gain the additional information as to the length of S phase. This parameter could not be measured in as many tumours as the labelling index, but was still available for 67/87 tumour samples (77%), and was shown to be independent of the labelling index. It showed markedly less variability between tumours, though, and not a single subgroup comparison showed a difference in median T_s between groups. Theoretically this is compatible with a view that the S phase is a relatively standardised process within cells, taking place at a rather fixed rate in all cells. If this is indeed the case, then measuring it is not going to provide any useful information, since variation in cell production rates will reside almost entirely in variation in the proportion of in-cycle cells, which can be measured by static methods. It is too early to come to this conclusion yet. The fact that length of S phase shows no relationship to known prognostic factors does not necessarily mean that it is of no predictive value, as this may only indicate that it gives information independent of that available from other

data. Conversely, the labelling index will almost certainly prove to be prognostic in univariate analysis because of its close association with histological grade. Because of this very association it may provide little or no additional information, though. Only continued observation and subsequent multivariate analysis will answer the question as to the prognostic power of tumour cell kinetics as measured with bromodeoxyuridine.

Before considering the results obtained from RIHC for EGFR, since this is a relatively novel method, we need to ask whether it is a valid one. In terms of the cell pellets used as standards, the answer to this is in the affirmative- the grain counts are in linear proportion to the EGFR expression by those lines. However, these preliminary studies used only 2 lines (the ZR-75-1 can only really be considered a negative control rather than a standard), and more need to be studied to draw up a true standard curve to more thoroughly prove this point. In the tumours the matter is not even as simple as this, since the cell density cannot be assumed to be the same in all cases. For this reason the grain count can only be expressed as grains *per unit of area*, not per cell. This is the same for ligand binding, where levels can only be expressed per mass of membrane protein. In either case, it could be argued that receptor density within the tissue might just as easily be the biologically important variable as receptor number per cell. With RIHC it would be possible to do separate cell counts in order to correct to bring the counts down to numbers per cell, as this would be a useful extension of this work.

In terms of reproducibility the answer to the original question is also yes, the results are very consistent for the pellets and normal breast between runs, and for different people doing the counting, but this is not proof that the results are accurate. Counts do accord with immunohistochemistry, both in the literature and in our hands, but since this is a method based on that technique this is not entirely surprising. A comparison with ligand binding would be desirable, and will be an area for future study. There may well be differences in individual tumours, but it would be hoped that overall the results tended to be correlated. In cases of difference it would be helpful to ascertain from the histology whether this might be due to presence of distracting elements in the tumour which would cause problems for ligand binding- a substantial component of normal or in-situ disease, or small areas of positive tumour with a large negative stromal component. In fact if there are no such differences, then RIHC has no advantage over ligand binding.

In comparison to routine immunohistochemistry, RIHC only has an advantage if the quantification which it provides is of any additional value. The advantage applies at top and bottom of the expression range though. Immunohistochemistry embraces a wide variety of staining systems for visualising primary antibody binding, and these are of different sensitivity and specificity. Therefore, at what level of EGFR expression staining becomes apparent is inconstant- there is an unknown and variable threshold

for positivity at the bottom end. There is also a problem in interpretation, given that the staining pattern needs to be taken into account if, as is often the case, only some of the tumour cells stain positively- what percentage is regarded as making the tumour as a whole EGFR positive? At the top end, once the tumour does cross the threshold on immunohistochemistry, then further increase in expression will not make it more positive. All this said, a simple plus or minus answer, whatever its threshold, may turn out to provide all the biological and prognostic information of a more accurate value. This can only be assessed by testing this hypothesis in a substantial tumour series, and this is another important area for future work with RIHC.

In subjective terms, RIHC is time-consuming, and requires scrupulous attention to the emulsion coating and grain counting if reproducible results are to be obtained. The need for the use of radioactive materials is also a relative disadvantage, and it is difficult to see that this is ever going to be more than a research tool (but then so are ligand binding methods for EGFR). Its potential lies in the possibility of using it to quantify levels of any antigen for which an antibody with good specificity and high affinity is available. An example is *erbB-2*, for which good antibodies are available in quantity, and where quantification is not possible at the protein level in other ways, because of the lack of a ligand to use for binding assays. This is in fact the next antigen I intend to study, in the same series of tumours, but future efforts need not be directed toward this class of compounds, or even to cell surface antigens.

The levels of expression recorded in normal breast samples are quite consistent between the 9 specimens analysed. Whilst I have argued against trying to equate grain counts with receptor numbers per cell, the level seen is of the order of that in the EJ cells, or in normal skin samples that I have also used with this assay. These are EGF responsive tissues, and so this is at least potentially a biologically significant level of expression. It was noted in the introduction that immunohistochemists have intermittently reported in the literature that EGFR is detectable in normal breast, particularly in relation to the myoepithelial cells. RIHC does not localise receptors as accurately as immunohisto-chemistry, but the examples shown demonstrate that the grains are distributed over all of the lobule and not just its basement layer as would be expected if all of the receptors were present on the myoepithelial cells.

This raises the issue of how accurate the localisation of receptors is with RIHC, which depends upon how far from the molecule of origin any emission travels before converting a grain within the emulsion. The 30keV γ emission of I-125 could potentially travel a histologically long way in the emulsion before conversion, if its angle of exit happened to be low (by which I mean that if its path were at right angles to the plane of the section it would not matter, but if it were nearly in the plane of the

section it would have a long course in the emulsion). Fortunately it is not this γ emission which converts the silver grains, but rather low energy β particles created by internal conversion of the primary emission, which only have a very short course (Wilson Angerson, personal communication). Thus the grains will lie within a few μm at most of the points of origin of the particle which gave rise to them.

The question must also be raised as to the true normality of tissue taking from reduction mammoplasty specimens. It is theoretically possible that very large breasts (requiring reduction mammoplasty) are so because of aberration of EGFR expression, but to my knowledge there is absolutely no evidence that this is so. These women are also younger on average than the breast cancer patients, and it is certainly possible that there is variation in EGFR expression with age (and perhaps especially with menopausal status). This is explored within the data gained in this study, though, and no relationship was found, but few of the specimens are from patients as young as the reduction mammoplasty group. It is difficult to obtain fresh (ie surgical) samples of unimpeachably normal breast for study. Normal areas are present within breast cancers, but breast within which a tumour has developed cannot be considered normal, nor areas of fibrocystic disease subject to biopsy. Tissue adjacent to fibroadenomata would be accepted by most, but given that these lesions need only be enucleated, it would require separate consent to carry out further biopsy at the time of surgery, which would be ethically difficult given the increased possibility of complications or cosmetic deformity.

Some areas of normal breast seen within the cancer specimens were counted, out of interest, and have the same level of expression as seen in the reduction mammoplasty controls. There is thus no evidence in our material that there is any field change in EGFR expression in the cancer containing breast.

The most striking result in terms of the levels of expression seen in breast cancers is that virtually all the tumours show lower levels of EGFR than the normal breast from which they derived. That is, the great majority of breast cancers show downregulation of EGFR. This certainly fits with the observation that amplification is a rare event in respect of the EGFR gene, and the incidence of true overexpression in this study (3%), fits with the low incidence of amplification observed by others (Rajkumar & Gullick, 1994). It would be very interesting to look to see whether the overexpressers in the current series are in fact those with amplification, but at the moment this is purely speculative.

The currency of the idea that significant numbers of breast cancers *overexpress* EGFR arises from the ligand binding studies, which if read carefully never say this. They correctly say that 40% of breast cancers detectably *express* EGFR (eg Fox et al,

1994), but do not provide comparison with normal breast. This may be because normal breast, with its very low content of breast epithelial cells is probably a poor tissue for ligand binding studies, and may well give spuriously low estimates of EGFR content for this same reason. For whatever reason, and despite the scattering of reports from histochemists that EGFR is quite detectable in normal breast, there has been a misconception that levels of EGFR in normal breast are low, and that the expression detected in tumours is therefore an overexpression. The current results suggest that this is wrong. Does this matter? Is this any more than a semantic exercise? I would answer that it is, for it is important to way that we think about the biology of EGFR in breast cancers. For a start it suggests that there may be selection against expression in carcinogenesis, or suppression of expression. This would be consistent with a role for EGFR as a differentiation signalling mechanism rather than a mitogenic one in breast tissue. This is doubly important if we relate this to the clinical situation, where we want to know why tumours grow and how we can stop them. Research is going on in targetting EGFR as an anti-tumour therapy for breast cancer (among other tumours, like squamous carcinomata, where the rationale is stronger). If EGFR is a differentiation signal, then this is biologically an undesirable thing to do. Furthermore, if levels of expression in tumours are really low relative to normal tissues, then there is a negative therapeutic window, that is, normal tissue toxicity will be produced before any therapeutic effects. These are only notes of caution, and it will be interesting to see whether this type of approach is of value, but there must be some dubiety in light of the results presented here.

The literature on the relationship between EGFR expression and pathological prognostic factors is confused. In general, both immunohistochemical and ligand binding studies have failed to show associations with nodal status and tumour size, as was the case here, and less often this has also been found for tumour grade as well (for references, see introductory section of Chapter 10). However, others have found such relationships in respect of each of these, and in this series the relationship with tumour grade is very strong, in line with Castellani et al (1994) and Bolla et al (1992). The former of these was an immunohistochemical study, the latter used ligand binding, so the difference in the literature would not seem to be based on technique; nor can the failure to establish this relationship be blamed on lack of statistical power since 3 of the 4 negative studies were larger than the current one. Given the close relationship I have found this disparity in other studies is a mystery.

In the light of my findings about the levels of EGFR expression in tumours versus normal tissue, and the hypothesis that it may not be a mitogenic, but rather a differentiation, signal, it is interesting that the level of expression as determined by RIHC is nevertheless very strongly related to cell proliferation as measured by BUDR

incorporation in vivo. It is striking that mean labelling index in the 40% of tumours with greater than 10% of normal levels of EGFR expression is more than 3 times higher than that in the low/non expressing tumours, and this is certainly in keeping with the consensus in the literature using Ki-67 (references in Chapter 10).

Can we reconcile these findings? It could well be that the association of EGFR and labelling index is no more than that, and is not causal. Both are related to tumour grade, and may simply be joint markers of poor tumour differentiation, for instance. It is also possible that EGFR is playing a different role in the tumours (mitogenesis) than it does in the normal breast, by virtue of its reduced numbers or varying in second messenger pathways, for example. Ligand availability might also alter the signal transduced by a given number of EGFR molecules on the cell surface, and the current data provide no information about levels of ligand to which these receptors are exposed. It must also be remembered that the receptor is internalised after ligand binding, and high levels of ligand exposure could thus give a falsely low impression of EGFR expression on RIHC if the antibody did not recognise these internalised receptors. Another useful field for further study would therefore be to analyse the levels of EGF, TGF α and other EGFR ligands in these tumours.

GENERAL

DISCUSSION

In the second chapter, I identified three reasons for studying tumour cell kinetics:

- for prognostic information;
- as an guide to the use of radio- and chemo-therapy; and
- as a tool for studying tumour biology.

I also stated a single general aim for the current investigation. So then, just what is "the potential use of flow cytometric methods for the determination of tumour cell kinetics", in the light of the experimental work reported here, and in terms of the three factors above?

One thing that emerges clearly is that for all the increasing sophistication of the technology being brought to bear, the current methods for measuring the division of cell populations *in vivo* provide only a very limited description of the process. Flow cytometric SPF emerges as markedly subjective, poorly reproducible, and poorly correlated with thymidine and bromodeoxyuridine labelling when this is assessed critically. This would seem to be more than adequate reason for the finding that it is of limited prognostic help- even if cell kinetics were a potent predictor of outcome, this is simply not an accurate enough measurement. The bromodeoxyuridine-based kinetic method scores better in these areas (with lesser subjectivity as evidenced by inter-observer variation, better reproducibility, and greater consistency with parallel techniques and previous literature), and might yet prove to be an improvement in terms of predicting outcome for this reason. Only more time and more patients would determine this- even if the survival advantage was twice that observed for SPF, this would require 300-400 patients to be followed for 5 or preferably 10 years.

One of the advantages bromodeoxyuridine was to bring was the addition of the new dimension of dynamic measurement, the ability to assess the rate of cell cycle transit. Whilst it seems to be capable of doing this, we were forced to the preliminary conclusion in the last chapter that this parameter seems to be a relatively fixed characteristic, the small degree of variation in which is of little biological significance. It is unlikely to add much to the prognostic information given. This raises the possibility of using an *in vitro* method for bromodeoxyuridine labelling (analagous to thymidine labelling, but without the radioactivity). This would provide the static but not the (probably irrelevant) dynamic data of *in vivo* labelling. The loss of the *in vivo* element is potentially important though, in that the behaviour of small pieces of tissue in culture is not necessarily the same as that of the tumour mass *in situ*.

Two major issues are still not addressed adequately by these methods. One is that of cell loss. This concept was introduced in the very first chapter, and has lain dormant since, for the simple reason that none of the techniques for studying cell kinetics has anything to tell us about this aspect of tumour growth. Its potential importance is easily illustrated using the data that I have obtained. If we substitute in equation 8 from the first chapter,

$$\emptyset = 1 - \frac{T_{\text{pot}}}{T_d}$$

using the median value for T_d from the literature review, of about 100 days, and the median value of T_{pot} which we have found in this series, of about 15 days, then we obtain $\emptyset = 0.85$, that is, 85% of cells produced within the tumours die rather than complete a further cycle. This has the very important consequence that the overall rate of tumour growth becomes more sensitive to alteration in cell loss than alteration in cell production. This is readily apparent if we simply rearrange equation 8 in the form,

$$T_d = \frac{T_{\text{pot}}}{(1 - \emptyset)}$$

To bring about a doubling in T_d requires a doubling of T_{pot} , but from a baseline of 0.85, \emptyset need only increase to 0.925 to create the same effect. A much smaller proportional change in cell loss is required to bring about a given alteration in overall growth rate. It is this which makes the inability to measure this parameter a critical shortcoming in cell kinetic methodology, and is unlikely that better measures of prognosis will be forthcoming until they take account of this factor. Put very simply, cell loss rate is much more important in determining tumour growth than cell proliferation rate. The recent interest in the mechanism of cell loss by programmed cell death, or apoptosis (Wyllie, 1992), was discussed in Chapter 1. Methods for identifying apoptosis on a cell-by-cell basis have been developed (Ansari et al, 1993; Wijsman et al, 1993; Gorczyca et al, 1994), and a very fruitful extension of the current work would be to make some measurement of cell loss by these means, in parallel with cell proliferation estimates. This could potentially increase the prognostic information, but more importantly might give a much more accurate idea of the mechanism of action of molecular abnormalities. For instance, overexpression of *c-erbB-2* which has prognostic implication, yet no demonstrable effect upon cell proliferation in this study, might act via an increase in apoptotic rate.

The other Trojan horse in the cell kinetic stockade is heterogeneity. To the extent that rates of cell growth vary throughout a tumour, any approach based upon single or few samples is limited by the unknown degree to which the samples used reflect the situation in the rest of the tumour. It is hard to see that this can ever be overcome, since in clinical practice, one does not have access to all of a tumour for study of a single factor, nor would one want to do this to the exclusion of all other information about it. The critical matter is not what to do about this particular problem, but to be aware of its extent. The only information available about this comes from the Mt Vernon group report upon the kinetics of colon cancer as determined using BUDR (Rew et al, 1991). They analysed multiple biopsies from over half of the 100 tumours which they studied, and present detailed data in relation to six of these (their table 3). This shows that very

large variations exist. In the first tumour in that table, for instance, the range of values of labelling index in different areas of the tumour was from 2.4% to 10.7%, and in the last the range for T_s was 13.1 hrs to 35.1 hrs. These are important differences by anyone's reckoning, and this is an important area for further study. If heterogeneity is indeed this large, then it might simply be that a single sample approach for cell kinetics, however comprehensive, will never be of help in determining prognosis.

It becomes apparent that prognostication is not where I see cell kinetics as being of use. In terms of providing a guide as to who might most benefit from the administration of radio- or chemo-therapy, and how these should be individually scheduled, the situation is not so glum. This is because the issue of cell loss is not necessarily relevant here, for what might be important in determining the response to cell cycle related therapies is not so much how fast the cell population is actually increasing in size, but rather how fast it is trying to increase. For in this case, it is what each individual cell is doing that matters, as that is the level at which the therapy operates. The more cells in cycle at any given point in time, the more are susceptible to agents which disrupt that process, and what would have happened to them subsequently, that is whether they would have lived or died, does not need to be known. Furthermore, the rate at which they are dividing, even if it is not biologically important to the natural history of the tumour, might well determine tumour survival when therapy is given, if it allows repopulation between courses of therapy such that the cumulative effect of treatment is lost. So there remains a potential place for this information in individualising patient therapy, albeit with the remaining problem of heterogeneity. It will be very interesting to see what emerges from the current crop of trials looking to use cell kinetic data as a means of selecting patients for accelerated radiotherapy (Lochrin et al, 1992; Wilson 1991).

The investigation of tumour biology remains to be considered as a field for the use of tumour cell kinetics. This has been explored in a preliminary way here, in looking at differences between aneuploid and diploid tumours, and between EGFR, *c-erbB-2* and oestrogen receptor positive and negative tumours. We have shown that although all tumours are cytogenetically DNA aneuploid but only become recognisable as such on flow cytometry at some arbitrary level of abnormality, this crude distinction does have biological significance, since the aneuploid tumours as a group have different cell kinetics to their diploid fellows. Similarly, even a small group of patients for whom data as to ER expression are available show that this factor clearly identifies groups of tumours with quite different characteristics- tumours which have escaped from this control mechanism show significantly faster potential growth. In the case of *erbB-2*, although this has been shown to be a prognostic factor in human breast cancer, and despite the fact that it is a growth factor receptor, its expression does not correlate with the rate of cellular proliferation, suggesting that it does not act as an important determinant of cellular growth. As an individual question, this requires closer investigation before it can be written off so blithely, based as it is on a binary

classification of tumours as positive or negative for the oncogene. To assess this properly requires a method of quantifying expression which will provide much greater power in determining whether there is any relationship between expression and growth. This is exactly what has been done for EGFR in this study, and the results of this are a very marked difference in kinetics based on level of expression. The difference in findings for ER, EGFR and *c-erbB-2* illustrate very well the way in which this type of experiment may help in working out which factors are functionally important in determining the growth of breast cancers.

The question as to which measure of cellular proliferation to use remains open. Flow cytometric SPF emerges poorly from our critical examination, bromodeoxyuridine rather better. The failure of cell cycle transit to differ between groups does hint that it may not be a biologically important parameter. If this is the case, then there is less reason to go to the bother of *in vivo* labelling. It would come back into its own if any way of assessing actual tumour growth were developed, as it would then be possible to work back to cell loss, and thereby fill in one of the great gaps in our ability to describe the process of proliferation. Compared with staining for Ki-67 or PCNA, or their eventual successors, the use of bromodeoxyuridine retains the advantage that it is a functional, *in vivo* measure of cell cycle activity. Despite the greater difficulty of using it, this alone is a reasonable case for keeping it in parallel with simpler methods as a tool for exploring the cell biology of cancer, and as a potential guide to patient treatment.

The conclusions from all of the foregoing, in stark terms, are then:

- S phase fraction is a subjective measurement, of poor reproducibility and very limited prognostic use.
- bromodeoxyuridine labelling index is more valid and more reproducible, but the dynamic cell cycle information gained by this method is probably to no benefit.
- cell kinetic measurements of the type used in this work have two major shortcomings:
 - they do not account for heterogeneity of kinetics within the tumour; and
 - they do not account for cell loss within the tumour cell population.

The methods need to be adapted in order to address these problems.

- proliferation markers do have an important role to play in untangling the many abnormalities in the growth control mechanism in tumours, to determine which are more likely to be causal. Cell kinetic measurements are a means not an end, in the study of tumour biology.

REFERENCES

- Aaltomaa S, Lipponen P, Eskelinen M et al. Mitotic indexes as prognostic predictors in female breast cancer. *J Cancer Res Clin Oncol* 1992; 118: 75-81
- Aaltomaa S, Lipponen P, Papinaho S, Syrjanen K. Proliferating cell nuclear antigen (PC10) immunolabelling and other proliferation indices as prognostic factors in breast cancer. *J Cancer Res Clin Oncol* 1993; 119: 288-94
- Abercrombie M. Estimation of nuclear population from microtome sections. *Anat Rec* 1946; 94: 239-47
- Allison DC, Ridolpho PF, Anderson S, Bose K. Variations in ³H-thymidine labelling of S-phase cells in solid mouse tumours. *Cancer Research* 1985; 45: 6010-6014
- Almendral JM, Huebsch D, Macdonald-Bravo H, Blundell PA, Bravo R. Cloning and sequence of the human nuclearprotein cyclin: homology with DNA binding proteins. *PNAS* 1987; 84: 1575-9
- Anbazhagan R, Gelber RD, Bettelheim R, Goldhirsch A, Gusterson BA. Association of *c-erbB-2* expression and S-phase fraction in the prognosis of node positive breast cancer. *Ann Oncol* 1991; 2: 47-53
- Ansari B, Coates PJ, Greenstein BD, Hall PA. In situ end-labelling detects DNA strand breaks in apoptosis and other physiological and pathological states. *J Pathol* 1993; 170: 1-8
- Arnerlöv C, Emdin SO, Lundgren B et al. Breast carcinoma growth rate described by mammographic doubling time and S-phase fraction. Correlations to clinical and histopathologic factors in screened population. *Cancer* 1992; 70: 1928-34
- Atkin NB, Richards BM. Deoxyribonucleic acid in human tumours as measured by microspectrophotometry of Feulgen stain : a comparison of tumours arising at different sites. *Br J Cancer* 1956; 10: 769-86
- Atkin NB. Modal deoxyribonucleic acid value and survival in carcinoma of the breast. *Br Med J* 1972; i: 271-2

- Auer G, Eriksson E, Azavedo E, Caspersson T, Wallgren A. Prognostic significance of nuclear DNA content in mammary adenocarcinomas in humans. *Cancer Res* 1984; 44: 394-6
- Baak JPA, van Dop H, Kurver PHJ, Hermans J. The value of morphometry to classic prognosticators in breast cancer. *Cancer* 1985; 56: 374-82
- Barker S, Panahy C, Puddefoot JR, Goode AW, Vinson GP. Epidermal growth factor receptor and oestrogen receptors in the non-malignant part of the cancerous breast. *Br J Cancer* 1989; 60: 673-7
- Barnard NJ, Hall PA, Lemoine NR, Kadar N. Proliferative index in breast carcinoma determined in situ by Ki67 immunostaining and its relationship to clinical and pathological variables. *J Pathol* 1987; 152: 287-95
- Barnes DM, Meyer JS, Gonzalez JG, Gullick WJ, Millis RR. Relationship between *c-erbB-2* immunoreactivity and thymidine labelling index in breast carcinoma in situ. *Breast Cancer Res Treat* 1991; 18: 11-17
- Beerman H, Kluin PM, Hermans J, van der Velde CJH, Cornelisse CJ. Prognostic significance of DNA-ploidy in a series of 690 primary breast cancer patients. *Int J Cancer* 1990; 45: 34-9
- Begg AC, Hofland I, Moonen L et al. The predictive value of cell kinetic measurements in a European trial of accelerated fractionation in advanced head and neck tumours- an interim report. *Int J Radiat Oncol Biol Phys* 1990; 19: 1449-53
- Begg AC, McNally N, Shrieve DC, Kärcher H. A method to measure the duration of DNA synthesis and the potential doubling time from a single sample. *Cytometry* 1985; 6: 620-6
- Bellantone R, Scambia G, Battaglia F et al. Presence of epidermal growth factor receptors may identify a more aggressive class of breast neoplasm. *Breast Disease* 1993; 6: 119-25
- Bello LJ. Regulation of thymidine kinase synthesis in human cells. *Exptl Cell Res* 1974; 89: 263.

- Betta PG, Bottera G, Pavesi M, Pastormerlo M, Bellingeri D, Tallarida F. Cell proliferation in breast carcinoma assessed by a PCNA grading system and its relation to other prognostic variables. *Surg Oncol* 1993; 2: 59-63
- Bilous M, Milliken J, Mathijs JM. Immunocytochemistry and in situ hybridisation of epidermal growth factor receptor and relation to prognostic factors in breast cancer. *Eur J Cancer (A)* 1992; 28: 1033-7
- Blanco G, Holli K, Heikkinen M, Kallioniemi O-P, Taskinen P. Prognostic factors in recurrent breast cancer: relationships to site of recurrence, disease-free interval, female sex steroid receptors, ploidy and histological malignancy grading. *Br J Cancer* 1990; 62: 142-6
- Bland JM. *An introduction to medical statistics.* Oxford Univ. Press: Oxford. 1987
- Bland JM, Altman DG. Statistical methods for assessing agreement between two methods of clinical measurement. *Lancet* 1986; i: 307-10
- Bolla M, Chedin M, Colonna M, Marron J, Rostaing-Puissant B, Chambaz E. Prognostic value of epidermal growth factor in a series of 303 breast cancers. *Eur J Cancer (A)* 1992; 28: 1052-4
- Bouzabar N, Walker KJ, Griffiths K et al. Ki-67 immunostaining in primary breast cancer: pathological and clinical associations. *Br J Cancer* 1989; 59: 943-7
- Boyd MF, Meakin JW, Hayward JL, Brown TC. Clinical estimation of the growth rate of breast cancer. *Cancer* 1981; 48: 1037-42
- Bravo R, Frank R, Blundell PA, Macdonald-Bravo H. Cyclin/PCNA is the auxiliary protein to DNA polymerase-delta. *Nature* 1987; 326: 515-20
- Brown BW, Atkinson EN, Thompson JR, Montague ED. Lack of concordance of growth rates of primary and recurrent breast cancer. *JNCI* 1987; 78: 425-35
- Bullough WS. Mitotic activity in tissues of dead mice, and tissues kept in physiological salt solutions. *Exp Cell Res* 1950; 1: 410-20

- Buttayan R, Zakeri Z, Lockshin R, Wolgemuth D. Cascade induction of *c-fos*, *c-myc*, and heat shock 70k transcripts during regression of the rat ventral prostate gland. *Mol Endocrinol* 1988; 2: 650-7
- Calvert RJ, Satchithanandam S. Comparison of plasma and tissue thymidine kinase activities (letter). *Br J Cancer* 1989;59:660
- Castellani R, Visscher DW, Wykes S, Sarkar FH, Crissman JD. Interaction of transforming growth factor-alpha and epidermal growth factor receptor in breast carcinoma: an immunohistologic study. *Cancer* 1994; 73: 344-9
- Challappan SP, Hiebert S, Mudryj M, Horowitz JM, Nevins JR. The E2F transcription factor is a cellular target for the Rb protein. *Cell* 1991; 65: 1053-61
- Charlson ME, Feinstein AR. A new clinical index of growth rate in the staging of breast cancer. *Amer J Med* 1980; 69: 527-36
- Charpin C, Devictor B, Bonnier P et al. Epidermal growth factor receptor in breast cancer: correlation of quantitative immunocytochemical assays to prognostic factors. *Breast Cancer Res and Treat* 1993; 25: 203-10
- Clark GM, Dressler LG, Owens MA, Pounds G, Oldaker T, McGuire WL. Prediction of relapse or survival in patients with node-negative breast cancer by DNA flow cytometry. *New Engl J Med* 1989; 320: 627-33
- Clark GM, McGuire WL. Follow up study of HER-2/*neu* amplification in primary breast cancer. *Cancer Res* 1991; 51: 944-8.
- Clayton F. Pathologic correlates of survival in 378 lymph node-negative infiltrating ductal breast carcinomas. *Cancer* 1991; 68: 1309-17
- Collins VP, Loeffler RK, Tivey H. Observations on growth rates of human tumours. *Am J Roentg* 1956; 76: 988-1000
- Cooke T, Stanton PD, Winstanley J, Murray G, Croton R, Holt S, George W. Long term prognostic significance of thymidine labelling index in primary breast cancer. *Eur J Cancer* 1992; 28: 424-6

- Cornelisse C, van der Velde C, Caspers R, Moolenaar A, Hermans J. DNA ploidy and survival in breast cancer patients. *Cytometry* 1987; 8: 225-34
- Damjanov I, Mildner B, Knowles BB. Immunohistochemical localization of the epidermal growth factor receptor in normal human tissues. *Lab Invest* 1986; 55: 588-92
- Dawson AE, Norton JA, Weinberg DS. Comparative assessment of proliferation and DNA content in breast carcinomas by image analysis and flow cytometry. *Am J Pathol* 1990; 136: 1115-24
- de Fazio A, Leary J, Hedley DW, Tattersall MH. Immunohistochemical detection of proliferating cells *in vivo*. *J Histochem Cytochem* 1987; 35: 571-4
- de Moulin D. A short history of breast cancer. Kluwer:Dordrecht. 1989
- Dervan PA, Magee HM, Buckley C, Carney DN. Proliferating cell nuclear antigen counts in formalin-fixed paraffin-embedded tissue correlate with Ki-67 in fresh tissue. *Am J Clin Pathol* 1992; 97(Suppl 1): S21-8
- Dische S, Saunders MI. The rationale for continuous, hyperfractionated, accelerated radiotherapy. *Int J Radiat Oncol Biol Phys* 1990; 19: 1317-20.
- Dittadi R, Donisi PM, Brazzale A, Cappelozza L, Brusca G, Gion M. Epidermal growth factor receptor in breast cancer: comparison with non-malignant breast tissue. *Br J Cancer* 1993; 67: 7-9
- Dyson JED, Simmons DM, Daniel J, McLaughlin JM, Quirke P, Bird CC. Kinetic and physical studies of cell death induced by chemotherapeutic agents or hyperthermia. *Cell Tissue Kinet* 1986; 19: 311-24
- El-Diery WS, Tokino T, Velculescu VE. WAF1, a potential mediator of p53 tumour suppression. *Cell* 1993; 75: 817-25
- Fabrikant JL, Wisseman CL, Vitak MJ. The kinetics of cellular proliferation in normal and malignant tissues. *Radiology* 1969; 92: 1309-16
- Fantl WJ, Johnson DE, Williams LT. Signalling by receptor tyrosine kinases. *Annu. Rev. Biochem.* 1993; 62: 453-81.

- Feichter G, Czech W, Goerttler K et al. Comparison of S-phase fractions measured by flow cytometry and autoradiography in human transplant tumours. *Cytometry* 1988; 9: 605-11
- Fisher B, Gunduz N, Costantino J et al. DNA flow cytometric analysis of primary operable breast cancer. *Cancer* 1991; 68: 1465-75
- Forster G, Cooke TG, Cooke LD, Stanton PD, Bowie G, Stell PM. Tumour growth rates in squamous carcinoma of the head and neck measured by *in vivo* bromodeoxyuridine incorporation and flow cytometry. *Br J Cancer* 1992; 65: 698-702.
- Fournier Dv, Weber E, Hoeffken W, Bauer M, Kubli F, Barth V. Growth rate of 147 mammary carcinomas. *Cancer* 1980; 45: 2198-207
- Fowler JF. Potential for increasing the differential response between tumours and normal tissues : can proliferation rate be used? *Int J Radiat Onc Biol Phys* 1985; 12: 641-5
- Fox SB, Smith K, Hollyer J, Greenall M, Hastrich D, Harris AI. The epidermal growth factor receptor as a prognostic marker: results of 370 patients and a review of 3009 patients. *Breast Cancer Res and Treat* 1994; 29: 41-9
- Friedlander ML, Hedley DW, Taylor IW. Clinical and biological significance of aneuploidy in human tumours. *J Clin Pathol* 1984; 37: 961-74
- Frierson HF. Ploidy analysis and S-phase fraction determination by flow cytometry of invasive adenocarcinomas of the breast. *Amer J Surg Path* 1991; 15: 358-67
- Fuhr JE, Frye A, Kattine AA, van Meter S. Flow cytometric determination of breast tumour heterogeneity. *Cancer* 1991; 67: 1401-5
- Gasparini G, Pozza F, Meli S, Reitano M, Santini G, Bevilacqua P. Breast cancer cell kinetics: immunocytochemical determination of growth fractions by monoclonal antibody Ki-67 and correlation with flow cytometric S-phase and with some features of tumour aggressiveness. *Anticancer Res* 1991; 11: 2015-21

- Gasparini G, Bevilacqua P, Pozza F et al. Value of epidermal growth factor receptor status compared with growth fraction and other factors for prognosis in early breast cancer. *Br J Cancer* 1992; 66: 970-6
- Gasparini G, Boracchi P, Bevilacqua R, Mezzetti M, Pozza F, Weidner N. A multiparametric study on the prognostic value of epidermal growth factor receptor in operable breast carcinoma. *Breast Cancer Res and Treat* 1994; 29: 59-71
- Gerdes J, Schwab U, Lemke H, Stein H. Production of a mouse monoclonal antibody reactive with a human nuclear antigen associated with cell proliferation. *Int J Cancer* 1983; 31: 13-20
- Gerdes J, Lemke H, Baisch H et al. Cell cycle analysis of a cell proliferation-associated human nuclear antigen defined by monoclonal antibody Ki-67. *J Immunol* 1984; 133: 1710-5
- Gerdes J, Li L, Schlueter C et al. Immunobiochemical and molecular biologic characterisation of the cell proliferation-associated nuclear antigen that is defined by monoclonal antibody Ki-67. *Am J Pathol* 1991; 138: 867-73
- Gershon-Cohen J, Berger SM, Klickstein HS. Roentgenography of breast cancer moderating concept of 'biologic predeterminism'. *Cancer* 1963; 16: 961-4
- Goodson WH, Ljung B-M, Moore DH et al. Tumour labelling indices of primary breast cancers and their regional lymph node metastases. *Cancer* 1993; 71: 3914-9
- Gorczyca W, Tuziak T, Kram A, Melamed MR, Darzynkiewicz Z. Detection of apoptosis-associated DNA strand breaks in fine-needle aspiration biopsies by in situ end labeling of fragmented DNA. *Cytometry* 1994; 15: 169-75
- Gratzner HG. Monoclonal antibody to 5-bromo- and 5-iodo-deoxyuridine : a new reagent for detection of DNA replication. *Science* 1982; 218: 474-5
- Gu Y, Turck CW, Morgan DO. Inhibition of CDK2 activity in vivo by an associated 20k regulatory subunit. *Nature* 1993; 366: 707-10
- Haagensen CD. Diseases of the breast. Saunders: Philadelphia. 1956

- Hall PA, Levison DA, Woods AL et al. Proliferating cell nuclear antigen (PCNA) immunolocalization in paraffin sections: an index of cell proliferation with evidence of deregulated expression in some neoplasms. *J Pathol* 1990; 162: 285-94
- Hannon GJ, Beach D. p15 (INK4B) is a potential effector of TGF-beta induced cell cycle arrest. *Nature* 1994; 371: 257-61
- Harper JW, Adami GR, Wei N, Keyomarsi K, Elledge SJ. The p21 CDK-interacting protein cip-1 is a potent inhibitor of G1 cyclin-dependent kinases. *Cell* 1993; 75: 805-16
- Hatschek T, Bjelkenkrantz K, Carstensen J et al. Cytophotometric estimation of cell proliferation in breast cancer. Correlation to the clinical course during long-term follow up. *Acta Oncol* 1989; 28: 801-6
- Hatschek T, Gröntoft O, Fagerberg G et al. Cytometric and histopathologic features of tumours detected in a randomized mammography screening program: correlation and relative prognostic influence. *Breast Cancer Res Treat* 1990; 15: 149-60
- Hatschek T, Carstensen J, Fagerberg G, Stål O, Gröntoft O, Nordenskjöld B. Influence of S-phase fraction on metastatic pattern and post-recurrence survival in a randomized mammography trial. *Breast Cancer Res Treat* 1989; 14: 321-7
- Hedley DW, Rugg C, Gelber R. Association of DNA index and S-phase fraction with prognosis of node positive early breast cancer. *Cancer Res* 1987; 47: 4729-35
- Hedley DW, Freidlander ML, Taylor IW. Application of DNA flow cytometry to paraffin-embedded archival material for the study of aneuploidy and its clinical significance. *Cytometry* 1985; 6: 327-33
- Hedley DW, Freidlander ML, Taylor IW, Rugg CA, Musgrove EA. Method for analysis of cellular DNA content of paraffin-embedded tissue. *J Histochem Cytochem* 1983; 31: 1333-5
- Hedley DW. Flow cytometry using paraffin-embedded tissue : five years on. *Cytometry* 1989; 10: 229-41
- Hiddeman W, von Bassewitz DB, Kleinemeier H-J et al. DNA stemline heterogeneity in colorectal cancer. *Cancer* 1986; 58: 258-63

- Hockenbery C, Nuñez G, Milliman C, Schreiber RD, Korsmeyer SJ. *Bcl-2* is an inner mitochondrial membrane protein that blocks programmed cell death. *Nature* 1990; 348: 334-6
- Hockenbery C, Zutter M, Hickey W, Nahm M, Korsmeyer SJ. *Bcl-2* protein is topographically restricted in tissues characterized by apoptotic cell death. *Proc Natl Acad Sci USA* 1991; 88: 6961-5
- Hoshino T, Barker M, Wilson CD, Boldrey EB, Fewer D. Cell kinetics of human gliomas. *J Neurosurg* 1972; 37: 15-26
- Howard A, Pelc SR. Nuclear incorporation of ³²P as demonstrated by autoradiographs. *Exp Cell Res* 1951; 2: 178-87
- Howard A, Pelc SR. Synthesis of desoxyribonucleic acid in normal and irradiated cells and its relation to chromosome breakage. *Heredity, Suppl.* 6, 1953, 261-73
- Ito S, Hoshino T, Prados MD, Edwards MSB. Cell kinetics of medulloblastomas. *Cancer* 1992; 70: 671-8
- Joensuu H, Toikkanen S, Klemi PJ. DNA index and S-phase fraction and their combination as prognostic factors in operable ductal breast carcinoma. *Cancer* 1990; 66: 331-40
- Johnson HA, Bond VP. A method of labelling tissues with tritiated thymidine *in vitro* and its use in comparing rates of proliferation in duct epithelium in fibradenoma and in carcinoma of the breast. *Cancer* 1961; 14: 639
- Kallioniemi O-P, Blanco G, Alavaikko M et al. Improving the prognostic value of DNA flow cytometry in breast cancer by combining DNA index and S-phase fraction. *Cancer* 1988; 62: 2183-90
- Kallioniemi O-P, Holli K, Visakorpi T, Koivula T, Helin HH, Isola JJ. Association of *c-erbB-2* protein over-expression with high rate of cell proliferation, increased risk of visceral metastasis and poor long-term survival in breast cancer. *Int J Cancer* 1991; 49: 650-5.

- Kallioniemi O-P, Joensuu H, Klemi P, Koivula T. Inter-laboratory comparison of DNA flow cytometric results from paraffin-embedded breast carcinomas. *Breast Cancer Res Treat* 1990; 17: 59-61
- Kallioniemi O-P. Comparison of fresh and paraffin-embedded tissue as starting material for DNA flow cytometry and evaluation of intratumour heterogeneity. *Cytometry* 1988; 9: 164-9
- Kerr JFR, Winterford CM, Harmon BV. Apoptosis: its significance in cancer and cancer therapy. *Cancer* 1994; 73: 2013-26
- Kerr JFR, Wyllie AH, Currie AR. Apoptosis: a basic biological phenomenon with wide-ranging implications in tissue kinetics. *Br J Cancer* 1972; 26: 239-57
- Key G, Becker MH, Duchrow M et al. New Ki-67 equivalent murine monoclonal antibodies (MIB 1-3) prepared against recombinant parts of the Ki-67 antigen. *Anal Cell Pathol* 1992; 4: 181-5
- Klijn JGM, Look MP, Portengen H, Alexieva-Figusch J, van Putten WLJ, Fockens JA. The prognostic value of epidermal growth factor receptor (EGF-R) in primary breast cancer: results of a 10 year follow-up study. *Breast Cancer Res and Treat* 1994; 29: 73-83
- Kreis W, Arlin Z, Yagoda A, Jones BRL, Fiori L. Deoxycytidine and deoxythymidine kinase activities in plasma of mice and patients with neoplastic disease. *Cancer Res* 1982;42:2514.
- Kusama S, Spratt JS, Donegan WL, Watson FR, Cunningham C. The gross rates of growth of human mammary carcinoma. *Cancer* 1972; 30: 594-9
- Lala PK, Patt HM. A characterization on the boundary between the cycling and resting states in ascites tumour cells. *Cell Tissue Kinet* 1968; 1: 137-46
- le Doussal V, Tubiana-Hulin M, Friedman S, Hacene K, Spyrtos F, Brunet M. Prognostic value of histologic grade nuclear components of Scarff-Bloom-Richardson (SBR). *Cancer* 1989; 64: 1914-21

- Lees JA, Buchkovick KJ, Marshak DR, Anderson CW, Harlow E. The retinoblastoma protein is phosphorylated on multiple sites by human cdc2. *EMBO* 1991; 10: 4279-90
- Leonardi E, Girlando S, Serio G et al. PCNA and Ki-67 expression in breast carcinoma: correlations with clinical and biological variables. *J Clin Pathol* 1992; 45: 416-9
- Lew D, Reed S. A proliferation of cyclins. *Trends Cell Biol* 1992; 2: 77-81
- Lipponen PK, Eskelinen MJ. Cell proliferation of transitional cell bladder tumours determined by PCNA/cyclin immunostaining and its prognostic value. *Br J Cancer* 1992; 66: 171-6
- Ljungberg B, Stenling R, Roos G. DNA content in renal cell carcinoma with reference to tumour heterogeneity. *Cancer* 1985; 56: 503-8
- Lloveras B, Edgerton S, Thor AD. Evaluation of *in vitro* bromodeoxyuridine labelling of breast carcinomas with the use of a commercial kit. *Am J Clin Pathol* 1991; 95: 41-7
- Lochrin CA, Wilson GD, McNally NJ, Dische S, Saunders MI. Tumour cell kinetics, local tumour control, and accelerated radiotherapy: a preliminary report. *Int J Rad Oncol Biol Phys* 1992; 23: 87-91
- McGuire W, Dressler L. Emerging impact of flow cytometry in predicting recurrence and survival in breast cancer patients. *J Natl Cancer Inst.* 1985; 75: 405-11
- McKenna PG, O'Neill KL, Abram WP, Hannigan BM. Thymidine kinase activities in mononuclear leukocytes and serum from breast cancer patients. *Br J Cancer* 1988; 57:619-22.
- Macklis RM, Lin JY, Beresford B, Atcher RW, Hines JJ, Humm JL. Cellular kinetics, dosimetry, and radiobiology of α -particle radioimmunotherapy: induction of apoptosis. *Radiat Res* 1992; 130: 220-6

- McNally NJ. Can cell kinetic parameters predict the response of tumours to radiotherapy? *Int J Radiat Biol* 1989; 56: 777-86.
- Merkel DE, McGuire WL. Ploidy, proliferative activity and prognosis. DNA flow cytometry of solid tumours. *Cancer* 1990 ; 65 : 1194-205
- Meyer JS, Bauer WC. *In vitro* determination of tritiated thymidine labelling index (LI) - evaluation of a method utilising hyperbaric oxygen and observations on the LI of human mammary carcinoma. *Cancer* 1975; 36: 1374-80
- Meyer JS, Koehm SL, Hughes JM et al. Bromodeoxyuridine labelling for S-phase measurement in breast carcinoma. *Cancer* 1993; 71: 3531-40
- Meyer JS, Province M. Proliferative index of breast cancer by thymidine labelling : prognostic power independent of stage, estrogen and progesterone receptors. *Breast Cancer Res Treat* 1988; 12: 191-204
- Meyer JS, Friedman E, McCrate MM, Bauer WC. Prediction of early course of breast carcinomas by thymidine labelling. *Cancer* 1983; 51: 1879-86
- Meyer JS, McDivitt RW. Reliability and stability of the thymidine labelling index of breast carcinoma. *Lab Invest* 1986; 54: 160-4
- Minckwitz V, Kaufmann M, Schmid H, Goertler K, Bastert G. Epidermal growth factor receptor and S-phase fraction as prognosticator combination in node negative primary breast cancer. *Breast* 1993; 2: 229-33
- Miyachi K, Fritzler MJ, Tan EM. Autoantibody to nuclear antigen in proliferating cells. *J Immunol* 1978; 121: 2228-34
- Möller P, Mechtersheimer G, Kaufmann M et al. Expression of epidermal growth factor receptor in benign and malignant primary tumours of the breast. *Virchows Archiv A* 1989; 414: 157-64
- Murray GD, Miller R. Statistical comparison of two methods of clinical measurement. *Br J Surg* 1990; 77: 384-7

- Nicholson RI, McClelland RA, Finlay P et al. Relationship between EGF-R, *c-erbB-2* protein expression and Ki-67 immunostaining in breast cancer and hormone sensitivity. *Eur J Cancer (A)* 1993; 29: 1018-23
- Nicholson RI, McClelland RA, Gee JMW et al. Epidermal growth factor receptor expression in breast cancer: association with response to endocrine therapy. *Breast Cancer Res and Treat* 1994; 29: 117-25
- Noda A, Ning Y, Venable SF, Pereira-Smith OM, Smith JR. Cloning of senescent cell-derived inhibitors of DNA synthesis using an expression screen. *Expl Cell Res* 1993; 211: 90-8
- Noguchi M, Thomas M, Kitagawa H et al. The prognostic significance of proliferating cell nuclear antigen in breast cancer: correlation with DNA ploidy, *c-erbB-2* expression, histopathology, lymph node metastases and patient survival. *Int J Oncol* 1993; 2: 985-9
- O'Neill KL, Abram WP, McKenna PG. Serum thymidine kinase levels in cancer patients. *Ir J Med Sci* 1986;155:272.
- O'Neill KL, Abram WP, Hannigan BM, McKenna PG. Elevated serum and mononuclear leukocyte thymidine kinase activities in patients with cancer. *Ir Med J* 1987;80:264.
- O'Reilly SM, Campeljohrn RS, Barnes DM et al. DNA index, S-phase fraction, histological grade and prognosis in breast cancer. *Br J Cancer* 1990; 61: 671-4
- Ozawa S, Ueda M, Ando N, Abe O, Shimizu N. Epidermal growth factor receptors in cancer tissues of oesophagus, lung, pancreas, colorectum, breast and stomach. *Jpn J Cancer Res* 1988; 79: 1201-7
- Peters G. Stifled by inhibitions *Nature* 1994; 371: 204-5
- Phillipe E, Le Gal Y. Growth of seventy-eight recurrent mammary cancers : quantitative study. *Cancer* 1968; 21: 461-7
- Pines J. Cyclins and cyclin-dependent kinase: take your partners. *TIBS* 1993; 18: 195-7
- Pines J. Cell cycle control. Presentation at EUSOMA meeting, London, Nov 1994

- Polyak K, Lee MH, Erdjument-Bromage H et al. Cloning of p27 (Kip1), a cyclin-dependent kinase inhibitor and a potential mediator of extracellular antimitogenic signals. *Cell* 1994; 78: 59-66
- Popert RJ, Joyce AD, Thomas DJ, Walmsley BH, Coptcoat MJ. Bromodeoxyuridine labelling of transitional cell carcinoma of the bladder- an index of recurrence? *Br J Urol* 1993; 71: 279-83
- Quirke P, Dyson JED, Dixon MF, Bird CC, Joslin CAF. Heterogeneity of colorectal adenocarcinomas evaluated by flow cytometry and histopathology. *Br J Cancer* 1985; 51: 91-106
- Rajkumar T, Gullick WJ. The type I growth factor receptors in human breast cancer. *Breast Cancer Res Treat* 1994; 29: 3-9
- Railo MJ, Smitten KV, Pekonen E. The prognostic value of epidermal growth factor receptor (EGFR) in breast cancer patients- results of a follow-up study on 149 patients. *Acta Oncologica* 1994; 33: 13-7
- Remvikos Y, Gerbault-Seurrau M, Vielh P, Zafroni B, Magdelénat H, Dutrillaux B. Relevance of DNA ploidy as a measure of genetic deviation : a comparison of flow cytometry and cytogenetics in 25 cases of breast cancer. *Cytometry* 1988; 9: 612-8
- Rew DA, Campbell ID, Taylor I, Wilson GD. Proliferation indices of invasive breast carcinomas after *in vivo* 5-bromo-2'-deoxyuridine labelling: a flow cytometric study of 75 tumours. *Br J Surg* 1992; 79: 335-9
- Rew DA, Taylor I, Weaver PC, Wilson GD. The proliferation characteristics of human colorectal carcinoma measured *in vivo*. *Br J Surg* 1991; 78: 60-6
- Riccardi A, Danova M, Dionigi P et al. Cell kinetics in leukaemia and solid tumours studied with *in vivo* bromodeoxyuridine and flow cytometry. *Br J Cancer* 1989; 59:898-903
- Richards GE. Mammary cancer. Part I. *Br J Radiol* 1948; 21: 109-16

- Roncucci L, Pedroni M, Scalmati A et al. Cell kinetic evaluation of colorectal tumours after *in vivo* administration of bromodeoxyuridine. *Int J Cancer* 1992; 52: 856-61
- Sarraf CE, Bowen ID. Proportions of mitotic and apoptotic cells in a range of untreated experimental tumours. *Cell Tissue Kinet* 1988; 21: 45-9
- Sasaki K, Matsumura K, Murakami T, Tsuji T. Measurement of bromodeoxyuridine labelling index, Ki-67 score and Ag-NOR count in breast carcinomas. *Oncology* 1992; 49: 147-53
- Sawhney N, Hall PA. Ki-67- structure, function, and new antibodies. *J Pathol* 1992; 168: 161-2
- Searle J, Lawson TA, Abbott PJ, Harmon B, Kerr JFR. An electron microscopic study of the mode of cell death induced by cancer chemotherapeutic agents in populations of proliferating normal and neoplastic cells. *J Pathol* 1975; 116: 129-38
- Serrano M, Hannon GJ, Beach D. A new regulatory motif in cell cycle control causing specific inhibition of cyclin D/CDK4. *Nature* 1993; 366: 704-7
- Shaw P, Bovey R, Tardy S, Sahli R, Sordat B, Costa J. Induction of apoptosis by wild-type p53 in a human colon tumour-derived cell line. *Proc Natl Acad Sci USA* 1992; 89: 4495-9
- Shibuya M, Ito S, Davis RL, Wilson CB, Hoshino T. A new method for analyzing the cell kinetics of human brain tumours by double labelling with bromodeoxyuridine *in situ* and with iododeoxyuridine *in vitro*. *Cancer* 1993; 71: 3109-13
- Shrestha P, Yamada K, Wada T et al. Proliferating cell nuclear antigen in breast lesions: correlation of *c-erbB-2* oncoprotein and EGF receptor and its clinicopathological significance in breast cancer. *Virchows Archiv-A* 1992; 421: 193-202
- Silvestrini R. Feasibility and reproducibility of the 3H-thymidine labelling index in breast cancer. *Cell Prolif* 1991; 24: 437-45

- Silvestrini R, Daidone M, Valagussa P, DiFronzo G, Mezzanotte G, Bonadonna G. Cell kinetics as a prognostic indicator in node-negative breast cancer. *Eur J Cancer Clin Oncol* 1989; 25: 1165-71
- Silvestrini R, Daidone M, Valagussa P et al. 3H-thymidine labelling index as a prognostic indicator in node-positive breast cancer. *J Clin Oncol* 1990; 8: 1321-7
- Slamon DJ, Clark GM, Wong SG, Levin WJ, Ullrich A, McGuire WL. Human breast cancer : correlation of relapse and survival with amplification of the HER-2/*neu* oncogene. *Science* 1987; 235:177-82
- Spratt JS, Heuser L, Kuhns JG et al. Association between the actual doubling times of primary breast cancer with histopathologic characteristics and Wolfe's parenchymal mammographic patterns. *Cancer* 1981; 47: 2265-8
- Stål O, Wingren S, Carstensen J et al. Prognostic value of DNA ploidy and S-phase fraction in relation to estrogen receptor content and clinicopathological variables in primary breast cancer. *Eur J Cancer Clin Oncol* 1989; 25: 301-9
- Steel GG. Growth kinetics of tumours. Oxford, Clarendon Press. 1977
- Stenkvist B, Bengtsson E, Dahlqvist B et al. Predicting breast cancer recurrence. *Cancer* 1982; 50: 2884-93
- Stephenson R, Gay H, Fair W, Melamed M. Effect of section thickness on quality of flow cytometric DNA content determinations in paraffin-embedded tissues. *Cytometry* 1986; 7: 41-4
- Tachibana M, Deguchi N, Baba S, Jitsukawa S, Hata M, Tazaki H. Prognostic significance of bromodeoxyuridine high labelled bladder cancer measured by flow cytometry: does flow cytometric determination predict the prognosis of patients with transitional cell carcinoma of the bladder? *J Urol* 1993; 149: 739-43
- Tauchi K, Hori S, Itoh H, Osamura RY, Tokuda Y, Tajima T. Immunohistochemical studies on oncogene products (*c-erbB-2*, EGFR, *c-myc*) and oestrogen receptor in benign and malignant breast lesions. *Virchows Archiv A* 1989; 416: 65-73

- Taylor A, Jones OW, Grishaver MA. Effect of 5-fluorouracil on the release of thymidine kinase from hepatoma cells *in vitro*. *Cancer Res* 1981;41:192.
- Tinnemans MM, Schutte B, Lenders MH, Ten Velde GP, Ramaekers FC, Blijham GH. Cytokinetic analysis of lung cancer by *in vivo* bromodeoxyuridine labelling. *Br J Cancer* 1993; 67: 1217-22
- Toi M, Tominaga T, Osake A, Toge T. Role of epidermal growth factor receptor expression in primary breast cancer: Results of a biochemical study and an immunocytochemical study. *Breast Cancer Res and Treat* 1994; 29: 51-8
- Toikkanen S, Joensuu H, Klemi P. The prognostic significance of nuclear DNA content in invasive breast cancer - a study with long-term follow-up. *Br J Cancer* 1989; 60: 693-700
- Tommasi S, Paradiso A, Mangia A et al. Biological correlation between HER-2/*neu* and proliferative activity in breast cancer. *Anticancer Res* 1991; 11: 1395-400
- Toyoshima H, Hunter T. p27, a novel inhibitor of G1 cyclin-CDK protein kinase activity, is related to p21. *Cell* 1994; 78: 67-74
- Travers MT, Barrett-Lee PJ, Berger U et al. Growth factor expression in normal, benign, and malignant breast tissue. *Br Med J* 1988; 296: 1621-4
- Tsutsumi Y, Naber SP, DeLellis RA et al. *neu* oncogene protein and epidermal growth factor receptor are independently expressed in benign and malignant breast tissues. *Hum Pathol* 1990; 21: 750-8
- Tubiana M, Koscielny S. Cell kinetics, growth rate and the natural history of breast cancer. *Eur J Cancer Clin Oncol* 1988; 24: 9-14
- Tucker SL, Chan KS. The selection of patients for accelerated radiotherapy on the basis of tumour growth kinetics and intrinsic radiosensitivity. *Radiotherapy Oncol* 1990; 18: 197-211

- Umekita Y, Enokizono N, Sagara Y et al. Immunohistochemical studies on oncogene products (EGF-R, *c-erbB-2*) and growth factors (EGF, TGF- α) in human breast cancer: their relationship to oestrogen receptor status, histological grade, mitotic index and nodal status. *Virchows Archiv (A)* 1992; 420: 345-51
- Veronese SM, Gambacorta M, Gottardi O, Scanzi F, Ferrari M, Lampertico P. Proliferation index as a prognostic marker in breast cancer. *Cancer* 1993; 71: 3926-31
- Vindeløv LL, Hansen HH, Christensen IB et al. Clonal heterogeneity of small-cell anaplastic carcinoma of the lung demonstrated by flow cytometric DNA analysis. *Cancer Res* 1980; 40: 4295-300
- Walker NI, Bennett RE, Kerr JFR. Cell death by apoptosis during involution of the lactating breast in mice and rats. *Am J Anat* 1989; 185: 19-32
- Waterfield MD, Mayes EL, Stroobant P et al. A monoclonal antibody to human epidermal growth factor receptor. *J Cell Biol* 1982; 20: 149-61.
- White RA, Terry NHA, Meistrich ML, Calkins DP. Improved method for computing potential doubling time from flow cytometric data. *Cytometry* 1990; 11: 314-7.
- Wijsman JH, Jonker RR, Keijzer R, van der Velde CJH, Cornelisse CJ, van Dierendonck. A new method to detect apoptosis in paraffin sections: in situ end-labeling of fragmented DNA. *J Histochem Cytochem* 1993; 41: 7-12
- Wilson GD. Assessment of human tumour proliferation using bromodeoxyuridine-current status. *Acta Oncol.* 1991; 30: 903-10
- Wilson GD, McNally NJ, Dische S. Measurement of cell kinetics in human tumours *in vivo* using bromodeoxyuridine incorporation and flow cytometry. *Br J Cancer* 1988; 58: 423-31
- Wilson GD, McNally NJ, Dunphy E, Karcher H, Pfragner R. The labelling index of human and mouse tumours assessed by bromodeoxyuridine staining *in vitro* and *in vivo* and flow cytometry. *Cytometry* 1985; 6: 641-7

- Winstanley J, Cooke TG, Murray GD et al. The prognostic significance of *c-erbB-2* in primary breast cancer. *Br J Cancer* 1991; 63: 447-50.
- Wintzer HO, Zipfel I, Schulte-Monting J, Hellerich U, von Kleist S. Ki-67 immunostaining in human breast cancers and its relationship to prognosis. *Cancer* 1991; 67: 421-8
- Wyllie AH. Apoptosis and the regulation of cell numbers in normal and neoplastic tissues: an overview. *Cancer Metast Rev* 1992; 11: 95-103
- Xiong Y, Hannon GJ, Zhang H, Casso D, Kobayashi R, Beach D. p21 is a universal inhibitor of cyclin kinases. *Nature* 1993; 366: 701-4
- Yousof N, Khan S, Sheikh Y, Hyams D, Bokhari J, Raza A. Cell cycle parameters and DNA ploidy in colorectal carcinomas. *J Surg Res* 1991; 51: 457-62

APPENDICES

Appendix I: Raw data from the study of tumour ploidy and S phase fraction. Data are presented from the 281 patients in whom ploidy was calculated. Column 1 identifies the case by its accession number in the Liverpool Breast Cancer Series, and column 2 the half peak coefficient of variation of the diploid G0/G1 peak in the histogram used for analysis. In column 4 tumour ploidy is coded as D for diploid and A for aneuploid. * in the final column indicates that SPF was not obtainable for that tumour.

Series No.	CV	DNA Index	Ploidy	SPF(%)
7	5.6	1.0	D	4.6
8	4.1	1.4+2.3	A	*
12	5.6	2.1	A	20.8
18	4.5	1.0	D	7.1
19	4.9	1.2+1.5	A	*
23	5.0	1.8	A	13.7
24	7.3	1.6	A	6.3
30	9.2	1.6+2.3	A	*
31	8.0	1.0	D	7.0
54	7.7	1.8	A	*
59	5.8	2.0	A	11.6
60	5.1	1.0	D	5.3
66	6.7	1.0	D	7.4
75	8.5	1.5	A	*
78	7.6	1.0	D	*
88	7.8	2.0	A	*
90	5.0	2.5	A	17.4
94	8.0	2.0	A	3.4
95	5.8	1.0	D	7.5

Series No.	CV	DNA Index	Ploidy	SPF(%)
98	3.5	1.7	A	12.1
99	8.6	1.6	A	*
101	6.0	1.0	D	1.6
110	4.7	1.0	D	5.3
115	4.2	1.7	A	3.7
118	4.5	1.0	D	3.3
125	9.2	1.7	A	*
129	4.9	1.0	D	3.1
131	6.9	1.2	A	5.2
132	7.1	1.0	D	2.0
141	5.0	1.0	D	*
144	6.3	1.3	A	2.1
145	8.1	1.0	D	3.5
148	8.4	2.0	A	4.5
153	8.4	1.5	A	*
155	5.9	1.0	D	3.1
162	8.1	1.9	A	16.8
163	6.4	1.0	D	3.7
164	8.6	2.1	A	*
168	6.1	2.0	A	17.7
171	8.0	1.6	A	14.4
172	6.8	1.0	D	*
173	7.2	1.0	D	2.4
174	5.2	1.9	A	10.2
175	4.5	1.0	D	4.9
177	6.1	1.0	D	2.8
179	7.9	1.0	D	4.7

Series No.	CV	DNA Index	Ploidy	SPF(%)
181	5.2	1.7	A	21.7
203	5.2	1.4	A	*
205	7.1	1.0	D	4.0
207	6.4	1.8	A	*
220	4.5	1.0	D	6.7
221	7.9	1.1	A	*
230	5.7	1.0	D	3.7
231	4.3	1.2	A	12.9
236	6.6	1.5	A	5.9
239	7.7	1.0	D	7.3
245	6.6	2.1	A	9.5
249	8.1	1.0	D	5.5
250	7.0	1.0	D	8.3
256	7.6	1.7	A	13.3
258	4.7	3.3	A	*
266	6.7	1.6	A	12.3
272	6.5	1.7	A	12.8
283	7.3	1.4	A	7.9
297	7.4	1.6	A	*
301	4.5	1.2+1.8	A	*
304	5.2	1.5	A	9.1
307	9.9	1.3	A	*
310	5.8	2.0	A	9.4
319	5.1	1.0	D	5.6
322	7.8	1.4	A	13.5
323	3.5	1.8	A	6.0
324	3.8	1.9	A	8.3

Series No.	CV	DNA Index	Ploidy	SPF(%)
325	5.1	1.2	A	16.7
331	3.0	1.0	D	3.1
334	6.7	1.5	A	11.9
338	7.5	1.0	D	5.6
340	4.7	1.9	A	12.9
342	6.6	2.2	A	12.2
346	5.7	1.0	D	5.6
361	3.7	1.0	D	6.4
363	4.8	1.3	A	10.9
370	7.7	1.0	D	3.9
373	5.6	1.0	D	3.1
379	7.5	1.2	A	25.9
384	5.2	1.0	D	4.1
386	4.7	1.4	A	8.2
390	4.6	1.8	A	12.3
391	6.5	1.7	A	9.0
393	5.0	2.7	A	39.8
395	8.1	2.0	A	15.0
396	5.3	1.0	D	1.3
399	6.3	1.0	D	4.1
404	6.6	1.7	A	8.4
408	6.2	2.5	A	25.8
409	6.8	2.1	A	2.8
413	4.4	1.0	D	4.7
414	7.6	1.0	D	7.8
419	4.1	1.0	D	4.7
425	9.8	2.0	A	*

Series No.	CV	DNA Index	Ploidy	SPF(%)
426	3.4	1.5	A	8.4
433	4.6	1.0	D	3.4
436	8.1	1.0	D	4.5
437	4.1	1.8	A	8.3
440	3.8	1.4	A	9.9
441	3.5	2.4	A	8.1
451	7.0	0.8+2.8	A	*
452	7.6	1.0	D	5.2
456	6.4	1.6	A	11.3
458	5.4	1.0	D	10.1
459	5.2	1.5	A	5.4
461	6.6	2.0	A	*
465	4.4	1.7	A	10.7
470	3.7	0.9	A	9.6
471	4.8	2.0	A	21.1
472	3.9	1.4	A	*
474	2.5	0.9	A	6.6
475	7.2	1.0	D	3.8
476	4.3	1.0	D	3.7
477	5.5	1.3	A	4.5
479	6.3	1.7	A	8.7
480	6.0	1.0	A	9.7
483	8.0	1.7	A	6.2
484	5.8	1.0	D	7.7
486	4.3	1.0	D	2.1
488	7.5	2.0	A	6.3

Series No.	CV	DNA Index	Ploidy	SPF(%)
492	4.6	2.7	A	*
495	7.5	1.0	D	3.6
496	4.8	1.0	D	4.6
498	5.8	1.0	D	2.4
500	7.8	1.6	A	*
502	9.5	1.6	A	*
503	6.7	1.8	A	6.7
504	5.1	1.6+2.1	A	*
508	4.4	1.0	D	7.9
515	5.2	1.0	D	6.6
518	7.2	1.9	A	*
520	7.8	3.2	A	20.4
521	5.6	1.8	A	2.3
529	4.4	1.0	D	4.6
530	5.2	1.8	A	10.8
532	3.9	2.0	A	16.3
536	4.6	1.0	D	4.8
541	4.6	1.0	D	3.1
546	4.2	1.0	D	4.3
547	8.8	1.0	D	*
548	2.8	1.8	A	8.0
556	7.6	1.7	A	*
558	5.1	1.0	D	2.7
559	3.8	1.0	D	2.5
560	4.9	1.9	A	5.7
565	5.0	1.0	D	2.8
567	4.8	2.0	A	5.2

Series No.	CV	DNA Index	Ploidy	SPF(%)
568	3.7	1.0	D	0.8
569	4.9	1.0	D	1.4
570	4.1	2.0	A	5.1
571	4.1	1.0	D	4.9
575	5.3	2.8	A	13.6
578	5.8	2.7	A	23.7
582	4.1	1.0	D	3.1
591	5.4	1.7	A	10.9
594	6.0	1.7	A	3.3
598	6.9	1.0	D	7.2
602	8.0	1.8	A	2.5
604	6.0	0.7	A	3.1
605	9.4	0.8+1.5+1.9	A	*
607	4.0	1.7	A	14.0
611	5.8	1.0	D	2.5
612	7.5	2.1+3.0	A	*
622	5.9	1.0	D	6.9
641	6.7	0.6	A	6.2
642	7.1	1.8	A	12.0
648	4.3	1.6	A	*
649	6.4	1.7	A	13.3
650	3.8	2.0	A	7.6
651	3.9	2.0	A	14.0
653	7.8	1.0	D	4.1
660	3.6	1.5	A	*
661	4.3	2.1	A	27.6
663	4.9	1.0	D	3.3

Series No.	CV	DNA Index	Ploidy	SPF(%)
664	5.3	3.0	A	*
666	3.7	1.4+1.7+1.9	A	*
667	5.1	2.0	A	7.0
668	5.4	1.0	D	3.3
669	4.7	2.0	A	3.8
670	4.9	1.7	A	12.8
672	3.9	1.8	A	7.4
677	6.6	1.6	A	10.6
678	5.1	1.6	A	15.8
680	4.4	2.0	A	10.2
682	5.4	1.5	A	6.7
683	4.6	1.8	A	13.4
684	4.0	1.0	D	2.1
685	4.1	1.7	A	2.7
686	5.2	1.0	D	4.2
691	7.0	1.0	D	7.3
692	3.9	2.1	A	9.2
693	4.1	1.5	A	14.3
694	9.2	2.1	A	*
697	4.2	1.9	A	11.5
698	4.9	0.9+1.8	A	*
700	8.9	1.0	D	*
701	7.2	2.1	A	6.0
702	3.3	1.6	A	16.7
703	4.5	1.7	A	11.3
705	4.1	2.2	A	6.3
706	5.4	0.7	A	*

Series No.	CV	DNA Index	Ploidy	SPF(%)
711	3.9	1.7+1.9	A	*
712	4.0	1.4	A	17.0
715	4.4	2.2	A	11.3
721	6.0	1.8	A	21
723	4.9	1.0	D	3.6
724	4.3	1.9	A	7.6
726	5.8	1.0	D	1.7
727	8.2	1.8	A	10.5
730	5.4	0.7+1.7	A	*
731	6.3	1.0	D	2.3
732	6.2	2.1	A	*
733	5.2	1.0	D	3.9
734	7.6	1.8	A	5.8
735	4.5	1.9	A	21.5
737	4.0	1.0	D	1.9
741	5.5	1.4+1.7	A	*
743	6.3	1.0	D	1.8
745	5.6	2.0	A	9.0
748	8.3	1.0	D	2.3
752	4.9	1.0	D	6.7
753	3.7	1.1+2.1	A	3.6
756	2.8	1.8	A	16.1
758	5.6	1.5	A	21.0
762	5.7	2.1	A	*
763	5.8	1.6	A	9.6
771	3.6	1.7+1.9+3.0	A	*
772	5.9	1.8	A	16.2

Series No.	CV	DNA Index	Ploidy	SPF(%)
776	6.3	2.0	A	20.5
779	4.9	3.1	A	*
783	7.7	1.0	D	4.3
786	3.9	1.8	A	7.1
788	3.0	0.8	A	10.2
797	5.1	1.4	A	9.9
800	3.4	2.0	A	12.1
802	4.2	1.0	D	2.4
803	7.9	1.0	D	3.7
808	6.1	1.0	D	4.4
809	6.7	1.7+2.7	A	*
822	7.0	1.5	A	*
823	7.8	2.0	A	*
824	6.9	1.0	D	4.5
828	9.4	1.5+2.1	A	*
829	6.0	1.0	D	3.4
836	8.2	2.2	A	*
839	7.0	1.9	A	10.3
841	6.6	2.1	A	2.2
846	6.4	1.0	D	2.7
849	6.5	1.0	D	3.3
853	4.8	1.7	A	21.8
857	4.0	1.0	D	3.2
867	6.3	1.0	D	2.7
882	4.7	1.0	D	4.5
885	7.0	1.0	D	3.3

Series No.	CV	DNA Index	Ploidy	SPF(%)
886	6.8	2.4	A	1.9
896	4.4	1.2+1.9	A	*
899	5.5	1.0	D	2.2
905	6.5	1.0	D	5.7
906	5.2	1.7	A	12.3
908	5.5	2.2	A	*
917	5.4	1.9	A	6.0
919	8.5	1.9	A	*
920	7.1	1.6	A	16.3
924	7.1	1.6	A	16.7
929	6.3	1.0	D	6.0
930	5.7	1.0	D	3.0
932	6.5	2.7	A	23.9
956	6.5	1.9	A	10.5
969	6.0	1.9	A	11.6
973	9.0	1.0	D	*
977	6.0	1.9	A	16.0
978	6.1	1.4	A	18.4
981	5.3	1.0	D	5.3
984	6.4	1.0	D	5.0
987	3.3	2.0	A	9.7

Appendix Ia: Pathological data for patients in ploidy series for whom SPF is available. Columns are: pt no- accession number in Liverpool Ploidy Series; meno- menopausal status, 1=pre, 2=post; t,n- pT,pN by TNM classification; grade- modified Bloom and Richardson system; er- 1=<5fmol/mg, 2= \geq 5fmol/mg; erbB-2- 1=pos- itive, 2=negative. *=not available

	pt no	meno	t	n	grade	er	erbB-2
1	7	2	2	2	3	1	2
2	12	2	2	1	2	2	2
3	18	1	3	1	*	1	2
4	20	2	1	1	1	1	2
5	22	2	1	1	2	1	2
6	23	2	2	2	*	1	1
7	24	1	2	1	*	1	2
8	31	2	2	2	*	1	*
9	33	1	2	2	3	2	2
10	36	2	2	2	*	2	2
11	50	2	2	1	3	2	2
12	56	1	2	2	3	2	2
13	59	2	2	2	3	2	2
14	60	2	2	2	1	1	2
15	66	2	1	1	2	2	1
16	75	2	2	1	3	1	2
17	81	1	2	2	3	2	1
18	84	1	3	2	3	2	2
19	90	2	2	2	3	1	2
20	94	2	3	1	*	2	2
21	98	1	3	1	2	2	2
22	101	2	1	2	3	2	2
23	112	2	2	1	*	2	2
24	113	1	2	2	2	2	2
25	115	2	2	1	*	2	2
26	118	2	3	1	*	1	1
27	125	2	2	1	*	1	2
28	129	1	2	2	1	2	2
29	131	2	2	2	*	1	2
30	132	2	2	2	*	1	2
31	145	2	2	2	2	1	2
32	148	2	2	1	*	1	2
33	153	2	2	1	1	2	1
34	155	2	2	1	1	1	2
35	161	2	3	2	1	1	*
36	162	2	2	2	*	2	1
37	163	2	2	1	*	1	2
38	164	2	2	2	*	1	2
39	168	2	3	1	*	1	2

	pt no	meno	t	n	grade	er	erbB-2
40	171	1	2	1	*	2	2
41	173	2	2	1	*	2	2
42	174	1	2	1	1	1	2
43	175	2	2	2	*	1	2
44	177	2	2	2	*	1	2
45	181	*	2	2	2	1	2
46	189	2	2	1	2	1	1
47	205	1	1	1	1	1	2
48	220	2	2	1	*	2	2
49	229	2	3	2	1	1	*
50	230	2	2	1	*	1	2
51	231	1	3	1	1	2	2
52	236	2	2	1	*	2	2
53	239	2	2	1	*	1	2
54	245	2	2	2	*	1	1
55	249	2	2	2	*	1	2
56	250	2	3	2	3	1	2
57	256	2	2	2	3	1	2
58	266	2	2	1	3	1	2
59	272	2	3	2	2	2	1
60	283	1	1	1	*	1	2
61	304	2	3	1	*	2	2
62	307	2	2	2	*	2	2
63	310	1	1	2	2	1	2
64	319	1	2	2	*	1	2
65	322	2	2	1	*	2	2
66	323	2	2	1	*	1	2
67	324	2	2	1	2	1	2
68	325	2	2	1	2	1	1
69	331	2	3	2	3	2	2
70	334	1	3	1	*	2	2
71	338	1	3	2	*	1	2
72	340	1	2	1	2	1	2
73	346	1	2	2	*	2	2
74	361	2	3	1	2	1	2
75	363	1	3	1	3	1	1
76	370	1	3	1	2	2	1
77	373	2	2	2	2	1	2
78	379	2	2	1	*	2	2
79	384	1	2	2	3	1	1
80	386	2	1	1	*	1	2
81	390	1	2	1	2	2	2
82	391	2	2	1	2	1	2
83	393	2	3	1	*	1	1
84	395	2	2	2	*	2	2
85	396	2	2	2	*	1	2
86	399	*	2	1	*	1	2

	pt no	meno	t	n	grade	er	erbB-2
87	404	2	3	2	*	1	2
88	408	2	2	2	*	1	2
89	409	2	*	1	*	1	2
90	413	2	1	2	*	1	1
91	414	2	1	1	2	2	*
92	419	2	2	2	2	1	2
93	426	2	3	1	*	1	1
94	433	2	2	2	1	1	1
95	436	2	2	2	2	1	2
96	437	1	2	1	1	2	1
97	440	2	1	1	*	1	2
98	441	2	2	2	*	1	2
99	452	2	3	1	*	1	1
100	456	2	2	2	3	2	2
101	458	2	2	1	3	2	2
102	459	2	2	1	*	*	*
103	465	2	2	2	1	2	2
104	470	2	2	1	1	1	2
105	471	*	2	1	1	1	2
106	474	2	3	2	3	2	1
107	477	2	1	1	*	1	2
108	479	2	3	1	*	1	1
109	480	1	2	1	*	1	2
110	484	2	2	1	*	2	2
111	486	1	2	1	1	1	2
112	488	2	2	2	1	1	2
113	495	2	2	1	2	2	2
114	498	2	2	2	1	2	2
115	503	2	2	1	3	1	2
116	508	2	*	*	*	2	1
117	515	2	2	1	1	1	2
118	520	*	2	2	3	2	*
119	521	2	2	1	1	1	2
120	522	2	2	1	2	1	*
121	529	2	2	2	3	1	1
122	530	*	3	1	1	1	2
123	532	2	2	1	*	2	1
124	536	2	2	1	3	1	2
125	541	2	3	2	1	1	2
126	543	*	2	1	1	1	2
127	546	2	2	1	2	1	2
128	548	1	2	2	*	2	1
129	559	*	2	1	*	*	2
130	560	*	*	1	*	1	2
131	565	1	2	2	3	2	2
132	568	2	2	2	1	1	2
133	569	2	2	2	*	1	2

	pt no	meno	t	n	grade	er	erbB-2
134	570	2	3	2	3	2	1
135	571	2	2	2	2	1	1
136	575	2	2	1	*	2	2
137	578	2	3	2	*	2	2
138	582	2	2	1	*	1	2
139	591	2	2	2	1	2	2
140	594	2	2	1	3	2	2
141	598	1	1	1	1	2	2
142	602	2	2	1	*	1	2
143	604	2	2	2	1	1	2
144	607	1	2	2	3	2	2
145	622	2	2	1	*	1	1
146	637	2	2	2	2	2	2
147	641	2	1	1	*	1	2
148	642	2	3	2	1	1	1
149	649	2	2	1	*	2	1
150	650	2	2	2	1	1	2
151	651	2	2	2	2	2	2
152	653	2	2	2	1	1	2
153	661	2	3	1	*	2	2
154	663	*	2	1	*	1	1
155	667	2	2	1	*	*	1
156	668	2	2	1	*	1	2
157	669	1	2	1	*	2	2
158	670	2	3	1	*	2	*
159	677	2	2	1	1	2	2
160	678	*	2	2	3	2	2
161	680	2	3	2	3	2	2
162	681	1	3	2	2	2	2
163	682	1	2	2	3	1	2
164	683	1	2	2	2	2	1
165	684	2	2	1	3	2	1
166	685	2	1	1	1	1	2
167	686	2	2	1	*	2	2
168	689	1	2	1	*	1	2
169	691	2	*	1	*	1	2
170	692	2	2	1	1	1	2
171	693	1	2	1	2	2	2
172	694	2	2	1	2	1	2
173	697	1	2	1	*	2	2
174	699	*	2	1	2	2	2
175	701	2	2	1	3	1	2
176	702	2	1	2	*	2	2
177	703	2	2	1	*	2	1
178	705	2	2	1	*	1	1
179	712	2	2	2	3	2	2
180	713	2	2	2	*	1	2

	pt no	meno	t	n	grade	er	erbB-2
181	715	2	*	1	*	2	1
182	721	2	3	2	*	1	2
183	723	2	3	1	*	1	2
184	724	2	2	2	1	1	2
185	726	2	2	1	1	2	2
186	727	2	2	1	1	1	1
187	731	2	2	1	*	2	1
188	733	1	3	1	*	1	2
189	734	1	3	2	*	1	2
190	735	*	2	2	3	2	2
191	737	2	3	1	*	1	2
192	743	1	2	2	1	2	2
193	745	2	2	1	*	1	1
194	748	2	*	1	*	1	2
195	753	2	2	1	*	1	2
196	756	1	2	2	3	1	1
197	763	*	2	1	*	2	2
198	772	1	3	2	3	1	2
199	776	2	3	1	*	2	2
200	783	2	2	1	*	1	2
201	786	1	3	1	2	2	1
202	788	1	3	1	*	2	1
203	797	1	1	1	*	1	2
204	800	2	3	2	*	1	1
205	802	*	*	*	*	*	2
206	808	1	2	1	2	1	2
207	824	*	*	*	*	*	2
208	839	2	2	1	*	1	2
209	846	2	2	1	2	1	2
210	849	2	2	1	1	2	2
211	853	1	2	2	2	1	1
212	867	2	1	1	2	2	2
213	882	2	2	1	2	1	*
214	885	2	2	2	*	*	2
215	886	2	2	2	1	2	2
216	899	*	*	1	*	*	1
217	906	1	2	2	3	2	1
218	917	2	2	1	*	1	2
219	919	2	2	1	*	1	1
220	930	2	*	1	2	*	1
221	932	2	2	2	1	1	1
222	956	2	2	1	1	2	1
223	984	2	2	1	3	1	1
224	987	2	1	2	3	1	2

Appendix II: Raw data from SPF reproducibility studies carried out on histograms derived from breast cancer lumpectomy specimens. Results are shown for 91 tumours from which two or more estimates of SPF could be made. The first column identifies the tumour by its number in the series from which these were drawn. Column 2 gives the half peak coefficient of variation of the diploid G0/G1 peak of the histogram used for analysis, and the next column the DNA index of the tumour population (DNA index 1.0 = diploid). There follow the 10 estimates of SPF upon the histogram- the first two letters identify the observer with PS = the author and SO = Ms Sarah Oakes; the following numbers 1 & 2 represent the first and second series of estimates by each observer; and the final letter gives the model used where R = rectangular, T = trapezoidal, Q = quadratic, and M = multiple broadened rectangles. * = no estimate made.

No.	CV	DI	PS1R	PS1T	PS1Q	PS1M	PS2R	PS2T	PS2Q	PS2M	SO1R	SO2R
1	7.6	1.6	16.8	8.0	8.6	20	16.8	8.0	8.6	6	16.8	16.8
3	5.4	1.0	6.1	5.7	5.3	50	*	*	*	*	*	*
4	4.8	1.5	8.9	7.4	*	-11	6.1	6.1	32.1	-11	*	*
5	4.5	1.0	2.7	2.5	0.7	-2	2.7	2.5	0.7	-5	2.7	2.8
6	5.6	1.0	6.4	4.7	*	-1	6.8	4.9	3.0	1	10.0	11.2
7	4.2	1.0	3.2	3.5	6.1	10	5.3	5.1	6.6	-2	7.2	6.5
9	3.3	1.7	13.5	12.4	21.3	-3	20.8	17.8	31.3	3	22.4	15.0
10	5.7	1.9	17.3	18.5	18.6	4	19.2	18.9	30.4	12	20.6	15.3
11	4.9	1.7	17.9	13.0	9.8	-15	24.5	14.6	*	-104	*	*
12	5.7	1.8	21.1	14.4	44.5	-11	22.1	14.8	42.4	-21	23.4	25.2

No.	CV	DI	PS1R	PS1T	PS1Q	PS1M	PS2R	PS2T	PS2Q	PS2M	SO1R	SO2R
17	4.4	1.0	6.7	6.4	8.5	-8	6.2	6.1	7.9	-8	9.6	7.3
18	4.7	1.8	18.5	17.6	35.3	6	17.4	12.9	12.7	-20	*	*
19	5.5	2.0	11.6	8.6	14.8	-11	11.6	8.4	20.1	-43	8.4	8.4
20	4.6	1.0	2.3	2.1	2.3	-9	2.3	2.0	3.7	-5	4.5	4.6
21	7.4	1.0	3.9	3.1	9.3	-4	*	*	*	*	*	*
22	4.4	1.0	10.3	9.3	*	90	8.5	8.2	*	23	11.3	11.0
23	4.6	1.0	5.1	4.6	4.8	0	3.7	3.4	2.2	-3	7.4	7.4
24	3.1	1.2	5.2	5.2	5.8	-2	4.4	4.4	5.3	-9	*	*
25	5.3	1.0	4.2	2.9	*	-28	3.4	2.3	4.2	-21	3.4	3.6
26	5.5	1.0	6.1	5.8	4.2	-3	6.5	6.4	3.3	-11	6.5	7.1
27	3.8	1.8	5.3	4.5	7.2	-9	4.2	4.5	6.4	-9	*	5.3
28	2.8	1.0	1.0	1.2	1.5	-14	1.6	1.3	1.7	-3	1.6	1.6
29	3.4	1.0	2.5	2.0	3.3	-15	*	*	*	*	*	*
32	3.6	1.0	6.1	6.2	6.9	-14	4.7	4.6	4.5	-20	7.3	8.8
33	4.1	1.0	1.3	0.8	3.5	-16	1.2	0.6	5.3	-24	2.8	2.8
34	3.8	1.8	9.9	9.9	9.9	-23	*	*	*	*	*	*
35	4.5	1.0	14.8	14.1	15.7	10	13.8	13.1	14.8	20	15.2	17.8

No.	CV	DI	PS1R	PS1T	PS1Q	PS1M	PS2R	PS2T	PS2Q	PS2M	SO1R	SO2R
37	2.5	1.0	1.9	1.8	1.9	-15	2.0	1.9	2.2	-11	1.9	1.9
38	2.5	1.7	7.5	4.6	10.8	-20	4.9	4.9	*	-68	11.2	6.3
39	7.1	1.0	5.2	4.6	5.5	5	6.0	4.9	1.9	22	7.9	7.9
41	4.2	1.3	7.2	7.1	8.0	2	5.3	5.6	6.8	-5	*	7.2
44	4.7	2.3	12.8	13.0	15.1	-3	12.5	10.6	2.0	-8	15.0	19.1
46	8.5	1.0	6.1	6.2	7.4	4	6.0	5.7	5.5	5	6.1	6.0
47	6.1	1.0	2.4	1.9	6.7	-3	2.4	2.1	4.6	-11	2.4	4.8
48	4.4	1.7	9.3	10.1	12.5	-11	9.4	10.1	11.8	-17	*	*
49	7.2	1.0	1.7	1.2	1.6	-10	1.7	1.2	1.6	1	1.7	1.7
50	2.4	1.0	1.1	1.3	1.7	-11	1.1	1.2	1.9	-13	2.7	2.7
51	3.6	1.8	8.5	8.2	10.6	0	8.4	8.2	10.3	2	10.0	8.4
52	5.0	1.0	4.9	4.8	5.9	-8	4.9	4.6	4.9	-8	5.3	5.3
53	5.4	1.6	11.3	9.7	13.2	12	10.9	8.1	*	9	10.2	9.8
54	5.7	1.0	2.9	2.7	6.0	0	*	*	*	*	*	*
55	3.4	1.3	7.5	7.3	7.0	-10	7.4	7.1	7.3	-12	9.8	*
56	3.7	1.0	3.4	3.2	4.1	-16	4.4	3.9	5.2	-17	6.0	6.0
57	4.3	1.0	3.3	3.0	7.1	18	3.3	3.0	7.1	17	6.3	4.6
59	6.0	1.0	1.1	0.9	3.6	49	2.3	1.2	9.7	-10	1.6	2.5

No.	CV	DI	PS1R	PS1T	PS1Q	PS1M	PS2R	PS2T	PS2Q	PS2M	SO1R	SO2R
61	3.7	1.0	2.5	2.5	1.9	23	2.8	2.5	2.9	2	3.3	2.3
63	3.4	1.0	4.1	4.0	4.3	-8	4.2	4.1	4.2	-11	4.2	4.2
64	3.6	1.0	5.0	5.1	4.9	-10	5.0	5.1	4.9	-13	5.0	5.1
65	5.0	1.0	6.7	5.8	3.4	-4	4.4	4.3	4.1	-2	6.7	6.7
66	3.7	1.0	5.0	5.1	7.2	-42	6.1	6.2	8.8	10	*	*
67	3.3	1.6	*	*	*	67	15.1	16.8	12.3	8	*	*
69	4.1	2.0	5.4	3.9	15.2	-2	5.3	4.3	6.4	-22	8.3	5.4
72	2.9	1.0	2.3	1.9	3.4	-1	1.9	1.5	2.2	-11	2.4	1.9
74	6.7	2.3	*	*	*	5	16.2	14.4	2.5	38	19.2	19.3
75	3.5	1.9	12.6	12.5	14.9	4	11.9	11.0	25.2	1	12.6	12.5
76	3.3	1.6	7.3	6.4	8.5	-4	8.2	8.0	9.9	-10	12.4	11.5
77	3.6	1.8	10.5	9.7	13.9	-1	10.1	9.1	15.2	-7	10.4	17.7
78	7.8	1.0	4.9	3.8	*	22	4.8	*	*	18	4.7	4.4
79	5.5	1.0	*	*	*	*	*	*	*	*	7.4	8.0
82	4.9	2.2	12.2	10.0	10.5	-7	12.1	9.9	10.4	-4	12.4	13.2
83	5.3	1.0	4.5	4.1	6.2	-4	2.8	2.3	5.3	-3	5.0	5.0
85	2.8	1.0	2.0	2.0	2.1	-54	2.0	1.7	1.5	-12	2.1	2.0

No.	CV	DI	PS1R	PS1T	PS1Q	PS1M	PS2R	PS2T	PS2Q	PS2M	SO1R	SO2R
87	5.2	2.0	6.8	6.5	6.1	0	6.5	6.3	6.3	2	6.8	6.7
89	6.1	2.0	26.3	24.3	29.2	23	26.2	23.4	22.9	22	27.0	26.0
90	6.4	1.0	2.5	2.6	2.3	22	*	*	*	*	*	*
91	4.2	1.0	5.0	4.7	6.0	-8	4.6	4.3	5.8	-9	7.2	6.7
92	4.8	1.0	3.8	3.6	1.9	3	2.5	2.2	2.9	-7	5.1	5.1
93	3.9	1.5	7.1	7.7	10.5	0	10.7	11.0	13.9	-1	4.6	6.2
94	5.1	1.0	2.8	2.9	2.7	21	2.4	2.6	1.2	22	4.6	4.6
95	4.3	1.0	3.0	2.8	3.2	-6	4.3	3.8	4.8	-5	5.0	5.0
96	4.0	1.8	9.4	8.7	11.0	0	9.4	8.5	9.7	-1	9.5	9.5
98	3.0	1.8	24.6	24.8	28.0	13	18.7	19.4	20.5	-14	*	*
99	4.2	1.7	6.9	8.5	9.3	-17	6.9	7.9	4.2	18	6.8	*
100	8.2	1.6	16.2	16.1	30.6	-7	14.7	11.7	43.3	-18	*	*
101	3.7	1.9	13.0	12.9	16.2	5	13.0	12.8	16.1	0	15.1	15.0
102	3.4	1.5	19.9	19.1	25.9	4	21.5	*	*	-19	*	*
104	3.8	1.0	1.3	1.3	1.1	-5	1.3	1.4	1.1	-5	2.6	2.1
105	3.5	1.9	11.7	11.0	12.9	4	8.9	9.0	8.9	-12	10.4	16.6
106	7.6	1.0	4.9	4.6	6.1	3	4.9	4.7	6.1	3	6.6	6.6
107	4.2	1.9	16.8	17.9	20.9	5	16.8	17.1	17.5	-9	21.7	16.8

No.	CV	DI	PS1R	PS1T	PS1Q	PS1M	PS2R	PS2T	PS2Q	PS2M	SO1R	SO2R
108	5.7	1.6	22.2	14.9	18.3	21	22.2	14.9	18.3	15	*	*
109	4.6	1.0	0.9	0.9	1.3	-10	0.9	0.5	3.8	-6	1.0	1.0
110	6.1	1.3	3.0	3.1	4.0	-4	2.8	2.8	3.7	5	*	*
111	3.1	2.6	29.9	27.7	21.3	-36	29.7	27.5	21.2	-20	*	19.5
112	5.1	1.0	1.6	1.5	2.8	2	*	*	*	*	*	*
114	8.4	1.0	8.0	6.5	*	22	8.7	7.5	*	33	7.6	7.8
115	6.9	1.0	2.3	2.3	*	3	5.4	6.5	*	1	8.0	8.0
116	4.3	1.0	4.5	4.2	7.0	-4	4.0	4.2	5.9	-4	4.7	6.5
117	4.7	1.6	*	*	*	*	6.0	4.9	6.9	9	*	*
118	4.7	1.7	17.5	16.6	22.9	-8	16.0	15.9	23.0	-10	18.2	15.0
119	7.1	1.0	2.4	2.0	2.7	9	3.3	2.9	5.1	19	3.2	3.2

Appendix III: Characteristics of patients and tumours labelled with bromodeoxyuridine, and basic histogram parameters for each tumour. Numbers in the first column have simply replaced the patient's names, these being in alphabetical order, the three patients with bilateral tumours being identified by the suffixes L & R (for left and right). Meno = menopausal status. T & N = tumour size and nodal status, using the TNM classification. ER = oestrogen receptor status, 0 for negative (<5fmol/mg protein), and 1 for positive. n = number of labelled undivided cells available for calculation of T_s . CV = half peak coefficient of variation of the diploid G_0/G_1 peak. DI = DNA index. * means not available, P (in DI column) means polyploid.

No	Age	Meno	T	N	ER	n	CV	DI
1	69	post	2	0	*	484	3.2	1.0
2	49	*	1	1	0	649	4.2	2.0
3	82	post	2	1	*	259	*	1.0
4	59	post	2	1	0	498	7.2	1.0
5	65	post	1	0	*	661	4.0	P
6	61	post	*	*	*	309	3.9	1.6
7	84	post	2	1	*	191	4.4	1.0
8	52	post	1	0	*	411	3.5	1.0
9	51	post	3	1	1	932	5.6	1.7
10	74	post	3	0	*	1107	4.2	1.0
11	77	post	1	*	*	183	4.9	1.0
12	77	post	2	0	0	482	13.7	1.0
13	58	post	3	0	0	1095	4.9	1.5
14	70	post	2	*	1	296	4.1	1.0
15	66	post	*	*	*	256	5.5	1.3
16	59	post	1	0	0	2523	2.7	1.7
17	62	post	1	0	*	161	4.9	1.0
18	48	pre	2	1	*	2253	8.2	1.5
19	59	post	2	1	*	1672	*	1.4
20	*	*	*	*	*	1524	5.2	1.4
21	77	post	2	0	1	187	3.3	1.7
22	56	post	*	*	*	1022	3.8	1.7

No	Age	Meno	T	N	ER	n	CV	DI
23	36	pre	3	0	*	203	3.7	1.5
24	46	pre	1	*	0	555	4.4	1.4
25	57	post	2	1	0	1199	13.9	1.0
26	60	post	2	1	*	3605	4.8	3.0
27	55	post	3	0	1	4624	11.4	1.0
28L	61	post	*	*	*	1243	*	1.2
28R	61	post	*	*	*	163	*	1.0
29	64	post	1	1	*	257	4.9	1.8
30	40	pre	1	0	*	815	6.5	1.4
31	48	*	2	0	1	179	4.6	1.0
32	69	post	2	1	1	79	9.6	1.0
33	52	post	*	1	0	1193	4.9	1.6
34	66	post	2	1	*	956	11.9	1.6
35	63	post	2	0	1	109	4.8	1.3
36	69	post	2	0	*	213	4.1	1.6
37	65	post	2	0	*	720	5.3	1.0
38	55	post	2	1	*	1193	3.3	1.6
39	63	post	*	*	*	1380	*	1.0
40	*	pre	*	*	*	762	5.2	1.6
41	64	*	*	*	*	233	5.5	1.0
42	*	post	*	*	*	210	3.9	1.0
43	68	post	2	0	*	419	3.8	1.5
44L	48	*	1	1	1	145	3.8	2.1
44R	48	*	1	0	1	274	3.6	1.7
45	68	post	1	*	*	225	*	2.8
46	66	post	3	*	*	711	*	1.9
47	51	*	1	0	*	871	3.9	1.6
48	70	post	*	*	*	148	4.1	1.0
49	65	post	1	0	0	453	7.2	1.6
50	60	post	2	*	*	546	*	1.8
51	39	pre	1	0	*	504	*	1.0
52	62	post	3	0	0	896	5.5	1.5

No	Age	Meno	T	N	ER	n	CV	DI
53	*	*	*	*	*	633	*	1.2
54	53	post	3	1	1	426	3.3	1.0
55	65	post	*	*	*	856	12.8	1.0
56	47	pre	1	0	1	797	4.5	1.0
56	74	post	*	*	*	2271	7.2	2.0
58	70	post	1	0	*	1520	9.0	1.0
59L	71	post	1	0	1	991	5.3	1.8
59R	71	post	1	0	1	231	5.8	1.0
60	*	*	*	*	*	664	3.9	1.6
61	71	post	*	1	1	348	5.7	1.0
62	49	*	3	1	1	588	5.7	1.6
63	68	post	2	0	*	331	3.6	1.9
64	53	*	2	0	*	2630	5.9	1.4
65	52	post	2	0	0	1862	4.2	3.0
66	55	post	*	1	1	687	4.0	2.0
67	90	post	2	*	*	1271	10.3	1.0
68	75	*	*	*	*	747	7.7	1.0
69	59	post	*	*	*	303	7.6	1.8
70	73	post	1	1	*	1890	8.9	2.0
71	61	post	*	*	*	421	5.8	1.0
72	58	post	1	0	0	302	4.7	2.9
73	*	*	*	*	*	135	4.3	1.6
74	*	*	*	*	*	181	5.7	1.0
75	67	post	*	*	*	431	8.1	1.9
76	68	post	2	1	*	55	7.4	1.0
77	68	post	*	*	*	148	4.4	1.0
78	54	post	3	*	*	2272	5.0	1.5
79	69	post	*	*	*	133	5.7	1.0
80	71	post	*	*	*	169	5.9	1.0
81	56	post	1	0	*	226	7.6	1.0

Appendix IV: Kinetic parameters for each of the 84 tumours in which one or more could be calculated. The identification number in column 1 is the same as in the previous appendix. Subsequent columns are: PI- tumour ploidy (D diploid, A aneuploid); BLI- bromodeoxyuridine labelling index; TLI- total labelling index; ILI- immunohistochemical labelling index; SPF- S phase fraction; Ts- length of S phase in hours; Tpot- potential doubling time in days. Missing values are shown as *.

No.	PI.	BLI	TLI	ILI	SPF	T _s	T _{pot}
1	D	1.4	1.61	*	12.8	11.6	27.6
2	A	8.4	4.32	5.37	16.0	32.0	12.7
3	D	0.5	0.58	*	2.3	11.9	79.2
4	D	1.1	1.29	0.05	1.7	17.0	51.5
5	A	5.3	3.21	5.83	*	*	*
6	A	2.1	1.75	*	25.0	15.5	24.7
7	D	0.9	1.05	*	14.8	19.8	73.2
8	D	1.1	1.18	*	2.5	10.3	31.2
9	A	7.6	2.91	7.25	15.8	10.7	4.7
10	D	3.1	3.94	2.58	5.7	16.4	17.7
11	D	1.1	1.22	1.28	5.5	9.5	28.8
12	D	3.3	4.42	4.66	*	14.5	14.6
13	A	3.2	3.40	4.19	7.2	9.8	10.2
14	D	1.2	1.33	1.29	3.1	13.5	37.5
15	A	0.9	1.05	1.45	3.9	*	*
16	A	8.9	7.80	12.43	12.7	14.2	5.3
17	D	0.5	0.60	0.90	3.2	13.7	91.1
18	D	5.3	3.35	6.77	23.9	12.7	8.0
19	D	8.6	8.35	*	22.6	*	*
20	A	10.2	8.09	7.53	17.5	11.2	3.7
21	A	0.8	0.68	0.49	5.3	12.2	50.7
22	A	4.3	3.46	*	8.6	16.0	12.4
23	A	2.4	1.19	4.92	14.9	10.5	14.6
24	A	4.4	5.33	0.00	30.8	9.7	7.3

No.	Pl.	BLI	TLI	ILI	SPF	T _s	T _{pot}
25	D	2.0	2.49	5.91	*	7.5	12.5
26	A	12.2	7.63	13.76	18.1	21.3	5.8
27	D	7.2	8.24	2.87	*	10.0	4.6
28L	A	3.9	2.72	*	4.3	6.9	5.9
28R	D	0.5	0.52	*	1.7	9.3	62.2
29	A	3.2	1.27	1.05	6.5	13.6	14.2
30	A	10.2	8.22	9.65	39.1	*	*
31	D	0.4	0.48	*	2.4	18.4	153.3
32	D	0.8	0.95	0.85	3.7	22.3	92.8
33	A	8.5	5.08	*	*	*	*
34	A	6.4	4.57	*	*	16.5	8.6
35	A	1.2	1.14	0.64	11.4	14.0	38.8
36	A	1.6	0.78	2.47	6.3	12.0	25.1
37	D	1.6	1.90	2.76	3.3	10.3	21.5
38	A	8.2	4.43	7.97	15.7	*	*
39	D	2.7	2.98	*	3.3	8.7	10.8
40	A	5.2	3.29	*	20.6	17.7	11.4
41	D	2.3	2.89	*	23.6	24.8	35.9
42	D	0.9	1.03	*	8.7	12.1	44.8
43	A	12.9	6.89	*	40.7	*	*
44L	A	0.8	0.67	1.78	5.0	19.8	82.5
44R	A	1.2	0.66	*	7.7	*	*
45	A	7.8	2.13	*	10.4	*	*
46	A	7.2	2.52	*	7.0	22.7	10.5
47	A	4.0	1.90	1.76	14.3	*	*
48	D	0.8	0.88	*	5.2	10.2	42.4
49	A	2.9	1.20	*	17.0	*	*
50	A	6.7	4.47	*	6.0	8.9	4.4
51	D	1.3	1.64	*	5.9	22.7	58.1
52	A	3.6	2.65	9.48	20.0	14.5	13.4
53	A	2.8	2.32	*	*	17.4	20.7
54	D	0.8	0.91	2.17	2.7	11.8	49.2

No.	Pl.	BLI	TLI	ILI	SPF	T _s	T _{pot}
55	D	2.5	2.99	*	*	9.3	12.5
56	D	4.5	4.89	11.17	8.8	10.7	7.9
57	A	9.7	5.93	10.56	11.7	19.8	6.8
58	D	4.1	4.74	6.83	5.3	4.8	3.9
59L	A	5.1	3.41	*	8.0	13.6	8.9
59R	D	1.9	2.15	2.12	5.8	10.5	18.5
60	A	7.9	4.26	4.18	16.9	*	*
61	D	1.0	1.17	1.37	3.2	10.6	35.5
62	A	4.8	2.89	3.54	33.0	*	*
63	A	5.4	1.55	*	8.5	13.6	8.4
64	A	5.1	3.76	7.52	25.6	*	*
65	A	7.9	5.06	7.30	12.6	14.9	6.3
66	A	6.7	3.78	*	16.8	13.7	6.8
67	D	3.6	4.00	3.02	*	8.8	8.1
68	D	3.3	3.89	*	3.6	11.1	11.2
69	A	3.5	3.39	4.94	7.3	*	*
70	A	6.4	7.82	*	12.4	8.5	4.4
71	D	0.8	0.90	1.36	0.8	*	*
72	A	6.9	1.65	11.13	8.5	11.9	5.7
73	A	2.5	2.65	2.27	19.1	17.3	23.0
74	D	3.3	2.73	0.30	4.0	12.2	12.3
75	A	1.6	1.59	2.96	3.6	16.7	34.8
76	D	0.8	0.91	0.19	9.2	17.1	71.1
77	D	0.6	0.67	*	7.7	15.9	88.2
78	A	7.1	6.95	*	15.5	11.7	5.5
79	D	1.5	1.77	1.65	6.5	16.1	35.9
80	D	1.0	1.21	4.41	4.7	*	*
81	D	1.7	*	*	*	9.3	18.2

Appendix IVa: Results of immunohistochemistry for *c-erbB-2* in the BUdR-labelled tumours. No. = patient number in the bromodeoxyuridine series (as in Appendices III and IV). *erbB-2* = 0-negative, 1-positive, *-not available.

No	<i>erbB-2</i>
1	0
2	1
3	1
4	0
5	0
6	1
7	0
8	*
9	0
10	0
11	0
12	0
13	0
14	1
15	0
16	1
17	0
18	1
19	0
20	0
21	1
22	*
23	1
24	*
25	1
26	1
27	0
28L	0
28R	1
29	0
30	1
31	0
32	0
33	1
34	0
35	0
36	0
37	1
38	1
39	0
40	1

No	<i>erbB-2</i>
41	0
42	0
43	0
44L	1
44R	1
45	1
46	1
47	1
48	0
49	1
50	*
51	0
52	0
53	0
54	0
55	*
56	1
57	0
58	0
59L	0
59R	0
60	1
61	0
62	0
63	1
64	0
65	0
66	*
67	0
68	*
69	*
70	0
71	1
72	1
73	1
74	0
75	0
76	1
77	0
78	*
79	0
80	0
81	*

Appendix V: Data for patients whose tumours were assayed for EGFR by radioimmunohistochemistry. Columns: 'BUDR' - patient's number in the cell kinetic series, where applicable; 'Grains' - grain count per 10^{-2}mm^2 per hour of exposure; 'EGFR' - EGFR expression as % of normal breast in that batch; 'T' - TNM system pT; 'N' - TNM system pN; 'Gr.' - histological tumour grade, modified Bloom and Richardson scale; 'ER' - biochemical oestrogen receptor expression (0 = $<20\text{fmol/mg}$, 1 = $\geq 20\text{fmol/mg}$); 'LI', 'T_s', 'T_{pot}' - kinetic parameters as in Appendix IV. Missing values are shown as *.

No.	BUDR	Grains	EGFR	Age	T	N	Gr.	ER	LI	T _s	T _{pot}
1	1	0.75	5.4	69	2	0	2	*	1.4	11.6	27.6
2	2	0.00	0.0	49	1	1	2	0	8.4	32.0	12.7
3		0.54	3.8	*	3	*	3	*	*	*	*
4	3	2.62	25.3	82	2	0	3	*	0.5	11.9	79.2
5	4	0.78	5.2	59	2	1	2	0	1.1	17.0	51.5
6		7.13	48.2	53	1	0	*	*	8.1	13.3	5.5
7	5	1.98	22.0	65	2	0	3	*	5.3	*	*
8		0.19	2.0	53	2	1	*	*	*	*	*
9		0.00	0.0	68	2	0	*	*	*	*	*
10		0.00	0.0	63	1	0	*	*	*	*	*
11		0.34	3.8	61	3	*	*	*	*	*	*
12		4.35	29.4	50	2	0	*	*	*	*	*
13	9	3.40	28.6	51	3	1	3	1	7.6	10.7	4.7
14	10	29.20	245.1	74	3	0	2	*	3.1	16.4	17.7
15		0.21	1.7	62	1	1	*	1	*	*	*
16		0.75	5.7	76	1	0	3	*	*	*	*
17		0.81	5.7	47	1	*	*	*	*	*	*
18	11	0.10	0.8	77	2	0	3	*	1.1	9.5	28.8
19	12	89.40	749.3	77	2	0	3	0	3.3	14.5	14.6
20		0.57	4.3	63	2	1	*	*	*	*	*
21		1.69	16.9	63	1	0	*	*	*	*	*
22	13	0.00	0.0	58	4	0	2	0	3.2	9.8	10.2
23		8.11	76.6	59	2	1	3	*	*	*	*
24		3.29	33.8	92	1	*	*	0	*	*	*
25		0.40	2.7	62	2	0	*	*	*	*	*
26	14	0.23	2.2	70	2	*	1	*	1.2	13.4	37.5
27		0.80	6.7	45	1	0	*	*	*	*	*
28		0.33	3.3	53	1	*	*	*	*	*	*
29	18	1.24	12.0	48	2	1	2	*	5.3	12.7	8.0
30	20	7.49	72.3	75	2	1	3	*	10.3	11.2	3.7
31	21	0.25	2.4	77	2	0	2	1	0.8	12.2	50.7

No.	BUDR	Grains	EGFR	Age	T	N	Gr.	ER	LI	T _s	T _{pot}
32		0.83	8.2	46	4	0	*	0	*	*	*
33		1.20	11.6	58	2	1	*	*	*	*	*
34		6.8	49.9	*	1	0	*	0	6.3	20.8	11.0
35		0.18	1.8	67	4	1	*	*	*	*	*
36	25	3.16	30.5	57	2	1	3	0	2.0	7.5	12.5
37		6.92	68.8	82	4	*	*	0	*	*	*
38		0.21	2.1	45	2	0	*	*	*	*	*
39		0.45	4.6	54	2	1	*	1	*	*	*
40		0.62	6.1	57	1	1	*	*	*	*	*
41		0.00	0.0	74	2	*	*	*	*	*	*
42	26	0.06	0.4	60	2	1	3	*	12.2	21.3	5.8
43		7.33	49.6	61	2	1	*	*	*	*	*
44		6.53	75.2	47	2	1	*	1	*	*	*
45	27	1.89	12.4	55	3	0	3	1	7.2	10.0	4.6
46		0.35	2.4	44	2	0	*	1	*	*	*
47		0.14	1.7	65	2	1	*	*	*	*	*
48		0.27	2.6	65	2	1	*	1	*	*	*
49		1.55	15.5	57	2	1	*	*	*	*	*
50		0.22	2.1	59	1	0	*	0	*	*	*
51		0.51	5.0	77	2	1	*	*	2.5	6.6	8.8
52		0.04	0.4	80	1	0	*	*	2.1	13.6	21.6
53		0.00	0.0	78	2	1	*	1	*	*	*
54	32	0.69	4.6	48	2	0	1	1	0.4	18.4	153.3
55	33	1.98	19.1	69	2	1	2	1	0.8	22.3	92.8
56		0.71	7.2	76	2	1	*	1	*	*	*
57	34	22.6	189.1	52	4	1	3	*	8.5	*	*
58	36	0.70	4.6	63	1	0	2	1	1.2	14.0	38.8
59	38	0.42	3.4	65	2	1	1	0	1.6	10.3	21.5
60		0.17	1.7	67	2	0	*	*	1.6	9.6	20.0
61		0.49	5.6	64	*	0	*	*	*	*	*
62		0.04	0.3	76	2	1	*	1	*	*	*
63	41	2.60	21.3	47	2	1	3	*	5.2	17.7	11.4
64		0.37	4.2	59	3	*	*	*	*	*	*
65		4.07	27.6	84	1	1	*	*	*	*	*
66	43	1.00	7.2	77	2	1	1	0	0.9	12.1	44.8
67		0.19	2.0	67	2	1	*	1	*	*	*
68		0.73	8.4	59	2	1	*	1	2.8	12.4	14.8
69	45	0.00	0.0	48	2	0	*	1	0.8	19.8	82.5
70		0.68	5.0	62	1	0	*	*	1.1	12.7	38.5
71		0.24	2.4	61	1	1	*	0	3.2	17.5	18.2
72		6.34	42.9	50	2	0	*	0	*	*	*
73		4.95	52.8	58	*	1	*	*	*	*	*
74	50	0.85	6.3	80	2	0	1	*	0.8	10.2	42.4

No.	BUDR	Grains	EGFR	Age	T	N	Gr.	ER	LI	T _s	T _{pot}
75	56	0.17	1.1	53	3	1	2	1	0.8	11.8	49.2
76	58	0.70	5.3	47	1	0	3	*	4.5	10.7	7.9
77		0.32	3.2	75	2	0	*	1	*	*	*
78		1.13	11.6	66	2	1	*	0	5.2	31.8	20.4
79		0.62	7.5	72	1	*	1	*	*	*	*
80	61	2.93	28.3	71	1	0	3	1	5.1	13.6	8.9
81		0.25	2.8	45	1	0	*	1	*	*	*
82		18.23	156.8	64	1	1	*	*	*	*	*
83	63	2.94	24.8	51	2	0	3	*	7.9	*	*
84	64	1.09	9.2	71	*	1	1	1	1.0	10.6	35.5
85	67	2.36	15.5	52	2	0	3	0	5.1	*	*
86	68	1.06	10.2	52	2	0	3	0	7.9	14.9	6.3
87		0.25	2.5	56	2	0	*	1	*	*	*
88	71	0.26	2.6	75	2	1	2	1	3.3	11.1	11.2
89	72	0.25	3.5	59	2	0	2	1	3.5	*	*
90		6.49	43.9	68	2	1	*	*	*	*	*
91		7.51	50.8	67	2	0	*	0	2.3	*	*
92		0.20	1.7	92	2	0	*	0	*	*	*
93	73	0.28	2.6	73	2	1	3	*	6.4	8.5	4.4
94	74	0.00	0.0	61	2	0	2	*	0.8	*	*
95		0.19	1.9	47	1	0	*	1	*	*	*
96	75	4.48	36.8	58	1	0	3	0	6.9	11.9	5.7
97	76	1.18	9.9	75	2	*	3	*	2.5	17.3	23.0
98		9.07	61.3	40	1	1	*	*	*	*	*
99	81	2.07	20.6	54	2	0	*	0	7.1	11.7	5.5
100		0.50	5.7	61	4	0	*	*	3.1	10.7	11.5
101		0.29	2.9	46	1	0	*	1	*	*	*
102		0.28	2.9	*	2	0	*	1	*	*	*
103		6.84	63.5	63	2	*	*	*	*	*	*
104	83	10.1	85.1	71	2	0	3	*	1.0	*	*
105	84	0.53	4.5	56	1	0	3	*	1.7	9.3	18.2